

PREDICTION OF INHIBITION OF HYDRATE FORMATION
USING THE PFGC EQUATION OF STATE

By

ALI IFTIKHAR MAJEED

Bachelor of Science in Chemical Engineering
Boğaziçi University
Istanbul, Turkey
1979

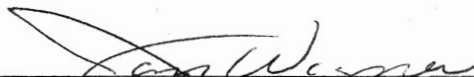
Master of Science
Oklahoma State University
Stillwater, Oklahoma
1981

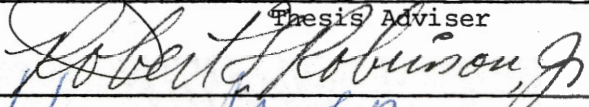
Submitted to the Faculty of the Graduate College
of the Oklahoma State University
in partial fulfillment of the requirements
for the Degree of
DOCTOR OF PHILOSOPHY
December, 1983

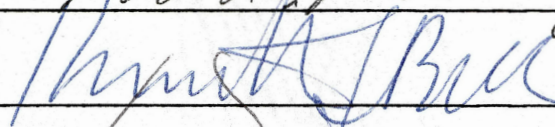
Thesis
1983D
M233P

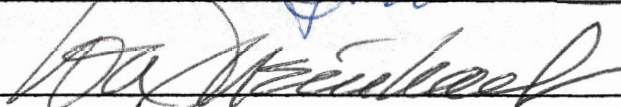
PREDICTION OF INHIBITION OF HYDRATE FORMATION
USING THE PFGC EQUATION OF STATE


Thesis Approved:



Thesis Adviser








Dean of the Graduate College

PREFACE

The Parameters from Group Contribution (PFGC) equation of state introduced by Cunningham and Wilson was developed into a useful engineering tool. Group parameters and binary group interaction coefficients were derived for paraffins, olefins, cycloparaffins, aromatics some inorganics, methanol, glycols and water. The gas phase fugacity, gas solubility in the aqueous phase, the activity coefficient of water and the solubility of the components in the gas phase are reliably predicted by the PFGC equation for multicomponent systems containing light hydrocarbons, nitrogen, carbon dioxide, hydrogen sulfide, methanol and glycols. The thermodynamic properties calculated using the PFGC equations are used in the technique developed by Parrish and Prausnitz to predict the hydrate forming conditions for mixtures of light hydrocarbons, nitrogen, carbon dioxide and hydrogen sulfide. The activity coefficient of water calculated by the PFGC equation is used in the hydrate model as modified by Menten, Parrish and Sloan to account for the presence of the inhibitor in the aqueous liquid phase. The inhibition of hydrate formation in the presence of methanol or glycols and the vaporization losses for the inhibitor are intrinsically handled by the PFGC equation of state and the hydrate model. The results from this work are very encouraging and provide the engineer with a theoretically consistent alternative to the classical Hammerschmidt equation.

The author wishes to express his deep sorrow and regret at the sad demise of Dr. J. H. Erbar, his major advisor. The knowledge, experience, encouragement and guidance provided by Dr. Erbar is posthumously acknowledged.

The author would also like to thank Dr. Jan Wagner, Dr. Kenneth J. Bell, Dr. Robert N. Maddox, Dr. Robert L. Robinson, Dr. Wayne A. Meinhart and Dr. Ruth C. Erbar for their invaluable guidance and assistance. Special thanks are due to Mr. Arild Wilson for his encouragement and support.

A note of thanks is given to Mr. C. Brewer and Mrs. E. Strubel for their assistance in the literature search. Thanks are expressed to Mrs. Teresa Tackett for her excellent work in typing and editing this thesis.

Financial support from the School of Chemical Engineering and the OSU Foundation is sincerely appreciated.

Finally, special gratitude is expressed to my parents, Mr. and Mrs. H. A. Majeed, my brother Waqar, my sister Neelofur, and to my wife Jana Yasmine, for their love, sacrifices, support, prayers and encouragement during this work.

TABLE OF CONTENTS

Chapter	Page
I. INTRODUCTION	1
II. LITERATURE REVIEW	5
History of Gas Hydrates	5
Hammerschmidt's Discovery	6
Early Experimental Data	6
Empirical Predictive Techniques	7
Van der Waals and Platteeuw's Model	8
Modifications by McKoy and Sinanoğlu	12
Validity Test by Marshall, Saito and Kobayashi	13
Further Work by Nagata and Kobayashi	15
Computer Program by Parrish and Prausnitz	17
Interaction Parameter by Ng and Robinson	21
Further Work by Holder, Corbin and Papadopoulos	22
Choice of Cell Size and Contribution of Subsequent Water Shells	24
Hydrate Formation in Multicomponent Mixtures	25
Generalized Model by Holder, Papadopoulos and John	27
Prevention and Removal of Hydrates	31
Hammerschmidt Equation	32
Work of Deaton and Frost	35
Experimental Work by Jacoby and Kobayashi, Withrow, Williams and Katz	36
Use of Global Injection to Inhibit Hydrate Formation	36
Modification of Hammerschmidt Equation by Nielsen and Bucklin	37
Improved Model by Menten, Parrish and Sloan	38
Experimental Work by Erickson, Len, Ng and Robinson	38
III. MODEL DEVELOPMENT	40
Statistical Thermodynamic Model for Hydrates	40
Activity Coefficient of Water in Hydrate Model.	43
Equation of State for Thermodynamic Properties	44
Derivation of the PFGC Equation of State	47
The Flory-Huggins Contribution	48
Group Contribution from a Modified Wilson Equation	51
Final Form of the PFGC Equation of State	53
Development of Fugacity Equation	55

Chapter	Page
Development of Calculation Procedure	60
Computer Program for Developing Parameters in PFGC Equation	62
Summary of This Work	65
 IV. RESULTS	 67
Fugacity Expression and New Calculation Procedure . . .	67
Pure Component Thermodynamic Property Prediction . . .	67
Vapor Liquid Equilibrium of Multicomponent Mixtures . .	80
Dry Light Hydrocarbon Systems	80
Aqueous Light Hydrocarbon Systems	122
Methanol and Glycol Systems	122
Multicomponent Test Mixtures	137
Prediction of Hydrate Forming Conditions for Pure Components	145
Multicomponent Hydrate Forming Conditions Prediction	145
Effect of Methanol and Glycols as Hydrate Inhibitors	163
 V. DISCUSSION OF RESULTS	 179
Quality of Pure Component Property Prediction	179
Quality of Vapor Liquid Equilibrium Predictions for Mixtures	183
Dry Light Hydrocarbon Systems	183
Aqueous Light Hydrocarbon Systems	186
Methanol and Glycol Systems	188
Multicomponent Test Mixtures	189
Quality of Predictions of Hydrate Forming Conditions for Pure Components	191
Quality of Prediction of Multicomponent Hydrate Forming Conditions	193
Quality of Prediction of the Effect of Methanol and Glycols as Hydrate Inhibitors	194
 VI. CONCLUSIONS AND RECOMMENDATIONS	 196
Conclusions	196
Recommendations	197
 BIBLIOGRAPHY	 200

LIST OF TABLES

Table	Page
I. Structural Properties of the Hydrate Lattice	20
II. Deviations in Vapor Pressure, Enthalpy and Volume Predictions for Pure Component Paraffin Hydrocarbons . . .	69
III. Deviations in Vapor Pressure, Enthalpy and Volume Predictions for Pure Component Olefin Hydrocarbons . . .	72
IV. Deviations in Vapor Pressure, Enthalpy and Volume Predictions for Pure Component Aromatic Hydrocarbons . . .	74
V. Deviations in Vapor Pressure, Enthalpy and Volume Predictions for Pure Component Cycloparaffin Hydrocarbons	75
VI. Deviations in Vapor Pressure, Enthalpy and Volume Predictions for Pure Component Non-Hydrocarbons	76
VII. Group Parameters for the PFGC Equation of State	81
VIII. Binary Group Interaction Parameters for the PFGC Equation of State	83
IX. CO ₂ Binary System Deviations in K-Value Predictions . . .	88
X. N ₂ Binary System Deviations in K-Value Predictions	92
XI. H ₂ S Binary System Deviations in K-Value Predictions	95
XII. C ₁ Binary System Deviations in K-Value Predictions	97
XIII. C ₂ Binary System Deviations in K-Value Predictions	102
XIV. C ₃ + Binary System Deviations in K-Value Predictions	105
XV. Benzene, Toluene Binary System Deviations in K-Value Predictions	108
XVI. Cycloparaffin Binary System Deviations in K-Value Predictions	110

Table	Page
XVII. H ₂ O Binary Systems Deviations in Phase Concentration Predictions	123
XVIII. Methanol Binary System Deviations in K-Value Predictions .	130
XIX. Glycol Binary System Deviations in K-Value Predictions . .	132
XX. Nominal Compositions of Multicomponent Test Mixtures . . .	138
XXI. Comparison of Experimental and Calculated Equilibrium Phase Densities for Test Mixture III	141
XXII. Reference Thermodynamic Properties of the Empty Hydrate and Liquid Water at 0°C and Zero Pressure	146
XXIII. Optimal Kihara Parameters and Deviations in Pure Component Hydrate Forming Temperature Predictions	147
XXIV. Deviations in Hydrate Forming Temperature Predictions for Hydrocarbon Mixtures	159

LIST OF FIGURES

Figure	Page
1. General Phase Behavior of a Pure Hydrocarbon or Hydrocarbon Mixture in Equilibrium with Gas Hydrates	2
2. The PFGC Equation of State	45
3. Simplified Logic Flow Diagram of the Fitting Program	64
4. Comparison of Predicted and Experimental Vapor Pressure Data for Selected Hydrocarbons	78
5. Comparison of Predicted and Experimental Vapor Pressure Data for Selected Non-Hydrocarbons	79
6. Comparison of Predicted and Experimental K-Values for Methane in the Methane-Ethane System	112
7. Comparison of Predicted and Experimental K-Values for Ethane in the Methane-Ethane System	113
8. Comparison of Predicted and Experimental K-Values for Methane in the Methane-Propane System	114
9. Comparison of Predicted and Experimental K-Values for Propane in the Methane-Propane System	115
10. Comparison of Predicted and Experimental K-Values for Methane in the Methane-CO ₂ System	116
11. Comparison of Predicted and Experimental K-Values for Carbon Dioxide in the Methane-CO ₂ System	117
12. Comparison of Predicted and Experimental K-Values for Nitrogen in the Nitrogen-Methane System	118
13. Comparison of Predicted and Experimental K-Values for Methane in the Nitrogen-Methane System	119
14. Comparison of Predicted and Experimental K-Values for Methane in the Methane-Toluene System	120
15. Comparison of Predicted and Experimental K-Values for Toluene in the Methane-Toluene System	121

Figure	Page
16. Comparison of Predicted and Experimental Phase Solubilities for the Methane-Water System	127
17. Comparison of Predicted and Experimental Phase Compositions for the Ethylene-Water System	128
18. Comparison of Predicted and Experimental Phase Compositions for the Hydrogen Sulfide-Water System	129
19. Comparison of Predicted and Experimental K-Values for Water in the TEG-Water System	133
20. Comparison of Predicted and Experimental K-Values for TEG-Water System	134
21. Comparison of Predicted and Experimental K-Values for Ethane in the Methanol-Ethane System	135
22. Comparison of Predicted and Experimental K-Values for Hydrogen Sulfide in the Methanol-H ₂ S System	136
23. Comparison of Predicted and Experimental Vapor Phase Water Solubilities for Test Mixture I at 220.3°F	139
24. Comparison of Predicted and Experimental K-Values for Components of Test Mixture II at 998 psia	140
25. Comparison of Predicted and Experimental Bubble Point Pressures for Test Mixture IV	142
26. Comparison of Predicted and Experimental Volume Percent Liquid for Test Mixture IV	143
27. Comparison of Predicted and Experimental Bubble Point Pressures for Test Mixture V	144
28. Comparison of Predicted and Experimental Hydrate Forming Conditions for Methane	148
29. Comparison of Predicted and Experimental Hydrate Forming Conditions for Ethane	149
30. Comparison of Predicted and Experimental Hydrate Forming Conditions for Propane	150
31. Comparison of Predicted and Experimental Hydrate Forming Conditions for Isobutane	151
32. Comparison of Predicted and Experimental Hydrate Forming Conditions for Methane-n-Butane Mixtures	152

Figure	Page
33. Comparison of Predicted and Experimental Hydrate Forming Conditions for Ethylene	153
34. Comparison of Predicted and Experimental Hydrate Forming Conditions for Propylene	154
35. Comparison of Predicted and Experimental Hydrate Forming Conditions for Nitrogen	155
36. Comparison of Predicted and Experimental Hydrate Forming Conditions for Oxygen	156
37. Comparison of Predicted and Experimental Hydrate Forming Conditions for Hydrogen Sulfide	157
38. Comparison of Predicted and Experimental Hydrate Forming Conditions for Carbon Dioxide	158
39. Comparison of Predicted and Experimental Hydrate Forming Conditions for Methane-Ethane Mixtures	161
40. Comparison of Predicted and Experimental Hydrate Forming Conditions for Methane-Propane Mixtures	162
41. Effect of Methanol on Hydrate Forming Conditions for Methane	165
42. Effect of Methanol on Hydrate Forming Conditions for Ethane .	166
43. Effect of Methanol on Hydrate Forming Conditions for Propane	167
44. Effect of Methanol on Hydrate Forming Conditions for Carbon Dioxide	168
45. Effect of Methanol on Hydrate Forming Conditions for Hydrogen Sulfide	169
46. Effect of Methanol on Hydrate Forming Conditions for a Mixture Containing 89.51 Mole% Methane and 10.49 Mole% Ethane	170
47. Effect of Methanol on Hydrate Forming Conditions in a Mixture Containing 95.01 Mole% Methane and 4.99 Mole% Propane	171
48. Effect of Methanol on Hydrate Forming Conditions for a Mixture Containing 90.09 Mole% Methane and 9.91 Mole% Carbon Dioxide	172

Figure	Page
49. Effect of Methanol on Hydrate Forming Conditions in a Synthetic Natural Gas Mixture	173
50. Effect of Methanol on Hydrate Forming Conditions for a Synthetic Gas Mixture Containing Carbon Dioxide	174
51. Ratio of Vapor to Liquid Composition for Methanol-Natural Gas Mixture	175
52. Effect of Glycols on Hydrate Forming Conditions for a Mixture Containing 89.51 Mole% Methane and 10.49 Mole% Ethane	176
53. Effect of Glycols on Hydrate Forming Conditions in a Synthetic Natural Gas Mixture	177
54. Effect of Glycols on Hydrate Forming Conditions for a Synthetic Gas Mixture Containing Carbon Dioxide	178

CHAPTER I

INTRODUCTION

Gas hydrates form when certain non-polar or slightly polar gas molecules are physically contacted with water above or below the ice point. The main industrial interest in hydrates lies in predicting their formation and preventing them from plugging gas pipelines. Organic substances like methanol, ethylene glycol, diethylene glycol and triethylene glycol are used to inhibit the formation of these gas hydrates. The classical Hammerschmidt (78) equation is still widely used for determining the effect of inhibitors like methanol and glycols on hydrate forming conditions. There is a clear need for developing a theoretically sound and consistent method for predicting hydrate formation and hydrate inhibition effects.

The general phase behavior of a pure hydrocarbon or a hydrocarbon mixture in equilibrium with gas hydrates is qualitatively shown in Figure 1. The basic statistical thermodynamic model for predicting gas hydrates was derived by Van der Waals and Platteeuw (256). Parrish and Prausnitz (170) presented a computer program for calculating hydrate forming conditions for pure components and gas mixtures. Menten, Parrish and Sloan (148) proposed the use of the activity coefficient of water in the basic hydrate model to account for the presence of an inhibitor like methanol or glycol in the aqueous phase. If the gas

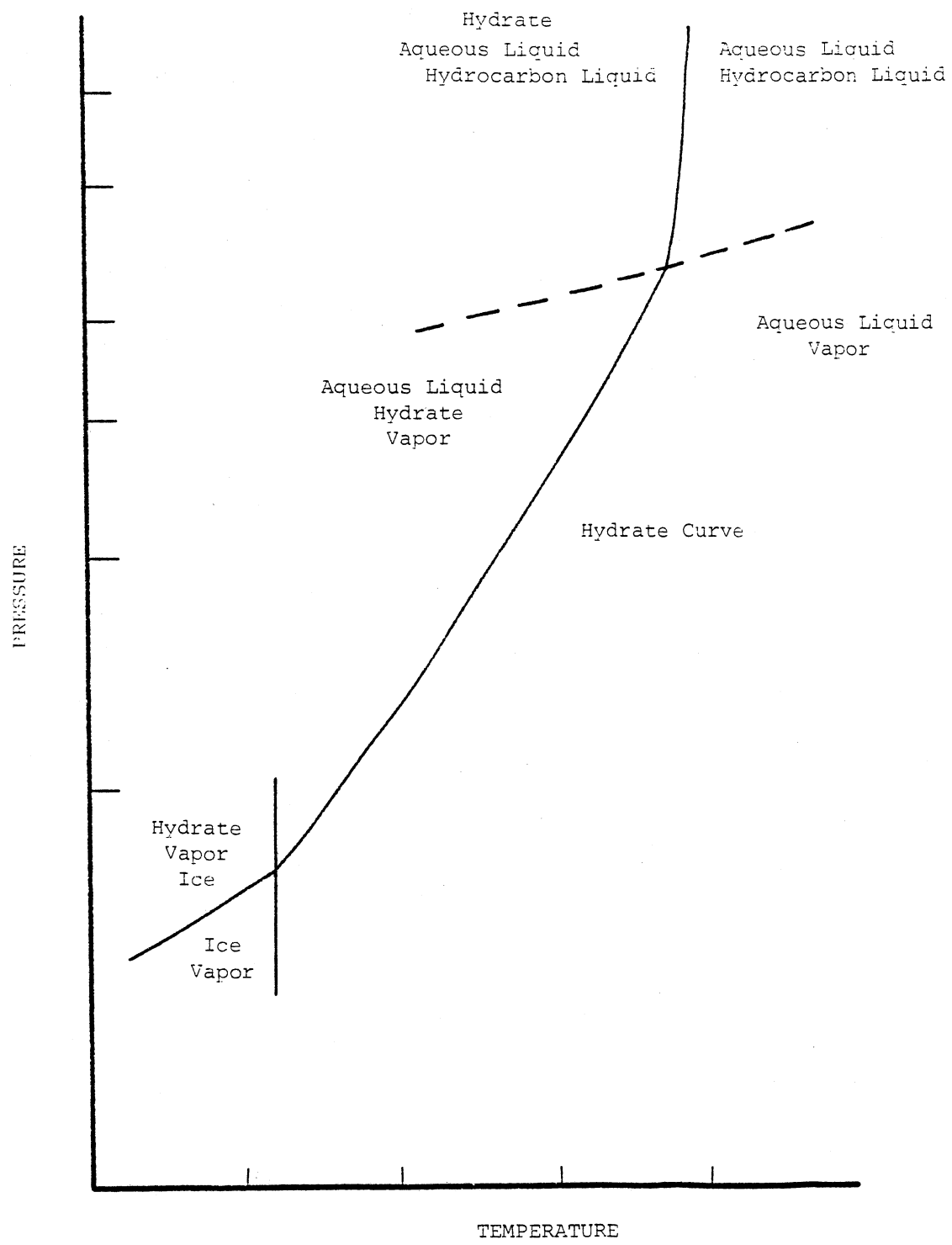


Figure 1. General Phase Behavior of a Pure Hydrocarbon or Hydrocarbon Mixture in Equilibrium with Gas Hydrates

phase fugacity, gas solubility in the aqueous phase, the activity coefficient of water in the presence of the inhibitor and the solubility of the inhibitor, in the gas phase is accurately determined by a single equation of state; the effect of inhibitors on hydrate forming conditions can be reliably and efficiently predicted. Moshfeghian, Shariat and Erbar (153) reported the use of the Parameter from Group Contributions (PFGC) equation of state to reliably predict the phase behavior of hydrocarbon, acid gas, methanol and water systems. The PFGC equation of state can be used as a single consistent source of thermodynamic data for use in the hydrate model for prediction of formation and inhibition of gas hydrates.

The purpose of this work is briefly summarized below:

1. Develop a computer program capable of solving the PFGC equation. Derive the fugacity expression for the PFGC equation so that the activity coefficient of water can be easily calculated.
2. Derive parameters for use in the PFGC equation to provide reliable thermodynamic properties for pure components. Accurate predictions are required for vapor pressures, volumetric properties and enthalpy departures for the liquid and vapor phase. Parameters are required for paraffins, olefins, cycloparaffins, aromatics, nitrogen, carbon dioxide, hydrogen sulfide, sulfur dioxide, methanol, glycols and water.
3. Use available literature data to check vapor liquid equilibrium predictions for light hydrocarbon systems with carbon dioxide, nitrogen, hydrogen sulfide, methanol, glycols and water. Revise the binary group interaction coefficients used in the PFGC equation as required. Evaluate

the quality of the thermodynamic properties predicted from the PFGC equation for multicomponent mixtures over a broad range of conditions.

4. Develop and correlate hydrate predictions using the Parrish and Prausnitz (170) model. Use the activity coefficient correction proposed by Menten, Parrish and Sloan (148). Derive new Kihara parameters for use in the hydrate model. Use the PFGC equation to predict gas phase fugacities, aqueous liquid phase gas solubilities, and the activity coefficient of water required by the hydrate model.

5. Develop, check and compare vapor-hydrocarbon liquid-aqueous liquid mutual solubilities for hydrocarbon, methanol, glycol and water systems. Derive the temperature dependent binary group interaction coefficients based on literature data.

6. Check and complete correlation of hydrate prediction and effect of methanol and glycols as hydrate inhibitors. Compare the inhibitor vaporization losses and inhibitor effectiveness quantitatively with literature data and qualitatively if no data are available.

The aim of this work is to provide the engineer with a reliable and accurate method for determining the effect of methanol and glycols on hydrate forming conditions of multicomponent gas mixtures over a broad range of conditions. The method should accurately determine vaporization losses for the inhibitor. The equilibrium phase behavior and thermodynamic properties for hydrocarbon, acid gas, methanol, glycol and water systems should also reliably be predicted by the same method.

CHAPTER II

LITERATURE REVIEW

History of Gas Hydrates

Faraday (59) attributed the discovery of the first known gas hydrate, a crystalline compound formed by cooling a solution of chlorine and water to 9°C, to Sir Humphrey Davy in 1810. Wroblewski, in 1882, reported a carbon dioxide hydrate. In 1878, Cailletet reported an acetylene hydrate and was the first to discover that a sudden decrease in pressure aided in the formation of these crystalline compounds. Woehler, in 1840, reported the hydrogen sulfide hydrate. Villard (254, 255) reported hydrates of methane, ethane, acetylene, and ethylene. Schutzenburger reported the first double hydrate-hydrogen sulfide and carbon disulfide and de Forcrand discovered a mixed hydrate of hydrogen sulfide and alcohol. In 1897 de Forcrand and Sully Thomas found that acetylene and carbon tetrachloride form a double hydrate. They also reported double hydrates of acetylene, ethylene, sulfur dioxide and carbon monoxide with ethylene chloride, ethylene bromide, methyl bromide and methyl iodide. The pioneering work of Faraday, Villard, de Forcrand, and others during the late nineteenth and early twentieth century has been compiled by Schroeder (229) and Katz (100). An extensive review of the hydrate literature is given by Byk and Fomina (23).

Hammerschmidt's Discovery

The first record of a clear realization that the natural gas industry's problem of pipeline freezing was caused by the formation of gas hydrates was the publication by Hammerschmidt (77) in 1934. In the course of his investigation Hammerschmidt (77) found that solid compounds known as gas hydrates had been reported in the literature many years before. These solid compounds, resembling snow or ice in appearance, were formed with methane, ethane, propane, and isobutane in the presence of water at elevated pressures and temperatures. Hammerschmidt (77) also discovered that the formation of gas hydrates in natural gas pipelines depends primarily upon pressure, temperature, and composition of the gas and water mixture. After these primary conditions are fulfilled, the formation of the hydrates is accelerated by high velocities of the gas stream, pressure pulsations, or inoculation with a small hydrate crystal. The work of Hammerschmidt (77) revived a subject that had laid dormant for nearly fifty years and brought out the importance of gas hydrates to the natural gas industry.

Early Experimental Data

In 1935 Deaton and Frost (45) at the Bureau of Mines carried out a comprehensive study of gas hydrates and their relation to the operation of natural gas pipelines. Information was obtained on the usual locations of hydrate freezes in pipelines, methods used to clear pipelines of such freezes, and the precautions ordinarily taken to avoid them. Experimental laboratory data were collected on the hydrate equilibrium temperatures and pressures for natural and pure gases.

Deaton and Frost (45) determined the practicability of using hydrate inhibitors like ammonia and alcohol in gas pipelines by making field tests. The only sure preventive measure found by the authors was to dehydrate the gas.

Empirical Predictive Techniques

Katz (101) and his co-workers did much of the early work on quantitative prediction of hydrate forming conditions by correlating dissociation pressures with gas gravity for several natural gas mixtures. Wilcox, Carson and Katz (266) developed the first reliable hydrate prediction method based on gas analysis. This method employs the vapor-solid equilibrium constants K in a manner analogous to vapor liquid equilibrium constants. A method comparable to a dew point calculation is used. Thus, the conditions of hydrate formation of a multicomponent gas mixture is found by the following condition:

$$\sum_i \frac{y_i}{K_{v-s_i}} = \sum_i z_i = 1.0 \quad (2.1)$$

where y and z are the mole fractions of component i in the vapor and the solid hydrate phase on a water free basis. The value of the vapor-solid equilibrium constant for a nonhydrate forming component is taken as infinity. For hydrate forming gases, the value of the vapor-solid equilibrium constant can be read from charts. As pointed out by Verma (253) there are two serious drawbacks to this approach. First, the use of a vapor-solid equilibrium constant does not distinguish between different hydrate structures. Second, the vapor-solid equilibrium constants have no explicit dependence on the concentration of the hydrate forming

components, and are assumed to be functions of temperature and pressure. The strong dependence of the vapor-solid equilibrium constants on the composition of the hydrate forming gas mixture has been shown by Marshall (138).

A technique for predicting hydrate formation conditions in natural gas mixtures based on the Clapeyron equation by McLeod and Campbell (146) was later superseded by the method by Trekel and Campbell (24). This method uses methane as a reference condition. The hydrate formation temperature is calculated by algebraically summing temperature displacements read from charts using the dry gas analysis. The temperature is corrected for the effect of pentanes and heavier components. The calculation is repeated at several different pressures and the best curve through these points represents the hydrate forming conditions for the mixture. This method does not distinguish between the different hydrate structures and is highly empirical in nature.

Van der Waals and Platteeuw's Model

The x-ray diffraction work carried out by Powell (173), Claussen (33), Pauling and Marsh (171), and Stackelberg and Muller (240) revealed that gas hydrates belong to a class of three dimensional inclusion compounds known as clathrates. The non-stoichiometric nature of gas hydrates was explained by suggesting fractional occupancy of the hydrate cavities. The gas hydrates may crystallize in either of two cubic structures, labelled Structure I and Structure II, depending on the size of the imprisoned guest molecules. The hydrated molecules are situated in cavities of two different sizes formed by a framework of water molecules linked together by hydrogen bonds. The unit cell of Structure

I contains forty-six water molecules enclosing two types of cavities:

1. Six pentagonal dodecahedral cavities consisting of twenty water molecules each located at the vertices and center of the unit cell.

2. Two tetrakaidecahedral cavities having two opposite hexagonal faces and twelve pentagonal faces serving to connect the regular dodecahedra.

The pentagonal dodecahedra are smaller than the two tetrakaidecahedra, having an average radius of 3.95 \AA , as compared with 4.30 \AA for the tetrakaidecahedra. Thus if all cavities were filled, the maximum hydrate number for Structure I would be $46/8$ or 5.75 .

The unit cell of Structure II is composed of 136 water molecules arranged to form sixteen smaller cavities and eight larger cavities. The smaller cavities are distorted dodecahedra with an average radius of 3.91 \AA , while the larger cavities are almost spherical with an average radius of 4.73 \AA . Structure II is formed only by hydrated molecules which are too large to fit within the cavities of Structure I.

Thermodynamically, gas hydrates are a solution of a gas in a solid. The solid solvent itself is metastable. The two components in the crystal are not joined together by ordinary chemical bonds, but it is the interaction of the encaged molecules with the surrounding network that stabilizes the complex. Van der Waals and Platteeuw (256) used a statistical partition function to describe the regular geometry and the non-stoichiometric nature of gas hydrates. The partition function of a hydrate containing only one type of cavity can be derived using the following assumptions:

1. There is either one or zero gas molecule in each cavity. Multiple occupation of the cavities by gas molecules is not possible.

Once encaged, gas molecules cannot leave the cavities.

2. The interaction of two gas molecules in neighboring cavities can be neglected. The gas molecule only interacts with the nearest neighboring water molecule. Only London forces are important for describing gas water interactions. All polar forces are assumed to be embodied in the hydrogen bonded lattice.

3. The contribution to the partition function of the cage forming water molecules in the metastable hydrate structure is not affected by the presence of the gas molecules in the hydrate lattice.

Other assumptions pointed out by Holder (84) are:

1. The encaged gas molecule has the same freedom to rotate within the cavity as it would in the gas phase. The dimensions of the cavity must be much larger than the largest dimensions of the gas molecule. The gas molecules are sufficiently small to prevent distortion of the hydrate lattice.

2. A specific potential function can accurately describe the water-gas interaction in the hydrate structure. This potential function can be the Lennard-Jones potential or the Kihara potential.

Verma (253) has examined some of these assumptions in detail. The assumption of single occupancy is easily satisfied, since the size of various cavities of either structure are small enough to contain only one gas molecule. The assumption of insignificant interaction between guest molecules in adjacent cavities is justified because of the relatively large separation of cavities. The assumption of free rotation in the cavity is justified for smaller sized, nearly spherical gas molecules like argon and methane. Also, McKoy and Sinanoğlu (145) used

a Boltzmann probability function to show that the gas molecule is confined very near the center of the cavity and therefore does not cause any serious distortion of the cavity and the rotational freedom of gas molecules is not seriously affected.

The Van der Waals and Platteew (256) model corresponds to a three dimensional generalization of localized adsorption without any gas-gas interaction. The chemical potential of the gas in the hydrate structure is described by a Langmuir-type isotherm and an analog of Raoult's law is used for the solid solvent. The difference between μ_w^β , the chemical potential of water in the empty hydrate lattice and μ_w^H , that in the filled hydrate lattice, is

$$\Delta\mu_w^H = \mu_w^\beta - \mu_w^H = -RT \sum_m v_m \ln(1 - \sum_j \phi_{mj}) \quad (2-2)$$

where

r = gas constant

v = number of cavities of type m per water molecule in the lattice.

The fraction of type m cavities occupied by the gas component 1 is given as

$$\phi_{m1} = C_{m1} f_1 / (1 + \sum_j C_{mj} f_j) \quad (2-3)$$

where

C = Langmuir constant,

f = Fugacity of the gas component 1, and

y = Mole fraction of gas component 1 in the vapor phase.

The Langmuir constant accounts for the gas-water interaction in the cavity. The Lennard-Jones-Devonshire cell theory was used to describe the average contribution to the potential energy due to the interaction of the gas molecule with any of the water molecules

constituting the wall of the cage as follows:

$$\epsilon(R) = 4\epsilon^* \left\{ \left(\frac{\sigma^*}{R}\right)^{12} - \left(\frac{\sigma^*}{R}\right)^6 \right\} \quad (2-4)$$

where R is the distance between the gas molecule and the particular water molecule considered. The energy parameter ϵ and the distance parameter σ are characteristic of the interaction of the gas with the water. For the distance parameter the "hard sphere approximation" was used. The "geometric mean relation" was used for the energy parameter. The Langmuir constant is given by

$$C(T) = 4\pi/kT \int_0^{\infty} \exp[-w(r)/kT] r^2 dr \quad (2-5)$$

where T is the absolute temperature, k is the Boltzmann constant, and $w(r)$ is the spherically symmetric cell potential which is a function of the cell radius, the coordination number, and the nature of the gas-water interaction.

Modifications by McKoy and Sinanoğlu

At the equilibrium dissociation pressure of the hydrate, the chemical potential of the free gas molecules over the gas hydrates and the molecules in the force field of the lattice is equal. The calculation of dissociation pressures by Van der Waals and Platteeuw (25c) is good only for the monoatomic gases and quasispherical molecules like methane, but is off by large factors for some non-spherical molecules like carbon dioxide and ethane. After examining the assumptions in the Van der Waals and Platteeuw (25c) model, it appears that, to a good approximation, lattice distortions are not significant, and the molecule is confined pretty much to the center of the cage and does not collide with the wall. An examination of the intermolecular potential

reveals that the discrepancy between the calculated and observed dissociation pressures is due to the inadequacy of the Lennard-Jones potential used. As an alternative, the use of the Kihara potential is suggested by McKoy and Sinanoğlu (145). The Kihara potential assigns a core to each molecule. It therefore includes the effect of the finite size of the molecules on their interaction. The core of a homopolar diatomic molecule is defined as the line segment between the nuclei. The energy of interaction between two such molecules is then assumed to be of the Lennard-Jones 12-6 type. However, the argument of the cell potential is now taken to be the shortest distance between the molecular cores and

$$\Phi(\rho) = \epsilon \left[\left(\frac{\rho}{\rho_m} \right)^{12} - 2 \left(\frac{\rho}{\rho_m} \right)^6 \right] \quad (2-6)$$

where

ϵ = The potential minimum, and

ρ_m = The position of the potential minimum.

With dissociation pressure as a criterion it is concluded that Lennard-Jones 12-6 potential is satisfactory for the hydrates of the monoatomic gases and methane; for rodlike molecules like nitrogen, oxygen, ethylene, ethane and carbon dioxide, the Kihara potential is more suitable.

Validity Test by Marshall,

Saito and Kobayashi

For the solid solution theory to be exact a unique set of molecular parameters should exist for all data on each gas hydrate. Marshall, Saito and Kobayashi (137) fitted the force constants for methane below the ice-hydrate-water-gas quadruple point where the solid

solution theory could be applied exactly. For methane, the set of molecular parameters which exhibited the least deviation from the data of Deaton and Frost (45) were chosen. The chemical potential difference between ice and hydrate along the equilibrium curve was calculated from the following equation:

$$d(\Delta\mu/RT) = - (\Delta H/RT^2)dT + (\Delta V/RT)dP \quad (2-7)$$

where

ΔH = Molar enthalpy difference,

ΔV = Molar volume,

T = Absolute temperature, and

P = Total pressure.

This equation holds for any value of dP and dT . On the equilibrium curve

$$dP = (dP/dT)dT \quad (2-8)$$

Integration of equation (2-7) between T and 273°K along the equilibrium curve gives

$$\Delta\mu/RT = - \int (\Delta H/RT^2)dT + \int (\Delta V/RT) \frac{dP}{dT} dT \quad (2-9)$$

The force constants fitted above were used to correlate experimental data above the gas-hydrate-water-gas quadruple point. The assumption was made that the chemical potential of water in contact with the equilibrium hydrate could be estimated from an ideal solution relationship. At constant temperature the pressure effect on the chemical potential difference becomes

$$(\partial\Delta\mu'/\partial P)_T = \Delta V' \quad (2-10)$$

Integrating equation (2-10) at constant temperature gives

$$\Delta\mu' = \Delta\mu'_0 + \Delta V'(P - P_0) \quad (2-11)$$

where $\Delta\mu_0$ and P_0 are values for the reference hydrate. Marshall, Saito and Kobayashi (137) used methane as the reference hydrate.

The following empirical combined laws which relate the force constants between unlike molecules were used to calculate the force constants of the encaged gas molecules:

$$\bar{\sigma} = \frac{1}{2} (\sigma_w + \sigma_k) \quad (2-12)$$

$$\bar{\epsilon} = (\epsilon_w \epsilon_k)^{1/2} \quad (2-13)$$

where

σ = Energy parameter, and

ϵ = Distance parameter

subscripts

w = Water, and

k = Encased gas molecules.

Using the above relationships, the Lennard-Jones-Devonshire force constants for methane, argon, and nitrogen were determined and found to be in agreement with (constants predicted from second virial coefficient) and viscosity data. These results point to the essential validity of the solid solution theory. Saito and Kobayashi (225) used the same parameters to calculate the dissociation pressures for ternary hydrate systems thus demonstrating the applicability of the Van der Waals and Platteeuw (256) theory for application above 32°F to ternary systems.

Further Work by Nagata and Kobayashi

Nagata and Kobayashi (157) made an attempt to derive a more realistic interaction function for the encaged rodlike molecules in the hydrate lattice. An effort was made to determine a set of potential parameters

which gives a good representation of experimental data over a wide range of temperatures using various intermolecular potential functions including the Kihara model.

The Kihara potential between a core molecule and a point molecule, i.e., the lattice molecule, is calculated. The core is defined as the rod which represents a homopolar diatomic molecule whose distance between the nuclei is l and whose radius is c , the center of the core being at a distance L from the point molecule. The Lennard-Jones potential as a function of the shortest distance between the core and the point molecule was used. The general expression derived for the potential of rodlike molecules reduces to the potential for spherical or line molecules as the limiting case. The parameters of the derived function are determined so as to agree with the experimental dissociation pressures.

For the nitrogen hydrate, a rodlike molecule model is used. A spherical core is used to calculate the dissociation pressure for the methane hydrate. A comparison of predicted dissociation pressures for the methane-nitrogen water system, obtained by using the Kihara potential and the Lennard-Jones potential, with experimental data shows that the Kihara model, which takes into account the shape and size of a caged molecule, is superior to the less realistic Lennard-Jones potential. Nagata and Kobayashi (158) extended their work to predict the dissociation pressures of ternary gas hydrates using data from binary hydrates. The methane-propane hydrate crystallizes in Structure II, while the methane and propane hydrates crystallize in Structure I and II, respectively. Good agreement was obtained in predicting results. The predicted hydrate pressures are higher than the observed data for methane-rich concentration regions.

Computer Program by Parrish and Prausnitz

Parrish and Prausnitz (170) presented a method for calculating hydrate-gas equilibria in multicomponent systems. The method, based on the theory of Van der Waals and Platteeuw, uses the Kihara potential with a spherical core:

$$\Gamma(r) = \infty, r < 2a$$

$$\Gamma(r) = 4\epsilon \left[\left(\frac{\sigma}{r-2a} \right)^{12} - \left(\frac{\sigma}{r-2a} \right)^6 \right], r > 2a \quad (2-14)$$

where

ϵ = Characteristic energy,

a = Core radius, and

$\sigma + 2a$ = Collision diameter.

The above equation describes the interaction between the gas molecule and one water molecule in the cavity wall. The cell potential can be obtained by summing all the gas-water interactions in the cell

$$w(r) = 2z\epsilon \left[\frac{\sigma^{12}}{R^{11}r} (\delta^{10} + \frac{a}{R} \delta^{11}) - \frac{\sigma^6}{R^5r} (\delta^4 + \frac{a}{R} \delta^5) \right] \quad (2-15)$$

where

$$\delta^N = [(1 - r/R - a/R)^{-N} - (1 + r/R - a/R)^{-N}] / N \quad (2-16)$$

and

$N = 4, 5, 10$ or 11 ,

z = Coordination number of the cavity, and

R = Cell radius of the cavity.

The equations listed above can be used to calculate the chemical potential difference between the empty hydrate lattice and filled hydrate lattice.

The chemical potential of water in the hydrate phase equals that in each of the other coexisting phases at equilibrium. If liquid water is present as a phase, then

$$\mu_w^H(T, P, \theta) = \mu_w^L(T, P) + RT \ln x_w \quad (2-17)$$

where

μ_w^L : Chemical potential of pure liquid water at T and P, and

x_w : Mole fraction of water in the liquid phase.

The chemical potential difference can be defined as

$$\Delta\mu_w^L = \mu_w^\beta - \mu_w^L \quad (2-18)$$

Using a reference hydrate the chemical potential can be calculated in two steps. First, for the reference hydrate, $\Delta\mu_w^L(T, P_r)$, at the given temperature, T, and the reference hydrate dissociation pressure, P_r , is found by using

$$\begin{aligned} \Delta\mu_w^L(T, P_r)/RT = \Delta\mu_w^L(T_o, P_o)/RT_o - \int_{T_o}^T (\Delta h_w^\alpha + \Delta h_w^f) RT^2 dT \\ + \int_{T_o}^T [\Delta v_w^\alpha + \Delta v_w^f]/RT (dP/dT) dT \end{aligned} \quad (2-19)$$

where

P_o = Dissociation pressure of the reference hydrate,

T_o = Ice-point temperature,

Δh_w^α = Molar difference in enthalpy between empty hydrate and ice,

Δv_w^α = Molar difference in enthalpy between empty hydrate and ice,

Δh_w^f = Molar difference in enthalpy between ice and water, and

Δv_w^f = Molar difference in enthalpy between ice and water.

The chemical potential difference at any T and P is given by

$$\Delta\mu_w^L(T, P) = \Delta\mu_w^L(T, P_R) + (\Delta v_w^g + \Delta v_w^f)(P - P_R) \quad (2-20)$$

Parrish and Prausnitz (170) have chosen the methane hydrate as the reference hydrate for Structure I for temperatures above 0°C. For temperatures below 0°C, xenon hydrate is the reference hydrate. The reference hydrate for Structure II below 0°C is the hydrate formed by bromochlorodifluoromethane, and hydrates of natural gas mixtures are the reference hydrates above 0°C. The pressure and temperature curves for reference hydrates are calculated from the following empirical relationship:

$$\ln P_R = A_R + B_R/T + C_R \ln T \quad (2-21)$$

where A, B, and C are constants fitted to represent the experimental data. Other thermodynamic properties used in the equations above were calculated by Parrish and Prausnitz (170) and are presented in Table I.

Kihara parameters for gases were estimated from second virial coefficient data and the final values for these parameters were found by minimizing the differences between experimental and calculated values of the chemical potential. The gas fugacities were calculated using the Redlich-Kwong equation. Integrals were evaluated numerically with the ten-point Gaussian quadrature formula. The computer program developed by Parrish and Prausnitz (170) can handle mixtures of hydrate-forming and nonhydrate-forming gases. The method is reported to be reliable; so that for a given pressure, the predicted temperature may be too high by at most 2°C and usually much less. This estimate applies to pressures up to 9000 psia.

TABLE I
STRUCTURAL PROPERTIES OF THE HYDRATE LATTICE (170)

	Structure I		Structure II	
Ideal composition (when cavities are fully occupied)	$M_1 \cdot 3M_2 \cdot 32H_2O$		$M_1 \cdot 2M_2 \cdot 17H_2O$	
Number of water molecules per unit cell	46		136	
Typical gases that form this hydrate structure	Methane Ethane Ethylene		Propane i-Butane n-Butane	
Type of Cavity	Small	Large	Small	Large
Number of cavities per unit cell	2	6	16	8
Cavity diameter, A°	7.95	8.60	7.82	9.46
Coordination number (number of water molecules surrounding a single cavity)	20	24	20	28

Interaction Parameter by Ng and Robinson

Ng and Robinson (159) proposed the introduction of a proportionality constant and an interaction constant into the equations used by Parrish and Prausnitz (170). The equation that was used for binary systems is given below:

$$\Delta\mu_w^L = RT [1 + 3(\alpha - 1)Y_1^2 - 2(\alpha - 1)Y_1^3] \quad (2-22)$$

$$[\sum_m v_m \ln(1 + \sum_j C_{mj} f_j) + \ln n_w]$$

where

α = Binary interaction constant ,

Y = Mole fraction in gas phase,

n_w = mole fraction of water,

C_{mj} = Langmuir constant, and

f_j = Fugacity of component j .

This modification showed considerable improvement over a wide range of concentration with only one adjustable interaction constant. The modified calculation method was extended to multicomponent mixture by rewriting the equation as:

$$\Delta\mu_w^L = RT [\prod_j \{1 + 3(\alpha_j - 1)Y_j^2 - 2(\alpha_j - 1)Y_j^3\}] \quad (2-23)$$

$$[\sum_m v_m \ln(1 + \sum_j C_{mj} f_j) + \ln n_w]$$

where α is the interaction constant between the least volatile and each of the other more volatile hydrate forming molecule j , and Y_j is the mole fraction of the component j . Ng and Robinson (159) also modified the program of Parrish and Prausnitz (170) to handle three-phase condensed liquid systems.

Ng and Robinson (159) investigated the role of n-butane in hydrate formation. Parrish and Prausnitz (170) indicated that n-butane does not form either Structure I or II hydrates because the molecule is too large to fit into the cavities. The experimental measurements show that n-butane does enter the hydrate lattice when hydrates are formed in the presence of methane at pressures from 150 to 15,000 psia over a temperature range from 0°F to about 55°F. At higher pressures and temperatures, n-butane ceases to enter the crystal and behaves like a nonhydrate former. N-butane must be considered as a hydrate former when initial hydrate forming conditions are predicted in mixtures where n-butane is a component and where the pressures are below about 15,000 psia.

Further Work by Holder, Corbin
and Papadopoulos

Holder, Corbin and Papadopoulos (85) have suggested that the chemical potential difference between water and the empty hydrate be calculated as

$$\frac{\Delta\mu}{RT_F} = \frac{\Delta\mu_w^0}{RT_0} - \int_{T_0}^{T_F} \frac{\Delta h_w}{RT^2} dT + \int_0^P \frac{\Delta v_w}{RT_F} dP - \ln x_w \quad (2-24)$$

where

μ = Chemical potential,

T = Absolute temperature,

h = Enthalpy,

v = Molar volume,

x = Mole fraction of water, and

P = Pressure

with subscripts

w = Water,

0 = Reference state, and

F = Any temperature

The first term on the right is an experimentally determined chemical potential difference between the unoccupied hydrate and pure water at some reference temperature, usually 0°C, and absolute pressure. The second term gives the temperature dependence of the enthalpy at constant (zero) pressure. The third term corrects the pressure to the final equilibrium pressure. Equation (3-24) has the advantage over the one presented by Parrish and Prausnitz (170) of avoiding simultaneous pressure and temperature corrections and eliminating the need for reference hydrate curves.

The temperature dependence of the enthalpy difference is given by

$$\Delta h_w = \Delta h_w^{\circ} + \int_{T_0}^T \Delta C_{p_w} dT \quad (2-25)$$

where ΔC_{p_w} is the heat capacity difference between the empty hydrate and pure water phases. The dependence of ΔC_{p_w} upon temperature is given by

$$\Delta C_{p_w} = \Delta C_{p_w}^{\circ} + b(T - T_0) \quad (2-26)$$

where

$\Delta C_{p_w}^{\circ}$ and b are constants based on experimental data. Argon, krypton, and methane gases were chosen for determining the reference chemical potential, enthalpies of Structure I hydrate, and estimation of useful Kihara parameters for water which describe the gas-water interactions in the hydrate phase. Argon, krypton, and methane are all relatively small spherical molecules which should fit the requirements of the Van der Waals and Platteeuw (256) model better than large or

asymmetric molecules. The following mixing rules were used for the Kihara parameters for the gases and water:

$$\sigma = (\sigma_{\text{H}_2\text{O}} + \sigma_{\text{gas}})/2$$

$$\epsilon = (\epsilon_{\text{H}_2\text{O}} + \epsilon_{\text{gas}})^{1/2}$$

$$a = a_{\text{gas}}/2$$

Kihara parameters were taken from second virial coefficient data, and values of σ and ϵ were minimized to match the deviation from experimental data.

Holder, Corbin and Papadopoulos (85) concluded that chemical potential, enthalpy, and heat capacity differences estimated for Structure I are only valid if the statistical model is valid. The mixing rules for the Kihara parameters are the weakest point in the model. It is unlikely that the present model will allow satisfactory predictions for large or highly asymmetric hydrate forming molecules, such as propane and isobutane. Modifications will have to be made to the model to account for both size and asymmetry.

Choice of Cell Size and Contribution of Subsequent Water Shells

John and Holder (93) examined the smoothed cell spherical potential model commonly used for describing the gas-water interactions in hydrates with respect to the characterization of the hydrate lattice structure. They compared gas-water potential energies calculated by using a discrete summation of individual interactions to those calculated by using a smoothed cell potential, where the water molecules forming the lattice case are mathematically "smeared" over a sphere of specified radius. The smoothed cell model predicts significantly different potentials than

the discrete summation average. The difference is most pronounced for tetrakaidecahedral cavities of Structure I hydrate in which case the effective coordination number changed from 24 to 21. John and Holder (93) note that the fact that predicted dissociation pressures are generally lower than experimental values, regardless of the gas species forming the hydrate, implies that the error in pressures is due to cavity characterization rather than to gas characterization. The error might be caused by inappropriate radii for the spherical shells. The use of the smoothed cell model leads to smaller Langmuir constants and will, to some degree, compensate for the error.

John and Holder (94) have also calculated the dispersion interactions between a gas molecule and second and third neighbor water molecules using quasi-spherical Kihara potentials. The redefining of the higher order shells makes it possible to separate the effects of cavity asymmetry from gas molecule asymmetry and to eliminate basic model inaccuracies. The effect of higher order shells can change the calculated Langmuir constants for a given set of Kihara parameters by several orders of magnitude. Higher order shells do have an effect on the stability of the hydrate, and these higher order potentials should be taken into account in determination of hydrate equilibria.

Hydrate Formation in Multicomponent

Mixtures

Holder and Hand (86) have expressed the need for a better data base for hydrate formation in the multicomponent mixtures. By studying the ethane-propane and methane-ethane-propane mixtures, they have demonstrated that both Structure I and Structure II hydrates can form

from a single mixture. An algorithm based on the Parrish and Prausnitz (170) approach for predicting hydrate-gas-water equilibria was developed for predicting equilibria in mixtures containing a methane-ethane-propane gas phase and a liquid water phase. The three Kihara parameters for each gas were adjusted for optimal values to give the best agreement with experimental data. These three parameters are the molecular diameter, σ , the potential well depth, ϵ , and the core radius, a . In addition to these individual gas parameters, system properties were also optimized. These properties are the difference in enthalpy between the unoccupied hydrate lattices and ice at 0°C and zero pressure, and the difference in chemical potential at the same conditions. The three spherical-core Kihara parameters were fitted to binary and ternary hydrate data. The following mixing rules were used:

$$\sigma_{\text{mix}} = 1/2(\sigma_{\text{H}_2\text{O}} + \sigma_{\text{gas}})$$

$$\epsilon_{\text{mix}} = (\epsilon_{\text{H}_2\text{O}} \cdot \epsilon_{\text{gas}})^{1/2}$$

$$a_{\text{mix}} = 1/2(a_{\text{H}_2\text{O}} + a_{\text{gas}})$$

Dissociation pressures were found to be insensitive to values of the core radius. Fitting the Kihara parameters, instead of using those obtained from the viscosity or second virial coefficient data, leads to a higher accuracy in the prediction of the dissociation pressure. The general shape of the calculated curves is in agreement with the experimental curves. The mixture containing the most methane produced the largest relative error because this mixture has dissociation pressures nearer to the Structure I - Structure II equilibrium conditions where errors tend to be largest.

For systems containing methane, ethane, and propane, the optimal values of the zero-point thermodynamic properties are in relatively good agreement with those expected from theoretical considerations. The zero-point enthalpic differences between the empty hydrate and ice are different from those used by Parrish and Prausnitz (170). A generalization of the technique of fitting the Kihara parameters to experimental data can be applied to predicting hydrate formation for multicomponent mixtures containing both hydrate formers and non-hydrate formers.

Generalized Model by Holder,

Papadopoulos and John

Holder, Papadopoulos and John (87) have applied the principle of corresponding states to the prediction of hydrate equilibria, resulting in good agreement between the Kihara parameters used for predicting hydrate equilibria and those obtained from virial coefficient and viscosity data. The model suggests a new method for calculating the Langmuir constant, C , in the following equation:

$$C = \frac{4\pi}{kT} \int_0^R (e^{-W(r)/kT}) r^2 dr \quad (2-27)$$

where

$W(r)$ = Smoothed cell radial potential function,

r = Radial distance of the gas molecule from cavity center,

k = Boltzmann's constant, and

T = Absolute temperature.

The smoothed cell radial potential function is modified such that

$$W(r) = W_1(r) + W_2(r) + W_3(r) \quad (2-28)$$

where W_1 , W_2 , and W_3 are the smoothed cell potential contributions of the first, second, and third shell of water molecules. The cell characteristics needed for the calculation of the cell potentials are tabulated by Holder, Papadopoulos, and John (87).

The modification to the smoothed cell potential mentioned above is not sufficient to predict hydrate equilibria except for spherical molecules such as argon, krypton, and methane. In the past, this deficiency has been overcome by adjusting the Kihara size and energy parameters so that good agreement with experimental data was obtained. The major difficulty in the above approach is that the Kihara parameters needed for calculating hydrate equilibria cannot be related to the Kihara parameters found from viscosity and second virial coefficient data. There are several sets of Kihara parameters which can calculate a single Langmuir constant. For gases which fit into two cavities, there exist many pairs of Langmuir constants which will closely predict the experimental dissociation pressures of the binary hydrates. Only one of these pairs can be correct. If the prediction of hydrate formation for only a single gas was required, the arbitrary selection of Kihara parameters would be useful although theoretically unsound. The wrong Kihara parameters, the wrong cell potentials, and the wrong Langmuir constants may lead to the right dissociation pressures. In practical cases hydrates are formed from gas mixtures. The Langmuir constants for each gas are independent of the composition of the gas and would be the same in the mixture as in the pure gas for each species.

The contribution to the chemical potential difference Δu_w is the sum of the contribution from the Structure I and the Structure II cavities;

$$\Delta\mu_w^H = \Delta\mu_I^H + \Delta\mu_{II}^H \quad (2-29)$$

In a pure gas hydrate, if $\Delta\mu_I^H$ is too low and $\Delta\mu_{II}^H$ is too high at a given pressure, their sum may be correct. Consider a gas hydrate formed from a mixture of methane and propane. The propane molecules do not fit into the Structure I cavity, and the Langmuir constant for propane in Structure II is about 600 times as large as that of methane. Therefore, $\Delta\mu_I^H$ will be determined solely from the methane Langmuir constant, and the propane Langmuir constant will determine the contribution of $\Delta\mu_{II}^H$. Errors in the methane and propane Langmuir constants will produce corresponding errors in $\Delta\mu_I^H$ and $\Delta\mu_{II}^H$ which, in most cases, will not be compensating. The dissociation pressure for the mixture can only be correct if the Langmuir constants used for each species are correct.

Theoretically, the Kihara parameters obtained from hydrate data and from virial coefficient and viscosity data should agree. When agreement is obtained between the two sets of Kihara parameters, the calculated Langmuir constants are more likely to accurately describe the contribution to hydrate stability between the large and the small cavities. Since the Langmuir constants are extremely sensitive to the Kihara parameters, it would not be possible to require that the parameters obtained from hydrate data and from virial coefficient and viscosity data be identical. The following mixing rules are used to describe the gas-water interactions in the hydrate cavities:

$$\sigma = (\sigma_g + \sigma_w)/2$$

$$\epsilon = (\epsilon_g \epsilon_w)^{1/2}$$

$$a = (a_g)/2$$

where

σ_g = Kihara distance parameter for gas-gas interactions,

σ_w = Kihara distance parameter for gas-water interactions,

ϵ_g = Kihara energy parameter for gas-gas interactions,

ϵ_w = Kihara energy parameter for gas-water interactions, and

a = Kihara core diameter of the gas molecule.

The mixing rules given above are somewhat arbitrary, and the variation between the parameters obtained from hydrate data and from virial coefficient and viscosity data can be attributed to a small binary interaction parameter type of correction, which is incorporated into the Kihara parameters used for the hydrate data. This approach will work without any further correction for spherical molecules. When non-spherical molecules are included, the model requires a modification for the effects of molecular asphericity.

Holder, Papadopoulos and John (87) have proposed the following perturbation-type model to correct for the fact that the gas-water interactions depart from the spherical smoothed cell potential. The Langmuir constant C is given by

$$C = Q^* C^*$$

where

$$C^* = \frac{4\pi}{kT} \int_0^R \exp\left(-\left[\frac{W_1(r) + W_2(r) + W_3(r)}{kT}\right]\right) r^2 dr \quad (2-30)$$

and Q^* is an empirical function that corrects the Langmuir constant due to the restricted motion of the gas molecule. The value of Q^* is chosen so that the Langmuir constant C is accurate. The Q^* factor accounts for all non-idealities in the molecular interactions between the gas and the hydrate cavity. To be theoretically valid, Q^* should exhibit certain

trends with molecular properties: (1) Q^* should be near one for spherical molecules in nearly spherical cavities, and Q^* should decrease as the molecular asymmetry (and the acentric factor increases). A non-spherical gas will have restricted movement in a spherical cavity and would be less stable than a spherical molecule. The lower stability will lead to a lower value of C . Hence, the acentric factor is a good correlating parameter. (2) Q^* should decrease as the size of the molecule increases. (3) Q^* should be proportional to the ratio of the molecular diameter to the cavity diameter. The quantity $(\sigma/R-a)$ is a measure of the degree of tightness with which a molecule fits into a cavity. (4) Q^* should decrease as the intermolecular attractiveness (as measured by ϵ) increases. An increase in ϵ leads to preference for certain orientations and internal rotation is more restricted as the value Q^* decreases. Thus ϵ/KT is used as a correlating parameter.

The following empirical corresponding states correlation for Q^* is proposed Holder, Papadopoulos and John (87):

$$Q^* = \exp(-a_0 [w(\sigma/R-a) (\epsilon/KT_0)]^n) \quad (2-31)$$

where a_0 and n are empirical parameters which depend on the particular cavity.

Prevention and Removal of Hydrates

Gas hydrates will not form in pipelines that do not contain liquid water. If a pipeline contains liquid water and the minimum line temperature is below the hydrate formation point, then gas hydrates may

form and restrict the flow of gas through the pipeline. The only positive manner to prevent hydrates is to dehydrate the gas to a water dew point temperature below any temperature the gas may encounter in transmission or distribution. Formation of gas hydrates may also be avoided by introducing inhibitors, like methanol and glycols, to lower the hydrate forming temperature. One way to remove hydrates is to reduce the line pressure on both sides of the hydrate plug, thus upsetting hydrate equilibrium and permitting evaporation. Raising the temperature above that of formation of the hydrate may also be useful in removal of hydrates. A brief review of the literature on hydrate prevention and removal is given below.

Hammerschmidt Equation

Hammerschmidt (78) has pointed out that the installation of dehydration plants for prevention of hydrate formation may not always be economically feasible. In cases such as gathering systems, small distribution systems, or distribution systems that operate where climatic or pressure conditions induce hydrate formation only at infrequent and short intervals. Points where hydrate formation is concentrated over a small area such as at regulator stations, meter runs, and aboveground piping. Emergency repairs of main line breaks under adverse water conditions might also be included in this category. The addition of antifreeze compounds is an attractive alternative to dehydration of the gas.

If a foreign substance is dissolved in a pure liquid, it will lower the freezing point of the pure liquid by a definite amount. The law of freezing point depression states that this depression in freezing point is directly proportional to the weight of dissolved substance in

a given amount of solvent. The freezing point depression of an ideal solution can be written as

$$\Delta T \cong \frac{RT_0^2}{\Delta H} \ln (1 + N/S) \quad (2-32)$$

where

T Freezing point depression,

T_0 = Normal freezing point,

H = Enthalpy of fusion per mole of solvent,

N = Moles of solute,

S = Moles of solvent, and

R = Gas constant.

If the solution is dilute, N is much smaller than S and the logarithm can be expanded in terms of N/S :

$$\ln(1 + \frac{N}{S}) = \frac{N}{S} - \frac{1}{2}(\frac{N}{S})^2 + \frac{1}{3}(\frac{N}{S})^3 \quad (2-33)$$

For dilute solutions where N is small, all powers of N/S greater than one can be neglected and

$$\Delta T \cong \frac{RT_0^2}{\Delta H} * \frac{N}{S} \quad (2-34)$$

Also

$$\frac{N}{S} = \frac{WM_1}{100M - MW} \quad (2-35)$$

where M_1 is the molecular weight of the solvent. Therefore

$$\Delta T = \frac{M_1 RT_0^2}{\Delta H} * \frac{W}{100M - MW} \quad (2-36)$$

Hammerschmidt (78) used more than 100 experimental determinations of the freezing point lowering in a gas hydrate system which contained either methanol, ethanol, isopropanol or ammonia in concentrations that ranged

from 5 to 20 weight percent of the antifreeze compound to obtain

$$\frac{M_1 RT_0^2}{\Delta H} = 2335 \quad (2-37)$$

or

$$\Delta T = \frac{2335W}{100M - MW} \quad (2-38)$$

Equation (2-36) is applicable to nonassociating compounds, such as most organic materials and ammonia. Hammerschmidt (78) has recommended the use of methanol in the control of hydrate formation because it has several desirable properties: It is noncorrosive; it does not react chemically with any constituent of the natural gas; it is soluble in all proportions with water; it is readily available and reasonable in cost; and it is 100 percent volatile under pipeline conditions; so that a solid residue cannot be deposited if the fluid in the line is partially or completely vaporized. The vapor pressure of methanol is greater than water, thereby preventing the deposition of additional moisture such as would occur if a lower vapor pressure fluid were present. Hammerschmidt (78) has noted that introducing the methanol as a vapor into the pipeline which contains flowing gas will prove to be more effective and economical than pumping the methanol into the line in liquid form. The reason for this is probably due to better and more uniform contact of the methanol vapor with the hydrate. In some cases addition of methanol liquid may fail to produce any beneficial results, whereas introducing methanol vapor into the same line and under the same conditions may be entirely successful in preventing and removing gas hydrates. In a methanol injection system, the amount of methanol to be injected should be sufficient to provide for the loss of methanol to the vapor phase and the solubility of the methanol in

any liquid hydrocarbon that may be present. The vapor pressure of methanol is high enough that significant quantities will vaporize.

Work of Deaton and Frost

According to Deaton and Frost (45) the only method found to be completely satisfactory in preventing the formation of hydrates in gas transmission lines is to dehydrate the gas entering the line to a water dew point low enough to preclude formation of hydrates at any point in the system. The dehydration techniques include water removal by hygroscopic solutions, solid absorbents, and solid adsorbents. Deaton and Frost (45) have also recognized the inhibiting effect of different organic and inorganic chemicals on hydrate formation. They have tabulated the effect of various inhibitors in reducing the temperature of hydrate formation for any given pressure and the percentage pressure increase required to form hydrates at any selected temperature when various inhibitors are added to water. The data presented by Deaton and Frost (45) shows that ammonia is more than twice as effective an inhibitor as methanol. There is a serious drawback in the use of ammonia. In the presence of water, ammonia reacts with carbon dioxide, which is usually present in small quantities in all natural gases, to form ammonium bicarbonate. Ammonium carbonate is a solid compound which causes greater difficulties than gas hydrates. Although ammonia may be useful in special cases Deaton and Frost (45) note that methanol is the most widely used inhibitor for the prevention of hydrates in gas transmission lines.

Experimental Work by Jacoby and Kobayashi,

Withrow, Williams and Katz

Jacoby (92) extrapolated the data taken by Hammerschmidt (78) for the use of methanol in the prevention of hydrate formation. Experimental data on hydrate decomposition temperature lowering for an aqueous liquid composition of 15 weight percent methanol were obtained for one natural gas mixture. Kobayashi, Withrow, Williams and Katz (113) experimentally determined the hydrate decomposition conditions for methane and propane in contact with solutions of sodium chloride brine and ethanol. The data indicate that for a given pressure, the temperature at which methane hydrates may exist is lowered 4° to 6°F by the presence of 15 percent by weight solution of ethanol. The reaction of methane to form the hydrate $\text{CH}_4 \cdot 7\text{H}_2\text{O}$ was studied by Kobayashi, Withrow, Williams and Katz (113) from the standpoint of chemical equilibrium to predict the effect of sodium chloride dissolved in water on the condition of hydrate formation.

Use of Glycol Injection to Inhibit Hydrate Formation

The formation of gas hydrates may also be inhibited by the injection of liquid glycol. Glycols have low volatility and are easily separated from liquid hydrocarbons and from the water they absorb. Ethylene, diethylene, and triethylene glycols have all been used for glycol injection. The most popular has been ethylene glycol because of its lower cost and somewhat superior characteristics. The glycol in the water must be present at the point where wet gas is cooled below its hydrate forming temperature. The injection must be done to achieve a good

distribution of the glycol throughout the equipment. The depression of the gas hydrate forming point is calculated by the use of the Hammerschmidt (78) equation with a different constant for the glycols as given below:

$$\Delta T = \frac{KW}{100M - MW} \quad (2-39)$$

where $K = 2200$ for ethylene glycol. Nielsen and Bucklin (161) note that the Hammerschmidt equation can be used to design glycol injection systems operating at temperatures as low as -40°F requiring about 0.4 mole fraction of ethylene glycol. The success of the Hammerschmidt equation at these conditions is due to a number of compensating factors. The strong negative deviations exhibited by water in glycol solutions is one of the compensating factors.

Modification of Hammerschmidt Equation by Nielsen and Bucklin

Nielsen and Bucklin (161) have modified the Hammerschmidt equation for concentrated methanol using

$$\ln\left(1 + \frac{N}{S}\right) = -\ln x_w \quad (2-40)$$

and

$$\Delta T = -\frac{2335}{M_1} \ln x_w \quad (2-41)$$

where

x_w = Mole fraction of water.

Although this form of the Hammerschmidt equation is only a better approximation, it has been used for the design of practical methanol hydrate control systems operating as low as -160°F .

Improved Model by Menten,

Parrish and Sloan

Menten, Parrish and Sloan (148) proposed the use of the activity coefficient of water in the basic model developed by Van der Waals and Platteeuw (256). The difference between the chemical potential of the empty hydrate and the chemical potential of liquid water is given as

$$\Delta\mu_w^L(T,P) = RT \sum_m v_m \ln(1 + C_{mf}) + RT \ln\gamma_w x_w \quad (2-42)$$

where γ_w represents the activity coefficient of water in the aqueous liquid phase. The activity coefficient of water is normally taken as 1.0 due to the fact that the water concentration is almost pure when hydrocarbons are the hydrate forming gases. With an inhibitor like methanol or glycol present in the aqueous liquid phase, only the activity coefficient need be changed to reflect the new activity of water. The inhibitor has a low vapor pressure and does not enter the hydrate structure. Data are presented by Menten, Parrish and Sloan (148) for hydrate inhibition with KCl, CaCl₂ and methanol. Calculations based on the data obtained indicate that there is a strong effect of a small deviation in the activity coefficient of water from unity. The method proposed by Menten, Parrish and Sloan (148) is considerably more accurate than the Hammerschmidt equation.

Experimental Work by Erichson,

Leu, Ng and Robinson

Erichson, Leu, Ng and Robinson (58) investigated the influence of methanol on hydrate forming conditions in methane, ethane, propane, and

carbon dioxide, and in two synthetic natural gas mixtures, one of which contained carbon dioxide. The Van der Waals and Platteeuw (256) model and the Parrish and Prausnitz (170) algorithm with the modification proposed by Ng and Robinson (159) were used to predict hydrate forming conditions in the presence of methanol. None of the experimental data on the mixtures was used in developing the prediction method, so the agreement between the experimental and calculated results verifies the ability to predict in the complete absence of any experimental data. The calculated results agree well in the transition region from Structure I to Structure II hydrates at higher pressures. The results were compared with the Hammerschmidt equation. The results compared favorably to the experimental data in the hydrocarbon systems but unfavorably in systems containing carbon dioxide.

CHAPTER III

MODEL DEVELOPMENT

Statistical Thermodynamic Model for Hydrates

Gas hydrates have a regular geometric structure and are non-stoichiometric in nature. Thermodynamically, hydrates are solutions of gases in a meta-stable solid structure formed by water molecules. Van der Waals and Platteeuw (256) derived the basic statistical thermodynamic equations for gas hydrates using a three dimensional Langmuir model for ideally localized absorption of spherical molecules in the cavities of a solid hydrate lattice structure. The model assumes the gas hydrates are a dilute solid solution obeying Raoult's law. Other assumptions in the model are the following:

1. Each cavity contains either one or zero gas molecules. Multiple occupancy of the cavities by gas molecules is not possible. The gas molecules, once engaged cannot leave the cavities.
2. Gas molecules only interact with the nearest water molecule. The interaction of two gas molecules in neighboring cavities can be neglected. The gas water interactions are described by London forces. All polar forces are assumed to be embodied in the hydrogen bonded lattice.
3. The presence of the gas molecules in the hydrate lattice does not affect the contribution to the partition function of the cage

forming water molecules in the metastable hydrate structure.

4. The dimensions of the cavity are larger than the largest dimensions of the gas molecule. The encaged gas molecule has the same freedom to rotate within the cavity as it would in the gas phase. The gas molecules are sufficiently small to prevent distortion of the hydrate lattice during this rotation.

5. The Kihara potential function can accurately describe the gas water interaction in the hydrate structure.

The difference between μ_w^β , the chemical potential of water in the empty hydrate lattice, and μ_w^H , the chemical potential in the filled hydrate lattice, is

$$\Delta\mu_w^H = \mu_w^\beta - \mu_w^H = -RT \sum_m v_m \ln(1 - \sum_j \theta_{mj}) \quad (3-1)$$

where

v_m = Number of cavities of type m per water molecule in the lattice.

The fraction of type m cavities occupied by gas component 1 is

$$\theta_{m1} = C_{m1} f_1 / (1 + \sum_j C_{mj} f_j) \quad (3-2)$$

where

C_{m1} = Langmuir constant, and

f_1 = Fugacity of gas component 1.

The Langmuir constant, C_{m1} , accounts for the gas water interaction in the cavity. Van der Waals and Platteeuw(256) showed that the Langmuir constant is given by:

$$C(T) = 4\pi/kT \int_0^\infty \exp[-w(r)/kT] r^2 dr \quad (3-3)$$

where

k = Boltzmann's constant,

T = Absolute temperature, and

$w(r)$ = Spherically symmetric cell potential

The spherically symmetric cell potential $w(r)$ is a function of the cell radius, the coordination number and the nature of the gas-water interaction. The Kihara potential with a spherical core is used,

$$\Gamma(r) = \infty, \quad r < 2a$$

$$\Gamma(r) = 4\epsilon \left[\left(\frac{\sigma}{r-2a} \right)^{12} - \left(\frac{\sigma}{r-2a} \right)^6 \right], \quad r > 2a \quad (3-4)$$

where

ϵ = Characteristic energy,

a = Core radius, and

$\sigma + 2a$ = Collision diameter.

In the presence of liquid water, Equation (3-1) can be written as

$$\Delta\mu_w^L(T,P) = RT \sum_m v_m \ln(1 + C_m f) + RT \ln x_w \quad (3-5)$$

where

$\Delta\mu_w^L(T,P)$ is the difference in the chemical potential of the water in the empty hydrate lattice and the chemical potential of pure liquid water at T and P , x_w is the mole fraction of water in the aqueous liquid phase.

When ice is present Equation (3-5) becomes

$$\Delta\mu_w^\alpha(T,P) = RT \sum_m v_m \ln(1 + C_m f) \quad (3-6)$$

where $\Delta\mu_w^\alpha(T,P)$ is the chemical potential difference at T and P between the empty hydrate lattice and ice.

The calculation procedure presented by Parrish and Prausnitz (170) is used to calculate $\Delta\mu_w^L(T,P)$ if liquid water is present and $\Delta\mu_w^G(T,P)$ if ice is present.

Activity Coefficient of Water
in Hydrate Model

As suggested by Menten, Parrish and Sloan (148), Equation (3-5) can be rewritten as

$$\Delta\mu_w^L(T,P) = RT \sum_m v_m \ln(1 + C_{mf}) + RT \ln\gamma_w x_w \quad (3-7)$$

where γ_w is the activity coefficient of water in the aqueous liquid phase.

When hydrocarbons are the hydrate forming gases, the water concentration in the aqueous liquid phase is almost pure. The activity coefficient of water is therefore taken as unity. In the presence of a hydrate inhibitor, like methanol or glycols, the activity coefficient of water is no longer close to 1.0, and a small deviation in the activity coefficient of water from unity can have a significant effect on the results of the prediction. The activity coefficient of water in the presence of methanol or glycols must be calculated and introduced into the basic hydrate model.

The use of the activity coefficient in the hydrate model is sufficient to account for the presence of the inhibitor since the inhibitor has a low vapor pressure and does not enter the hydrate structure. The introduction of the activity coefficient of water in the basic hydrate model provides a theoretically sound alternative to the Hammerschmidt (78) equation.

Equation of State for Thermodynamic Properties

The statistical model for hydrate prediction requires certain thermodynamic properties. The gas phase fugacity of the hydrate forming gases has to be calculated. When liquid water is present, the solubility of the hydrate forming gases in the aqueous liquid phase has to be determined. To be able to use Equation (3-7) to predict the effect of hydrate inhibitors like methanol and glycols on hydrate forming conditions, the activity coefficient of water in the presence of methanol and glycols must be accurately calculated at any given temperature and pressure. The solubility of the inhibitor in the gas phase must also be correctly known to be able to determine vaporization losses of the inhibitor. Furthermore, the gas phase fugacities, gas solubility in the aqueous phase, the activity coefficient of water, and the solubility of the inhibitor in the gas phase should be determined by a single procedure that is internally consistent to prevent any functional discontinuities in the properties over a wide range of temperature, pressure and compositions.

The Parameters from Group Contributions (PFGC) equation is an equation of state analogous to an activity coefficient equation. Introduced by Cunningham and Wilson (40), the PFGC equation requires that parameters be calculated only from group contributions. The PFGC equation is presented in Figure 2. Cunningham and Wilson (40) demonstrated the accuracy of the PFGC equation in predicting the vapor pressure and density of saturated hydrocarbons. Infinite dilution activity coefficients for light hydrocarbons in heavier hydrocarbons and activity coefficients for mixtures of light hydrocarbons and alcohols were also well represented by the PFGC equation. Moshfeghian, Shariat and

$$\frac{Pv}{RT} = Z = 1 - \frac{sv}{b} \ln\left(1 - \frac{b}{v}\right) - s + b\left(\frac{c}{b_H}\right) \sum_k^g \psi_k \left(\frac{b - b \sum_n^g \psi_n \tau_{nk}}{v - b + b \sum_n^g \psi_n \tau_{nk}} \right)$$

$$\begin{aligned} \frac{\mu_i}{RT} = & s_i \left(\frac{v}{b} - 1 \right) \ln\left(1 - \frac{b}{v}\right) + 1 - \frac{sb_i}{b} \left[\frac{v}{b} \ln\left(1 - \frac{b}{v}\right) + 1 \right] \\ & + \ln\left(\frac{RT}{v}\right) - \left(\frac{c}{b_H}\right) \left\{ \sum_k^g \left[m_{ik} b_k \ln\left(\frac{v - b + b \sum_n^g \psi_n \tau_{kn}}{v \tau_{kk}}\right) \right] \right. \\ & \left. + b \sum_k^g \left[\psi_k \left(\frac{-b_i + \sum_n^g m_{in} b_n \tau_{kn}}{v - b + b \sum_n^g \psi_n \tau_{kn}} \right) \right] \right\} \end{aligned}$$

$$\frac{\Delta H}{RT} = (Z-1) + \left(\frac{c}{b_H}\right) \frac{b^2}{T} \left\{ \sum_k^g \psi_k \left(\frac{\sum_n^g \psi_n \left(\frac{d\tau_{kn}}{dT}\right)}{v - b + b \sum_n^g \psi_n \tau_{kn}} \right) \right\}$$

$$b = \sum_i^c x_i b_i$$

$$b_i = \sum_k^g m_{ik} b_k$$

$$s = \sum_i^c x_i s_i$$

$$s_i = \sum_k^g m_{ik} s_k$$

$$\tau_{kn} = e^{-E_{kn}/T}$$

$$E_{kn} = K_{kn} [E_k + E_n] / 2.0$$

$$\psi_k = ? \quad \psi_n = ?$$

$$E_k = E_k^{(0)} + E_k^{(1)} \left(\frac{283.2}{T} - 1 \right) + E_k^{(2)} \left[\left(\frac{283.2}{T} \right)^2 - 1 \right]$$

Figure 2. The PFGC Equation of State

Erbar (153) used the PFGC equation to reliably predict the phase behavior of hydrocarbon, acid gas, methanol, and water systems. The PFGC equation can be used as a single consistent source of thermodynamic data for prediction of formation and inhibition of gas hydrates when coupled to the basic hydrate model. The PFGC equation can provide gas phase fugacities, gas solubility in the aqueous phase, the activity coefficient of water, and the solubility of the inhibitor in the gas phase.

An inherent advantage in the use of the PFGC, or any reliable equation of state, is the ease of adaptability to computer use. Once the appropriate partial derivatives have been obtained analytically, a computer program can be developed to iteratively solve for the different properties needed. The vapor pressure, liquid and vapor volumes, and liquid and vapor enthalpy departures can be calculated simultaneously. Additionally, for multicomponent mixtures, the vapor-liquid equilibrium K-ratios can also be calculated.

If reliably predicted vapor-liquid equilibrium K-ratios are available from the PFGC equation of state, any calculation technique, such as the one developed by Erbar (57), can be used to perform vapor-liquid-liquid equilibrium flash calculations. The results of such a flash calculation will yield compositions, volumetric properties, enthalpies, and entropies of each phase. The activity coefficient of water is also calculated. These properties can then be used in the hydrate prediction technique developed by Parrish and Prausnitz (170) for hydrate prediction. The modification of Menten, Parrish and Sloan (148) can be used to calculate the effect of hydrate inhibitors like methanol and glycols on hydrate forming conditions.

Derivation of the PFGC Equation of State

The Parameter for Group Contributions (PFGC) equation of state was proposed by Cunningham and Wilson (40) in 1974. The development of the model and the derivation of the equation is given by Cunningham (39). A summary of his work is presented below.

The Helmholtz free energy, A , and the statistical partition function, Q , are related by

$$A = -kT \ln Q \quad (3-8)$$

where

k = Boltzmann's constant, and

T = Absolute temperature.

The appropriate differentiation of the Helmholtz free energy gives the desired thermodynamic properties. The equation of state can be found by differentiating the Helmholtz free energy with respect to volume at constant temperature and composition.

$$P = - \left(\frac{\partial A}{\partial V} \right)_{T,n} \quad (3-9)$$

where

P = Total pressure,

V = Total volume, and

n = number of moles

Instead of theoretically deriving a partition function, Wilson (267) proposed that the Helmholtz free energy and the partition function were so closely related that an empirical form can be chosen to describe the free energy function. It was assumed that empirically derived equations which have successfully described the form of the excess Gibbs free energy could be used to model the Helmholtz free energy. The void

spaces between the molecules are identified as an additional component of the mixture designated as "holes." The volume fraction of each component is calculated. An arbitrary parameter is introduced for the volume of one mole of holes. The volume fractions are converted into mole fractions and substituted into any analytical equation for the Helmholtz free energy. The equations used as a basis for deriving the PFGC equation of state have been modified to handle molecules as solutions of one or more groups.

A modified Flory-Huggins equation accounts for entropy effects due to differences in molecule size. A modified Wilson equation is assumed to represent the activity coefficients of the individual groups in a mixture. It is assumed that molecular activity coefficients corrected for effects due to differences in molecular size can be calculated as the sum of group activity coefficients. The group activity coefficients are determined by the group composition rather than the molecular composition.

The Helmholtz free energy, A^{PFGC} , has two parts:

$$\frac{A^{\text{PFGC}}}{RT} = \frac{A^{\text{F.H.}}}{RT} + \frac{A^{\text{G}}}{RT} \quad (3-10)$$

where

$A^{\text{F.H.}}$ = Contribution from the Flory-Huggins entropy, and

A^{G} = Group contribution represented by a modified Wilson equation.

The Flory-Huggins Contribution

The Flory Huggins contribution to the Helmholtz free energy is given as

$$\frac{A^{\text{F.H.}}}{RT} = \sum_I n_I^* \ln \phi_I^* \quad (3-11)$$

where

ϕ_I^* = Volume fraction of component I, including holes, and

n_I^* = Number of moles of component I, including holes.

Equation (3-11) can be separated to account for the holes;

$$\frac{A^{F.H.}}{RT} = n_H \ln \phi_H + \sum_I n_I \ln \phi_I \quad (3-12)$$

where

n_H Is the total number of holes.

The total number of holes, n_H is equal to

$$n_H = \frac{V - \sum_j n_j b_j}{b_H} \quad (3-13)$$

where

j = Refers to each molecular component present, and

V = Total volume,

b_j = Volume of one mole of molecules j , and

b_H = Volume of one mole of holes.

The volume fraction of holes ϕ_H is given as

$$\phi_H = \frac{V - \sum_j n_j b_j}{V} \quad (3-14)$$

The volume fraction of the other components is given as

$$\phi_I = \frac{n_I b_I}{V} \quad (3-15)$$

Using the above relationships, equation (3-12) can be written as

$$\frac{A^{F.H.}}{RT} = \frac{V - \sum_j n_j b_j}{b_H} \ln \left(\frac{V - \sum_j n_j b_j}{V} \right) + \sum_I n_I \ln \left(\frac{n_I b_I}{V} \right) \quad (3-16)$$

letting

$$n = \sum_j n_j \quad (3-17)$$

and

$$b = \sum_j x_j b_j \quad \text{where } b_j = \sum_i n_{I_i} b_i \quad (3-18)$$

The free energy can be represented as

$$\frac{A^{\text{F.H.}}}{RT} = \frac{V - nb}{b_H} \ln \left(1 - \frac{nb}{V} \right) + \sum_I n_I \ln \left(\frac{n_I b_I}{V} \right) \quad (3-19)$$

The effect of b_H in equation(3-19) is much too strong for molecules consisting of more than one group. A new parameter, s , which is proportional to the external degrees of freedom per lattice site is introduced into equation (3-19). The equation (3-19) is adjusted to replace b_H with, s .

The final form of the Flory-Huggins contribution to the free energy is

$$\frac{A^{\text{F.H.}}}{RT} = ns \left(\frac{V}{nb} - 1 \right) \ln \left(1 - \frac{nb}{V} \right) + \sum_I n_I \ln \frac{n_I b_I}{V} \quad (3-20)$$

Equation (3-20) can be differentiated to give

$$\begin{aligned} \frac{P^{\text{F.H.}}}{RT} &= - \left(\frac{\partial}{\partial V} \frac{A^{\text{F.H.}}}{RT} \right)_{T,n} = \frac{ns}{nb} \ln \left(1 - \frac{nb}{V} \right) \\ &+ \frac{ns}{nb} (V - nb) \left[\frac{V + V - nb}{V(V - nb)} \right] + \sum_I \frac{n_I}{V} \end{aligned}$$

or, in the compressibility factor form

$$Z = \frac{P^{\text{F.H.}} V}{nRT} = 1 - s \left[\frac{V}{nb} \left(\ln \left(1 - \frac{nb}{V} \right) + 1 \right) \right] \quad (3-21)$$

Group Contribution from a Modified Wilson Equation

The second contribution to the PFGC Helmholtz free energy equation is a modified Wilson equation. The original Wilson equation is a two-parameter activity coefficient equation for the excess Gibb's free energy;

$$\frac{g^E}{RT} = - \sum_I x_I \ln \left(\sum_j x_I + x_J \Lambda_{IJ} \right) \quad (3-22)$$

where

x_I, x_J = Mole fractions, and

Λ_{IJ} = Molecular interaction parameters.

The modified equation for the Helmholtz free energy is

$$\frac{A^G}{RT} = - c \left(\sum_j n_j^* N_j \right) \sum_i \psi_i \ln \left(\frac{\sum_j \psi_j^* \lambda_{ij}}{\lambda_{ij}} \right) \quad (3-23)$$

The modifications include the addition of the parameter c , a universal constant related to the lattice coordination number and replacing the mole fractions with group fractions ψ_i^* where

$$\psi_i^* = \frac{\sum_j n_j^* m_{ji} v_i}{\sum_j n_j^* N_j} \quad (3-24)$$

with

n_j^* = Total number of molecules,

m_{ji} = Number of groups i per molecule j ,

v_i = Number of lattice sites per group i ,

N_j = Total number of lattice sites per molecule j .

The quantity N_j is also defined as

$$N_j = \sum_i n_{ji} v_i \quad (3-25)$$

The molecule interaction energy terms Λ_{ij} in the Wilson equation are replaced by group interaction terms λ_{ij} and

$$\lambda_{ij} = \lambda_{ji} = \exp^{-E_{ij}/kT} \quad (3-26)$$

where

E_{ij} = Interaction energy between groups i and j ,

T = Absolute temperature, and

K = Boltzmann constant.

A term for the vacant sites or holes must be added to the free energy equation. The group fraction for holes is defined as

$$\psi_H = 1 - \frac{nb}{V} \quad (3-27)$$

An additional term for holes results in

$$\begin{aligned} \frac{A^G}{RT} = & -c \left(\sum_j n_j^* N_j \right) \left[\psi_H \ln \left(\frac{\psi_H \lambda_{HH} + \sum_j \psi_j^* \lambda_{jH}}{\lambda_{HH}} \right) \right. \\ & \left. + \sum_i \psi_i^* \ln \left(\frac{\psi_H \lambda_{iH} + \sum_j \psi_j^* \lambda_{ij}}{\lambda_{ij}} \right) \right] \end{aligned} \quad (3-28)$$

Since the total volume divided by the volume of a lattice site is equal to the total number of sites,

$$\frac{V}{bH} = \sum_j n_j^* N_j \quad (3-29)$$

Assuming that a hole has an ideal interaction with either group and no interaction with other vacant lattice sites, the fundamental equation for the group contribution term is derived as

$$\frac{A^G}{RT} = -\frac{c}{b_H} bn \sum_i \psi_i \ln \left(\frac{V - nb + nb \sum_j \psi_j^* \lambda_{ij}}{V \lambda_{ii}} \right) \quad (3-30)$$

Equation (3-30) can be differentiated to give the pressures from group contribution

$$\frac{P^G}{RT} = \left(\frac{A}{RT} \right)_{T,n} = \frac{nc}{b_H} \sum_i \psi_i \frac{nb - nb \sum_j \psi_j \lambda_{ij}}{V - V - nb + nb \sum_j \psi_j \lambda_{ij}} \quad (3-31)$$

and in compressibility form

$$Z = \frac{cb}{b_H} \sum_i \left(\frac{nb - nb \sum_j \psi_j \lambda_{ij}}{V - nb + nb \sum_j \psi_j \lambda_{ij}} \right) \quad (3-32)$$

Final Form of the PFGC Equation of State

The Flory-Huggins and the Wilson contribution can be summed to give the final expression for the Helmholtz free energy:

$$\begin{aligned} \frac{A_{PFGC}}{RT} = & \sum_I n_I \ln \frac{n_I b_I}{V} + (V - nb) \frac{s}{b} \ln \left(\frac{V - nb}{V} \right) \\ & - \frac{ncb}{b_H} \sum_i \psi_i \ln \left(\frac{V - nb + nb \sum_j \psi_j \lambda_{ij}}{V \lambda_{ii}} \right) \end{aligned} \quad (3-33)$$

The PFGC equation of state derived from equation (3-33) is

$$\begin{aligned} Z = \frac{PV}{nRT} = & 1 - \frac{sV}{nb} \ln \left(\frac{V - nb}{V} \right) - s \\ & + b \left(\frac{c}{b_H} \right) \sum_i \psi_i \left(\frac{nb - nb \sum_j \psi_j \lambda_{ij}}{V - nb + nb \sum_j \psi_j \lambda_{ij}} \right) \end{aligned} \quad (3-34)$$

The primary variables in equation (3-34) are

c/b_H = A universal constant,

λ_{ij} = Interaction energy parameter between groups,

b_k = Volume of one mole of groups of type k , and

s_i = A parameter proportional to external degrees of freedom per lattice site.

Only three types of parameters corresponding to size, energy and degrees of freedom are required. These can be considered analogous to critical volume, critical temperature and the acentric factor, except that these parameters need to be known only for groups instead of molecules.

An interaction coefficient between groups has been defined for calculating E_{ij} from E_{ii} and E_{jj} as follows:

$$E_{ij} = a_{ij} \left(\frac{E_{ii} + E_{jj}}{2} \right) \quad (3-35)$$

where a_{ij} is the binary group interaction coefficient. For positive deviations from ideality, a_{ij} is less than unity. If a_{ij} is greater than unity, deviations are in the negative direction.

The group interaction energy E_{ii} is slightly temperature dependent. The following form is used:

$$E_{ii} = E_{ii}^{(0)} + E_{ii}^{(1)} \left[\frac{283.2}{T} - 1 \right] + E_{ii}^{(2)} \left[\left(\frac{283.2}{T} \right)^2 - 1 \right] \quad (3-36)$$

To predict the phase behavior of water hydrocarbon systems, Moshfeghian, Shariat and Erbar (153) defined different group interaction coefficients for the various phases present. One interaction coefficient per binary pair was defined for both the vapor phase and hydrocarbon-rich liquid. Another binary interaction coefficient was defined for the water-rich liquid phase. The water phase binary interaction coefficient usually had to be linearly temperature dependent to yield good hydrocarbon solubilities in the water-rich phase.

Development of Fugacity Equation

The thermodynamic expression for the fugacity of component k in a multicomponent mixture is given by

$$RT \ln \frac{f_k}{y_k^P} = \int_V^{\infty} \left[\left(\frac{P}{n_k} \right)_{T,V,n_j} - \frac{RT}{V} \right] dV - RT \ln z \quad (3-37)$$

The PFGC equation of state is given as

$$z = 1 - s \left[\frac{V}{nb} \ln \left(1 - \frac{nb}{V} \right) + 1 \right] + \left(\frac{c}{b_H} \right) (b) \sum_i^{NG} \psi_i \left[\frac{nb - nb \sum_j^{NG} \psi_j \lambda_{ij}}{V - nb + nb \sum_j^{NG} \psi_j \lambda_{ij}} \right] \quad (3-38)$$

Substituting $z = \frac{PV}{nRT}$ yields

$$\frac{PV}{nRT} = 1 - s \left[\frac{V}{nb} \ln \left(1 - \frac{nb}{V} \right) + 1 \right] + \left(\frac{c}{b_H} \right) (b) \sum_i^{NG} \psi_i \left[\frac{nb - nb \sum_j^{NG} \psi_j \lambda_{ij}}{V - nb + nb \sum_j^{NG} \psi_j \lambda_{ij}} \right] \quad (3-39)$$

Solving equation (3-39) explicitly for pressure yields

$$P = \frac{nRT}{V} - RT \left(\frac{ns}{nb} \right) \ln \left(1 - \frac{nb}{V} \right) - \frac{RT}{V} ns + \frac{RT}{V} \left(\frac{c}{b_H} \right) \sum_i^{NG} nb \psi_i \left[\frac{nb - nb \sum_j^{NG} \psi_j \lambda_{ij}}{V - nb + nb \sum_j^{NG} \psi_j \lambda_{ij}} \right] \quad (3-40)$$

Substituting $nb\psi_i = b_H \sum_I n_I m_{Ii} v_i$ gives (3-41)

$$P = \frac{nRT}{V} - RT \left(\frac{ns}{nb} \right) \ln \left(1 - \frac{nb}{V} \right) - \frac{RT}{V} ns + \frac{RT}{V} c \sum_i \left[\sum_I n_I m_{Ij} \psi_i \left(\frac{nb - b_H \sum_j \sum_I n_I m_{Ij} v_j \lambda_{ij}}{V - nb + b_H \sum_j \sum_I n_I m_{Ij} v_j \lambda_{ij}} \right) \right] \quad (3-42)$$

To partially differentiate equation (3-41) with respect to n_k the following identities can be used

$$ns = \sum_i^{NG} n_i s_i \quad \text{and} \quad \frac{\partial (ns)}{\partial n_k} = \sum_i^{NG} \frac{\partial n_i}{\partial n_k} s_i = s_k \quad (3-43)$$

Also,

$$nb = \sum_i^{NG} n_i b_i \quad \text{and} \quad \frac{\partial (nb)}{\partial n_k} = \sum_i^{NG} \frac{\partial n_i}{\partial n_k} b_i = b_k \quad (3-44)$$

and

$$\frac{\partial n}{\partial n_k} = \sum_i^{NG} \frac{\partial n_i}{\partial n_k} = 1 \quad (3-45)$$

Using the identities given above the following equation can be derived:

$$\begin{aligned} \left(\frac{\partial P}{\partial n_k} \right)_{T,V,n_j} &= \frac{\partial}{\partial n_k} \sum \frac{RT}{V} n_i - \frac{\partial}{\partial n_k} \left[RT \left(\frac{ns}{nb} \right) \ln \left(1 - \frac{nb}{V} \right) \right] \\ &\quad - \frac{\partial}{\partial n_k} \left[\frac{RT}{V} ns \right] \\ &\quad + \frac{\partial}{\partial n_k} \left[\frac{RT}{V} c \sum_i \left[\sum_I n_I m_{Ii} \psi_i \left(\frac{nb - b_H \sum_j \sum_I n_I m_{Ij} v_j \lambda_{ij}}{V - nb + b_H \sum_j \sum_I n_I m_{Ij} v_j \lambda_{ij}} \right) \right] \right] \end{aligned} \quad (3-46)$$

Thus

$$\begin{aligned}
& \left(\frac{\partial P}{\partial n_k} \right)_{T, V, n_j} \\
&= \frac{RT}{V} - RT \left\{ \ln \left(1 - \frac{nb}{V} \right) \frac{s_k}{nb} - \frac{ns}{nb} \frac{1}{\left(1 - \frac{nb}{V} \right)} \left(\frac{b_k}{V} \right) \right. \\
&\quad \left. - \frac{ns}{(nb)^2} \ln \left(1 - \frac{nb}{V} \right) \cdot b_k \right\} - s_k \frac{RT}{V} \\
&\quad + \frac{cRT}{V} \sum_i \left[m_{ki} v_i \left(\frac{nb - b_H \sum_j \sum_I n_{Ij}^m v_j \lambda_{ij}}{V - nb + b_H \sum_j \sum_I n_{Ij}^m v_j \lambda_{ij}} \right) \right] \\
&\quad + \left[\sum_I n_{Ii}^m v_i \cdot \left(\frac{(b_k - b_H \sum_j m_{kj} v_j \lambda_{ij}) (V - nb + b_H \sum_j \sum_I n_{Ij}^m v_j \lambda_{ij})}{(V - nb + b_H \sum_j \sum_I n_{Ij}^m v_j \lambda_{ij})^2} \right) \right. \\
&\quad \left. + \frac{(nb - b_H \sum_j \sum_I n_{Ij}^m v_j \lambda_{ij}) (+ b_k - b_H \sum_j m_{kj} v_j \lambda_{ij})}{(V - nb + b_H \sum_j \sum_I n_{Ij}^m v_j \lambda_{ij})^2} \right] \quad (3-47)
\end{aligned}$$

and

$$\begin{aligned}
& \left(\frac{\partial P}{\partial n_k} \right)_{T, V, n_j} \\
&= \frac{RT}{V} - RT \left\{ \ln \left(1 - \frac{nb}{V} \right) \frac{s_k}{nb} - \frac{ns}{nb} \frac{1}{\left(1 - \frac{nb}{V} \right)} \left(\frac{b_k}{V} \right) \right. \\
&\quad \left. - \frac{ns}{(nb)^2} \ln \left(1 - \frac{nb}{V} \right) \cdot b_k \right\} - s_k \frac{RT}{V} \\
&\quad + \frac{cRT}{V} \sum_i \left[m_{ki} v_i \left(\frac{nb - b_H \sum_j \sum_I n_{Ij}^m v_j \lambda_{ij}}{V - nb + b_H \sum_j \sum_I n_{Ij}^m v_j \lambda_{ij}} \right) \right] \\
&\quad + \sum_i \left[n_{Ii}^m v_i \frac{(b_k - b_H \sum_j m_{kj} v_j \lambda_{ij}) V}{(V - nb + b_H \sum_j \sum_I n_{Ij}^m v_j \lambda_{ij})^2} \right] \quad (3-48)
\end{aligned}$$

Replacing $v_i = \frac{b_i}{b_H}$ and using Equation (3-41), the above expression simplifies to

$$\begin{aligned}
 & \left(\frac{\partial P}{\partial n_k} \right)_{T, V, n_j} \\
 &= \frac{RT}{V} - RT \frac{s_k}{nb} \ln\left(1 - \frac{nb}{V}\right) + RT \frac{ns}{nb} \frac{b_k}{(V - nb)} \\
 &+ RT \frac{ns}{(nb)^2} b_k \ln\left(1 - \frac{nb}{V}\right) - RT \frac{s_k}{V} \\
 &+ RT \frac{c}{b_H} \left\{ \sum_i \left[m_{ki} b_i \frac{nb - nb \sum_j \psi_j \lambda_{ij}}{V(V - nb + nb \sum_j \psi_j \lambda_{ij})} \right] \right. \\
 &\left. + nb \sum_i \left[\psi_i \frac{(b_k - \sum_j m_{kj} b_j \lambda_{ij})}{(V - nb + nb \sum_j \psi_j \lambda_{ij})^2} \right] \right\} \quad (3-49)
 \end{aligned}$$

Equation (3-49) can be substituted in Equation (3-37) to yield the following expression

$$\begin{aligned}
 RT \ln \frac{f_k}{Y_k^P} &= \int_V^{\infty} \left[\frac{RT}{V} - RT \frac{s_k}{nb} \ln\left(1 - \frac{nb}{V}\right) + RT \frac{ns}{nb} \frac{b_k}{(V - nb)} \right. \\
 &+ RT \frac{ns}{(nb)^2} b_k \ln\left(1 - \frac{nb}{V}\right) - RT \frac{s_k}{V} \\
 &+ RT \frac{c}{b_H} \left\{ \sum_i \left[m_{ki} b_i \frac{nb - nb \sum_j \psi_j \lambda_{ij}}{V(V - nb + nb \sum_j \psi_j \lambda_{ij})} \right] \right. \\
 &\left. + nb \sum_i \left[\psi_i \frac{b_k - \sum_j m_{kj} b_j \lambda_{ij}}{(V - nb + nb \sum_j \psi_j \lambda_{ij})^2} \right] \right\}
 \end{aligned}$$

$$- \frac{RT}{V} \Big] dV - RT \ln Z \quad (3-50)$$

Integrating (3-50) yields

$$\begin{aligned} \ln \frac{f_k}{y_k^P} = & \left\{ - \frac{S_k}{nb} [(V - nb) \ln(V - nb) - V] - [V \ln V - V] \Big|_V^\infty \right\} \\ & + \left\{ \frac{ns}{nb} b_k \ln(V - nb) \Big|_V^\infty \right\} \\ & + \left\{ \frac{ns}{(nb)^2} b_k [(V - nb) \ln(V - nb) - V] - [V \ln V - V] \Big|_V^\infty \right\} \\ & + \frac{c}{b_H} \left[\left\{ \sum_i \left[m_{ki} b_i \ln \left(\frac{V - nb + nb \sum_j \psi_j \lambda_{ij}}{V} \right) \right] \Big|_V^\infty \right\} \right. \\ & \left. + \left\{ nb \sum \left[\psi_i \frac{(-b_k + \sum_j m_{kj} b_j \lambda_{ij})}{(V - nb + nb \sum_j \psi_i \lambda_{ij})^2} \right] \Big|_V^\infty \right\} \right] - \ln Z \quad (3-51) \end{aligned}$$

Equation (3-51) can be rearranged to

$$\begin{aligned} \ln \frac{f_k}{y_k^P} = & \left\{ \ln(V - nb) \left[\frac{S_k}{nb} (V - nb) + \frac{ns}{nb} b_k + \frac{ns}{(nb)^2} b_k (V - nb) \right] \right. \\ & + \ln V \left[\frac{S_k}{nb} V - \frac{ns}{(nb)^2} b_k V - S_k \right] \Big|_V^\infty \left. \right\} \\ & + \frac{c}{b_H} \left[\left\{ \sum_i \left[m_{ki} b_i \ln \left(\frac{V - nb + nb \sum_j \psi_j \lambda_{ij}}{V} \right) \right] \Big|_V^\infty \right\} \right. \\ & \left. + \left\{ nb \sum \left[\psi_i \frac{(-b_k + \sum_j m_{kj} b_j \lambda_{ij})}{(V - nb + nb \sum_j \psi_i \lambda_{ij})^2} \right] \Big|_V^\infty \right\} \right] - \ln Z \quad (3-52) \end{aligned}$$

Equation (3-52) simplifies to

$$\ln \frac{f_k}{y_k P} = \left\{ \left[s_k - \frac{s_k}{nb} v + \frac{ns}{(nb)^2} b_k v \right] \ln \frac{V-nb}{V} \right\} \\ + \frac{c}{b_H} \left\{ \left[\sum_i \left[m_{ki} b_i \ln \left(\frac{V - nb + nb \sum_j \psi_j \lambda_{ij}}{V} \right) \right] \right] \right\} \\ + \left\{ nb \sum_i \left[\psi_i \frac{(-b_k + \sum_j m_{kj} b_j \lambda_{ij})}{(V-nb+nb \sum_j \psi_i \lambda_{ij})^2} \right] \right\} - \ln Z \quad (3-53)$$

The limit of Equation (3-53) as $V \rightarrow \infty$ is zero. The final expression for the fugacity of component k in a mixture using the PFGC equation of state is given by

$$\ln \frac{f_k}{y_k P} = \left[\frac{s_k}{nb} v - \frac{ns}{(nb)^2} b_k v - s_k \right] \ln \left(1 - \frac{nb}{V} \right) \\ - \frac{c}{b_H} \left\{ \sum_i \left[m_{ki} b_i \ln \left(\frac{V-nb+nb \sum_j \psi_j \lambda_{ij}}{V} \right) \right] \right\} \\ + nb \sum_i \left[\psi_i \frac{(-b_k + \sum_j m_{kj} b_j \lambda_{ij})}{(V-nb+nb \sum_j \psi_i \lambda_{ij})} \right] \right\} - \ln Z \quad (3-54)$$

Development of Calculation Procedure

The PFGC equation of state is solved by a third order iteration process using the Richmond convergence method as given by Lapidus (123),

$$x_{i+1} = x_i - \frac{2f(x_i) \cdot f'(x_i)}{2[f'(x_i)]^2 - f(x_i) \cdot f''(x_i)} \quad (3-55)$$

The PFGC equation of state can be rearranged as

$$\frac{PV}{nRT} - 1 + \frac{sV}{nb} \ln\left(1 - \frac{nb}{V}\right) + s - \left(\frac{c}{b_H}\right) (b) \sum_i^{NG} \psi_i \left[\frac{nb - nb \sum_j \psi_j \lambda_{ij}}{V - nb + nb \sum_j \psi_j \lambda_{ij}} \right] = 0 \quad (3-56)$$

Replacing $\frac{nb}{V} = x$ gives

$$\frac{Pb}{xRT} - 1 + \frac{s}{x} \ln(1 - x) + s - \left(\frac{c}{b_H}\right) (b) \sum_i^{NG} \psi_i \left[\frac{x - x \sum_j \psi_j \lambda_{ij}}{1 - x + x \sum_j \psi_j \lambda_{ij}} \right] = 0 \quad (3-57)$$

Multiplying Equation (3-57) throughout by x and rearranging:

$$f(x) = (1-s)x - \frac{Pb}{RT} - s \ln(1-x) + \left(\frac{c}{b_H}\right) (b) \sum_i^{NG} \psi_i \left[\frac{x - x \sum_j \psi_j \lambda_{ij}}{1 - x + x \sum_j \psi_j \lambda_{ij}} \right] = 0 \quad (3-58)$$

The first derivative of Equation (3-58) is given as

$$f'(x) = 1 + s \left(\frac{x}{1-x}\right) + \left(\frac{c}{b_H}\right) b \sum_i^{NG} \psi_i \left[\frac{1}{(1-x+x \sum_j \psi_j \lambda_{ij})^2} - 1 \right] \quad (3-59)$$

The second derivative of Equation (3-59) is

$$f''(x) = \frac{s}{(1-x)^2} - \frac{2 \left(\frac{c}{b_H}\right) (b) \left[\sum_j^{NG} \psi_j \lambda_{ij} - 1 \right]}{(1-x+x \sum_j \psi_j \lambda_{ij})^3} \quad (3-60)$$

Equations (3-58) through (3-60) can be used in equation (3-55) to solve for x .

Computer Program for Developing Parameters
in PFGC Equation

The PFGC equation in its final form has five adjustable parameters s , b , E^0 , E^1 , and E^2 for each group where s corresponds to the degrees of freedom, b is the size parameter and E^0 , E^1 , and E^2 form the energy parameter. Additionally, one interaction coefficient per binary pair was defined for the vapor and hydrocarbon-liquid phases, and another binary interaction coefficient was defined for the water-rich liquid phase. In order to obtain values for s , b , E^0 , E^1 , and E^2 which lead to reliable prediction of thermodynamic properties, several steps were followed.

First groups were selected to represent the components of interest. Components that were identified by a single group were selected to obtain the pure group parameters for that group. An initial estimate was made for the values of the five group parameters. The PFGC equation was evaluated over the entire range of vapor pressure, volumetric and enthalpy departure data. The set of parameters that yield the lowest absolute average error in vapor pressure predictions were selected. Care was exercised to maintain reasonable quality of prediction for the volumetric and enthalpy departure properties.

Mixtures of different components were evaluated to obtain binary group interaction coefficients. The binary group interaction coefficients that yielded minimum absolute average error in equilibrium K-ratios for each component in the mixture were selected.

To aid in the evaluation and fitting of data to obtain reliable group parameters the MPMCGC program developed by Erbar (54) was used.

MPMCGC is a very elaborate multiproperty, multicomponent fit program written for the PFGC equation of state. A simplified flowsheet for the MPMCGC program appears in Figure 3. The program can be divided into four functional parts: input, property evaluation, fitting and output

The input section of the program reads in the data, checks it for reasonableness and, if necessary, modifies the data in selected spots to reduce the chances of program failure in later phases of the calculation. Selected diagnostic comments are made during the data checking phase of the program.

After successful completion of the input data checking phase, the program proceeds to evaluate the data using the group parameters supplied as part of input data. This evaluation is done by calculating vapor pressures, volumetric properties, and enthalpy departures at the given temperatures and pressures. The calculated results are then compared with the experimental data supplied as input data to the program. If the user has requested an evaluation only, the program skips to the output section. Otherwise, the program proceeds to the non linear fitting section of the program. In this section the designated calculations are carried out on each data point in the total data set. The group parameters for each group are varied to minimize the sum of relative errors in each of the properties specified in the total data set. The objective function in the nonlinear fitting program is optimized using Chandler's (26) modified version of Marquardt's nonlinear fitting algorithm. The absolute percent error in each point is used as a basis for comparison.

The nonlinear fitting program operations terminate when an iteration limit or a successful solution is reached. The output section

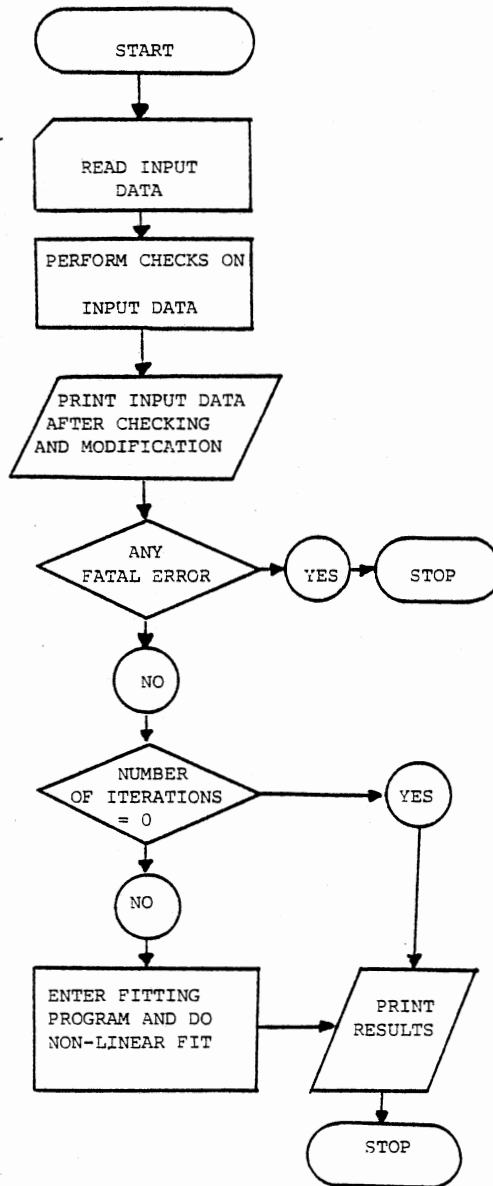


Figure 3. Simplified Logic Flow Diagram of the Fitting Program

of the program prints the final values of the fitted parameters and a detailed comparison for each individual data point. A summary of the final percentage errors for each type of data is also printed.

A detailed description of the MPMCGC program and its features is given by Erbar (54).

Summary of This Work

The following steps summarize the procedure to develop a reliable method for the prediction of the inhibition of gas hydrates using the PFGC equation of state.

1. Develop a computer program capable of solving the PFGC equation of state based on the Richmond convergence scheme using equation (3-55).
2. Use equation (3-54) to calculate the fugacity of individual components in a mixture.
3. Select the components for which thermodynamic properties are required. Using the new convergence scheme and the fugacity expression, derive parameters for pure components for the PFGC equation. Use vapor pressure, volumetric and enthalpy departure data from standard literature sources. Parameters are required for paraffins, olefins, cycloparaffins, aromatics, nitrogen, carbon dioxide, hydrogen sulfide, sulfur dioxide, methanol, glycols and water.
4. Using available literature data, check vapor-liquid equilibrium predictions for light hydrocarbon systems with carbon dioxide, nitrogen, hydrogen sulfide, methanol, glycols and water. Revise the binary group interaction coefficients used in the PFGC equation as required.

5. Calculate and use the activity coefficient of water as the ratio of its actual fugacity in a mixture to the pure component fugacity at the temperature and pressure of the mixture. Use equation (3-7) to predict hydrate formation conditions.

6. Develop and correlate hydrate predictions for the Parrish and Prausnitz (170) model for hydrate formation modified by equation (3-7). Derive new Kihara parameters for use in the hydrate model. Use the PFGC equation to predict gas phase fugacities, aqueous liquid phase gas solubilities, and the activity coefficient of water required by the hydrate model.

7. Develop, check, and compare vapor-hydrocarbon liquid-aqueous liquid mutual solubilities for hydrocarbon, methanol, glycol and water systems. Derive the temperature dependent binary group interaction coefficients based on literature data.

8. Complete and check correlation of hydrate prediction and effect of methanol and glycols as hydrate inhibitors. Compare inhibitor vaporization losses and inhibitor effectiveness quantitatively with literature data and qualitatively if no data are available.

CHAPTER IV

RESULTS

A brief summary of the results from the development of the PFGC equation of state for use in the prediction of inhibition of gas hydrates is given below.

Fugacity Expression and New Calculation Procedure

A computer program was developed to calculate the fugacity from the PFGC equation of state using equation (3-54). An iterative solution technique based on the Richmond convergence scheme was used to solve the PFGC equation of state. The results from the fugacity expression were found to be consistent with the results from the chemical potential expression derived by Cunningham and Wilson (40) and used by Moshfeghian, Shariat, and Erbar (153). The calculation procedure was exhaustively tested for accuracy. The Richmond convergence scheme provided improved speed and reliability in comparison with the direct substitution method previously used by Moshfeghian, Shariat, and Erbar (153).

Pure Component Thermodynamic Property Prediction

The GPA*SIM (70) program provides a list of components most

frequently used in the light hydrocarbon industry. The same component list was used for the selection of the paraffins, olefins, cycloparaffins, aromatics and inorganic substances. Methanol, ethylene glycol, diethylene glycol, and triethylene glycol were added to the pure component list.

Using available vapor pressure, volumetric, and enthalpy departure data from standard literature sources, pure component group parameters for use in the PFGC equation of state were derived. The primary target for the curve fitting process was to minimize the absolute percent error in vapor pressure prediction for each component. The comparison of the experimental and calculated vapor pressures for selected compounds is qualitatively shown in Figures 4 and 5. An evaluation of the prediction was made for volumetric properties and enthalpy departures of the liquid and vapor phases using available literature sources. Tables II through VI show the deviations in vapor pressure, enthalpy, and volume predictions for paraffins, olefins, aromatics, cycloparaffins, and some non-hydrocarbons. The temperature and pressure range evaluated, number of points, and percent absolute average error in vapor pressure are given in the tables. Deviations in the liquid and vapor volume and enthalpy departures are also presented. The deviations in pure component vapor pressures and liquid and vapor volumetric properties are expressed as absolute average errors based on the experimental value. The deviation in pure component liquid and vapor enthalpy departures is reported on a BTU/lb basis.

TABLE II

 DEVIATIONS IN VAPOR PRESSURE, ENTHALPY AND VOLUME PREDICTIONS FOR
 PURE COMPONENT PARAFFIN HYDROCARBONS

Compound	Temp. Range °F	Pres. Range PSIA	No. of Points	Absolute Average Deviation in Predicted Values					Reference No.
				Vapor Pressure (Percent)	Vapor Enthalpy Departure	Liquid Enthalpy Departure	Vapor Volume (Percent)	Liquid Volume (Percent)	
Methane	-290. + 440.	2.6 + 10000	120	2.25	3.81	2.19	3.79	7.11	67
*	-297.7 + 111.7	1.6 + 655.6	21	2.38					52
Ethane	-297.0 + 440.	0.0005 + 10000	98	2.64	2.67	1.60	4.94	3.25	68
Ethane	-252.7 + 89.3	0.024 + 89.3	39	3.60					52
Propane	-198.7 + 197.3	0.022 + 565.9	45	5.32					52
Iso-Butane	- 20.0 + 190.0	7.5 + 250	57	1.89	2.09	1.92	2.74	4.73	25
*	-162.67 + 269.3	0.023 + 502.7	49	6.99					52
N-Butane	-153.7 + 305.3	0.016 + 549.2	52	5.66					52
Iso-Pentane	- 0. + 460.0	2.18 + 5000	83	1.16	2.26	2.58	6.19	6.50	7, 230
*	-117.7 + 368.3	0.019 + 487.5	55	8.05					52
N-Pentane	-108.7 + 377.3	0.018 + 455.3	55	6.46					52
Neo-Pentane	- 0.67 + 314.3	5.952 + 437.12	36	3.75					52
N-Hexane	32. + 600.	0.876 + 600	69	1.95	0.73	3.38	8.40	2.86	25
*	- 63.7 + 449.3	0.022 + 421.8	58	5.64					52
N-Heptane	- 27.7 + 512.3	0.02 + 396.2	61	4.47					52

TABLE II (Continued)

Compound	Temp. Range °F	Pres. Range PSIA	No. of Points	Absolute Average Deviation in Predicted Values					Reference No.
				Vapor Pressure (Percent)	Vapor Enthalpy Departure	Liquid Enthalpy Departure	Vapor Volume (Percent)	Liquid Volume (Percent)	
N-Octane	63.7 → 449.3	0.021 → 342.2	62	3.45					52
N-Nonane	102.3 → 353.2	0.193 → 29.0	27	3.72					230
N-Decane	135.9 → 397.2	0.193 → 29.0	27	2.15					230
N-Undecane	167.2 → 438.4	0.193 → 29.0	27	0.45					230
N-Dodecane	196.7 → 476.7	0.193 → 29.0	27	1.70					230
N-Tridecane	224.9 → 512.7	0.193 → 29.0	27	3.61					230
N-Tetradecane	251.2 → 546.8	0.193 → 29.0	27	5.78					230
N-Pentadecane	276.4 → 578.8	0.193 → 29.0	27	7.86					230
N-Hexadecane	300.5 → 609.3	0.193 → 29.0	27	9.90					230
N-Heptadecane	321.6 → 638.6	0.193 → 29.0	27	13.16					230
2-Methyl Pentane	-81.7 → 431.3	0.016 → 420.7	58	14.8					52
3-Methyl Pentane	-72.7 → 440.3	0.022 → 425.4	58	6.43					52

TABLE II (Continued)

Compound	Temp. Range °F	Pres. Range PSIA	No. of Points	Absolute Average Deviation in Predicted Values					Reference No.
				Vapor Pressure (Percent)	Vapor Enthalpy Departure	Liquid Enthalpy Departure	Vapor Volume (Percent)	Liquid Volume (Percent)	
2,2 Dimethyl Butane	-45.0 → 170.0	0.180 → 32.20	44	3.75					230
2,3 Dimethyl Butane	-81.7 → 440.3	0.021 → 453.5	59	13.1					52

* Data used for evaluation but not fitted

TABLE III
 DEVIATIONS IN VAPOR PRESSURE, ENTHALPY AND VOLUME PREDICTIONS
 FOR PURE COMPONENT OLEFIN HYDROCARBONS

Compound	Temp. Range °F	Pres. Range PSIA	No. of Points	Absolute Average Deviation in Predicted Values					Reference No.
				Vapor Pressure (Percent)	Vapor Enthalpy Departure	Liquid Enthalpy Departure	Vapor Volume (Percent)	Liquid Volume (Percent)	
Ethylene	-272.5 + 49.8	0.018 + 742.1	63	3.08	3.96	4.77	9.50	3.81	8
*	-270.7 + 44.3	0.021 + 692.4	35	3.01					52
Propylene	-216.7 + 143.3	0.009 + 381.2	42	3.87	2.41	2.87	4.72	1.76	90
1-Butene	32. + 460.	18.6 + 1000.	42	3.22	1.82	2.71	27.5	2.48	25
Cis-2 -Butene	-144.7 + 323.3	0.018 + 603.2	53	14.10					52
Trans-2 -Butene	-153.7 + 305.3	0.014 + 546.1	52	3.87					52
Isobutene	-162.7 + 287.3	0.014 + 553.5	51	3.72					52
1,3 Butadiene	-115.0 + 60.0	0.166 + 30.10	18	3.87					52
1-Pentene	-177.7 + 368.3	0.016 + 476.8	55	3.22					230
Cis-2 -Pentene	-108.7 + 395.3	0.015 + 533.8	57	3.69					52
Trans-2 -Pentene	-108.7 + 386.3	0.016 + 502.9	56	3.69					52
2-Methyl- 1-Butene	-108.7 + 386.3	0.024 + 558.3	56	1.44					52

TABLE III (Continued)

Compound	Temp. Range °F	Pres. Range PSIA	No. of Points	Absolute Average Deviation in Predicted Values					Reference No.
				Vapor Pressure (Percent)	Vapor Enthalpy Departure	Liquid Enthalpy Departure	Vapor Volume (Percent)	Liquid Volume (Percent)	
3-Methyl 1-Butene	-126.7 + 350.3	0.021 + 492.0	54	2.76					52
2-Methyl 2-Butene	- 99.7 + 404.3	0.023 + 559.1	57	2.85					52
1-Hexene	- 72.7 + 440.3	0.02 + 426.7	58	3.22					52
1-Heptene	21.07 + 245.19	0.193 + 29.00	27	3.22					230
Propadiene	-150.0 + 5.0	0.15 + 29.4	34	5.11					230
1,2 Butadiene	-95.0 + 90.0	0.17 + 30.9	39	3.76					230

*Data used for evaluation but not fitted

TABLE IV
 DEVIATIONS IN VAPOR PRESSURE, ENTHALPY AND VOLUME PREDICTIONS
 FOR PURE COMPONENT AROMATIC HYDROCARBONS

Compound	Temp. Range °F	Pres. Range PSIA	No. of Points	Absolute Average Deviation in Predicted Values					Reference No.
				Vapor Pressure (Percent)	Vapor Enthalpy Departure	Liquid Enthalpy Departure	Vapor Volume (Percent)	Liquid Volume (Percent)	
Benzene	100.0 → 860.0	3.22 → 3000	66	1.60	2.80	3.94	12.33	6.55	25
* Benzene	62.3 → 552.22	1.247 → 710.38	56	1.34					52
Toluene	62.3 → 605.6	0.36 → 595.3	61	2.02	3.65	2.97	5.04	16.05	52
O-Xylene	26.3 → 674.3	0.020 → 538.9	73	1.66					52
M-Xylene	62.3 → 647.3	0.105 → 501.7	66	5.71					52
P-Xylene	17.33 → 647.3	0.017 → 500.3	71	1.86					52
Ethylbenzene	80.0 → 330.0	0.202 → 30.43	51	2.28					230

* Data used for evaluation but not fitted

TABLE V
 DEVIATIONS IN VAPOR PRESSURE, ENTHALPY AND VOLUME PREDICTIONS
 FOR PURE COMPONENT CYCLOPARAFFIN HYDROCARBONS

Compound	Temp. Range °F	Pres. Range PSIA	No. of Points	Absolute Average Deviation in Predicted Values					Reference No.
				Vapor Pressure (Percent)	Vapor Enthalpy Departure	Liquid Enthalpy Departure	Vapor Volume (Percent)	Liquid Volume (Percent)	
Cyclopentane	-40.0 → 160.0	0.20 → 29.3	41	1.25					230
Methyl Cyclopentane	-10.0 → 205.0	0.20 → 29.3	44	2.62					230
Cyclohexane	45.0 → 225.0	0.796 → 30.6	37	1.25					230
Methyl Cyclohexane	25.0 → 265.0	0.185 → 28.7	49	2.62					230
Ethyl Cyclopentane	30.0 → 265.0	0.182 → 29.1	48	1.47					230
Ethyl Cyclohexane	70.0 → 320.0	0.199 → 29.3	51	1.47					230

TABLE VI
 DEVIATIONS IN VAPOR PRESSURE, ENTHALPY AND VOLUME PREDICTIONS
 FOR PURE COMPONENT NON-HYDROCARBONS

Compound	Temp. Range °F	Pres. Range PSIA	No. of Points	Absolute Average Deviation in Predicted Values					Reference No.
				Vapor Pressure (Percent)	Vapor Enthalpy Departure	Liquid Enthalpy Departure	Vapor Volume (Percent)	Liquid Volume (Percent)	
Hydrogen	-300.0 → 500.0	1.0 → 5000.0	85		3.19		1.12		25
Nitrogen	-345.9 → 440.3	1.82 → 10000	137	1.86	2.77	1.34	9.32	1.77	241
Carbon Monoxide	-337.0 → 600.0	2.3 → 10000	67	4.19	5.56	1.47	6.31	17.4	25
Carbon Dioxide	-817.0 → 386.3	0.12 → 12328	96	6.49	2.23	1.83	13.3	12.2	91
Hydrogen Sulfide	- 76.4 → 340.0	14.7 → 10000	73	0.94	3.60	3.62	4.95	4.86	261
Sulfur Dioxide	40.0 → 480.0	26.6 → 4500	64	2.05	7.45	6.58	14.2	7.83	25
Water	32.0 → 684.0	0.089 → 2782.0	81	1.28	3.81	6.15	2.89	5.39	241
Methanol	32.0 → 464.0	0.571 → 1155.0	105	5.14	9.96	8.26	5.63	5.14	238
*	5.0 → 185.0	0.210 → 31.0	37	6.54					52
Ethylene Glycol	123.5 → 432.1	0.01 → 29.2	36	2.92	0.88	6.39	2.59	15.3	4

TABLE VI (Continued)

Compound	Temp. Range °F (T _r Range)	Pres. Range PSIA (P _r Range)	No. of Points	Absolute Average Deviation in Predicted Values					Reference No.
				Vapor Pressure (Percent)	Vapor Enthalpy Departure	Liquid Enthalpy Departure	Vapor Volume (Percent)	Liquid Volume (Percent)	
Diethylene Glycol	176.7 → 474.6	0.012 → 14.74	29	3.24	0.83	7.48	2.59	15.3	4
Triethylene Glycol	237.2 → 532.9	0.014 → 10.9	12	4.22	0.92	7.86	2.59	15.3	72
Oxygen	-297.3 → 181.0	14.696 → 736.0	26	4.83	2.67	3.24	10.67	19.2	25

* Data used for evaluation but not fitted.

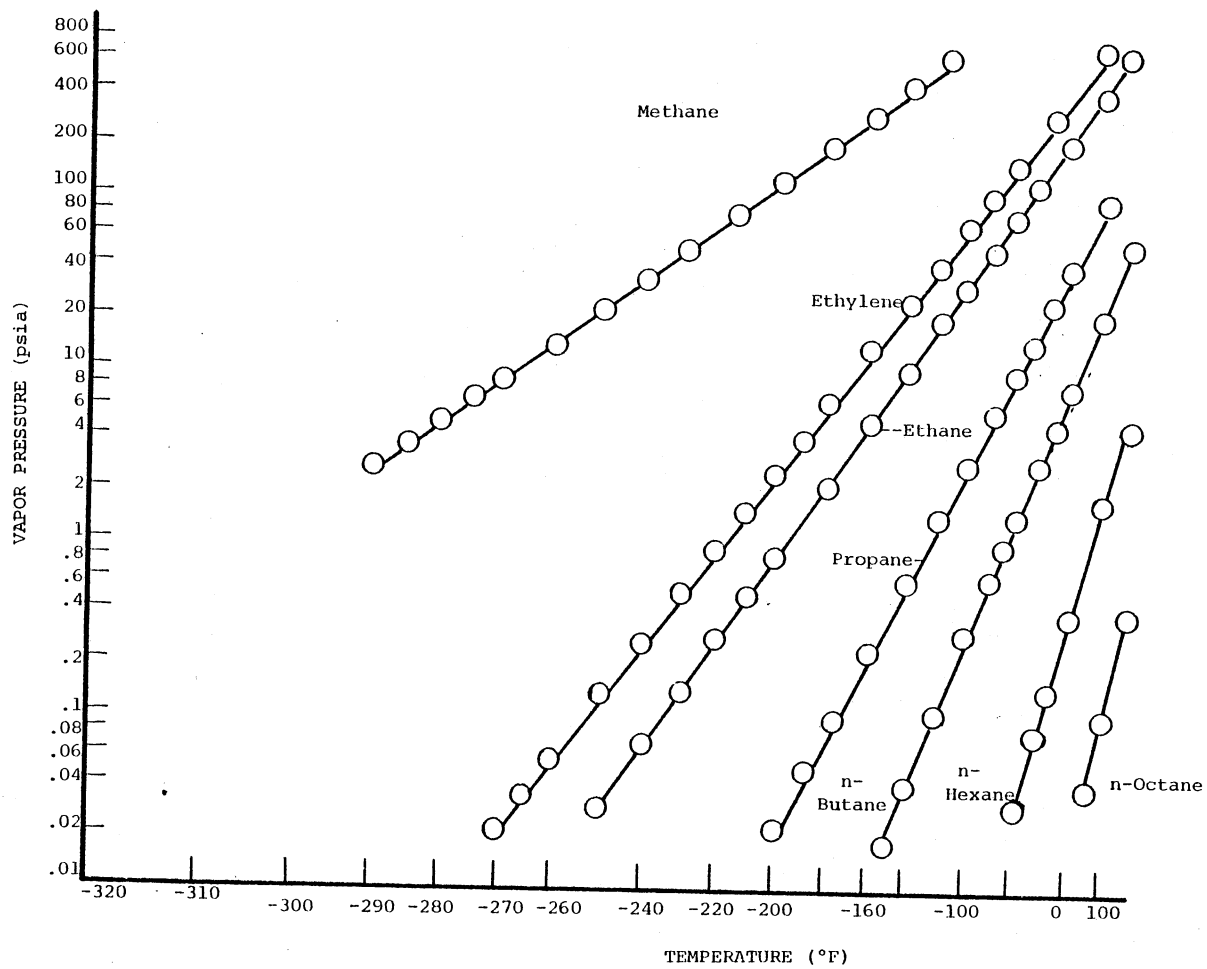


Figure 4. Comparison of Predicted and Experimental Vapor Pressure Data for Selected Hydrocarbons

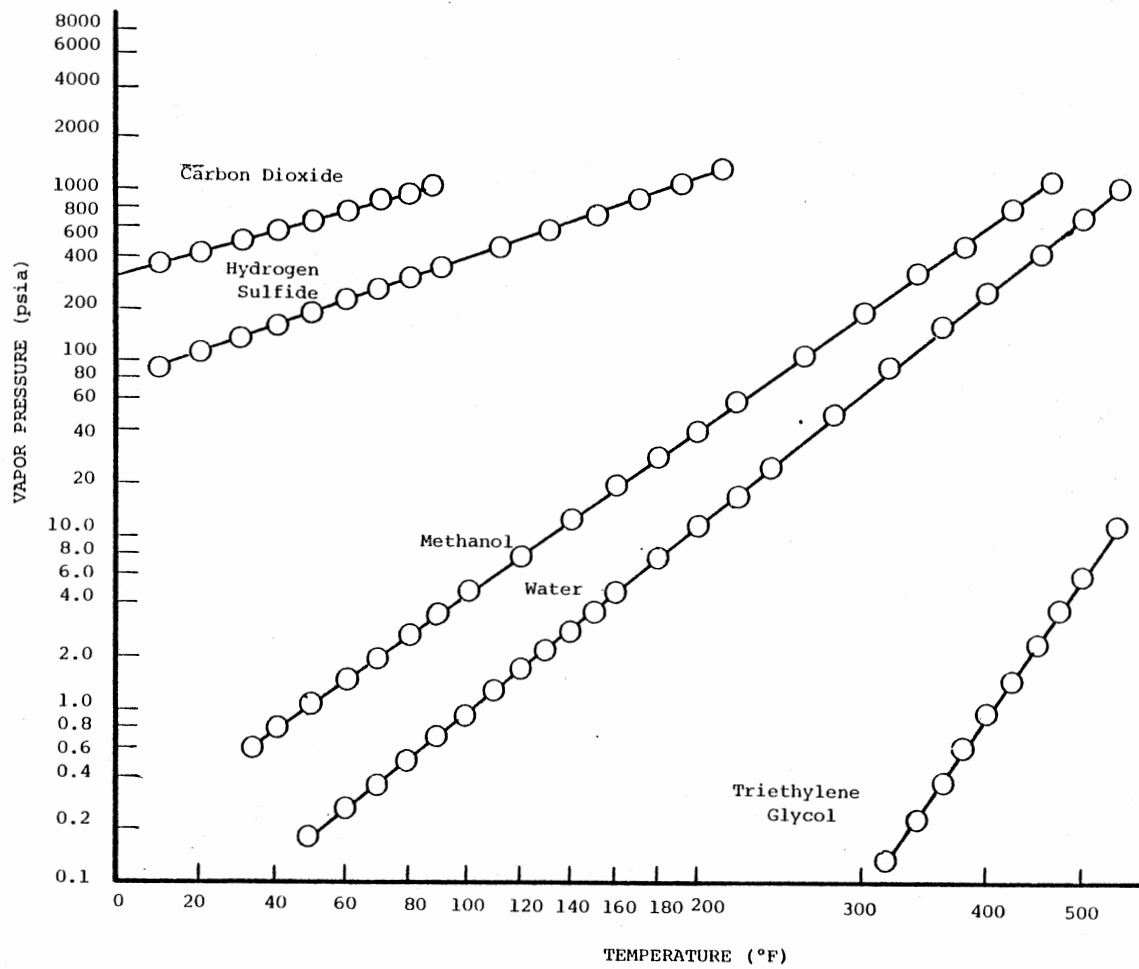


Figure 5. Comparison of Predicted and Experimental Vapor Pressure Data for Selected Non-Hydrocarbons

Vapor Liquid Equilibrium
of Multicomponent Mixtures

Using the pure component group parameters and extensive vapor liquid equilibrium literature data on mixtures, binary group interaction coefficients were derived for the PFGC equation of state. One interaction coefficient per binary pair was defined for both the vapor and hydrocarbon-liquid phases, and another binary interaction coefficient was defined for the water-rich liquid phase. The binary group interaction coefficients that minimized the absolute average error in equilibrium K-ratios, for mixtures, and vapor pressure, for pure components, over the given temperature and pressure range were selected. Table VII gives the final values of the group parameters for the PFGC equation of state. Table VIII contains a list of binary interaction coefficients for the groups used in the PFGC equation.

The evaluation of vapor liquid equilibrium of mixtures is classified as follows: 1) dry light hydrocarbon systems, 2) aqueous light hydrocarbon systems, 3) methanol and glycol systems, and 4) multi-component test mixtures.

Dry Light Hydrocarbon Systems

Binary mixtures of carbon dioxide, nitrogen, hydrogen sulfide, methane, ethane, ethylene, propane, benzene, toluene and a variety of cycloparaffins with light hydrocarbons were used to derive the vapor and hydrocarbon liquid phase binary group interaction coefficients. The components of each mixture, temperature and pressure range, and number of points evaluated are presented in Tables IX through XVI. The

TABLE VII
GROUP PARAMETERS IN THE PFGC EQUATION OF STATE

ID No.	Group	b	s	E_o	E_1	E_2
1	H ₂	0.3296	1.8729	-43.6787	8.2008	1.3592
2	CH ₄	0.5973	1.8982	-128.4301	-58.5361	7.5876
3	-CH ₃	0.3331	1.9780	-317.7900	-58.6300	6.0301
4	$\begin{array}{c} \\ \text{CH}_2 \\ \end{array}$	0.2668	0.4956	-270.0300	-77.8300	0.4678
5	$\begin{array}{c} \\ -\text{CH} \\ \end{array}$	0.2412	0.9260	-100.1300	-34.4800	0.3780
6	$\begin{array}{c} \\ -\text{C}- \\ \end{array}$	0.2587	-2.6435	-146.7097	-41.4111	0.0618
7	=CH ₂	0.3354	1.3235	-239.9300	-50.6490	1.5943
8	$\begin{array}{c} \diagup \\ \text{CH}_2 \\ \diagdown \end{array}$	0.3744	0.6333	-198.6450	-75.7460	0.3054
9	$\begin{array}{c} \diagup \\ \text{CH} \\ \diagdown \end{array}$	0.2580	0.3471	-257.1001	-193.8000	31.0000
10	$\begin{array}{c} \diagup \\ \text{C} \\ \diagdown \end{array}$	0.2619	0.2272	-313.2605	-112.2420	58.4559
11	-CH=	0.3108	-0.2419	-165.7000	-110.0200	-0.0083
12	N ₂	0.4450	2.3695	-118.3000	-33.2000	3.0000
13	CO ₂	0.3332	3.0920	-576.3110	-170.2465	0.1336
14	CO	0.4054	2.5992	-136.2700	-57.1000	6.4840
15	H ₂ S	0.4050	3.4335	-609.6001	-172.9000	16.0000
16	H ₂ O	0.2000	2.2000	-2651.3000	-2779.3000	858.5000
17	$\begin{array}{c} \\ \text{C}=\ \\ \end{array}$	0.2706	0.1938	-276.7700	-125.8000	48.0915
18	SO ₂	0.5822	2.7644	-522.3701	-267.7100	0.0673
19	CH ₃ OH	0.3732	5.5992	-1407.7700	-789.3101	108.0319
20	=C< (ortho)	0.2631	0.2246	-316.911	-112.0330	74.3827
21	=C< (para)	0.2598	0.2256	-305.792	-96.3310	63.5644

TABLE VII (Continued)

ID No.	Group	b	s	E_0	E_1	E_2
22	$\text{=C} \begin{smallmatrix} \diagup \\ \diagdown \end{smallmatrix} \text{(meta)}$	0.2619	0.2272	-313.2600	-112.2400	58.4560
23	=C=	0.6364	-0.6500	-75.0000	-101.3660	0.0011
24	—CH	0.6090	-0.4428	-40.0070	-17.5504	0.0165
25	O_2	0.4780	2.0756	-130.8700	-32.2969	2.0581
26	$\begin{array}{c} \\ \text{CH}_2\text{OH} \\ \end{array}$	0.5153	1.2009	-755.0500	-739.0801	103.1020
27	$\begin{array}{c} \quad \\ \text{CH}_2\text{OCH}_2 \\ \quad \end{array}$	0.1785	1.8880	-1011.2002	196.7524	-1.6264

TABLE VIII
 BINARY GROUP INTERACTION PARAMETERS FOR THE
 PFGC EQUATION OF STATE

No.	Group ID No.	Vapor and Hydrocarbon Liquid Phase		Aqueous Liquid Phase	
		$k_{ij} = a + bT$		$k_{ij} = c + dT$	
		a	b	c	d
	1-2	0.691	0	0.691	0
	1-3	0.411	0	0.411	0
	1-4	0.720	0	0.720	0
	1-5	0.460	0	0.460	0
	1-7	0.550	0	0.550	0
	1-8	0.695	0	0.695	0
	1-9	0.950	0	0.950	0
	1-10	0.050	0	0.050	0
	1-12	0.600	0	0.600	0
	1-16	0.113	0	0.113	-0.404
	2-3	0.945	0	0.945	0
	2-4	0.830	0	0.830	0
	2-5	0.700	0	0.700	0
	2-7	1.050	0	1.050	0
	2-8	0.850	0	0.850	0
	2-9	0.800	0	0.800	0
	2-10	0.100	0	0.100	0
	2-12	0.950	0	0.950	0
	2-13	0.765	0	0.765	0
	2-15	0.722	0	0.722	0
	2-16	0.263	0	0.125	0
	2-19	0.500	0	0.500	0
	2-21	1.430	0	1.430	0
	2-24	0.050	0	0.050	0
	2-26	0.600	0	0.600	0
	2-27	0.600	0	0.600	0

TABLE VIII (Continued)

No.	Group ID No.	Vapor and Hydrocarbon Liquid Phase		Aqueous Liquid Phase	
		$k_{ij} = a + bT$		$k_{ij} = c + dT$	
		a	b	c	d
	2-29	0.767	0	0.767	0
	3-4	1.010	0	1.010	0
	3-7	0.951	0	0.951	0
	3-11	0.974	0	0.974	0
	3-12	0.800	0	0.800	0
	3-13	0.850	0	0.850	0
	3-15	0.850	0	0.850	0
	3-16	0.335	0	0.210	0
	3-19	0.750	0	0.750	0
	3-20	1.026	0	1.026	0
	3-21	0.977	0	0.977	0
	3-26	0.695	0	0.695	0
	3-27	1.100	0	1.100	0
	3-29	0.700	0	0.700	0
	4-7	0.935	0	0.935	0
	4-8	1.115	0	1.115	0
	4-10	1.328	0	1.328	0
	4-11	0.962	0	0.962	0
	4-12	0.860	0	0.860	0
	4-13	0.850	0	0.850	0
	4-16	0.330	0	0.400	0
	4-17	1.101	0	1.101	0
	4-19	0.750	0	0.750	0
	4-20	0.677	0	0.677	0
	4-24	0.648	0	0.648	0
	4-26	0.888	0	0.888	0
	4-29	0.875	0	0.875	0
	5-7	0.850	0	0.850	0
	5-10	0.300	0	0.300	0

TABLE VIII (Continued)

No.	Group ID No.	Vapor and Hydrocarbon Liquid Phase		Aqueous Liquid Phase	
		$k_{ij} = a + bT$		$k_{ij} = c + dT$	
		a	b	c	d
	5-11	0.850	0	0.850	0
	5-12	0.400	0	0.400	0
	5-13	0.800	0	0.800	0
	5-16	0.250	0	0.470	0
	5-21	0.950	0	0.950	0
	5-26	1.100	0	1.100	0
	5-27	1.200	0	1.200	0
	6-21	5.500	0	5.500	0
	7-11	1.005	0	1.005	0
	7-12	0.900	0	0.900	0
	7-13	0.900	0	0.900	0
	7-15	0.840	0	0.840	0
	7-16	0.390	0	0.245	0
	7-71	0.991	0	0.991	0
	8-12	0.320	0	0.320	0
	8-13	0.920	0	0.920	0
	9-12	0.680	0	0.680	0
	8-13	0.920	0	0.920	0
	9-12	0.680	0	0.470	0
	9-13	0.920	0	0.805	0
	9-16	0.250	0	1.015	0
	9-19	0.805	0	0.974	0
	9-20	1.015	0	0.820	0
	9-21	0.974	0	1.240	0
	9-26	0.820	0	0.800	0
	9-27	1.240	0	0.880	0
	10-13	0.800	0	1.039	0
	10-15	0.880	0	0.990	0
	10-20	1.039	0	0.300	0

TABLE VIII (Continued)

No.	Group ID No.	Vapor and Hydrocarbon Liquid Phase		Aqueous Liquid Phase	
		$k_{ij} = a + bT$		$k_{ij} = c + dT$	
		a	b	c	d
	10-21	0.990	0	0.990	0
	11-12	0.300	0	0.300	0
	11-13	0.900	0	0.900	0
	11-16	0.250	0	0.350	0
	11-17	1.193	0	1.193	0
	12-13	0.780	0	0.780	0
	12-15	0.500	0	0.500	0
	12-16	0.318	0	0.318	-0.611
	12-19	0.500	0	0.500	0
	12-21	0.700	0	0.700	0
	12-24	1.200	0	1.200	0
	12-26	0.250	0	0.250	0
	12-27	0.350	0	0.350	0
	13-15	0.905	0	0.905	0
	13-16	0.550	0	0.358	0
	13-19	0.840	0	0.840	0
	13-24	0.050	0	0.050	0
	13-26	0.780	0	0.780	0
	13-27	1.160	0	1.160	0
	13-29	1.015	0	1.015	0
	14-16	0.080	0	-0.135	0
	15-16	0.530	0	0.256	0
	15-19	0.840	0	0.840	0
	15-24	0.200	0	0.200	0
	15-26	0.920	0	0.920	0
	15-27	1.120	0	1.120	0
	15-29	1.250	0	1.250	0
	16-19	0.908	0	0.908	0

TABLE VIII (Continued)

No.	Group ID No.	Vapor and Hydrocarbon Liquid Phase		Aqueous Liquid Phase	
		$k_{ij} = a + bT$		$k_{ij} = c + dT$	
		a	b	c	d
	16-25	0.220	0	0.110	0
	16-26	0.830	0	0.830	0
	16-29	0.800	0	0.800	0
	3-6	0.013	0	0.013	0
	4-6	0.405	0	0.405	0

TABLE IX

CO₂ BINARY SYSTEM DEVIATIONS IN K-VALUE PREDICTIONS

System	Temperature Range (°F)	Pressure Range (PSIA)	No. of Points	Percent Abs. Avg. Error			Reference No.
				K _{CO₂}	K _{2nd}	L/F	
CO ₂ (1) - CH ₄ (2)	-100.0 → 29.0	161.0 → 1146.0	45	8.51	4.89	9.61	47
	- 45.0 → 26.0	220.4 → 1235.6	36	11.13	7.28	5.42	43
	- 40.0 → 50.0	764.0 → 1187.0	13	15.85	7.76	1.74	96
	184.0 → 65.0	100.0 → 939.0	53	3.99	11.34	23.50	154
	26.3 → 26.3	556.0 → 1223.0	8	19.22	6.23	1.56	104
	-147.64 → 63.94	387.9 → 996.4	59	3.79	15.23	11.08	257
-159.0 → 29.0	300.0 → 1073.0	58	6.90	3.85	6.55	47	
CO ₂ (1) - C ₂ H ₆ (2)	- 9.67 → -9.67	209.1 → 309.6	12	1.28	1.92	29.90	43
	- 58.0 → 68.0	90.0 → 914.0	54	3.01	19.80	20.41	62
	- 60.0 → 60.0	101.6 → 813.0	37	5.18	21.6	21.62	75
	50.0 → 77.0	502.0 → 910.0	68	1.99	18.61	20.91	103
	- 4.36 → -4.36	233.7 → 333.6	12	3.32	3.33	38.00	156

TABLE IX (Continued)

System	Temperature Range (°F)	Pressure Range (PSIA)	No. of Points	Percent Abs. Avg. Error			Reference No.
				K _{CO₂}	K _{2nd}	L/F	
	32.0 → 32.0	360.0 → 577.0	14	4.97	2.86	45.0	248
	60.0 → 60.0	516.0 → 814.0	7	3.78	3.77	40.3	197
	-60.0 → 60.0	113.7 → 814.0	10	10.78	5.99	23.5	121
CO ₂ (1) - C ₃ H ₈ (2)	40.0 → 160.0	100.0 → 950.0	67	4.49	5.95	9.90	184
	-20.0 → 20.0	73.0 → 379.0	20	3.45	5.34	7.95	76
	-40.0 → 32.0	50.0 → 200.0	8	21.42	24.00	22.50	3
	- 4.36 → 4.36	233.67 → 333.6	12	18.30	17.20	27.30	156
CO ₂ (1) - nC ₄ H ₁₀ (2)	100.0 → 280.0	60.0 → 1150.0	54	7.45	7.07	9.11	167
	99.86 → 99.86	230.7 → 1024.3	9	4.99	17.60	8.71	200
	-49.3 → 50.0	4.8 → 599.0	29	12.20	6.89	3.72	213
	100.0 → 100.0	100.0 → 1095.0	10	4.76	8.76	2.30	50
	32.0 → 32.0	35.3 → 462.9	12	5.67	10.32	4.72	156
CO ₂ (1) - iC ₄ H ₁₂ (2)	100.0 → 250.0	105.0 → 1042.0	28	6.88	12.50	19.14	12
	32.0 → 32.0	39.7 → 505.0	18	11.10	12.22	5.83	156

TABLE IX (Continued)

System	Temperature Range (°F)	Pressure Range (PSIA)	No. of Points	Percent Abs. Avg. Error			Reference No.
				K_{CO_2}	K_{2nd}	L/F	
CO ₂ (1) - nC ₅ H ₁₂ (2)	40.1 → 220.0	33.0 → 1397.0	47	8.98	12.20	6.31	14
CO ₂ (1) - iC ₅ H ₁₀ (2)	40.0 → 220.0	22.0 → 1290.0	42	7.64	9.46	6.25	15
CO ₂ (1) - nC ₆ H ₁₄ (2)	104.0 → 248.0	113.0 → 1682.0	40	9.48	15.90	5.94	127
	77.0 → 104.0	83.7 → 1168.8	16	24.30	22.37	13.00	98
CO ₂ (1) - nC ₇ H ₁₆ (2)	99.5 → 399.3	27.0 → 1931.0	63	5.79	17.49	4.19	211
CO ₂ (1) - nC ₁₀ H ₂₂ (2)	40.0 → 460.0	50.0 → 2732.0	88	11.32	20.80	7.78	224
CO ₂ (1) - nC ₁₆ H ₃₄ (2)	372.9 → 735.08	284.5 → 749.5	31	11.21	12.21	8.16	231
CO ₂ (1) - C ₂ H ₄ (2)	13.98 → 77.0	403.0 → 1002.0	56	1.03	3.24		81
	32.0 → 32.0	556.9 → 637.8	14	2.79	4.33		74
	-42.88 → -4.36	138.1 → 379.9	25	1.34	4.36		156
	-58.0 → 68.0	106.2 → 941.6	52	0.85	3.01		152
CO ₂ (1) - C ₃ H ₆ (2)	-46.3 → 32.0	18.96 → 508.2	16	2.90	5.33	10.41	273
	- 4.36 → 32.0	66.13 → 505.5	25	4.85	3.59	9.80	156

TABLE IX (Continued)

System	Temperature Range (°F)	Pressure Range (PSIA)	No. of Points	Percent Abs. Avg. Error			Reference No.
				K_{CO_2}	K_{2nd}	L/F	
CO ₂ (1) - Benzene (2)	104.0 → 104.0	107.0 → 1120.0	15	6.59	11.09	3.97	219
	77.0 → 104.0	129.6 → 1124.1	17	2.07	24.82	7.77	98
CO ₂ (1) - Toluene (2)	248.18 → 517.46	141.52 → 743.9	21	14.05	3.82	3.70	232
	100.6 → 399.0	48.4 → 2218.0	34	10.63	19.20	11.76	214
CO ₂ (1) - Methylcyclo- hexane (2)	100.1 → 399.3	50.1 → 2160.0	31	9.69	13.22	8.88	216
CO ₂ (1) - Ethylcyclo- hexane (2)	100.0 → 400.0	25.4 → 2383.0	45	11.06	12.12	9.69	203
CO ₂ (1) - H ₂ S (2)	- 2.34 194.0	293.9 → 1175.7	85	3.53	8.30	21.42	102
	-55.0 180.0	100.0 → 1200.0	83	2.93	6.74	32.39	239
	100.0 → 100.0	600.0 → 600.0	2	3.10	9.50	19.00	198
	40.0 → 160.0	400.0 → 1000.0	2	3.75	4.50	12.50	199
CO ₂ (1) - N ₂ (2)	-67.0 → 32.0	255.0 → 1907.0	30	4.34	17.87	12.43	276
	32.0 → 32.0	587.8 → 1715.0	15	5.45	11.22	11.52	272
	26.33 → 26.33	496.7 → 1789.9	33	6.47	10.72	14.62	104

TABLE X

N₂ BINARY SYSTEM DEVIATIONS IN K-VALUE PREDICTIONS

System	Temperature Range (°F)	Pressure Range (PSIA)	No. of Points	Percent Abs. Avg. Error			Reference No.
				K _{N₂}	K _{2nd}	L/F	
N ₂ (1) - CH ₄ (2)	-213.0 → -145.0	500.0 → 500.0	9	3.19	4.78	16.14	242
	-288.7 → 252.7	32.7 → 281.2	45	1.84	4.12	3.24	169
	-240.0 → 130.0	40.5 → 710.0	101	4.74	6.19	11.03	111
	-258.1 → 135.7	28.5 → 716.0	83	4.58	4.65	12.11	107
	-280.0 → 150.0	25.0 → 650.0	97	4.25	6.40	8.43	31
	-240.0 → 151.1	50.7 → 721.7	27	8.46	6.84	19.27	29
N ₂ (1) - C ₂ H ₆ (2)	8.33 → 44.33	266.0 → 1378.5	49	8.15	7.02	14.89	105
	-210.0 → -110.0	50.0 → 1953.0	50	12.0	20.40	2.11	112
	-99.67 → 62.33	152.7 → 1913.7	31	13.70	13.74	10.19	151
N ₂ (1) - C ₃ H ₈ (2)	-254.3 → -239.7	21.8 → 450.0	30	(71.60)	--	15.03	132
	-274.0 → 176.0	68.0 → 2018.0	80	18.07	27.79	16.34	228
N ₂ (1) - nC ₄ H ₁₀ (2)	100.0 → 100.0	2018.0 → 4170.0	13	13.79	28.54	23.08	143

TABLE X

System	Temperature Range (°F)	Pressure Range (PSIA)	No. of Points	Percent Abs. Avg. Error			Reference No.
				K _{N₂}	K _{2nd}	L/F	
	100.0 → 280.0	236.0 → 3402.0	28	14.23	13.61	17.25	196
N ₂ (1) - iC ₄ H ₁₀ (2)	0.0 → 250.0	33.7 → 3013.0	53	11.19	14.28	6.84	212
N ₂ (1) - nC ₅ H ₁₀ (2)	-200.0 → 0.0	350.8 → 4506.5	21	22.05	26.14	13.24	121
N ₂ (1) - nC ₇ H ₁₆ (2)	90.0 → 360.0	1030.0 → 10025.0	32	24.59	21.90	17.78	2
	356.0 → 435.2	356.0 → 4085.0	21	15.45	14.43	7.41	21
N ₂ (1) - nC ₁₀ H ₂₂ (2)	100.0 → 280.0	80.0 → 5000.0	92	27.62	18.58	12.86	142
N ₂ (1) - C ₂ H ₄ (2)	- 99.67 → 8.33	223.56 → 1601.0	14	14.38	9.86	18.21	151
N ₂ (1) - C ₃ H ₆ (2)	-109.3 → 72.50	111.69 → 918.50	19	9.16	14.68	3.97	271
N ₂ (1) - Benzene (2)	167.0 → 257.0	900.86 → 4454.4	17	10.60	10.10	6.07	149
N ₂ (1) - Toluene (2)	104.0 → 391.1	514.0 → 14496.6	23	15.24	13.59	7.93	124
N ₂ (1) - m-Xylene (2)	104.0 → 391.1	333.6 → 14518.3	18	12.21	16.17	8.42	124
N ₂ (1) - Methylcyclohexane (2)	100.0 → 400.0	63.2 → 2447.0	28	10.42	12.25	2.94	204
N ₂ (1) - Ethylcyclohexane (2)	100.0 → 400.0	63.0 → 2957.0	41	14.34	29.67	3.24	203

TABLE X (Continued)

System	Temperature Range (°F)	Pressure Range (PSIA)	No. of Points	Percent Abs. Avg. Error			Reference No.
				K_{N_2}	K_{2nd}	L/F	
N ₂ (1) - H ₂ S(2)	1.90 → 160.0	251.0 → 3003.0	55	14.20	19.72	4.60	202
	- 99.4 → -49.3	20.4 → 1994.0	18	10.69	27.34	7.62	213
N ₂ (1) - CO ₂ (2)	- 67.0 → 32.0	255.0 → 1907.0	30	17.87	4.34	12.43	276
	32.0 → 32.0	587.8 → 1715.0	15	11.22	5.45	11.52	272
	26.33 → 26.33	496.7 → 1789.9	33	10.72	6.47	14.62	104

TABLE XI

H₂S BINARY SYSTEMS DEVIATIONS IN K-VALUE PREDICTIONS

System	Temperature Range (°F)	Pressure Range (PSIA)	No. of Points	Percent Abs. Avg. Error			Reference No.
				K _{H₂S}	K _{2nd}	L/F	
H ₂ S(1) - CH ₄ (2)	-120.0 → 200.0	200.0 → 1600.0	59	5.08	12.46	7.49	116
	40.0 → 160.0	200.0 → 195.0	59	3.03	8.24	3.27	182
	100.0 → 100.0	600.0 → 1800.0	3	5.00	9.67	12.00	198
	40.0 → 160.0	400.0 → 1600.0	5	3.30	12.60	7.80	199
	100.0 → 100.0	400.0 → 1900.0	16	2.54	8.75	3.35	50
H ₂ S(1) - C ₂ H ₆ (2)	-99.80 → 50.0	9.45 → 442.0	45	2.08	4.68	13.34	209
H ₂ S(1) - C ₃ H ₈ (2)	124.0 → 201.0	400.0 → 600.0	22	7.31	5.18	9.18	63
	-69.0 → 160.0	20.0 → 400.0	49	9.64	7.29	14.20	19
	-22.0 → 181.0	58.8 → 599.44	54	8.62	6.42	30.52	55
H ₂ S(1) - nC ₄ H ₁₀ (2)	100.0 → 250.0	69.4 → 1150.0	77	3.21	6.62	16.02	205
H ₂ S(1) - iC ₄ H ₁₀ (2)	40.1 → 220.0	30.0 → 894.0	37	3.07	3.67	26.20	201
H ₂ S(1) - nC ₅ H ₁₂ (2)	40.0 → 340.0	20.0 → 1302.0	60	4.66	6.04	5.29	188

TABLE XI (Continued)

System	Temperature Range (°F)	Pressure Range (PSIA)	No. of Points	Percent Abs. Avg. Error			Reference No.
				K_{H_2S}	K_{2nd}	L/F	
H ₂ S(1) - nC ₇ H ₁₆ (2)	100.0 → 400.0	81.9 → 1385.0	49	4.69	9.67	10.44	210
H ₂ S(1) - nC ₁₀ H ₂₂ (2)	40.0 → 340.0	20.0 → 1935.0	50	8.96	28.82	21.66	192
H ₂ S(1) - C ₃ H ₆ (2)	-22.0 → 59.0	44.09 → 235.0	24	7.79	12.69	17.72	55
H ₂ S(1) - Toluene (2)	100.0 → 400.0	29.5 → 1679.0	27	4.58	17.08	7.87	210
H ₂ S(1) - Methylcyclohexane (2)	100.0 → 400.0	38.4 → 1371.0	30	8.61	14.65	8.47	216
H ₂ S(1) - Ethylcyclohexane (2)	100.0 → 400.0	24.6 → 1813.0	27	5.46	18.98	5.97	204
H ₂ S(1) - CO ₂ (2)	2.34 → 194.0	293.9 → 1175.7	85	8.30	3.53	21.42	102
	-55.0 → 180.0	100.0 → 1200.0	83	6.74	2.93	32.39	239
	100.0 → 100.0	600.0 → 600.0	2	9.50	3.10	19.00	198
	40.0 → 160.0	400.0 → 1000.0	2	4.50	3.75	12.50	199
H ₂ S(1) - N ₂ (2)	1.9 → 160.0	251.0 → 3003.0	55	19.72	14.20	4.60	202
	-99.4 → -49.3	20.4 → 1994.0	18	27.34	10.69	7.62	213

TABLE XII

C₁ BINARY SYSTEM DEVIATIONS IN K-VALUE PREDICTIONS

System	Temperature Range (°F)	Pressure Range (PSIA)	No. of Points	Percent Abs. Avg. Error			Reference No.
				K _{C₁}	K _{2nd}	L/F	
CH ₄ (1) - C ₂ H ₆ (2)	-225.0 → -99.8	28.0 → 748.0	118	4.21	9.98	9.16	263
	-240.0 → 50.0	18.2 → 1000.0	33	4.98	10.05	11.67	109
	8.33 → 43.33	285.4 → 957.0	38	4.85	11.68	10.82	105
	-135.67 → 171.67	17.89 → 410.17	20	2.49	3.29	2.66	83
CH ₄ (1) - C ₃ H ₈ (2)	-176.0 → 32.0	50.0 → 1450.0	81	7.32	17.80	8.44	1
	40.0 → 190.0	100.0 → 1474.0	122	6.68	14.45	10.54	181
	-200.0 → 50.0	100.0 → 1200.0	29	5.90	20.41	4.34	174
	-254.3 → 160.0	6.1 → 1250.0	39	7.35	17.75	6.03	264
	-225.0 → -75.0	27.0 → 944.0	90	6.04	16.41	9.92	262
CH ₄ (1) - nC ₄ H ₁₀ (2)	70.0 → 130.0	40.0 → 1923.0	64	8.48	21.32	9.44	220
	-200.0 → 40.0	20.1 → 1822.0	105	8.33	22.42	18.14	48
	40.0 → 220.0	200.0 → 1923.0	25	11.21	12.74	24.33	265
	-160.0 → 50.0	20.0 → 1400.0	70	7.64	21.33	21.99	95

TABLE XII (Continued)

System	Temperature Range (°F)	Pressure Range (PSIA)	No. of Points	Percent Abs. Avg. Error			Reference No.
				K _{C1}	K _{2nd}	L/F	
CH ₄ (1) - iC ₄ H ₁₀ (2)	100.0 → 220.0	80.0 → 1600.0	38	8.92	9.76	11.78	165
CH ₄ (1) - nC ₅ H ₁₂ (2)	-147.9 → 32.02	20.1 → 2200.0	61	6.81	16.76	12.58	30
	-140.0 → 50.0	50.0 → 2200.0	64	6.42	17.63	11.02	96
	220.0 → 220.0	1001.0 → 1999.0	9	4.02	15.33	7.89	175
	100.0 → 340.0	20.0 → 2455.0	60	5.77	13.98	8.83	223
CH ₄ (1) - i-C ₅ H ₁₂ (2)	160.0 → 280.0	499.0 → 2191.0	21	10.34	14.90	13.43	175
	160.0 → 350.0	400.0 → 1000.0	28	12.02	9.72	19.66	5
CH ₄ (1) - nC ₆ H ₁₄ (2)	32.0 → 302.0	25.1 → 1736.0	49	7.07	27.13	16.76	235
	-131.24 → 32.0	19.9 → 2675.0	105	7.44	32.05	11.50	128
CH ₄ (1) - nC ₇ H ₁₆ (2)	-100.0 → 0.0	100.0 → 3000.0	67	6.82	45.22	12.37	27
	40.0 → 460.0	200.0 → 3328.0	97	8.69	38.92	10.01	185
CH ₄ (1) - nC ₈ H ₁₈ (2)	79.0 → 302.0	146.9 → 3865.0	35	11.60	12.51	8.76	115

TABLE XII (Continued)

System	Temperature Range (°F)	Pressure Range (PSIA)	No. of Points	Percent Abs. Avg. Error			Reference No.
				K _{C1}	K _{2nd}	L/F	
CH ₄ (1) - nC ₉ H ₂₀ (2)	-58.0 → 302.10	146.9 → 1469.0	136	10.59	43.73	9.59	118
CH ₄ (1) - nC ₁₀ H ₂₂ (2)	167.0 → 302.0	146.9 → 1469.0	26	14.53	10.73	3.98	114
	100.0 → 460.0	40.0 → 5000.0	157	9.13	25.42	10.89	179
	100.0 → 220.0	14.7 → 2000.0	33	10.92	11.39	5.40	122
	40.0 → 589.0	400.0 → 4000.0	50	8.39	29.90	6.34	264
CH ₄ (1) - Benzene(2)	150.0 → 150.0	100.0 → 4800.0	17	27.65	37.47	6.94	57
	298.22 → 442.4	288.19 → 3519.1	18	32.27	28.39	6.11	130
CH ₄ (1) - Toluene(2)	0.0 → 40.0	50.0 → 2500.0	24	19.88	33.87	3.13	129
	-100.0 → 0.0	100.0 → 3500.0	77	18.37	22.24	5.62	28
	300.74 → 518.0	439.1 → 3665.0	26	17.68	20.26	4.78	130
	150.0 → 150.0	100.0 → 5200.0	16	31.62	27.10	13.63	51
CH ₄ (1) - Methylcyclohexane(2)	-100.0 → 0.0	100.0 → 3750.0	99	19.42	37.95	12.22	110

TABLE XII (Continued)

System	Temperature Range (°F)	Pressure Range (PSIA)	No. of Points	Percent Abs. Avg. Error			Reference No.
				K_{C_1}	K_{2nd}	L/F	
CH ₄ (1) - Ethylcyclohexane (2)	100.0 → 400.0	59.0 → 3007.0	37	21.62	21.71	15.91	203
CH ₄ (1) - CO (2)	-255.0 → 125.0	100.0 → 698.0	30	6.72	9.01	22.51	110
CH ₄ (1) - CO ₂ (2)	-100.0 → 29.0	161.0 → 1146.0	45	4.89	8.51	9.61	47
	- 45.0 → 26.0	220.4 → 1235.6	36	7.28	11.13	5.42	43
	- 40.0 → 50.0	764.0 → 1187.0	13	7.76	15.85	1.74	96
	184.0 → 65.0	100.0 → 939.0	53	11.34	3.99	23.50	154
	26.3 → 26.3	556.0 → 1223.0	8	6.23	19.22	1.56	104
	-147.64 → 63.94	387.9 → 996.4	59	15.23	3.79	11.08	257
	-159.0 → 29.0	300.0 → 1073.0	58	3.85	6.90	6.55	47
	CH ₄ (1) - H ₂ S (2)	-120.0 → 200.0	200.0 → 1600.0	59	12.46	5.08	7.49
	40.0 → 160.0	200.0 → 195.0	59	8.24	3.03	3.27	182
	100.0 → 100.0	600.0 → 1800.0	3	9.67	5.00	12.00	198
	40.0 → 160.0	400.0 → 1600.0	5	12.60	3.30	7.80	199

TABLE XII (Continued)

System	Temperature Range (°F)	Pressure Range (PSIA)	No. of Points	Percent Abs. Avg. Error			Reference No.
				K_{C_1}	K_{2nd}	L/F	
CH ₄ (1) - H ₂ S (2)	100.0 → 100.0	400.0 → 1900.0	16	8.75	2.54	3.35	50
CH ₄ (1) - N ₂ (2)	-213.0 → -145.0	500.0 → 500.0	9	4.78	3.19	16.14	242
	-288.7 → 252.7	32.7 → 281.2	45	4.12	1.84	3.24	169
	-240.0 → 130.0	40.5 → 710.0	101	6.19	4.74	11.03	111
	-258.1 → 135.7	28.5 → 716.0	83	4.65	4.58	12.11	107
	-280.0 → 150.0	25.0 → 650.0	97	6.40	4.25	8.43	31
	-240.0 → 151.1	50.7 → 721.7	27	6.84	8.46	19.27	29

TABLE XIII

C₂ BINARY SYSTEM DEVIATIONS IN K-VALUE PREDICTIONS

System	Temperature Range (°F)	Pressure Range (PSIA)	No. of Points	Percent Abs. Avg. Error			Reference No.
				K _{C₂}	K _{2nd}	L/F	
C ₂ H ₆ (1) - CH ₄ (2)	-225.0 → -99.8	28.0 → 748.0	118	9.98	4.21	9.16	263
	-240.0 → 50.0	18.2 → 1000.0	33	10.05	4.98	11.67	109
	8.33 → 43.33	285.4 → 959.0	38	11.68	4.85	10.82	105
	-135.67 → 171.67	17.89 → 410.17	20	3.29	2.49	2.66	83
C ₂ H ₆ (1) - C ₂ H ₄ (2)	40.0 → 60.0	464.0 → 714.0	7	2.42	2.57	52.60	140
	-100.0 → 0.0	35.90 → 381.0	22	4.57	9.05	48.60	80
	14.0 → 68.0	280.1 → 703.2	15	2.62	9.28	41.70	61
C ₂ H ₆ (1) - C ₃ H ₆ (2)	10.0 → 160.0	100.0 → 722.0	29	4.92	4.11	20.57	141
C ₂ H ₆ (1) - C ₃ H ₈ (2)	-230.0 → 0.0	0.003 → 218.0	53	5.69	7.90	14.31	46
	0.0 → 50.0	100.0 → 400.0	5	2.40	6.80	25.30	174
	0.0 → 200.0	100.0 → 752.0	78	2.11	2.78	9.24	139
C ₂ H ₆ (1) - nC ₄ H ₁₀ (2)	150.0 → 250.0	509.0 → 805.0	19	3.30	4.07	16.73	245
C ₂ H ₆ (1) - iC ₄ H ₁₀ (2)	100.6 → 249.6	155.0 → 779.0	36	8.29	7.31	43.50	13

TABLE XIII (Continued)

System	Temperature Range (°F)	Pressure Range (PSIA)	No. of Points	Percent Abs. Avg. Error			Reference No.
				K_{C_2}	K_{2nd}	L/F	
C_2H_6 (1) - nC_5H_{12} (2)	40.0 → 340.0	50.0 → 955.0	68	5.56	7.92	21.99	178
C_2H_6 (1) - nC_6H_{14} (2)	150.0 → 350.0	25.0 → 1146.0	39	7.94	13.16	5.22	274
C_2H_6 (1) - nC_7H_{16} (2)	150.0 → 350.0	455.0 → 1215.0	32	11.29	13.41	17.10	147
C_2H_6 (1) - $nC_{10}H_{22}$ (2)	50.0 → 460.0	100.0 → 1715.0	112	14.53	22.66	6.18	186
C_2H_6 (1) - N_2 (2)	8.33 → 44.33	266.0 → 1378.5	49	7.02	8.15	14.89	105
	-210.0 → -110.0	50.0 → 1953.0	50	20.40	12.00	2.11	112
	- 99.67 → 62.33	152.7 → 1913.7	31	13.74	13.70	10.19	151
C_2H_4 (1) - N_2 (2)	- 99.67 → 8.33	223.56 → 1601.0	14	14.38	9.86	18.21	151
C_2H_6 (1) - H_2S (2)	- 99.80 → 50.0	9.45 → 442.0	45	4.68	2.08	13.34	209
C_2H_6 (1) - CO_2 (2)	- 9.67 → -9.67	209.1 → 309.6	12	1.92	1.28	29.90	43
	- 58.0 → 68.0	90.0 → 914.0	54	19.80	3.01	20.41	62
	- 60.0 → 60.0	101.6 → 813.0	37	21.60	5.18	21.62	75
	- 50.0 → 77.0	502.0 → 910.0	68	18.61	1.99	20.91	103
	- 4.36 → 4.36	233.7 → 333.6	12	3.33	3.32	38.00	156

TABLE XIII (Continued)

System	Temperature Range (°F)	Pressure Range (PSIA)	No. of Points	Percent Abs. Avg. Error			Reference No.
				K_{C_2}	K_{2nd}	L/F	
C ₂ H ₆ (1) - CO ₂ (2)	32.0 → 32.0	360.0 → 577.0	14	2.86	4.97	45.0	248
	60.0 → 60.0	516.0 → 814.0	7	3.77	3.78	40.3	197
	-60.0 → 60.0	113.7 → 814.0	10	5.99	10.78	23.5	121
C ₂ H ₄ (1) - CO ₂ (2)	13.98 → 77.0	403.0 → 1002.0	56	3.24	1.03		81
	32.0 → 32.0	556.9 → 637.8	14	4.33	2.79		74
	-42.88 → -4.36	138.1 → 379.9	25	4.36	1.34		156
	-58.0 → 68.0	106.2 → 941.6	52	3.01	0.85		152

TABLE XIV

C₃+ BINARY SYSTEM DEVIATIONS IN K-VALUE DEVIATIONS

System	Temperature Range (°F)		Pressure Range (PSIA)		No. of Points	Percent Abs. Avg. Error			Reference No.
						K _{C₃+}	K _{2nd}	L/F	
C ₃ H ₈ (1) - C ₃ H ₆ (2)	10.0	160.0	48.5	449.9	93	4.67	7.88	-	79
	10.0	190.0	49.9	613.6	73	4.23	5.53		183
	-20.0	130.0	26.4	323.8	69	5.86	8.98		134
	100.0	160.0	194.0	454.8	71	4.93	6.20		125
C ₃ H ₈ (1) - nC ₅ H ₁₂ (2)	160.0	370.0	100.0	650.0	69	6.19	7.15	16.60	222
C ₃ H ₈ (1) - iC ₅ H ₁₂ (2)	32.0	356.0	4.85	639.3	99	5.42	4.16	23.73	251
C ₃ H ₈ (1) - nC ₁₀ H ₂₂ (2)	40.0	460.0	25.0	1028.0	58	4.23	19.89	11.25	190
nC ₄ H ₁₀ (1) - nC ₁₀ H ₂₂ (2)	340.0	460.0	50.0	714.0	36	5.33	12.88	5.53	189
nC ₅ H ₁₂ (1) - Cyclo- hexane (2)	102.2	175.8	14.7	14.7	28	22.78	19.20	79.01	155
nC ₅ H ₁₂ (1) - Methycyclo- pentane (2)	97.16	158.72	14.7	14.7	44	9.82	5.85	15.32	155

TABLE XIV (Continued)

System	Temperature Range (°F)		Pressure Range (PSIA)		No. of Points	Percent Abs. Avg. Error			Reference No.
						K	K _{2nd}	L/F	
nC ₅ H ₁₂ (1) - Methylcyclohexane (2)	99.77	209.12	14.7	14.7	47	10.18	7.81	14.30	155
nC ₆ H ₁₄ (1) - Cyclohexane (2)	156.2	177.08	14.7	14.7	32	20.34	27.66		155
nC ₆ H ₁₄ (1) - Methylcyclopentane (2)	156.2	161.15	14.7	14.7	29	5.88	4.64		155
nC ₆ H ₁₄ (1) - Methylcyclohexane (2)	158.99	212.0	14.7	14.7	33	7.73	8.21		155
nC ₇ H ₁₆ (1) - Cyclohexane (2)	178.88	208.22	14.7	14.7	42	30.81	31.30		155
nC ₇ H ₁₆ (1) - Methylcyclohexane (2)	209.52	213.13	14.7	14.7	11	7.14	7.79		236
nC ₈ H ₁₈ (1) - 2-methylpentane (2)	50.0	104.0	0.23	6.60	48	4.23	7.71	10.42	131
nC ₈ H ₁₈ (1) - 3-methylpentane (2)	50.0	104.0	0.31	6.01	48	3.10	4.68	12.12	131

TABLE XIV (Continued)

System	Temperature Range (°F)		Pressure Range (PSIA)		No. of Points	Percent Abs. Avg. Error			Reference No.
						K	K _{2nd}	L/F	
nC ₈ H ₁₈ (1) - Ethylbenzene (2)	122.0	275.0	0.97	14.7	46	24.49	19.51	270	

TABLE XV

BENZENE, TOLUENE BINARY SYSTEMS DEVIATIONS IN K-VALUE PREDICTIONS

System	Temperature Range (°F)	Pressure Range (PSIA)	No. of Points	Percent Abs. Avg. Error			Reference No.
				K _{1st}	K _{2nd}	L/F	
Benzene (1) - CH ₄ (2)	150.0 → 150.0	100.0 → 4800.0	17	37.47	27.65	6.94	51
	298.22 → 442.4	288.19 → 3519.1	18	28.39	32.27	6.11	130
Benzene (1) - nC ₃ H ₈ (2)	100.0 → 400.0	20.0 → 850.0	73	7.75	9.92	25.70	64
Benzene (1) - nC ₇ H ₁₆ (2)	176.2 → 203.8	14.7 → 14.7	19	6.49	5.40	31.40	236
	124.7 → 141.44	3.48 → 7.73	20	5.93	6.15	25.61	162
	140.0 → 140.0	4.35 → 7.57	14	5.24	6.27	19.97	20
Benzene (1) - nC ₈ H ₁₈ (2)	179.8 → 238.7	14.7 → 14.7	19	9.84	8.71	34.39	236
Benzene (1) - CO ₂ (2)	104.0 → 104.0	107.0 → 1120.0	15	11.09	6.59	3.97	218
	77.0 → 104.0	129.6 → 1124.0	17	24.82	2.07	7.77	98
Benzene (1) - N ₂ (2)	167.0 → 257.0	900.86 → 4454.4	17	10.10	10.60	6.07	149
Toluene (1) - CO ₂ (2)	248.18 → 517.46	141.52 → 753.9	21	3.82	14.05	3.70	232
	100.6 → 399.0	48.4 → 2218.0	34	19.20	10.63	11.76	214

TABLE XV (Continued)

System	Temperature Range (°F)	Pressure Range (PSIA)	No. of Points	Percent Abs. Avg. Error			Reference No.
				K _{1st}	K _{2nd}	L/F	
Toluene (1) - H ₂ S(2)	100.0 → 400.0	29.50 → 1679.0	27	17.08	4.88	7.87	210
Toluene (1) - CH ₄ (2)	0.0 → 40.0	50.0 → 2500.0	24	33.87	19.88	3.13	129
	-100.0 → 0.0	100.0 → 3500.0	77	22.24	18.37	5.62	28
	300.74 → 518.0	439.1 → 3665.0	26	20.26	17.68	4.78	130
	150.0 → 150.0	100.0 → 5200.0	16	27.10	31.62	13.63	51
Toluene (1) - N ₂ (2)	104.0 → 391.0	514.0 → 14496.6	23	13.59	15.24	7.93	124

TABLE XVI

CYCLOPARAFFIN BINARY SYSTEM DEVIATIONS IN K-VALUE PREDICTIONS

System	Temperature Range (°F)	Pressure Range (PSIA)	No. of Points	Percent Abs. Avg. Error			Reference No.
				K _{1st}	K _{2nd}	L/F	
Methylcyclohexane (1) - CH ₄ (2)	-100.0 → 0.0	100.0 → 375.0	99	37.95	19.42	12.22	110
Ethylcyclohexane (1) - CH ₄ (2)	100.0 → 400.0	59.0 → 3007.0	37	21.71	21.62	15.91	203
Methylcyclohexane (1) - N ₂ (2)	100.0 → 400.0	63.2 → 2447.0	28	12.25	10.42	2.94	204
Ethylcyclohexane (1) - N ₂ (2)	100.0 → 400.0	63.0 → 2457.0	41	29.67	14.34	3.24	203
Methylcyclohexane (1) - H ₂ S (2)	100.0 → 400.0	38.40 → 1371.0	30	14.65	8.61	8.47	216
Ethylcyclohexane (1) - H ₂ S (2)	100.0 → 400.0	24.6 → 1813.0	27	18.98	5.46	5.97	204
Methylcyclohexane (1) - CO ₂ (2)	100.1 → 399.3	50.1 → 2160.0	31	13.22	9.69	8.88	216
Ethylcyclohexane (1) - CO ₂ (2)	100.0 → 400.0	25.4 → 2383.0	45	12.12	11.06	9.69	203

TABLE XVI (Continued)

System	Temperature Range (°F)	Pressure Range (PSIA)	No. of Points	Percent Abs. Avg. Error			Reference No.
				K _{1st}	K _{2nd}	L/F	
Cyclohexane (1) - nC ₅ H ₁₂ (2)	102.2 → 175.8	14.7 → 14.7	28	19.20	22.78	79.01	155
Methylcyclopentane (1) - nC ₅ H ₁₂ (2)	97.16 → 158.72	14.7 → 14.7	44	5.85	9.82	15.32	155
Methylcyclohexane (1) nC ₅ H ₁₂ (2)	99.77 → 209.12	14.7 → 14.7	47	7.81	10.18	14.30	155
Cyclohexane (1) - nC ₆ H ₁₄ (2)	156.2 → 177.08	14.7 → 14.7	32	27.66	20.34		155
Methylcyclopentane (1) - nC ₆ H ₁₄ (2)	156.02 → 161.15	14.7 → 14.7	29	4.64	5.88		155
Methylcyclohexane (1) - nC ₆ H ₁₄ (2)	158.99 → 212.0	14.7 → 14.7	33	8.21	7.73		155
Cyclohexane (1) - nC ₇ H ₁₆ (2)	178.88 → 208.22	14.7 → 14.7	42	31.30	30.81		155
Methylcyclohexane (1) - nC ₇ H ₁₆ (2)	209.52 → 213.13	14.7 → 14.7	11	7.79	7.14		236

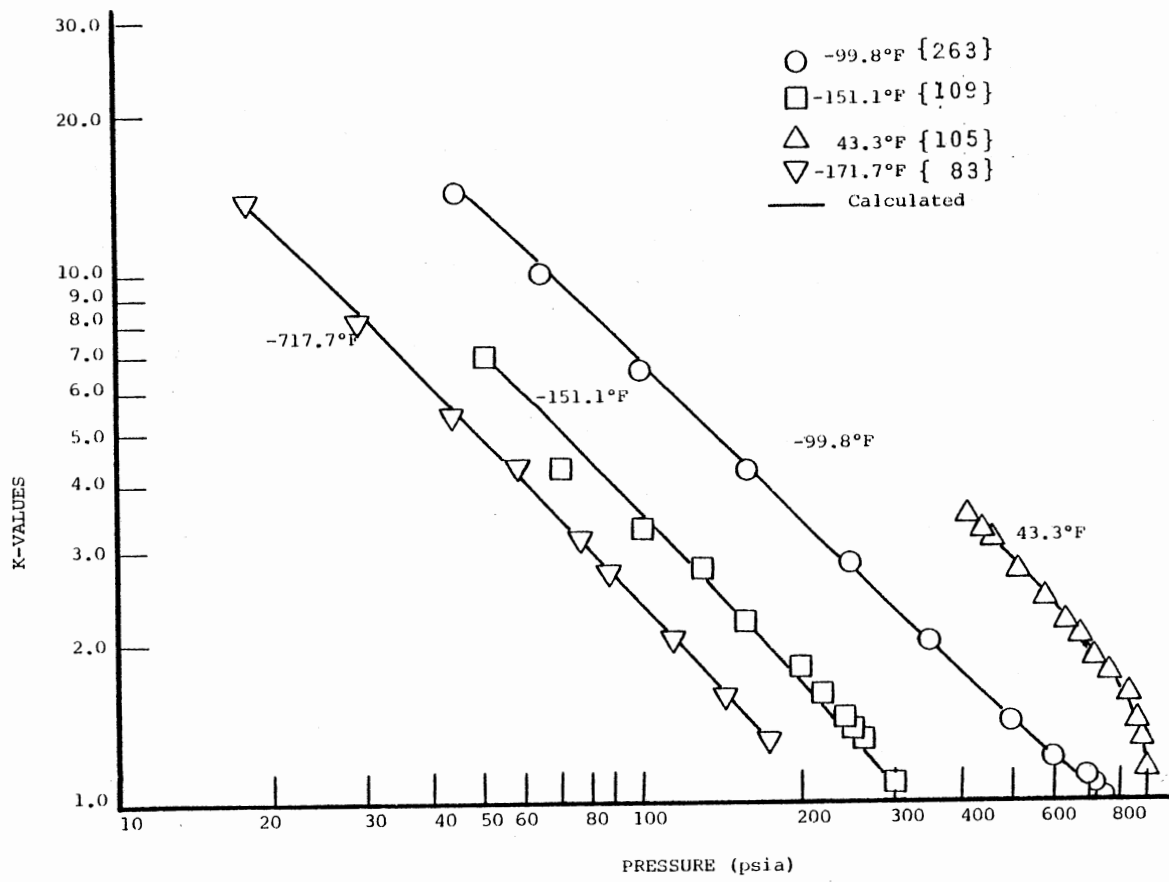


Figure 6. Comparison of Predicted and Experimental K-Values for Methane in the Methane-Ethane System

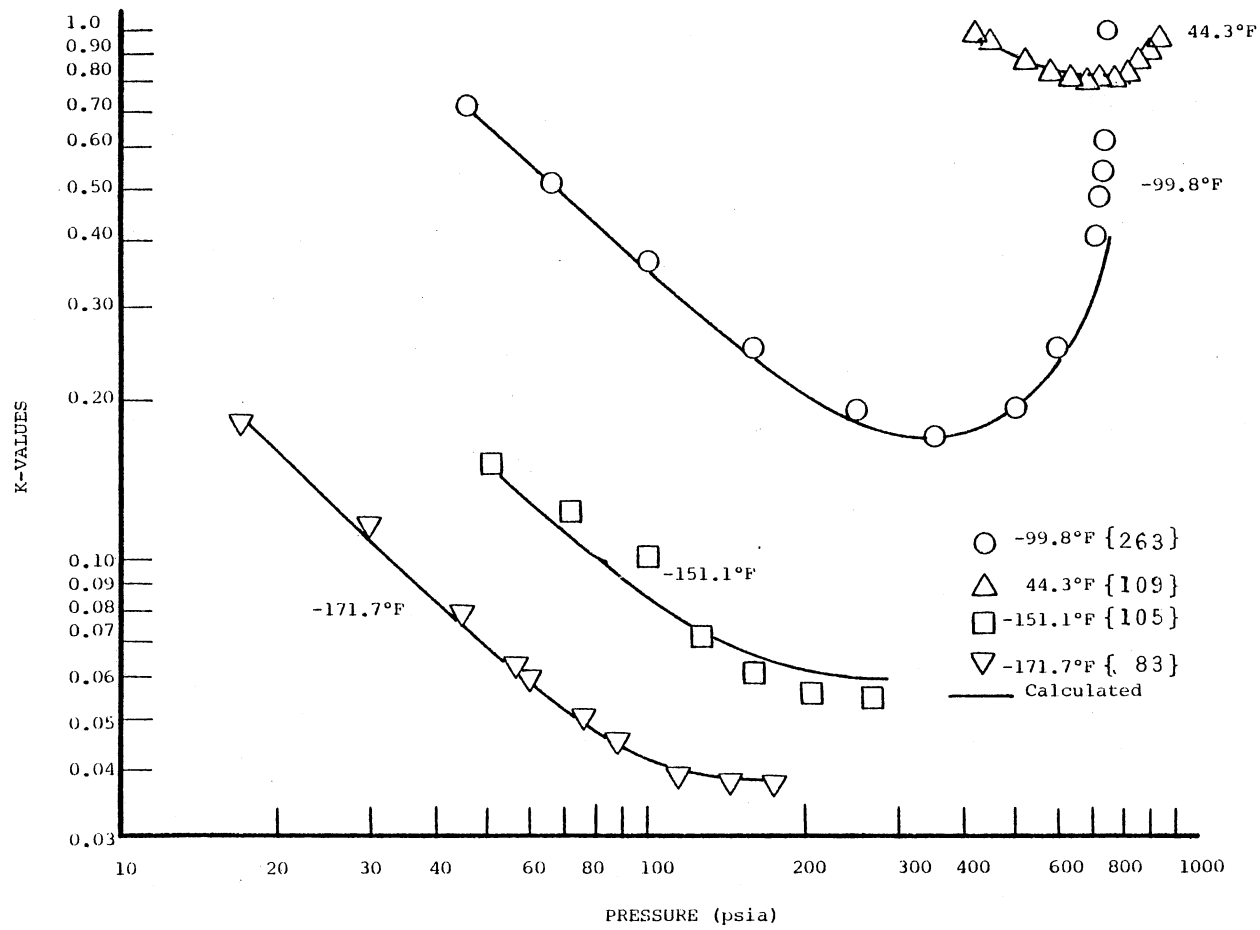


Figure 7. Comparison of Predicted and Experimental K-Values for Ethane in the Methane-Ethane System

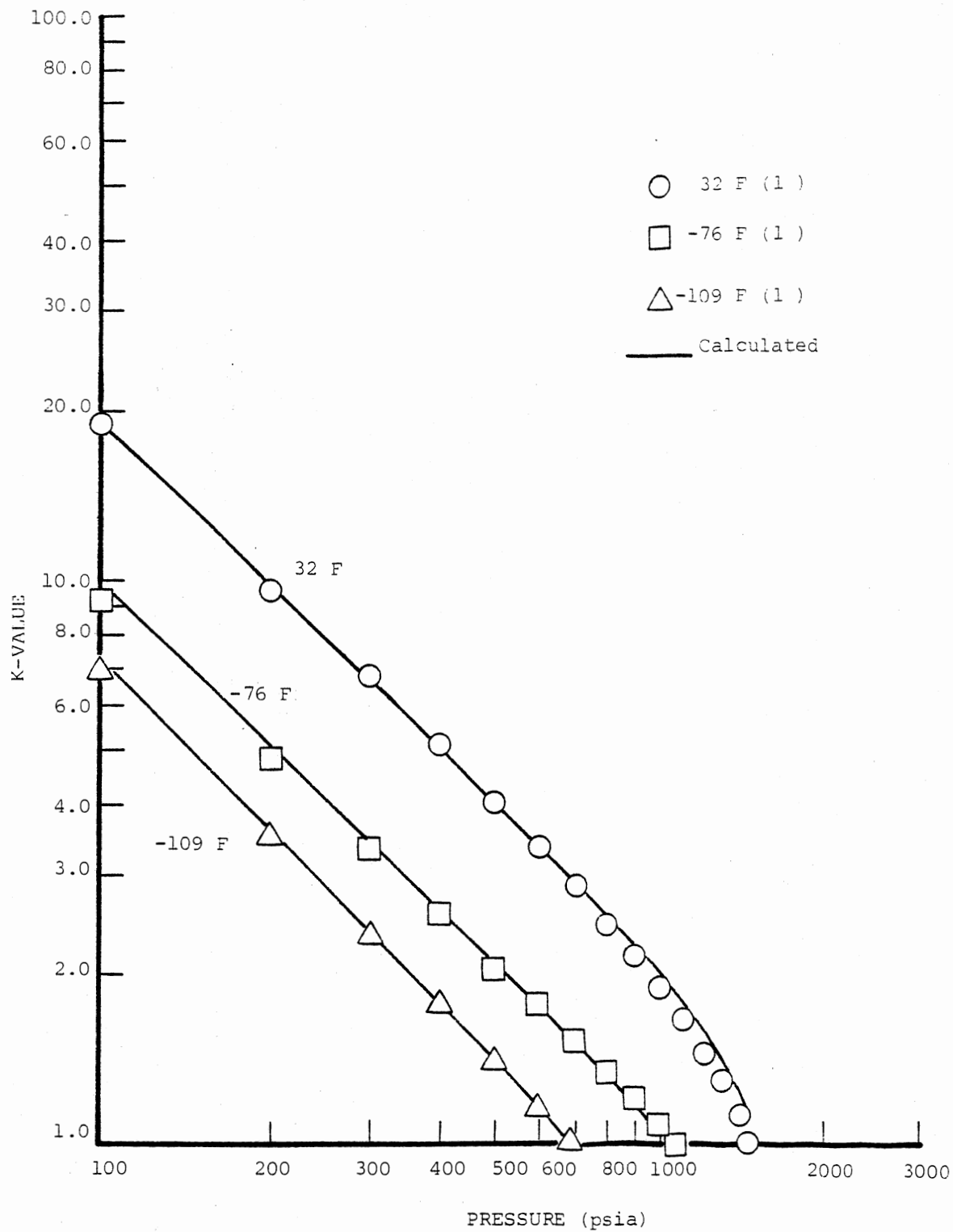


Figure 8. Comparison of Predicted and Experimental K-Values for Methane in the Methane-Propane System

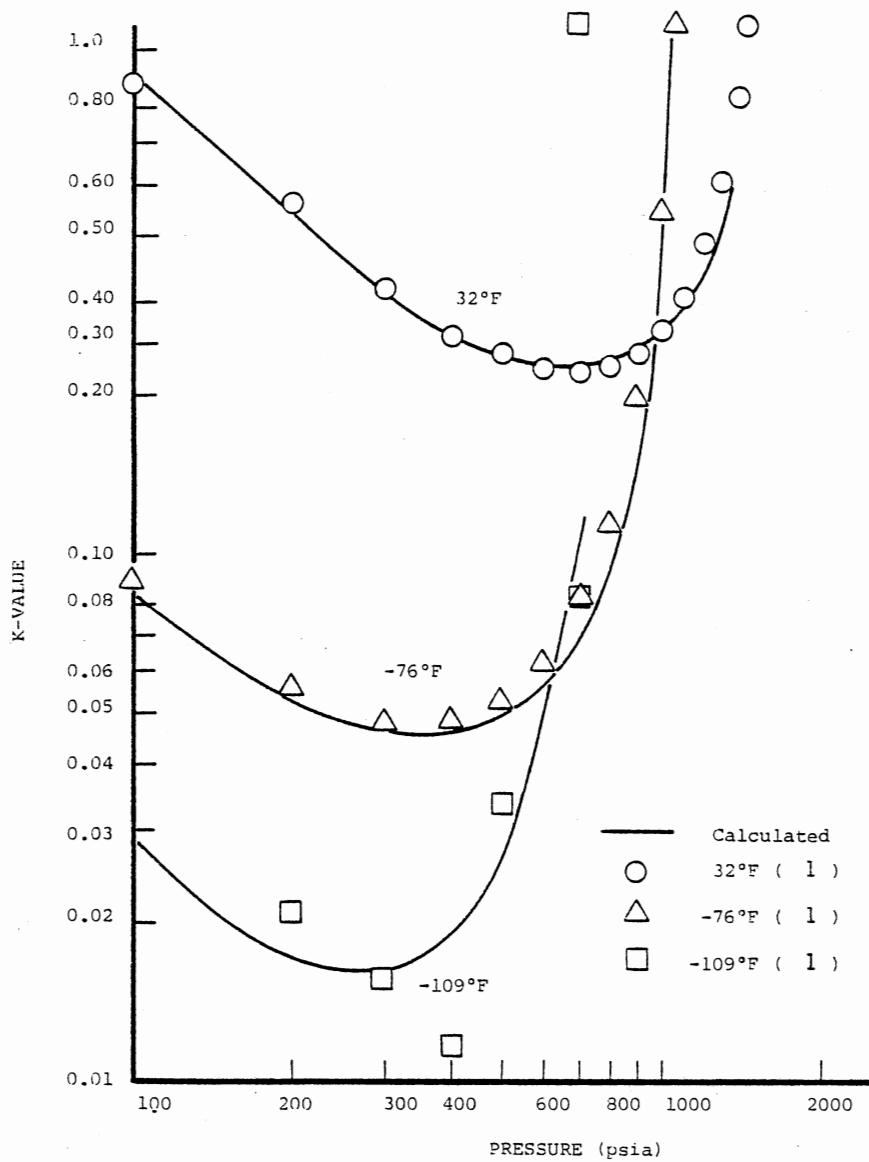


Figure 9. Comparison of Predicted and Experimental K-Values for Propane in the Methane-Propane System

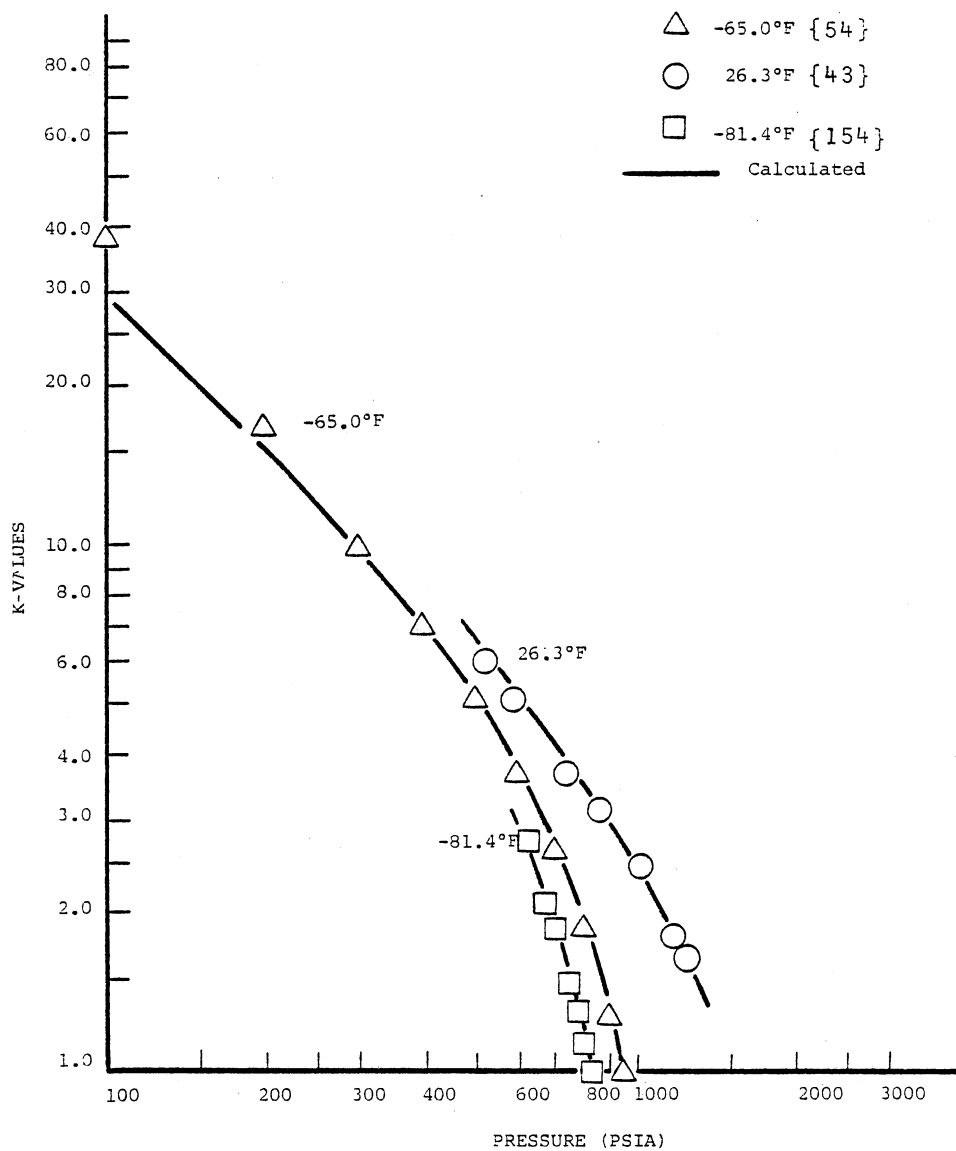


Figure 10. Comparison of Predicted and Experimental K-Values for Methane in the Methane-CO₂ System

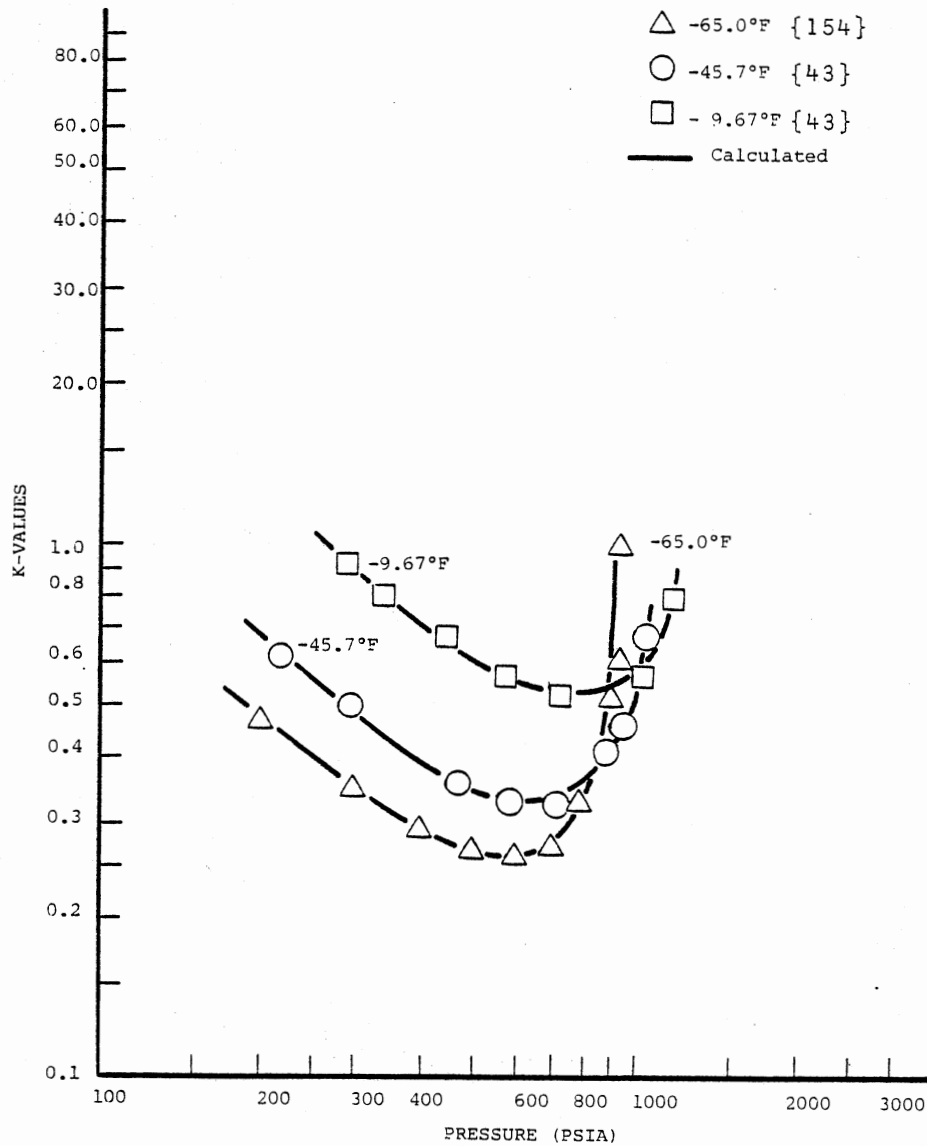


Figure 11. Comparison of Predicted and Experimental K-Values for Carbon Dioxide in the Methane-CO₂ System

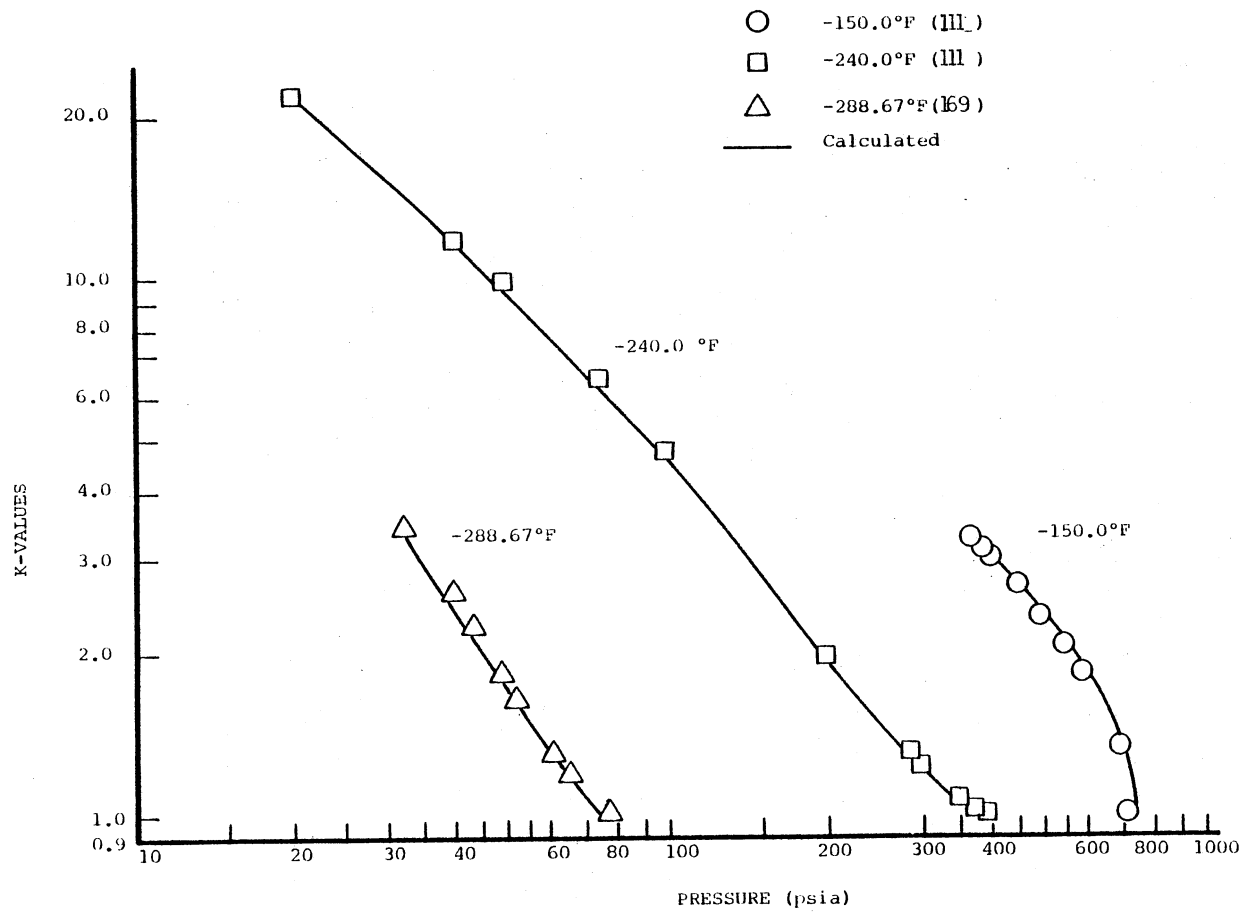


Figure 12. Comparison of Predicted and Experimental K-Values for Nitrogen in the Nitrogen-Methane System

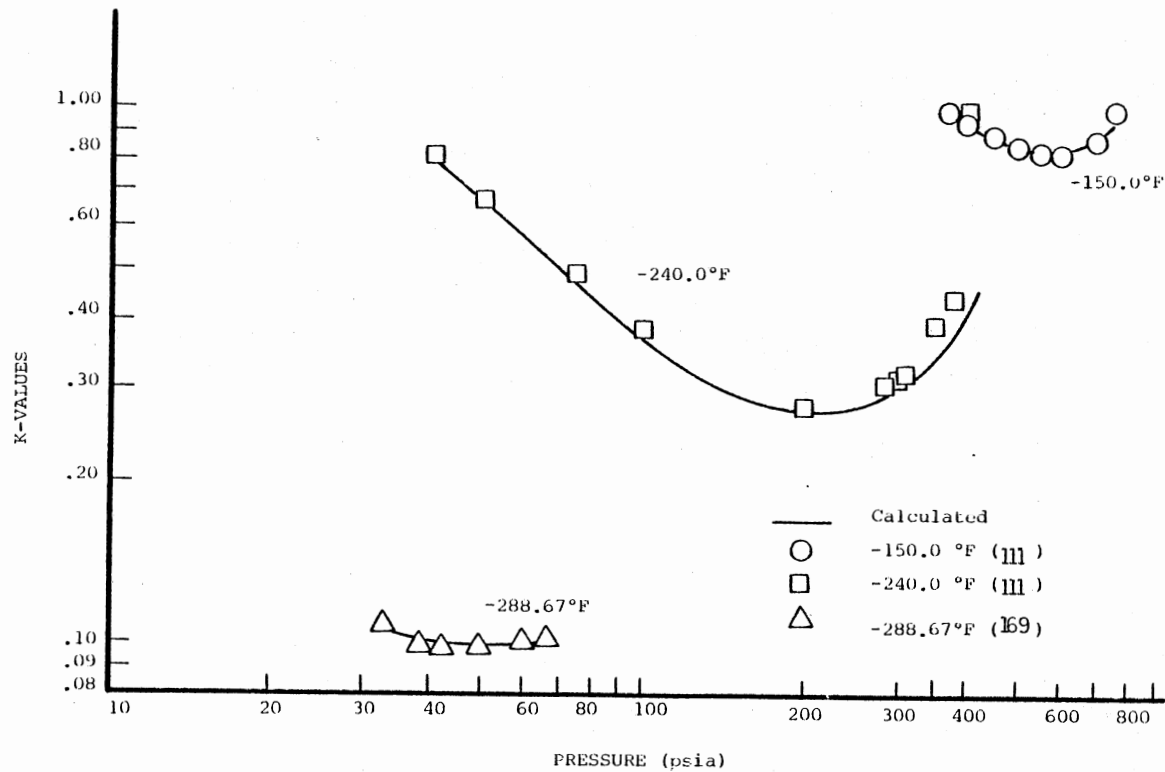


Figure 13. Comparison of Predicted and Experimental K-Values for Methane in the Nitrogen-Methane System

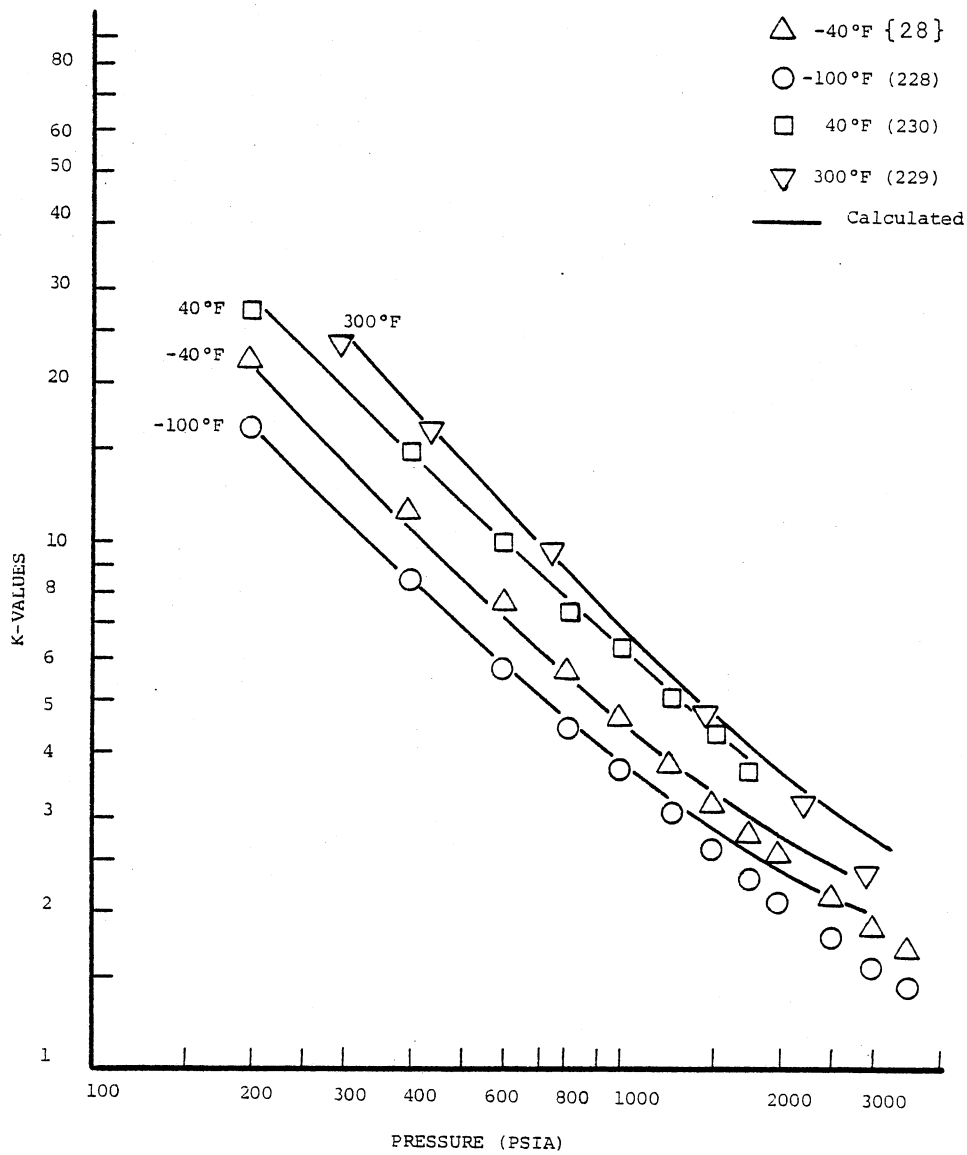


Figure 14. Comparison of Predicted and Experimental K-Values for Methane in the Methane-Toluene System

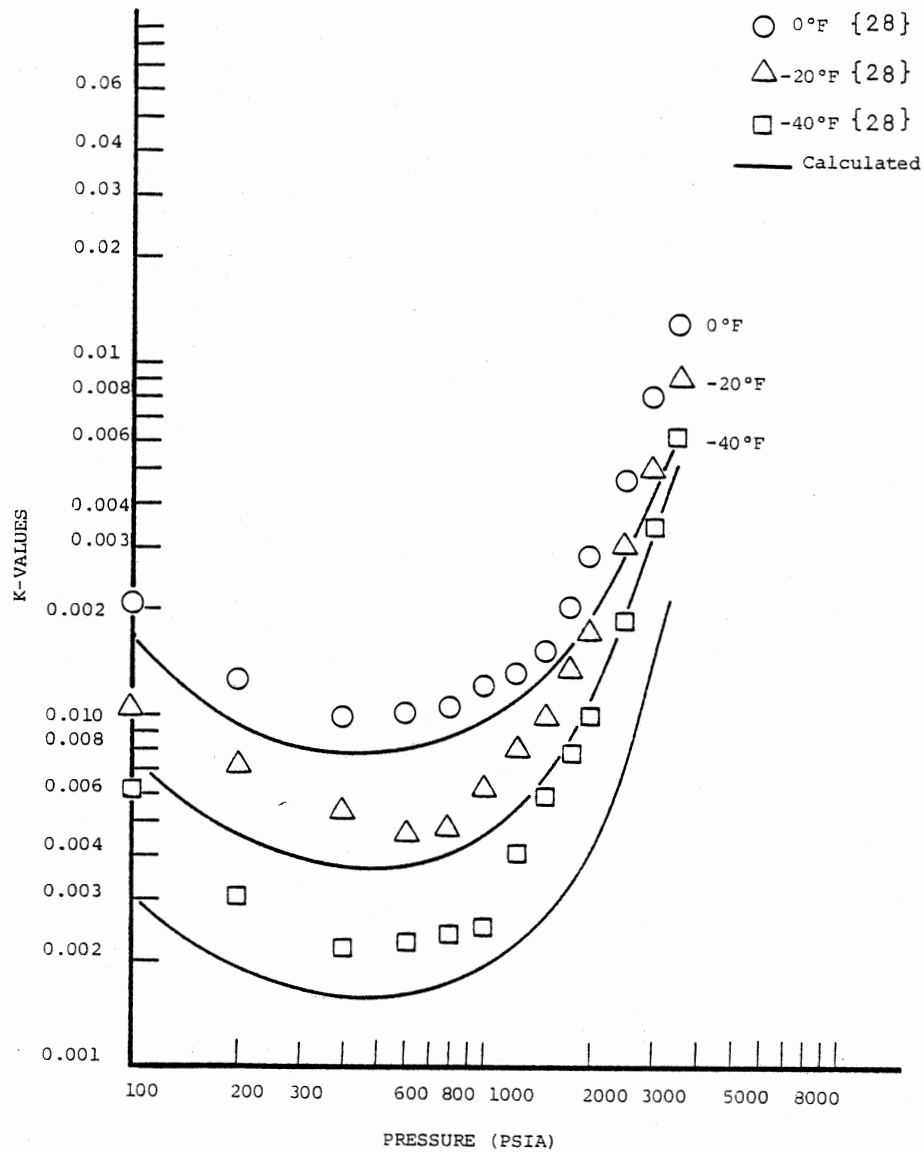


Figure 15. Comparison of Predicted and Experimental K-Values for Toluene in the Methane-Toluene System

absolute average deviation in predicted equilibrium ratios, liquid/feed ratios and the literature reference for each mixture are also given. The deviations in prediction of equilibrium K-ratios for components of selected binary mixtures is qualitatively shown in Figures 6 through 15.

Aqueous Light Hydrocarbon Systems

Mixtures of water with light hydrocarbons, carbon dioxide, hydrogen sulfide, nitrogen and carbon monoxide were used to derive the binary group interaction coefficients for the water rich liquid phase. The absolute average error in predicted phase composition for each phase was minimized. Table XVII gives a list of the systems evaluated, temperature and pressure range, number of points, and percent absolute average error in the smaller component concentration in each phase. Some of the nonhydrocarbon water binary group interaction coefficients for the PFGC equation were found to be temperature dependent and were fitted linearly with absolute temperature. The final values of the binary group interaction coefficients for aqueous systems and constants describing their dependence on temperature are included in Table XVIII.

Methanol and Glycol Systems

The PFGC equation of state has demonstrated the capability of handling systems containing methanol and glycols. Vapor liquid equilibrium data for methanol and glycol binary systems were used to derive the group interaction coefficients for the vapor and hydrocarbon-liquid and water-rich liquid phases. A summary of the results is presented in Tables XVIII and XIX. Percent absolute average errors in predicted

TABLE XVII

H_2O BINARY SYSTEMS DEVIATIONS IN PHASE
CONCENTRATION PREDICTIONS

System	Temperature Range (°F)		Pressure Range (PSIA)		No of Points	Percent Abs. Avg. Error in Smaller Component Conc.			Reference No.
						Vapor Phase	Hydrocarbon Liquid	Water	
$H_2O(1) - CH_4(2)$	100.0	460.0	387.6	9885.0	78	5.73			166
	25.0	100.0	23.2	92.3	12			0.94	194
	302.0	680.0	711.3	14226.0	45	7.33			243
	122.0	600.0	200.0	2450.0	16	3.49		1.84	269
$H_2O(1) - C_2H_6(2)$	100.0	460.0	200.0	10000.0	130	4.71			180
	100.0	340.0	400.0	10000.0	53			18.10	108
	392.0	712.0	2900.0	29007.0	12	18.51		14.36	42
$H_2O(1) - C_3H_8(2)$	60.0	280.0	14.7	511.7	76			11.64	10
	42.3	310.0	72.0	3000.0	240	7.16	12.90	10.51	108
$H_2O(1) - nC_4H_{10}(2)$	99.9	280.0	52.2	491.6	7	6.98	6.60	11.21	260
	100.0	460.0	20.0	10000.0	143		26.80	9.27	187
	671.0	687.2	3698.0	12038.0	5	9.36		16.86	42

TABLE XVII (Continued)

System	Temperature Range (°F)		Pressure Range (PSIA)		No of Points	Percent Abs. Avg. Error in Smaller Component Conc.			Reference No.
						Vapor Phase	Hydrocarbon Liquid	Water	
H ₂ O(1) - nC ₄ H ₁₀ (2)	100.0	280.0	52.2	934.7	115			21.80	126
H ₂ O(1) - nC ₅ H ₁₂ (2)	100.0	600.0	120.0	3000.0	32	9.81	31.66	18.50	269
H ₂ O(1) - nC ₆ H ₁₄ (2)	392.0	437.0	536.6	789.0	3	24.2			237
H ₂ O(1) - nC ₇ H ₁₆ (2)	392.0	473.0	413.4	984.8	5	16.6			237
H ₂ O(1) - nC ₈ H ₁₈ (2)	437.0	512.9	530.8	1112.5	5	13.66			237
	101.0	435.3	17.7	1285.0	6	5.99	18.10		268
H ₂ O(1) - nC ₉ H ₂₀ (2)	392.0	536.0	301.7	1305.4	6	18.67			237
H ₂ O(1) - nC ₁₀ H ₂₂ (2)	392.0	564.8	264.0	1446.0	7			21.43	237
H ₂ O(1) - nC ₁₂ H ₂₆ (2)	392.0	597.2	275.6	1929.0	6			17.20	237
H ₂ O(1) - nC ₁₆ H ₃₄ (2)	392.0	640.4	250.9	2320.6	6			28.80	237
H ₂ O(1) - nC ₂₀ H ₄₂ (2)	482.0	665.9	612.1	2683.2	7			17.00	237
H ₂ O(1) - C ₂ H ₄ (2)	95.0	212.0	66.9	7701.0	52	15.84			18
	99.9	280.2	497.2	4989.2	37	8.62		3.82	6

TABLE XVII (Continued)

System	Temperature Range (°F)		Pressure Range (PSIA)		No of Points	Percent Abs. Avg. Error in Smaller Component Conc.			Reference No.
						Vapor Phase	Hydrocarbon Liquid	Water	
H ₂ O(1) - C ₂ H ₄ (2)	100.0	250.0	17.0	543.0	49	10.75		44	
	334.4	662.0	1851.9	36740.0	35	28.40	36.30	226	
H ₂ O(1) - C ₃ H ₆ (2)	70.0	220.0	21.7	496.7	77	14.23		9	
	101.1	220.3	37.0	1252.5	26	12.98	8.67	144	
	330.8	572.0	1469.0	13887.8	16	5.63	33.62	226	
H ₂ O(1) - CO ₂ (2)	60.0	500.0	100.0	2940.0	40	8.50	6.26	269	
	77.0	212.0	251.3	746.6	22	4.22		38	
	122.0	662.0	2900.0	50759.0	68	12.46	24.52	246	
	302.0	662.0	1469.6	22044.0	116	9.27	16.02	244	
H ₂ O(1) - H ₂ S(2)	100.0	600.0	600.0	3000.0	31	13.49	11.90	269	
	100.0	600.0	50.0	2000.0	18	12.01	3.55	269	
	100.0	340.0	100.0	5000.0	55	16.56	19.28	253	
	86.0	338.0	250.0	340.0	34	15.28	23.10	22	

TABLE XVII (Continued)

System	Temperature Range (°F)		Pressure Range (PSIA)		No of Points	Percent Abs. Avg. Error in Smaller Component Conc.			Reference No.
						Vapor Phase	Hydrocarbon Liquid	Water	
H ₂ O(1) - N ₂ (2)	100.0	600.0	50.0	2000.0	16	7.84		3.81	269
H ₂ O(1) - CO(2)	100.0	600.0	50.0	2000.0	18	9.68		14.90	269

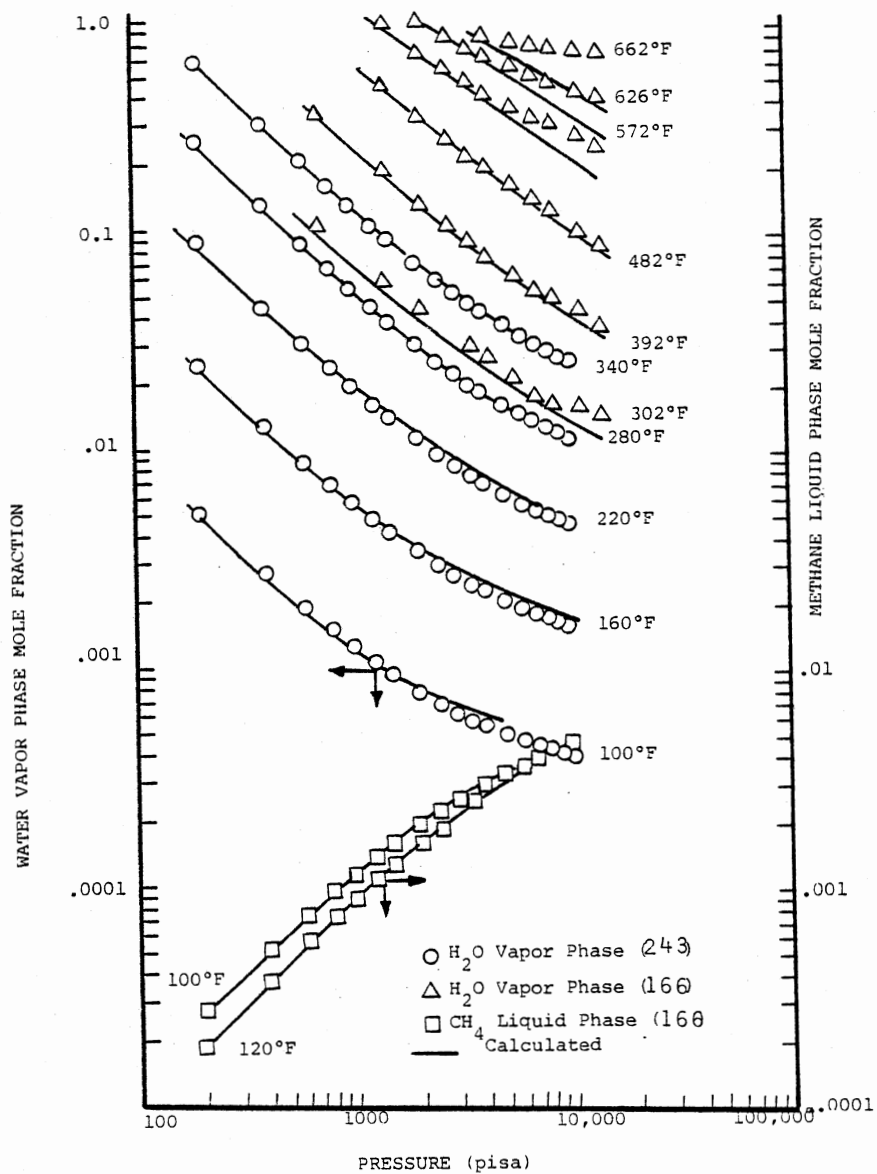


Figure 16. Comparison of Predicted and Experimental Phase Solubilities for the Methane-Water System

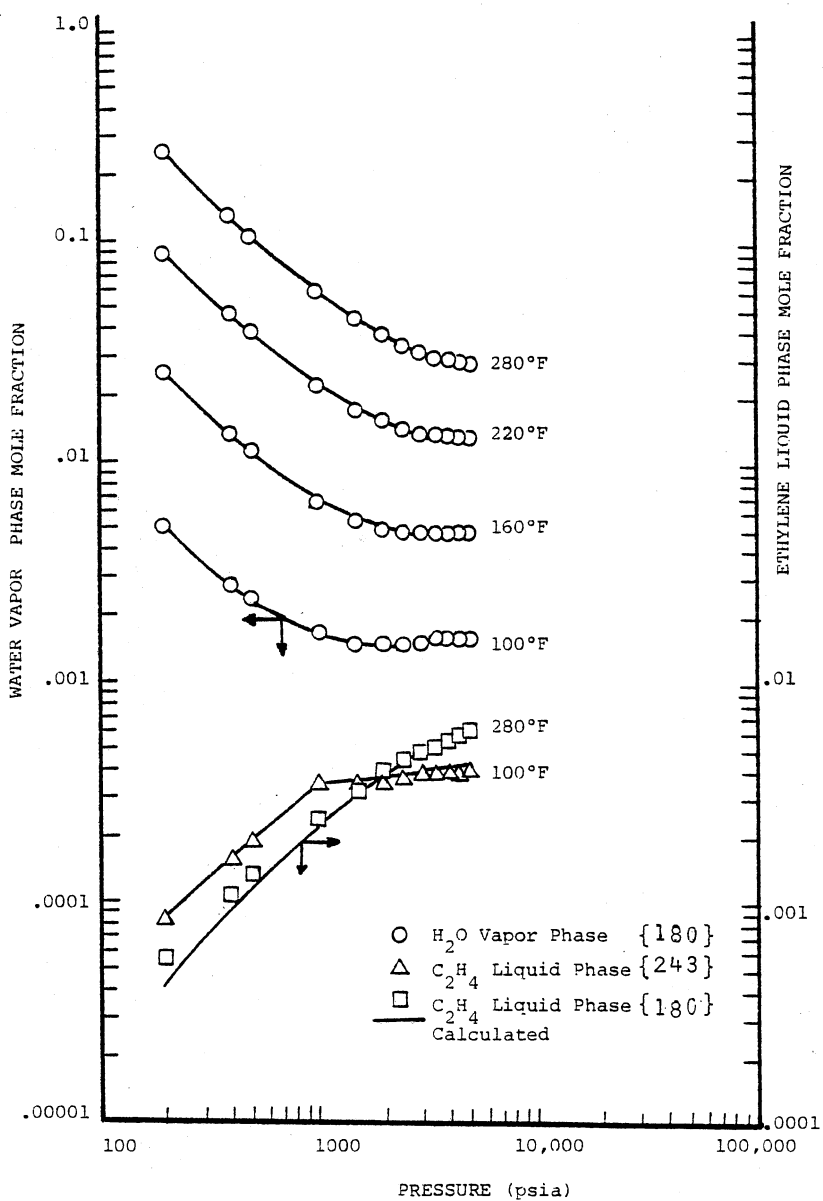


Figure 17. Comparison of Predicted and Experimental Phase Compositions for the Ethylene-Water System

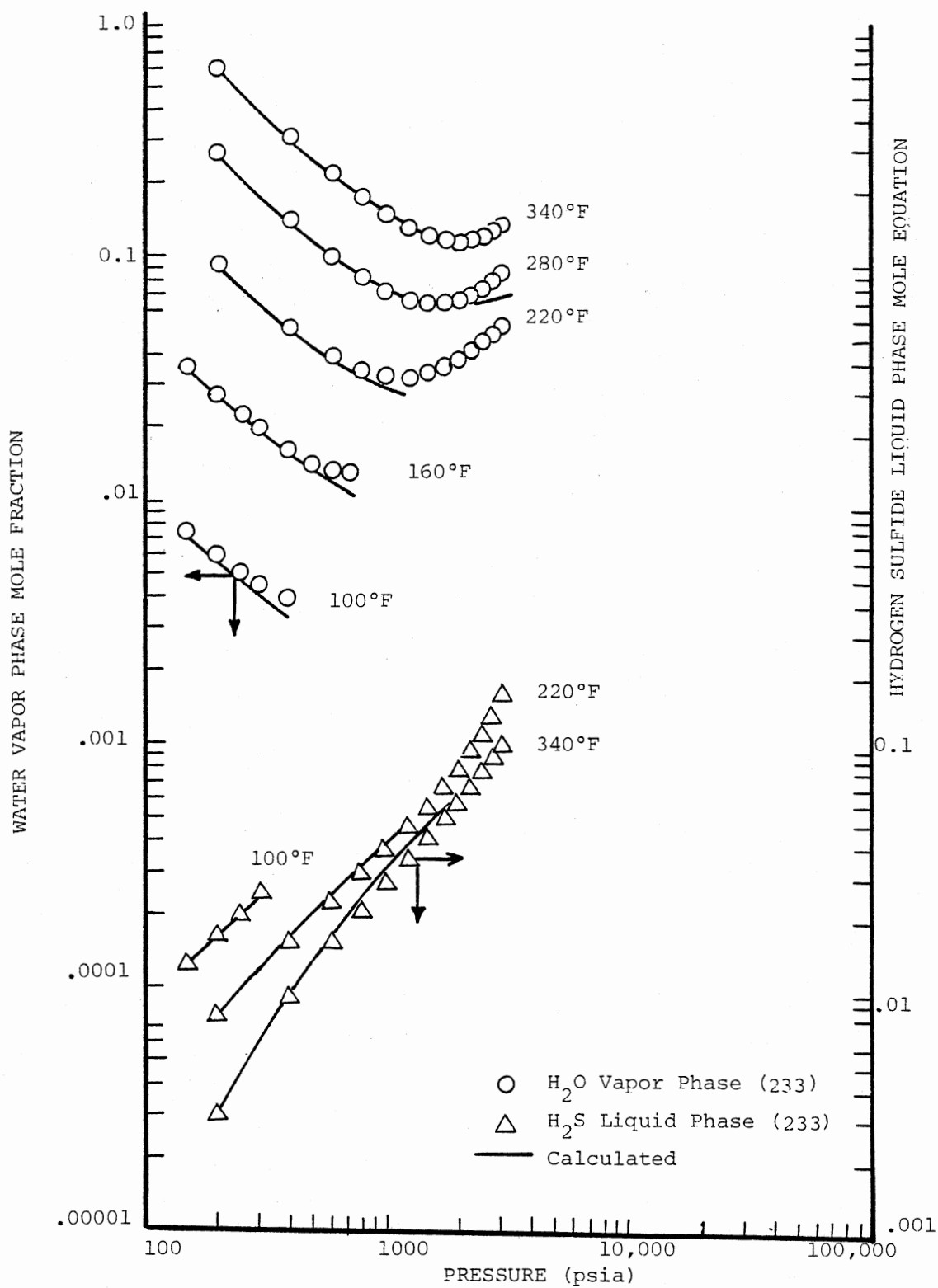


Figure 18. Comparison of Predicted and Experimental Phase Compositions for the Hydrogen Sulfide - Water System

TABLE XVIII

METHANOL BINARY SYSTEM DEVIATIONS IN K-VALUE PREDICTIONS

System	Temperature Range (°F)		Pressure Range (PSIA)		No. of Points	Percent Abs. Avg. Error			Reference No.
						K _{MeOH}	K _{2nd}	L/F	
Methanol (1) - Water (2)	212.0	482.0	15.1	994.0	51	16.78	7.62	34.1	73
	150.8	189.9	14.7	14.7	9	10.11	7.87	23.4	71
	116.8	198.1	6.77	14.7	29	12.74	9.67	14.58	246
	148.4	205.6	14.7	14.7	18	11.29	7.40	13.27	89
	152.42	201.4	14.7	14.7	14	13.71	5.65	21.95	275
	152.24	192.79	14.7	14.7	12	10.72	9.61	11.47	252
	150.8	203.0	14.7	14.7	10	12.82	14.73	16.24	99
	148.5	212.0	14.7	14.7	26	19.73	5.42	22.79	41
	205.5	358.2	44.1	164.6	110	14.35	9.75	24.86	82
	149.6	198.3	14.7	14.7	18	16.34	11.67	28.81	119
150.2	206.3	14.7	14.7	16	18.65	14.48	42.61	136	
Methanol(1) - H ₂ S(2)	-13.27	32.0	29.4	196.96	22		0.32	5.02	60
Methanol(1) - N ₂ (2)	76.73	98.33	514.4	922.9	8	7.99		1.88	60
Methanol(1) - CO ₂ (2)	77.0	77.0	31.7	873.8	11	24.3	6.14	26.8	97
	4.73	4.73	73.92	239.5	4		16.32	8.4	60
Methanol(1) - CH ₄ (2)	25.0	70.0	200.0	4000.0	57	12.5			92

TABLE XVIII (Continued)

System	Temperature Range (°F)		Pressure Range (PSIA)		No. of Points	Percent Abs. Avg. Error			Reference No.
						K	K _{2nd}	L/F	
Methanol(1) - C ₂ H ₆ (2)	-13.0	212.0	146.9	881.8	25	21.77	14.39	6.33	117
Methanol(1) - C ₂ H ₄ (2)	-45.1	-25.0	14.7	264.5	16		8.24*		234
Methanol(1)									
Isopentane (2)	75.6	88.9	14.7	14.7	16	34.57	31.80		164
Methanol(1) - Benzene (2)	144.9	159.2	14.7	14.7	10	30.29	25.88	55.40	88
Methanol(1) - Toulene (2)	148.1	213.1	14.7	14.7	10	13.59	21.08		11

*Indicate percent absolute average error in component mole fraction.

TABLE XIX

GLYCOL BINARY SYSTEM DEVIATIONS IN K-VALUE PREDICTIONS

System	Temperature Range (F)	Pressure Range (F)	No. of Points	Percent Abs. K. glycol	Abs. Avg. Error K ₂	Error L/F	Reference No.
Ethyleneglycol(1) - H ₂ O(2)	162.3 → 385.9	4.41 → 14.44	71	14.30	11.89	7.40	249
Diethyleneglycol(1)-H ₂ O(2)	117.0 → 240.0	1.93 → 14.70	20	21.79	17.72	-	66
Triethyleneglycol(1)-H ₂ O(2)	140.0 → 520.0	1.93 → 14.70	60	17.46	28.75	8.52	49
Triethyleneglycol(1)-CH ₄ (2)	50.0 → 120.0	100.0 → 2000.00	41	-	14.60	-	222
Ethyleneglycol(1)-CO ₂ (2)	78.0 → 220.0	219.0 → 1057.00	12	10.62	-	2.01	135
Triethyleneglycol(1)-CO ₂	32.0 → 86.0	14.7 → 734.00	18	15.52	-	4.91	133
Ethyleneglycol(1)-H ₂ S(2)	84.0 → 160.0	99.0 → 780.0	13	8.61	-	2.34	135
Triethyleneglycol(1)-H ₂ S(2)	120.0 → 200.0	14.7 → 164.7	15	12.89	-	4.16	17

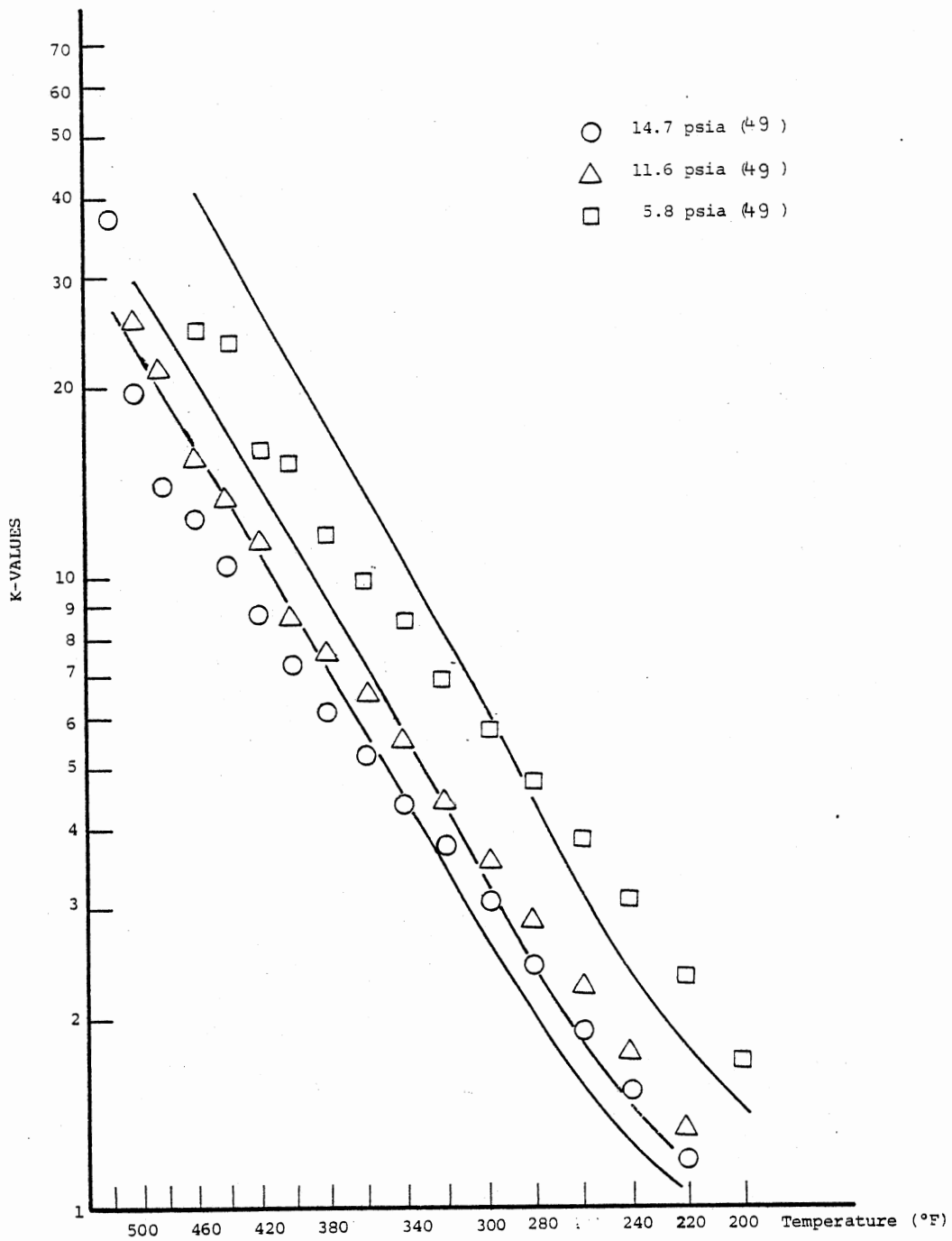


Figure 19. Comparison of Predicted and Experimental K-Values for Water in the TEG-Water System

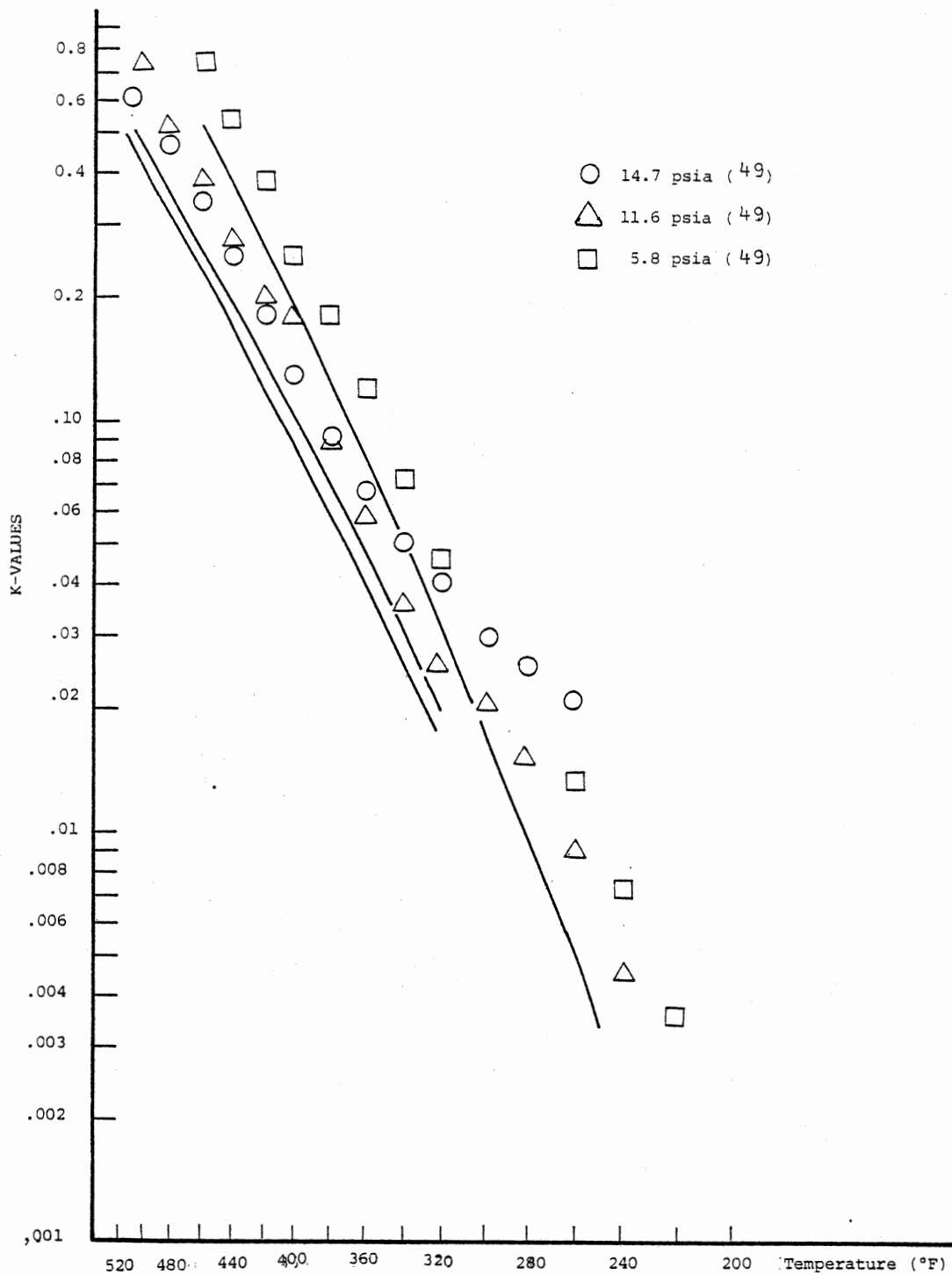


Figure 20. Comparison of Predicted and Experimental K-Values for TEG-Water System

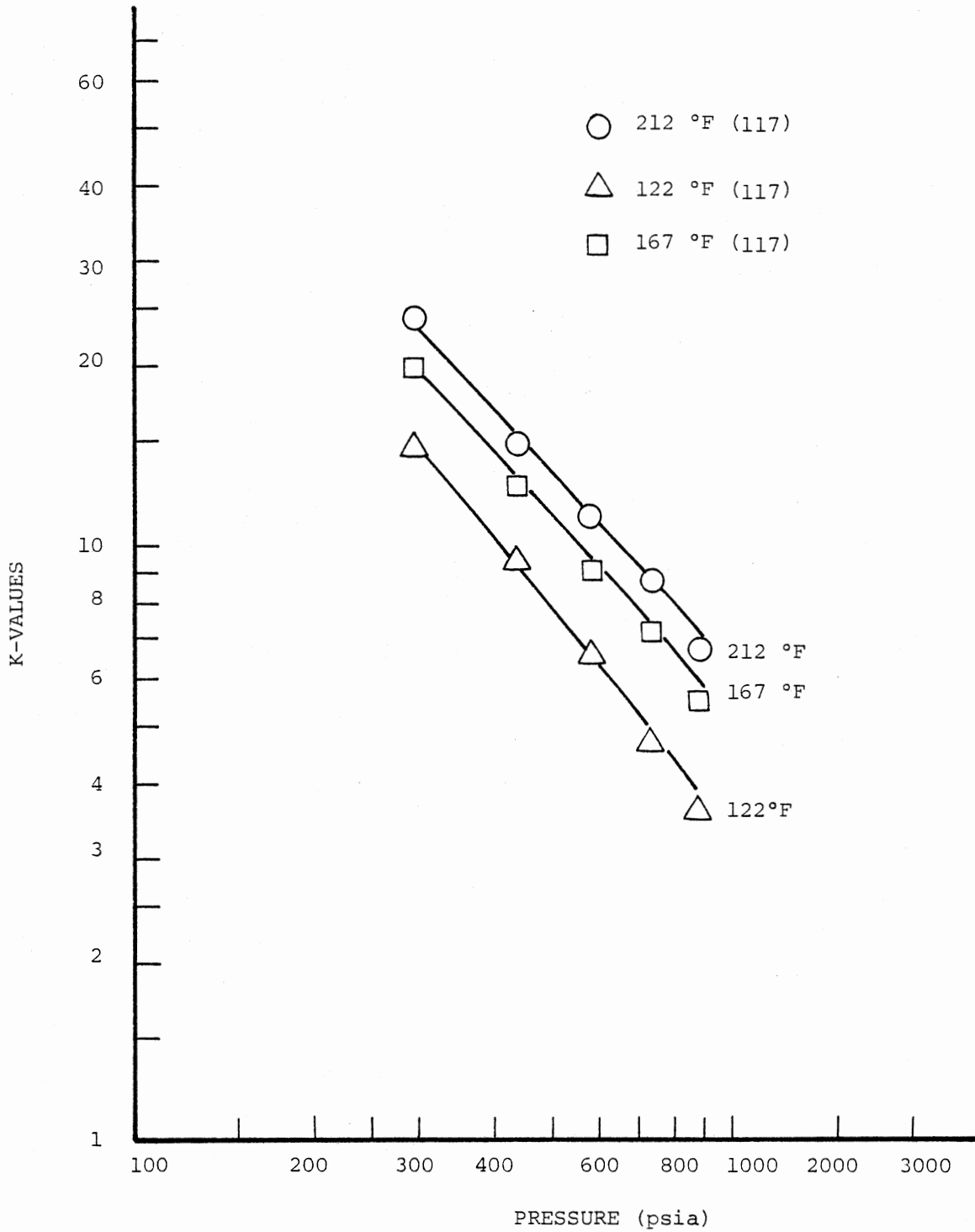


Figure 21. Comparison of Predicted and Experimental K-Values for Ethane in the Methanol-Ethane System

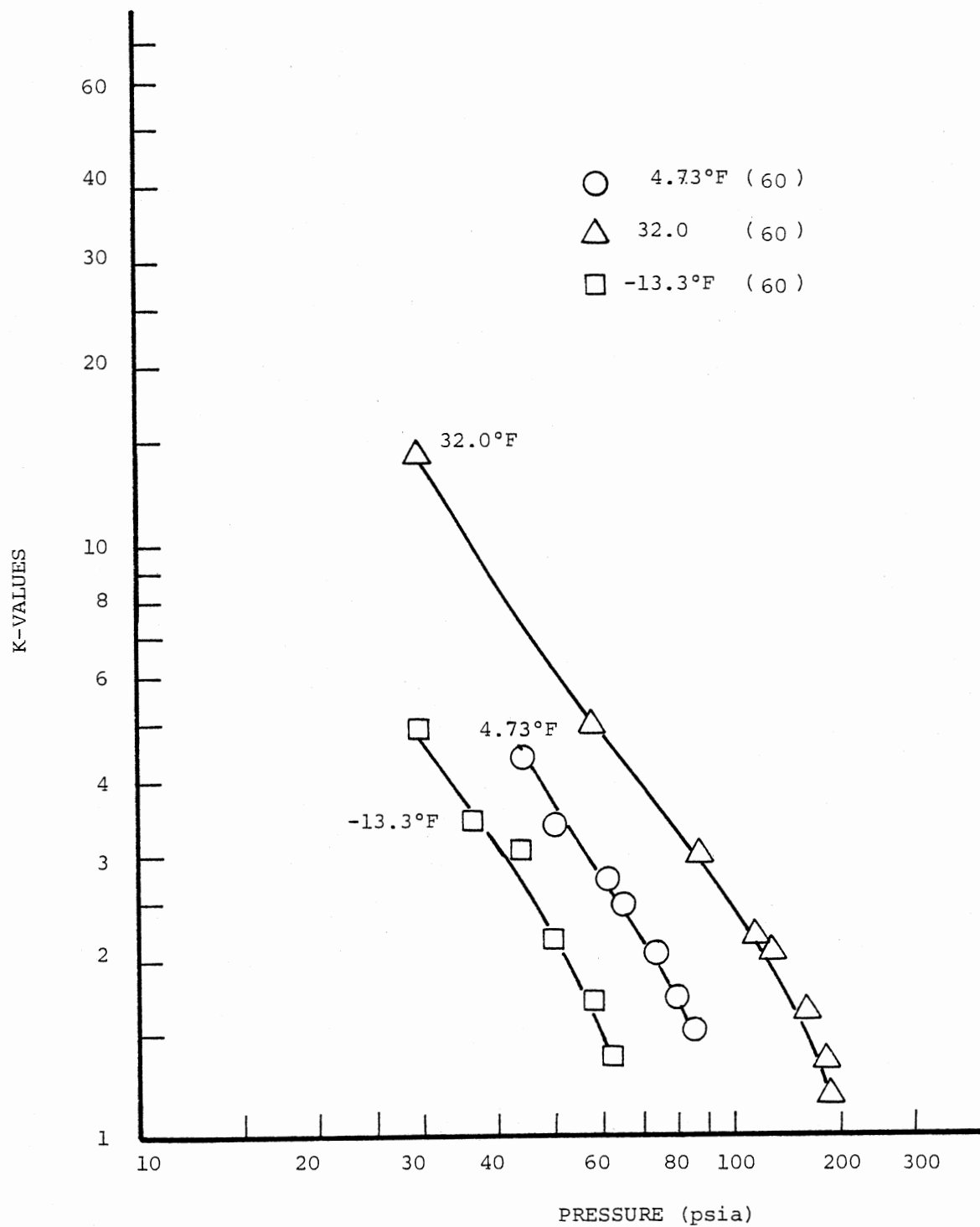


Figure 22. Comparison of Predicted and Experimental K-Values for Hydrogen Sulfide in the Methanol-H₂S System

equilibrium K-ratios, pressure and temperature ranges, number of points and references to the sources of data are included in the tables. Figures 19 through 20 qualitatively show the difference between experimental and calculated equilibrium K-ratios for selected methanol and glycol systems. The group parameters and binary group interaction coefficients for methanol and glycols are included in Table VII and VIII.

Multicomponent Test Mixtures

Several multicomponent test mixtures were used to evaluate the group parameters and the binary group interaction coefficients for the PFGC equation of state fitted to binary vapor liquid equilibrium data. Five selected systems are presented as test mixtures in Table XX.

Test Mixture I is used to show the comparison of predicted and experimental vapor phase water solubilities for typical light hydrocarbons containing carbon dioxide. The results are shown in Figure 23. Test Mixture II is a simulated natural gas mixture. Deviations in equilibrium K-ratios for each component in Test Mixture II are given in Figure 24. Test Mixture III was used to evaluate the equilibrium liquid and vapor phase densities for a typical sour gas system. The experimental and calculated liquid and vapor densities are compared in Table XXI. The prediction of phase equilibrium of a high nitrogen content synthetic natural gas was evaluated using Test Mixture IV. Comparison of calculated and experimental bubble point pressures is shown in Figure 25. The liquid volume fraction for Test Mixture IV was also evaluated and the results are given in Figure 26. Test Mixture V is a synthetic oil with the carbon dioxide content varying from 20 to 97 percent. Bubble point pressures at two different temperatures

TABLE XX

NOMINAL COMPOSITIONS OF MULTICOMPONENT TEST MIXTURES

Component	Moles In Test Mixture II (218)	Moles In Test Mixture III (218)	Moles In Test Mixture IV (118)	Moles In Test Mixture V (249)	Moles In Test Mixture I (57)
Methane	84.13	70.592	54.99	34.67	86.90
Ethane	4.67	6.860	7.09	3.13	7.40
Propane	2.34	2.967	3.65	3.96	2.20
i-Butane	--	--	--	--	0.51
n-Butane	0.93	--	2.06	5.95	0.43
n-Pentane	0.93	--	1.97	4.06	0.25
n-Hexane	--	--	--	3.06	0.18
n-Heptane	--	--	--	4.95	0.13
n-Octane	--	--	--	4.97	--
n-Decane	--	--	--	30.21	--
n-Tetradecane	--	--	--	5.04	--
Propylene	--	0.002	--	--	--
Nitrogen	7.00	7.026	30.25		
Carbon Dioxide	--	1.996	--	24.3 + 893.0	2.10
Hydrogen Sulfide	--	10.559	--	--	--
Water	--	--	--	--	100.00

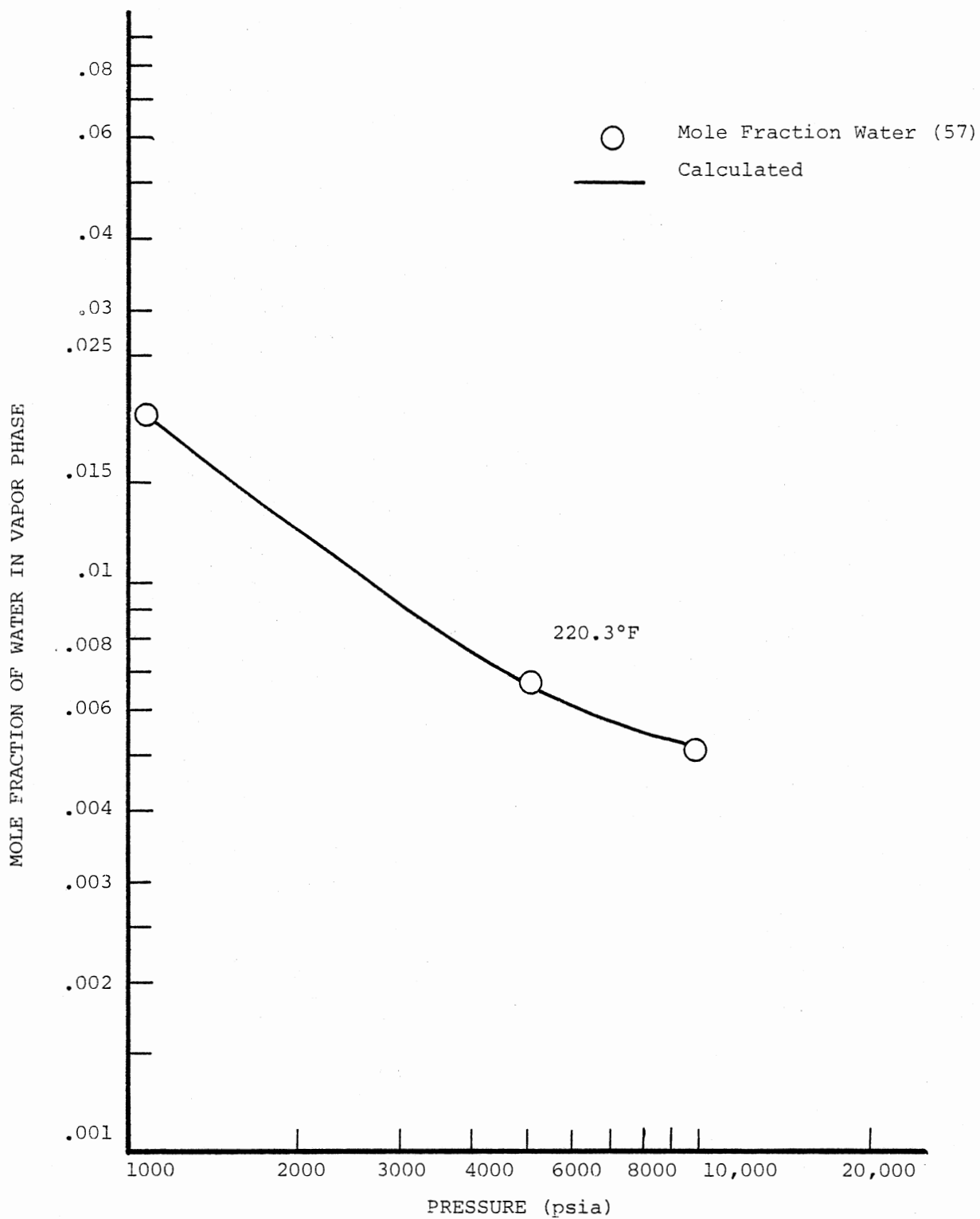


Figure 23. Comparison of Predicted and Experimental Vapor Phase Water Solubilities for Test Mixture I at 220.3 °F

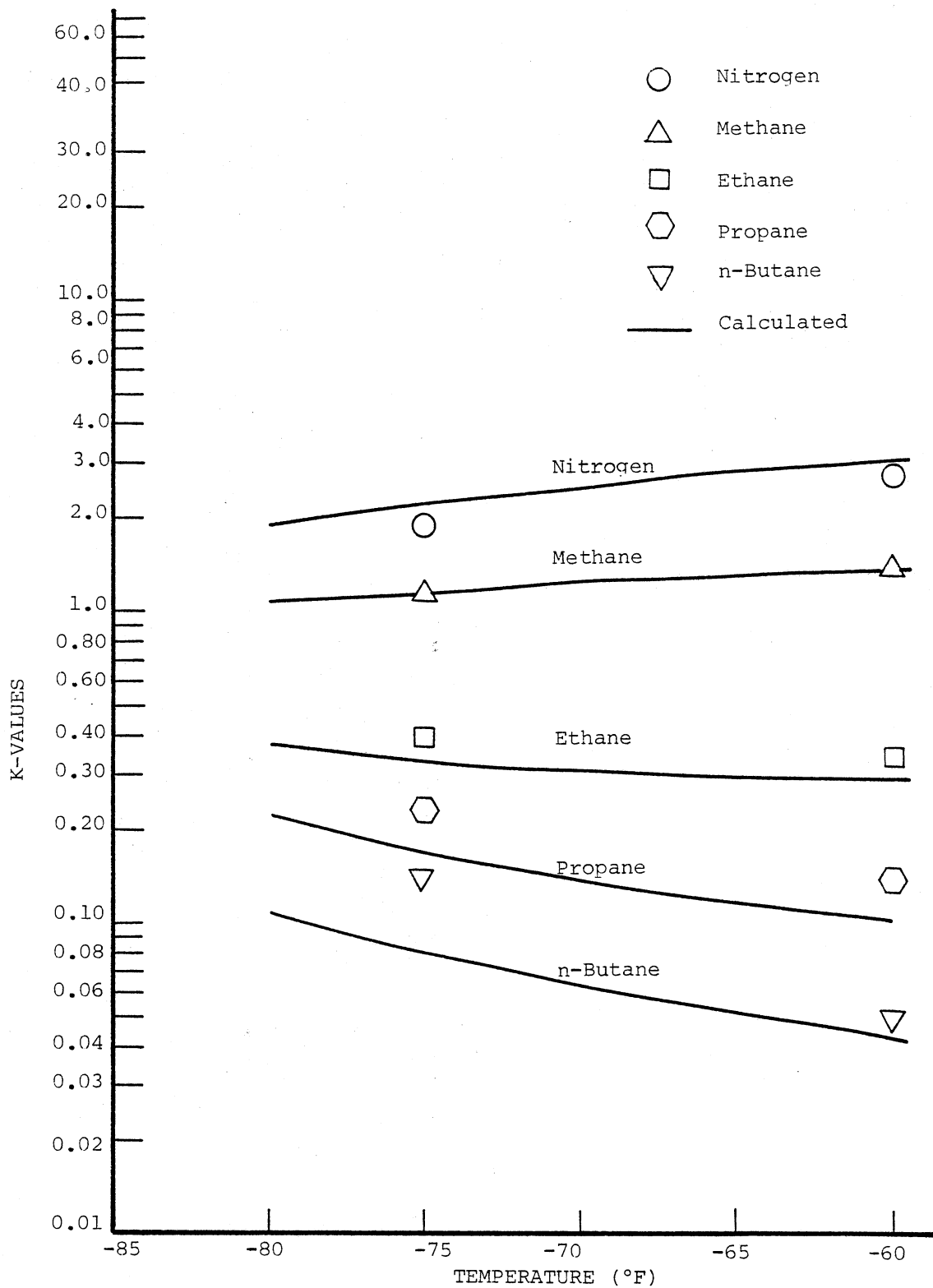


Figure 24. Comparison of Predicted and Experimental K-Values for Components of Test Mixture II at 998 psia (218)

TABLE XXI
 COMPARISON OF EXPERIMENTAL AND CALCULATED
 EQUILIBRIUM PHASE DENSITIES FOR
 TEST MIXTURE III (218)

Pressure (PSIA)	Temperature (DEG F)	Equilibrium Phase Densities (lb/ft ³)			
		Liquid		Vapor	
		Experimental	Calculated	Experimental	Calculated
398	-125.0	30.62	34.30	2.599	2.580
550	-100.0	30.66	33.46	3.588	3.881
599	- 99.3	29.79	31.13	4.050	4.347
716	- 74.9	30.80	31.69	4.695	5.033
799	- 75.0	29.59	28.75	5.587	5.978
901	- 50.0	30.79	29.67	6.033	6.530
1000	- 50.0	29.68	26.31	7.231	8.125
Percent Average Error		6.5		6.8	

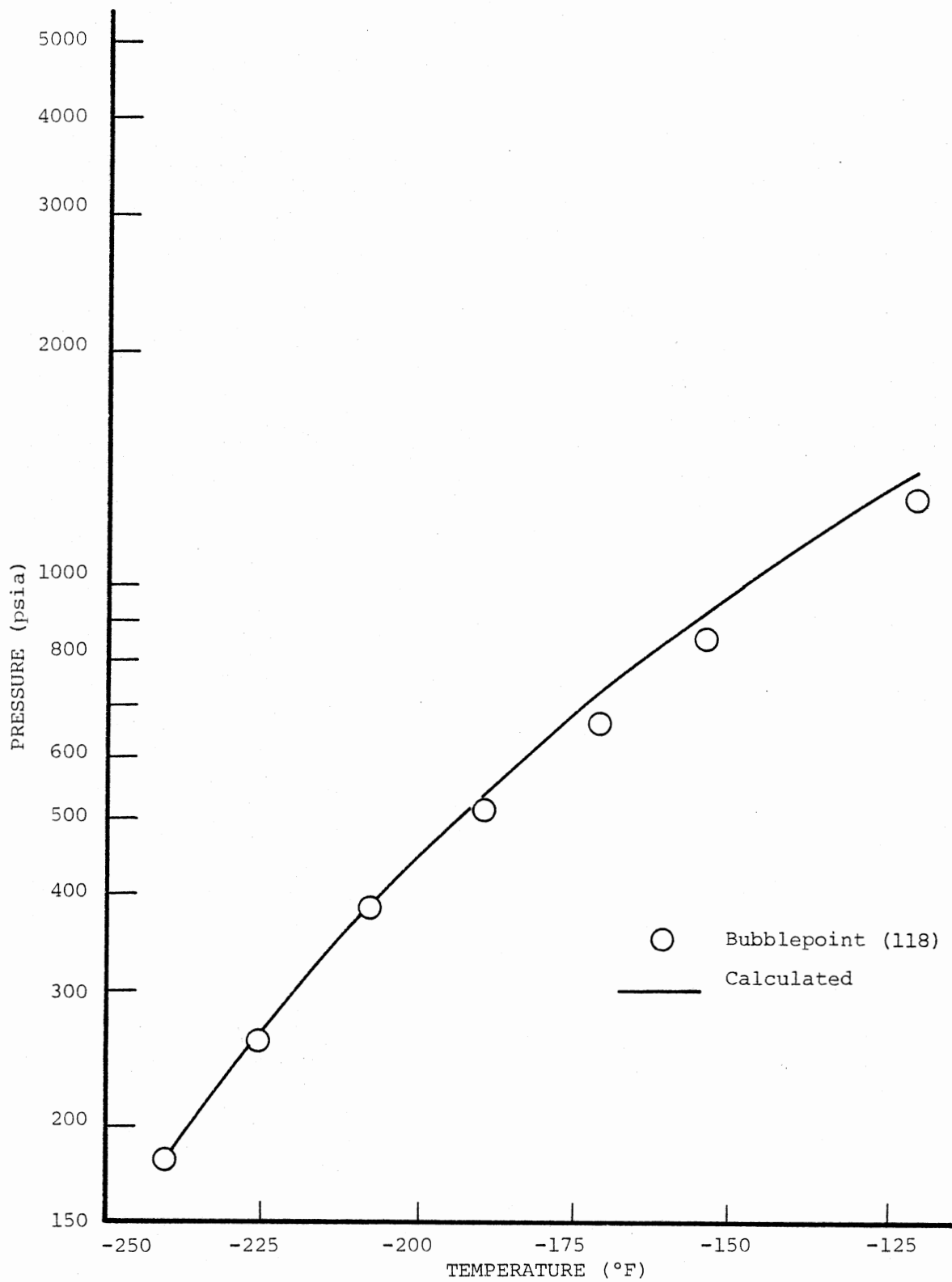


Figure 25. Comparison of Predicted and Experimental Bubble Point Pressures for Test Mixture IV

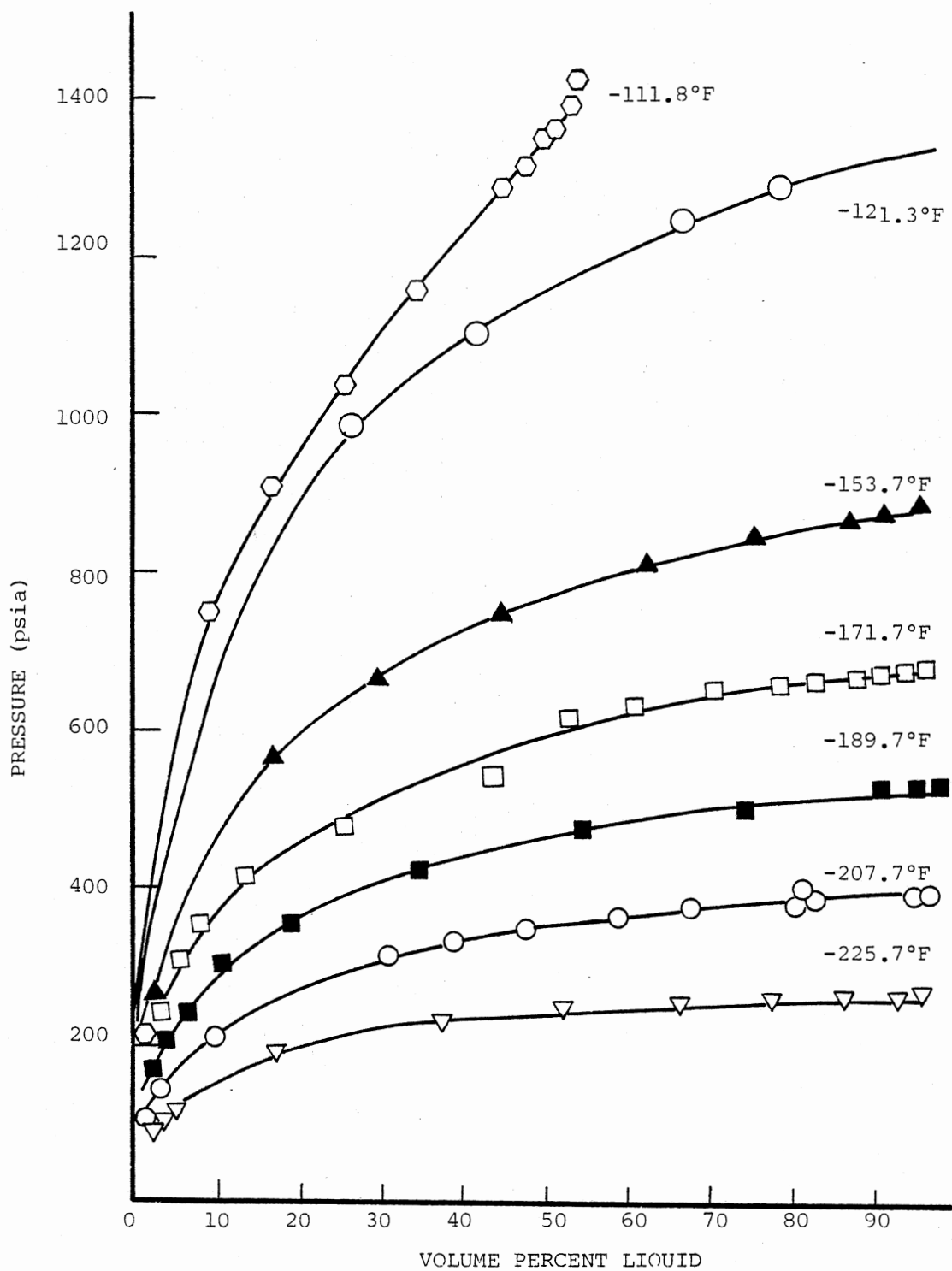


Figure 26. Comparison of Predicted and Experimental Volume Percent Liquid for Test Mixture IV (118)

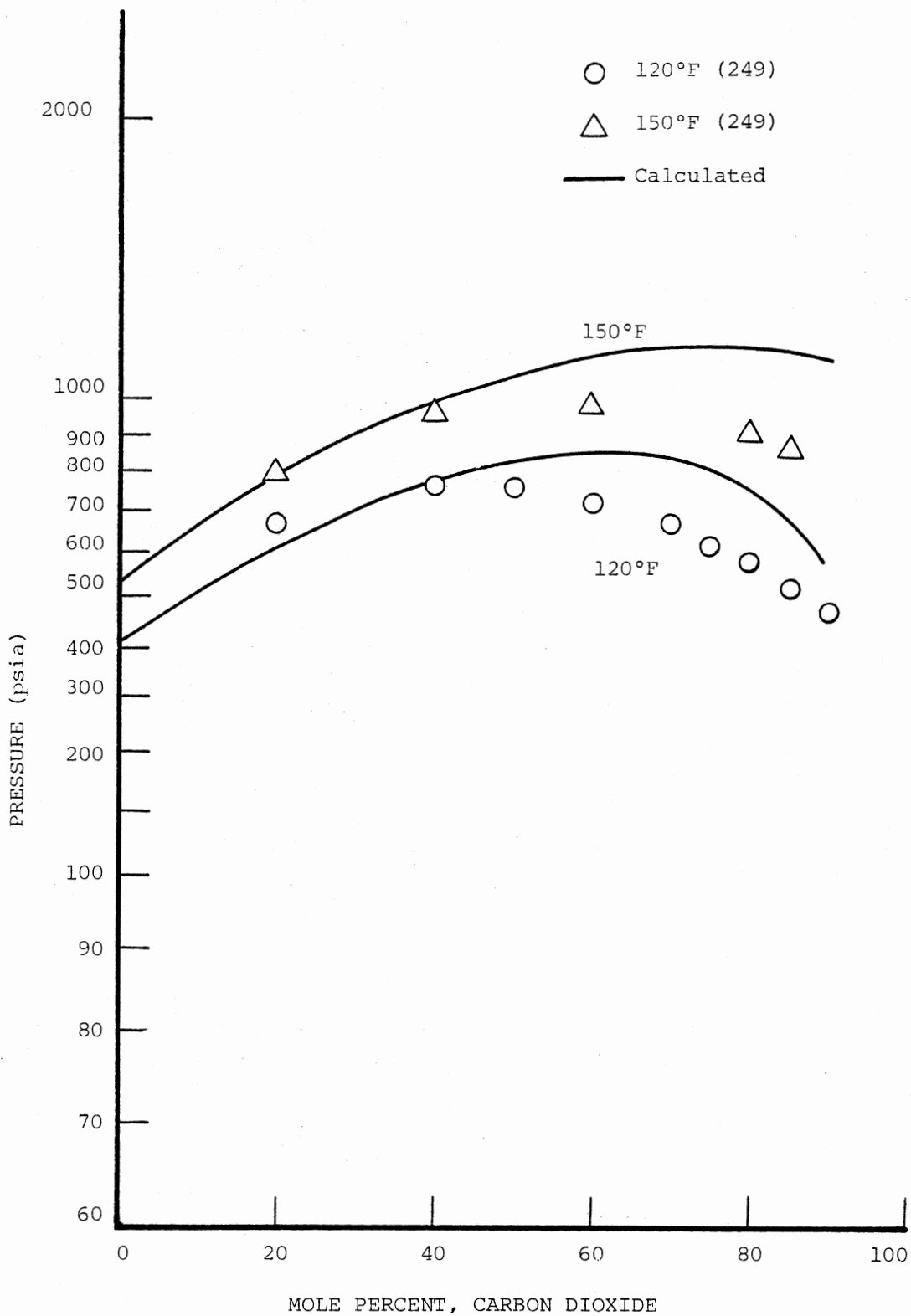


Figure 27. Comparison of Predicted and Experimental Bubble Point Pressures for Test Mixture V

were calculated and compared to experimental data. Deviations in bubble point pressures for different quantities of carbon dioxide are shown in Figure 27.

Prediction of Hydrate Forming Conditions for Pure Components

The mathematical model for prediction of hydrate forming conditions conceived by Van der Waals and Platteeuw (256) and developed by Parrish and Prausnitz (170) was used with the activity coefficient correction suggested by Menten, Parrish and Sloan (148). The reference properties used in the hydrate model are reported in Table XXII. The PFGC equation of state was used to predict gas phase fugacities, aqueous liquid phase gas solubilities, and the activity coefficient of water required by the hydrate model. Table XXIII gives the final values of the three Kihara parameters for each hydrate forming pure component. These parameters are based on minimizing the error in hydrate forming temperature conditions over the range of available data. The temperature and pressure range, number of points used, absolute average deviation in predicted hydrate forming temperatures and literature reference for each pure component is also included in Table XXIII. The comparison of experimental and calculated hydrate forming conditions for the pure components is graphically presented in Figures 28 through 38.

Multicomponent Hydrate Forming Conditions Prediction

As suggested by Ng and Robinson (159), a proportionality constant and an interaction constant were introduced into the equations used by

TABLE XXII

REFERENCE THERMODYNAMIC PROPERTIES OF THE EMPTY
HYDRATE (β) AND LIQUID WATER (L) AT 0°C AND
ZERO PRESSURE RELATIVE TO ICE (α) (170)

	Structure I	Structure II
$\mu_W^\beta - \mu_W^\alpha$ (cal/mol)	302.0	211.0
$h_W^\beta - h_W^\alpha$ (cal/mol)	275.0	193.0
$v_W^\beta - v_W^\alpha$ (cc/mol)	3.0	3.4
$h_W^L - h_W^\alpha$ (cal/mol)	1436.3	---
$C_P^L - C_P^\beta$ (cal/mol-°K)	9.11 - 0.0336(T-273.1)	--

TABLE XXIII

OPTIMAL KIHARA PARAMETERS AND DEVIATIONS IN PURE COMPONENT
HYDRATE FORMING TEMPERATURE PREDICTIONS

Compound Name	Optimal Kihara Parameters For Hydrate Prediction			Temperature Range (°F)	Pressure Range (°F)	No. of Points	Abs. Avg. Error In Temperature	Reference No.
	a (Å)	σ (Å)	ϵ/k (°K)					
Methane	0.30	152.76	3.2398	12.60 → 55.0	260.00 → 1419.00	18	1.2	45
				32.00 → 56.4	383.00 → 1567.00	4	0.5	195
				54.50 → 83.2	1395.00 → 9875.00	10	1.1	146
Ethane	0.40	175.36	3.3261	44.10 → 57.6	141.00 → 478.40	4	2.0	191
				14.70 → 56.0	45.40 → 396.00	24	1.3	45
				32.50 → 54.7	79.00 → 368.00	9	0.8	195
Propane	0.68	200.94	3.3030	10.50 → 39.0	14.47 → 58.24	19	1.95	45
				34.10 → 39.3	34.90 → 60.00	3	0.90	191
Isobutane	0.80	220.57	3.1244	32.05 → 35.42	16.66 → 24.45	24	0.52	219
n-Butane	0.75	169.41	3.4862	37.20 → 59.7	297.30 → 1989.90	18	2.20	215
Ethylene	0.47	172.87	3.1941	32.00 → 64.4	81.40 → 792.10	25	1.45	34
				62.78 → 81.14	683.40 → 8935.00	25	1.27	36
Propylene	0.65	202.42	3.2304	31.80 → 33.7	67.92 → 86.90	12	1.35	32
Nitrogen	0.35	126.31	3.2198	24.80 → 64.2	1587.00 → 13902.00	43	2.40	35
Oxygen	0.36	166.37	2.7673	28.80 → 47.8	1477.00 → 4702.00	28	2.50	37
Carbon Dioxide	0.72	167.47	2.9681	33.00 → 49.5	192.00 → 627.00	19	1.33	45
Hydrogen Sulfide	0.36	204.59	3.2000	31.30 → 85.1	13.50 → 324.70	7	2.06	233
				33.80 → 44.7	15.90 → 29.50	4	1.94	120

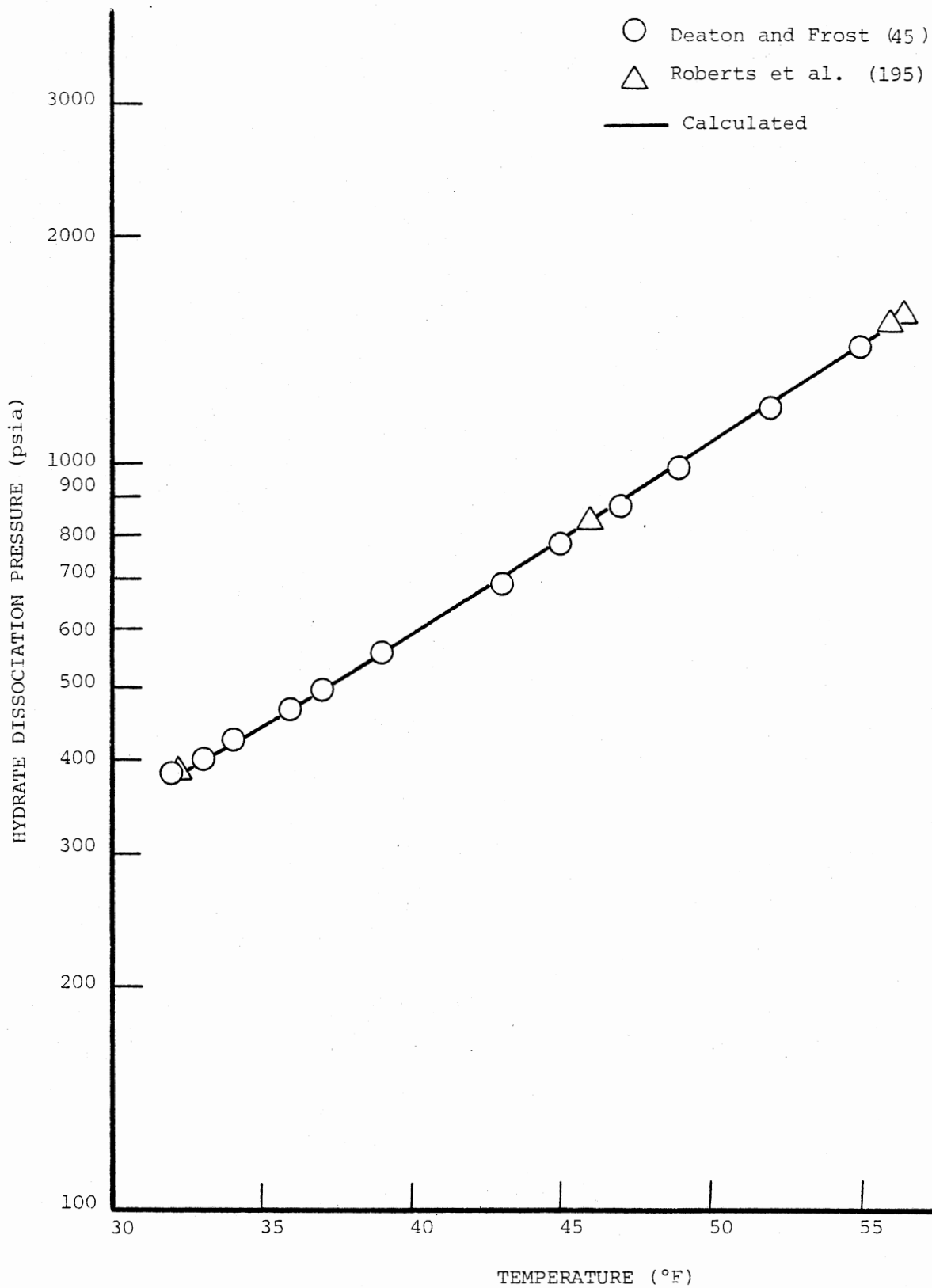


Figure 28. Comparison of Predicted and Experimental Hydrate Forming Conditions for Methane

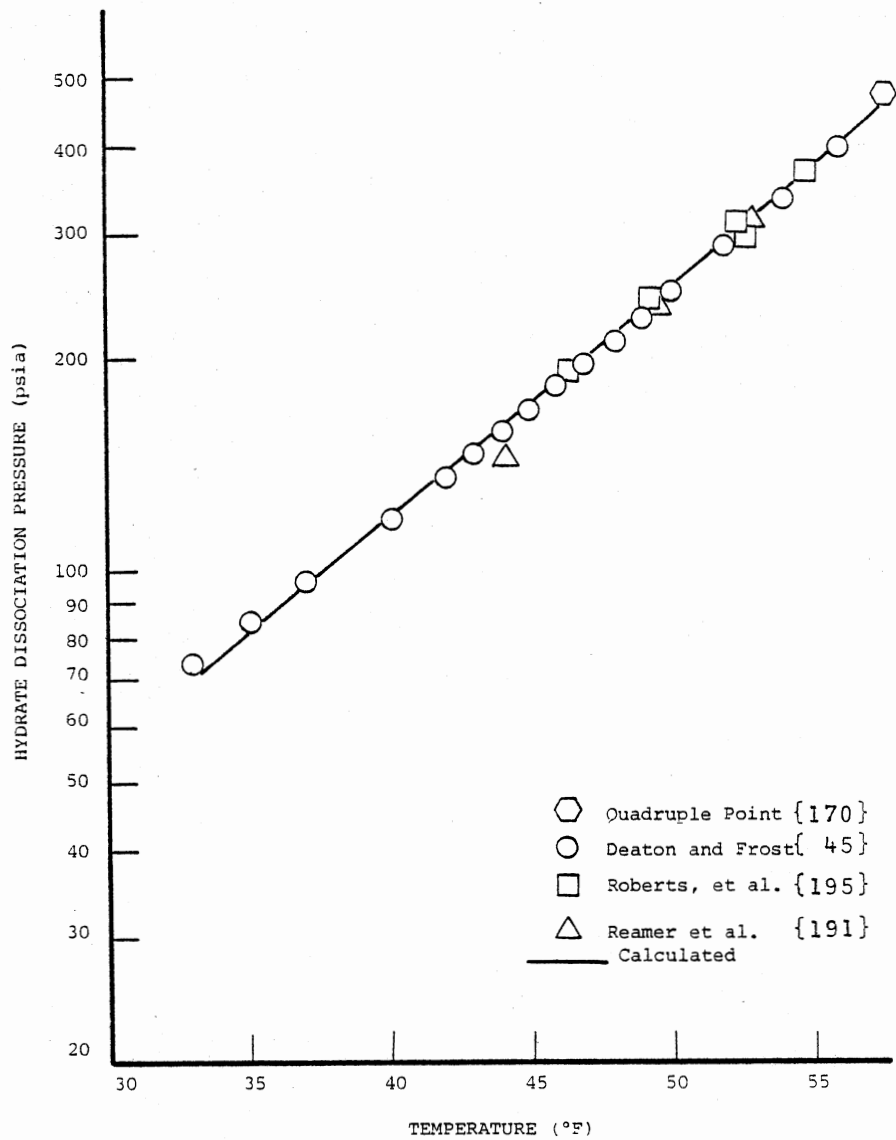


Figure 29. Comparison of Predicted and Experimental Hydrate Forming Conditions for Ethane

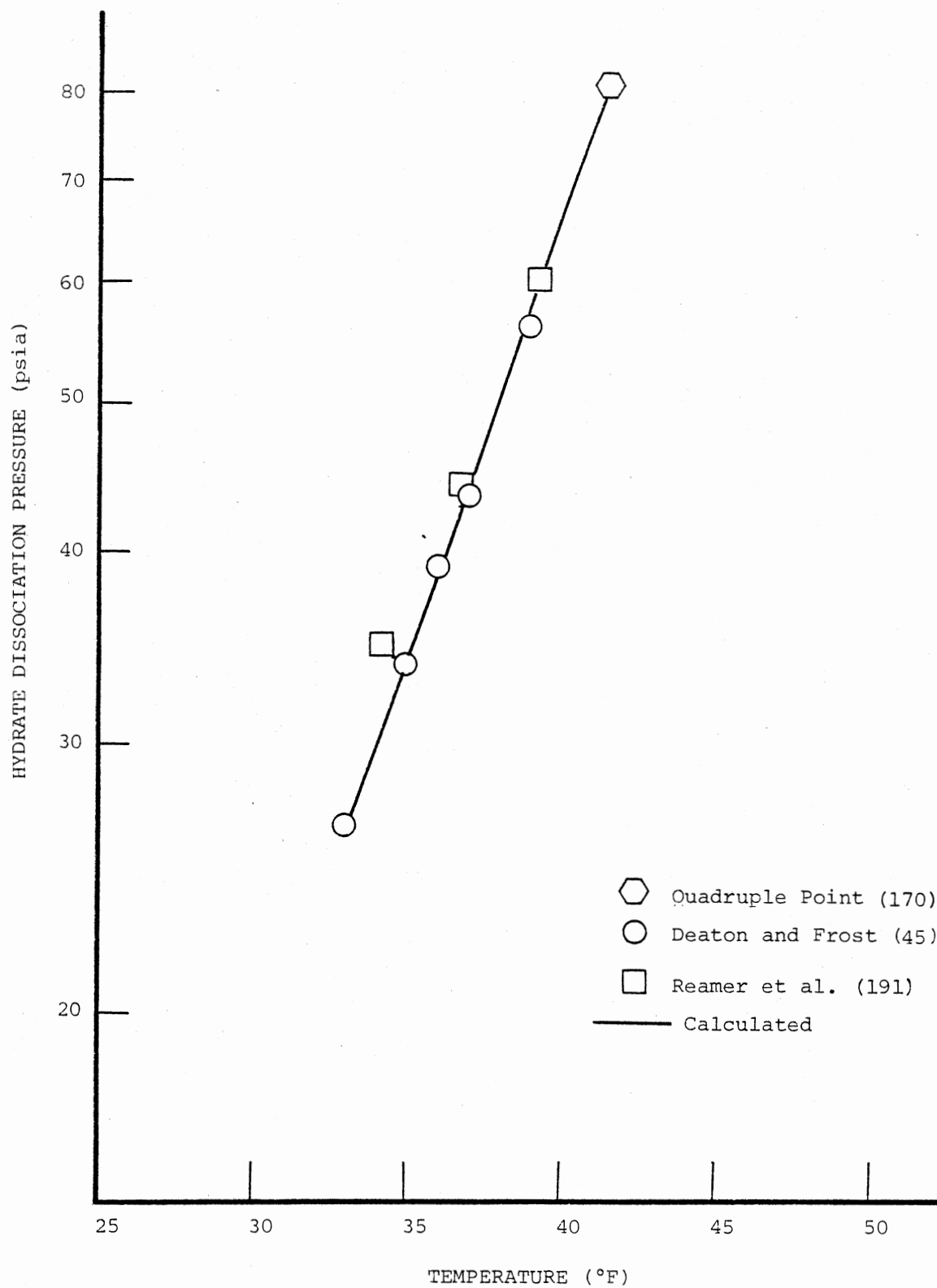


Figure 30. Comparison of Predicted and Experimental Hydrate Forming Conditions for Propane

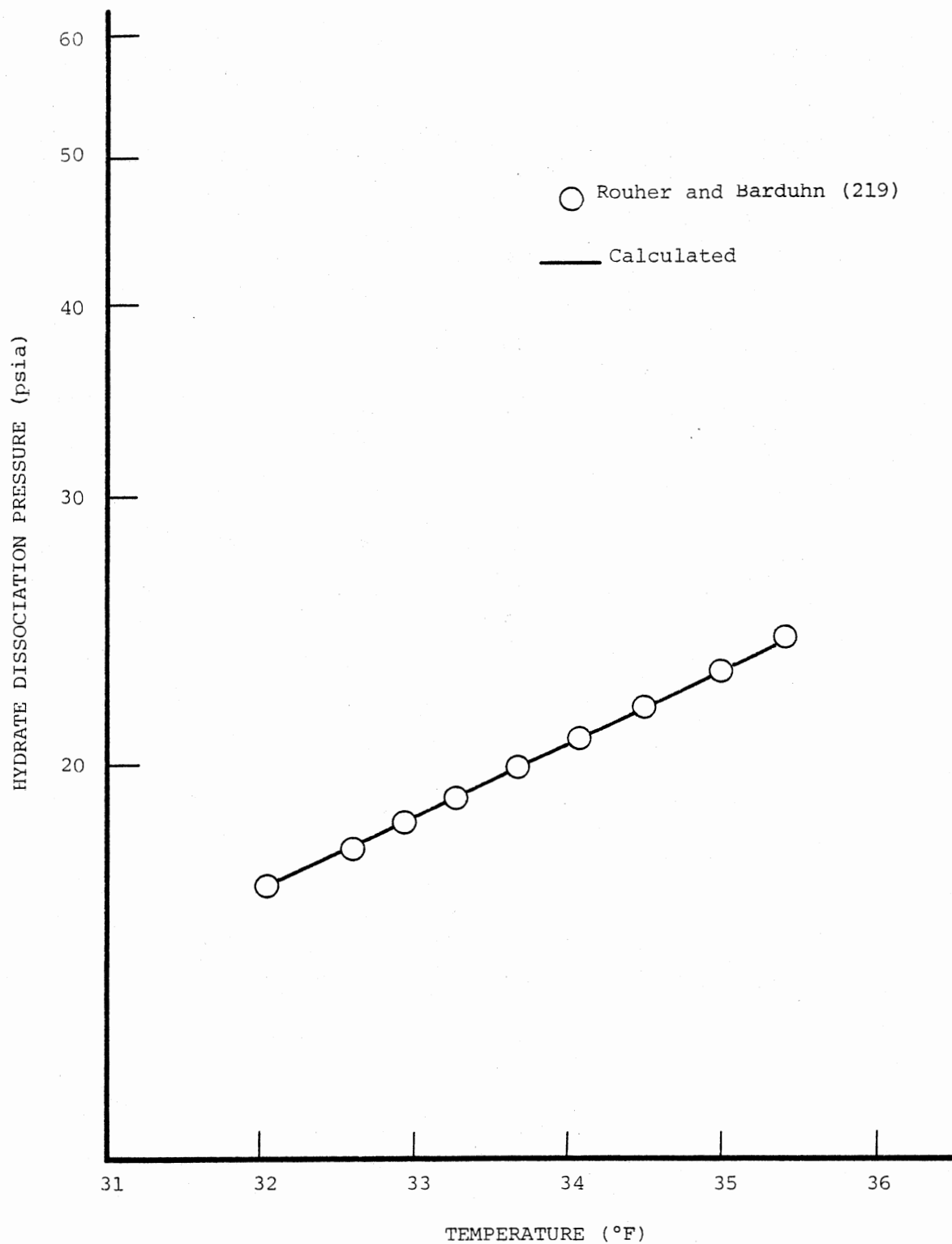


Figure 31. Comparison of Predicted and Experimental Hydrate Forming Conditions for i-Butane

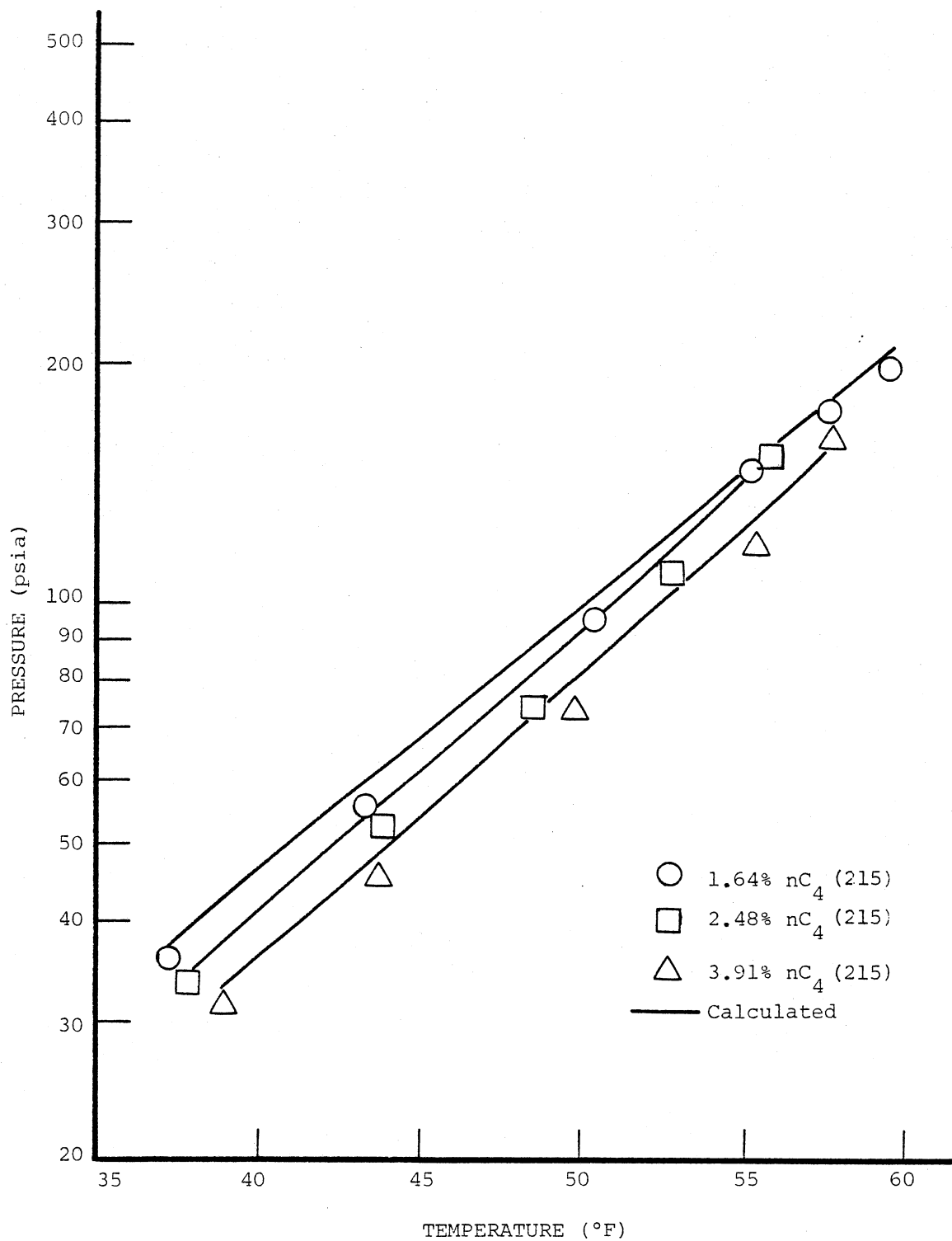


Figure 32. Comparison of Predicted and Experimental Hydrate Forming Conditions for Methane-n-Butane Mixtures

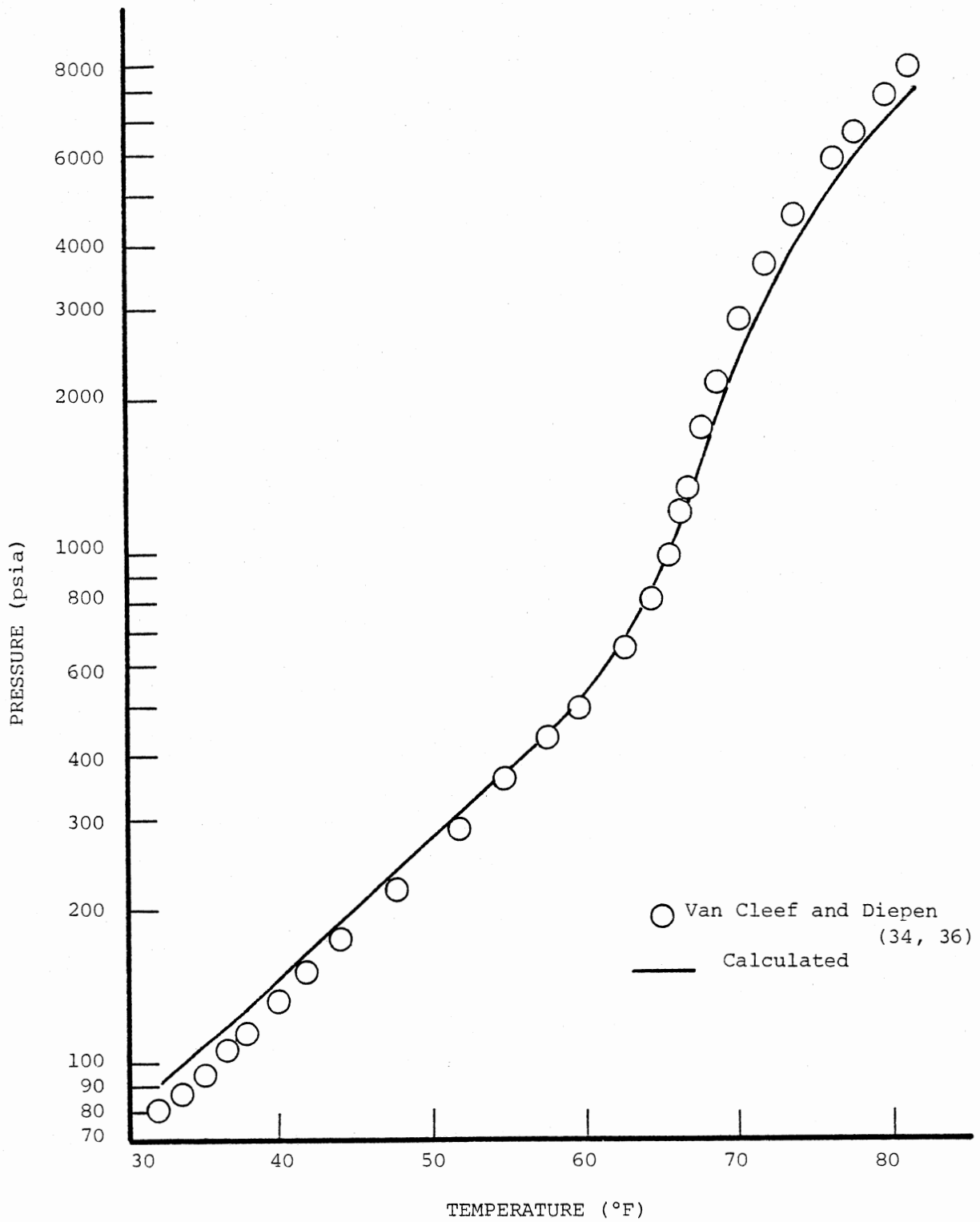


Figure 33. Comparison of Predicted and Experimental Hydrate Forming Conditions for Ethylene

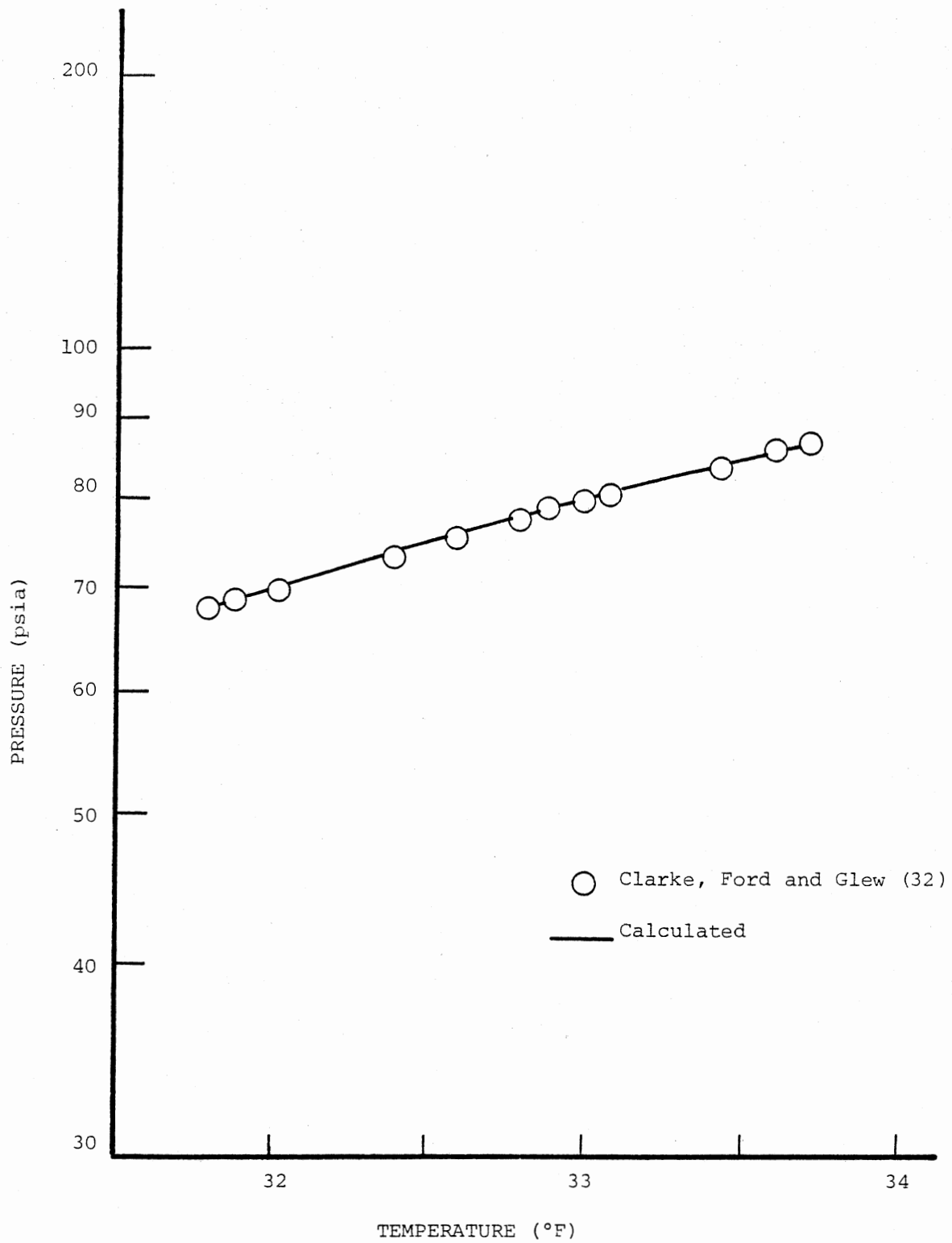


Figure 34. Comparison of Predicted and Experimental Hydrate Forming Conditions for Propylene

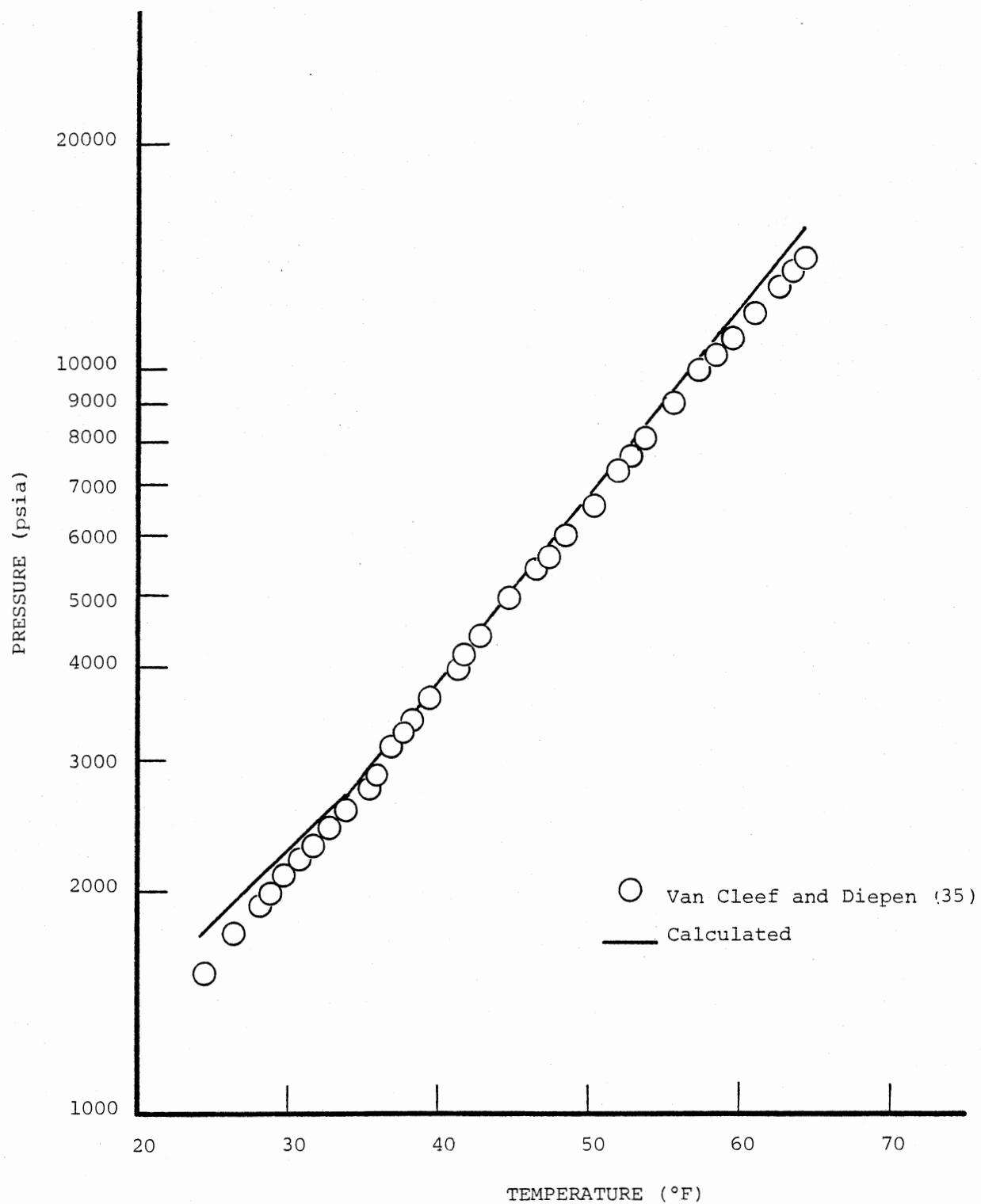


Figure 35. Comparison of Predicted and Experimental Hydrate Forming Conditions for Nitrogen

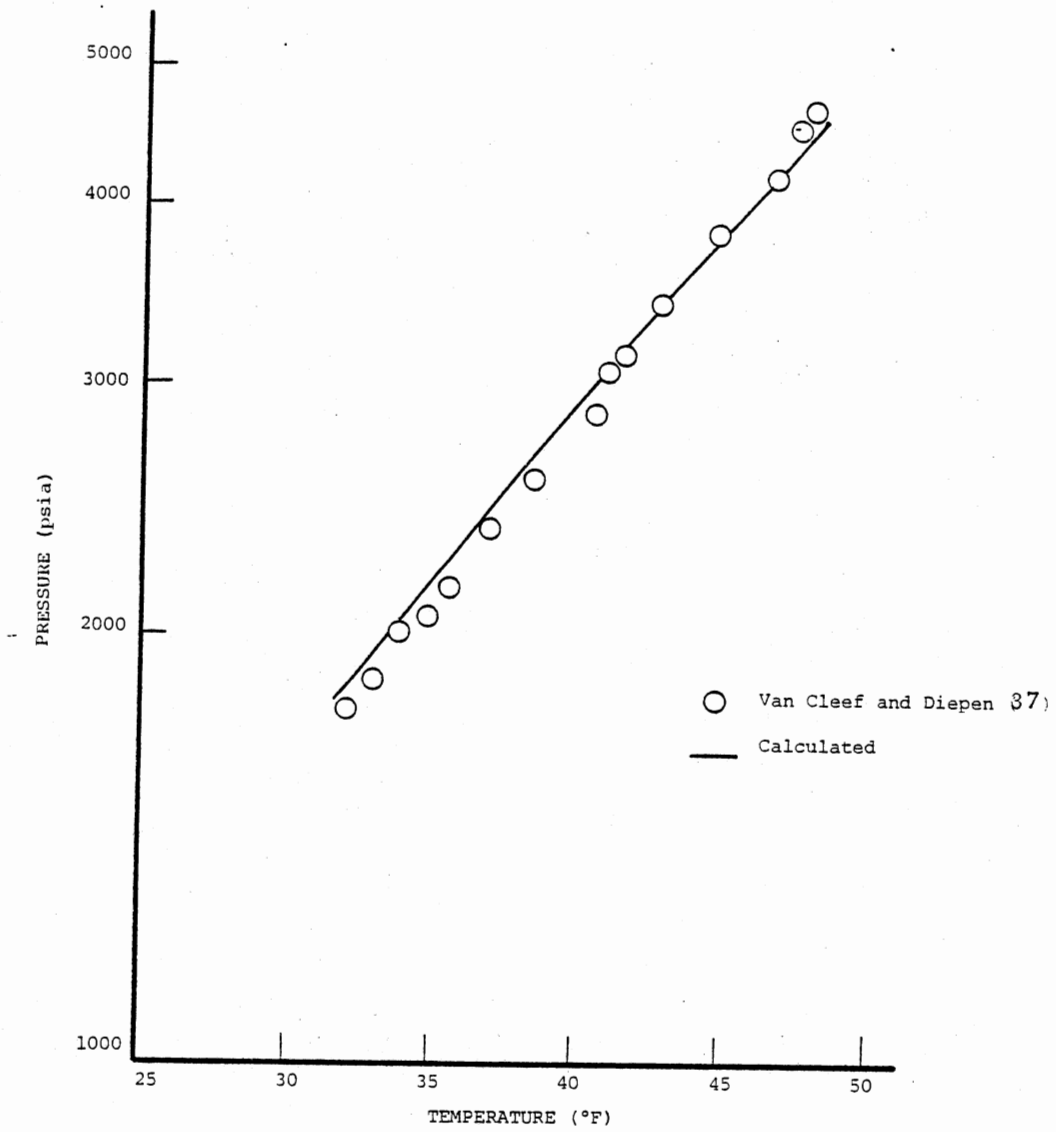


Figure 36. Comparison of Predicted and Experimental Hydrate Forming Conditions for Oxygen

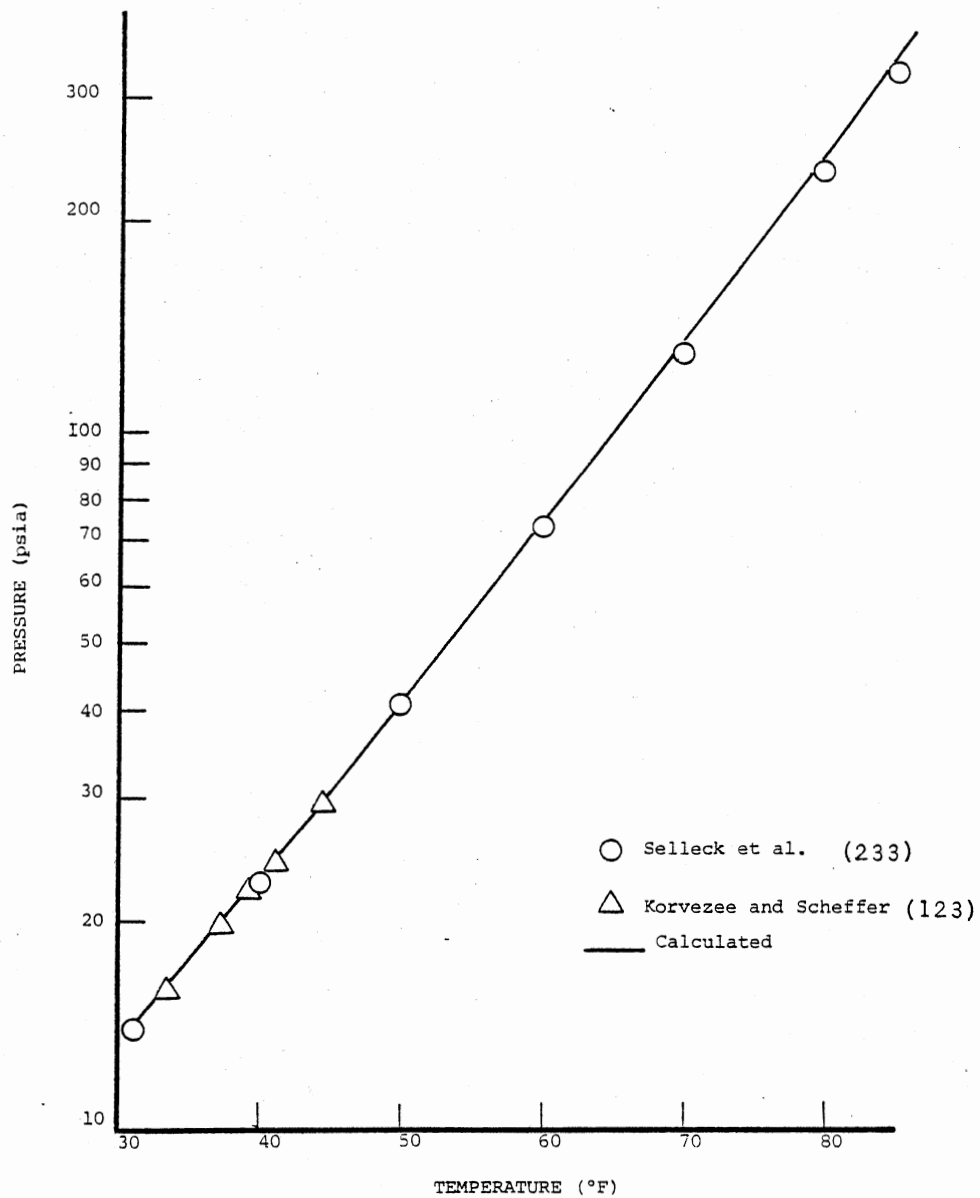


Figure 37. Comparison of Predicted and Experimental Hydrate Forming Conditions for Hydrogen Sulfide

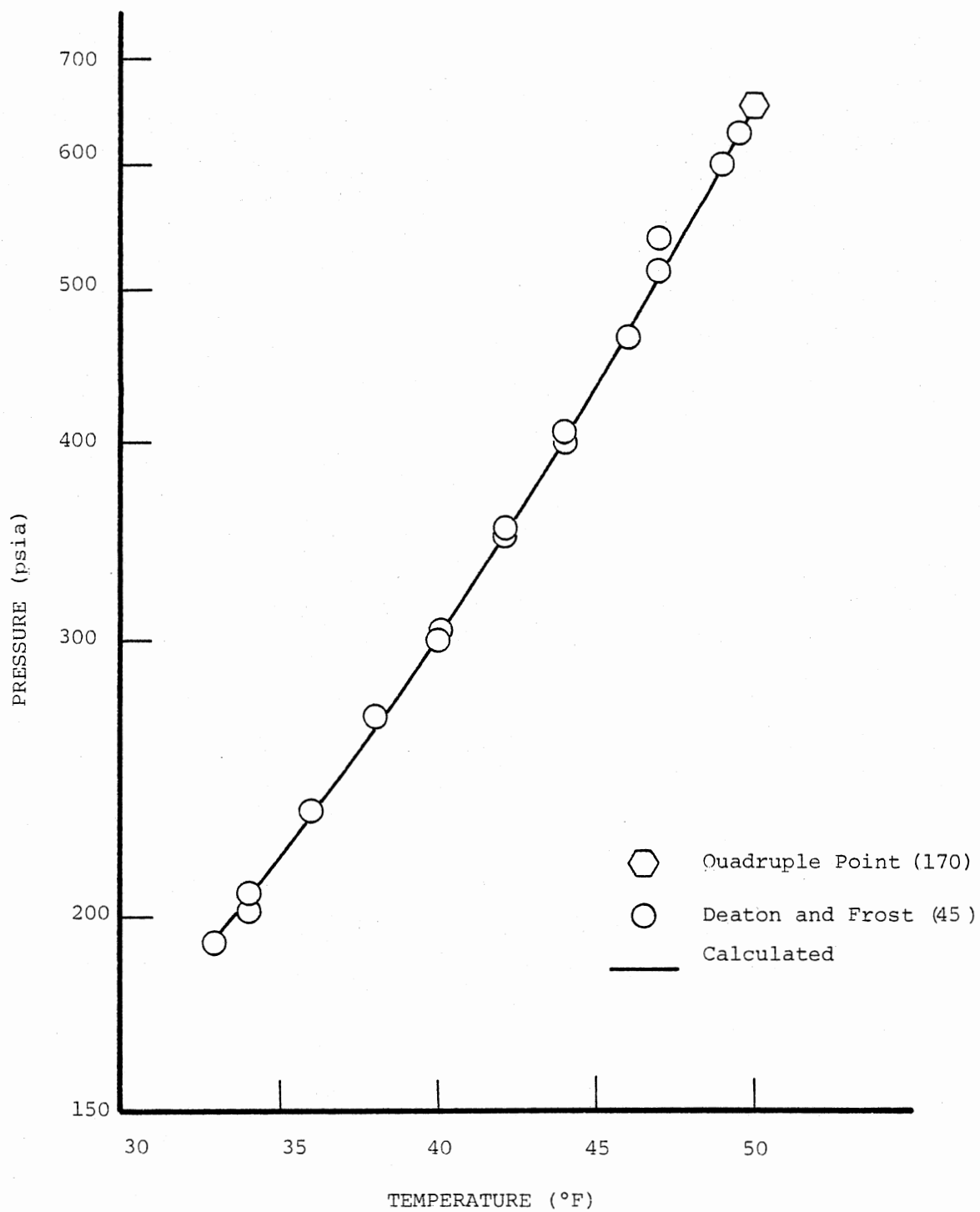


Figure 38. Comparison of Predicted and Experimental Hydrate Forming Conditions for Carbon Dioxide

TABLE XXIV
 DEVIATIONS IN HYDRATE FORMING TEMPERATURE PREDICTIONS FOR
 HYDROCARBON MIXTURES

Mixture	Temperature Range (°F)	Pressure Range (PSIA)	No. of Points	Abs. Avg. Error in Temperature (°F)	Ref. No.
Methane-Ethane	35.0 → 50.0	137.0 → 738.0	24	0.4	45
Methane-Propane	35.0 → 50.0	39.5 → 632.0	25	0.8	45
	54.1 → 72.5	263.0 → 1052.0	17	1.4	102
Methane-Isobutane	33.2 → 68.8	30.2 → 1460.5	46	3.1	217
	35.0 → 40.0	192.0 → 267.0	2	2.0	45
Methane-Butane	37.2 → 54.7	297.3 → 1989.9	18	2.1	215
Methane-Nitrogen	32.0 → 71.7	385.0 → 5100.0	65	2.5	207
Methane-Carbon Dioxide	36.2 → 54.5	289.0 → 1015.0	17	2.8	250
Methane-Hydrogen Sulfide	38.0 → 72.0	150.0 → 970.0	20	2.4	163
Methane-H ₂ S-CO ₂	40.0 → 60.0	110.0 → 765.0	20	3.0	206
Natural Gas A ²	35.0 → 69.5	91.0 → 1238.0	9	0.9	45
Natural Gas B	33.0 → 56.0	87.0 → 415.0	9	2.7	45
Natural Gas C	33.0 → 50.0	105.0 → 321.0	8	1.5	45
Natural Gas D	33.0 → 48.0	109.0 → 304.0	6	0.4	45
Natural Gas E	36.0 → 61.0	137.0 → 762.0	4	5.5	45
Natural Gas F	33.0 → 67.2	111.0 → 1362.0	9	2.9	45
Natural Gas G	33.0 → 65.0	110.0 → 1121.0	7	3.1	45
Natural Gas H	33.9 → 48.0	110.0 → 309.0	5	0.7	45
Natural Gas I	33.0 → 45.0	115.0 → 263.0	4	2.9	45

TABLE XXIV (Continued)

Mixture	Temperature Range (°F)	Pressure Range (PSIA)	No. of Points	Abs. Avg. Error in Temperature (°F)	Ref. No.
Natural Gas J	33.0 → 64.0	128.0 → 1216.0	23	1.8	45
Natural Gas K	34.0 → 55.1	155.0 → 666.0	6	1.3	45
Natural Gas L	33.0 → 62.0	183.0 → 1515.0	9	1.9	45
Natural Gas 2	53.2 → 83.9	1005.0 → 9925.0	8	0.5	146
Natural Gas 3	60.2 → 87.6	1015.0 → 9945.0	8	2.2	146
Natural Gas 4	63.2 → 88.3	1005.0 → 10005.0	10		146
Natural Gas 5	67.9 → 89.2	1075.0 → 9025.0	7		146
Natural Gas 6	48.9 → 82.2	835.0 → 9565.0	7	1.6	146
Natural Gas 7	53.9 → 82.2	1015.0 → 9925.0	11		146
Natural Gas 8	59.8 → 84.1	985.0 → 9205.0	7		146
Natural Gas 9	69.2 → 89.3	975.0 → 9185.0	13		146
Natural Gas 10	68.8 → 85.8	1965.0 → 9115.0	7		146
Natural Gas B	42.2 → 77.3	182.0 → 3963.0	9	2.7	266
Natural Gas C	40.2 → 72.3	232.0 → 3335.0	15	2.1	266
Natural Gas D	38.5 → 73.0	175.0 → 3270.0	12	2.2	266

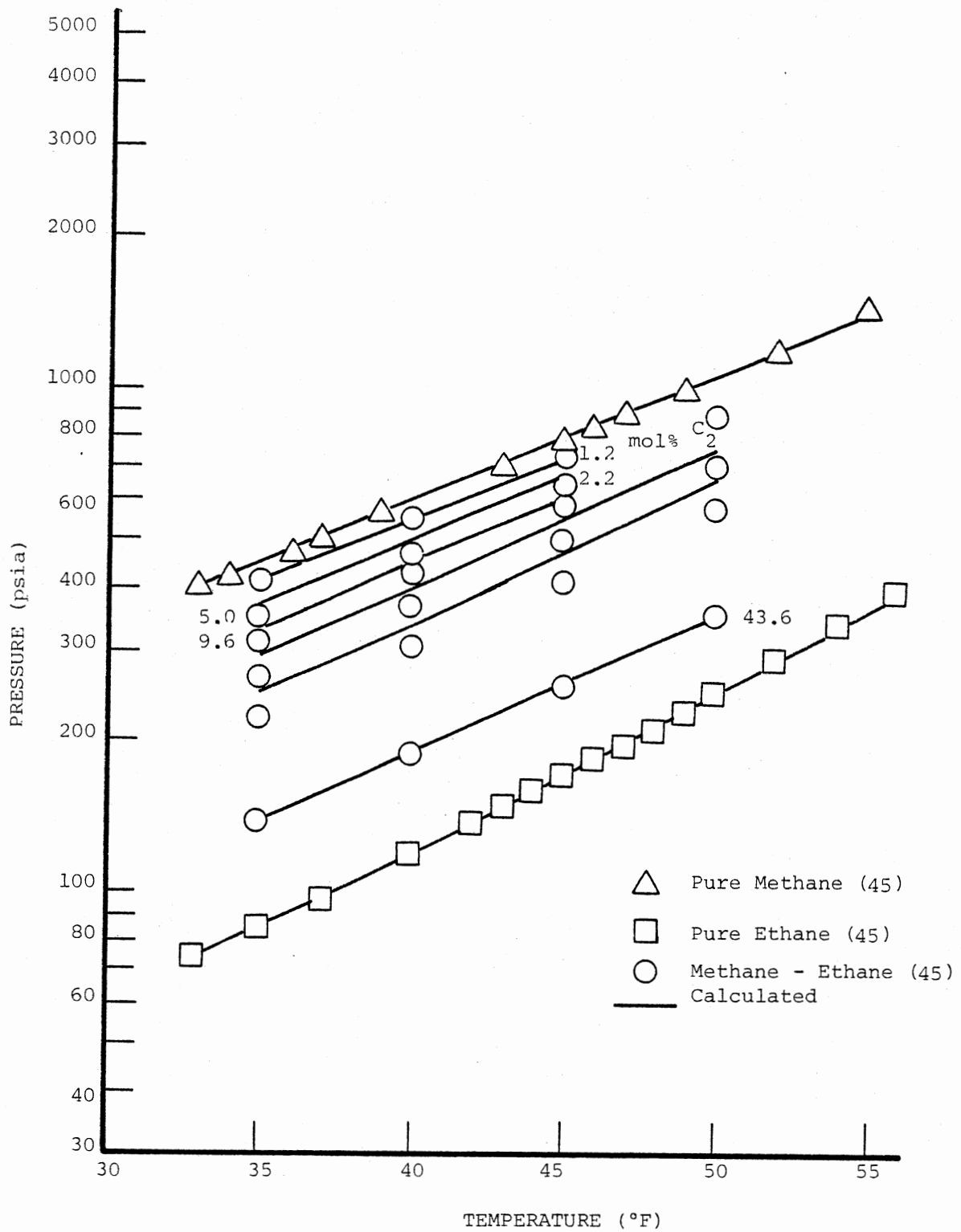


Figure 39. Comparison of Predicted and Experimental Hydrate Forming Conditions for Methane-Ethane Mixtures

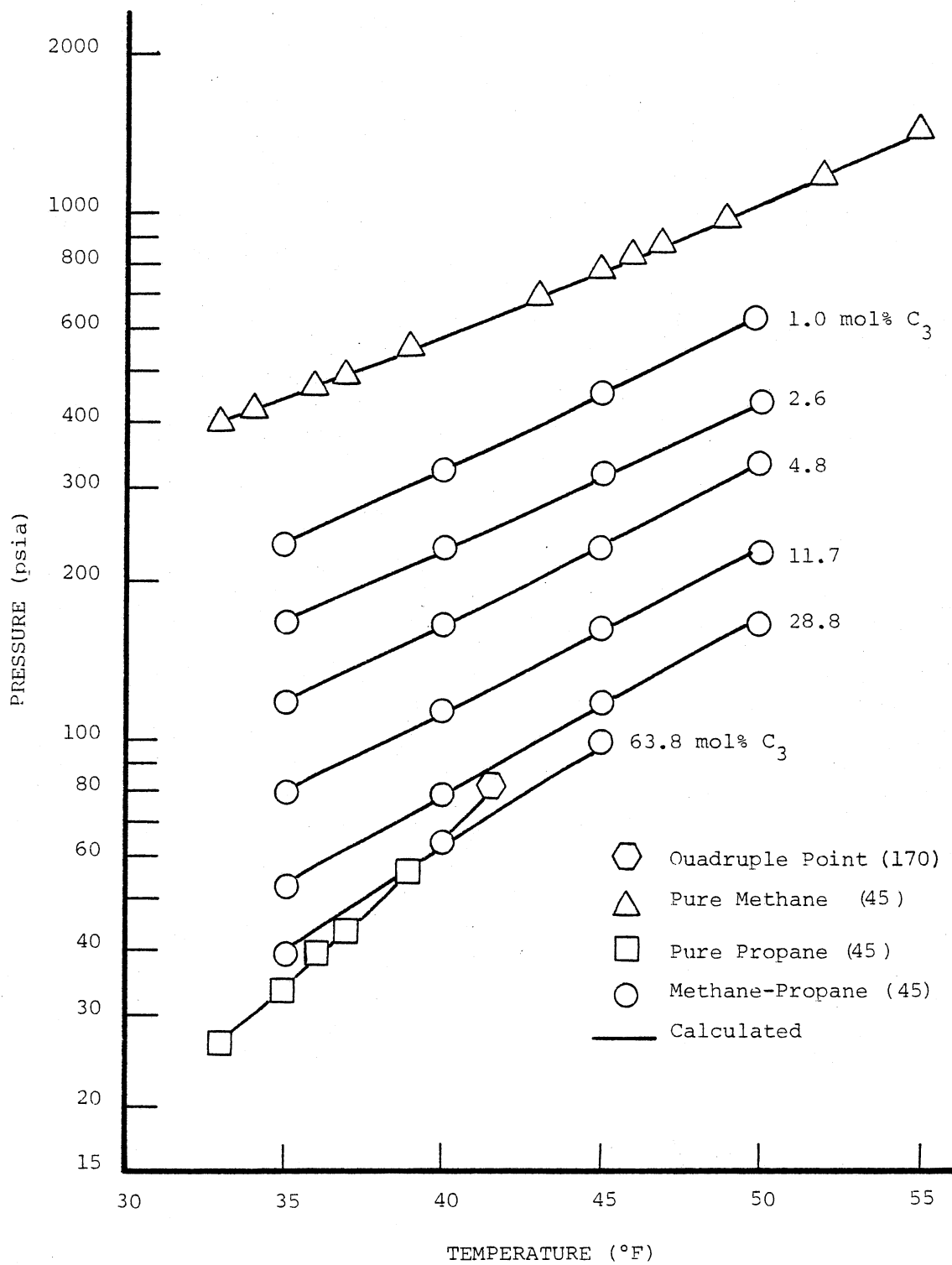


Figure 40. Comparison of Predicted and Experimental Hydrate Forming Conditions for Methane-Propane Mixtures

Parrish and Prausnitz (170). For the systems evaluated, no binary interaction constants for the hydrate model were used. The results of the evaluation for several light hydrocarbon systems are shown in Table XXIV. The temperature and pressure range, number of points evaluated, absolute average deviation in predicted hydrate forming temperatures and literature references to each of the systems are also included in Table XXIV. The comparison of experimental and predicted hydrate forming conditions for selected multicomponent mixtures are shown in Figures 39 through 40.

Effect of Methanol and Glycols as Hydrate Inhibitors

The activity coefficient modification to the basic hydrate model suggested by Menten, Parrish and Sloan (148) was used to calculate the effect of methanol and glycols on hydrate forming conditions.

Figures 41 through 50 show a comparison of the predicted and experimental hydrate forming conditions in the presence of methanol. The predictions from the Hammerschmidt equation (78) for systems containing methanol are also included. Methanol vaporization losses for a light hydrocarbon gas at various temperatures are shown in Figure 51.

No experimental data for the inhibition of hydrate formation in the presence of glycols are available for comparison. Figures 52 through 54 show the effect of addition of ethylene glycol, diethylene glycol and triethylene glycol as calculated by the PFGC equation. The change in hydrate forming conditions due to glycols was calculated by the new activity coefficient hydrate model. The predictions from the

Hammerschmidt equation (78) for systems containing glycols are also included in the figures for comparison.

The Hammerschmidt equation (78) follows the predictions from the PFGC and the new hydrate model very closely. The depression in the hydrate forming conditions calculated in the presence of methanol is 8°F for 10 wt% and 18°F for 20 wt%. For ethylene glycol the depression is 4°F for 10 wt% and 9°F for 20 wt%. For diethylene glycol the depression in the hydrate forming temperature calculated by the Hammerschmidt equation (79) is 5°F for 10 wt% and 10°F for 20 wt%.

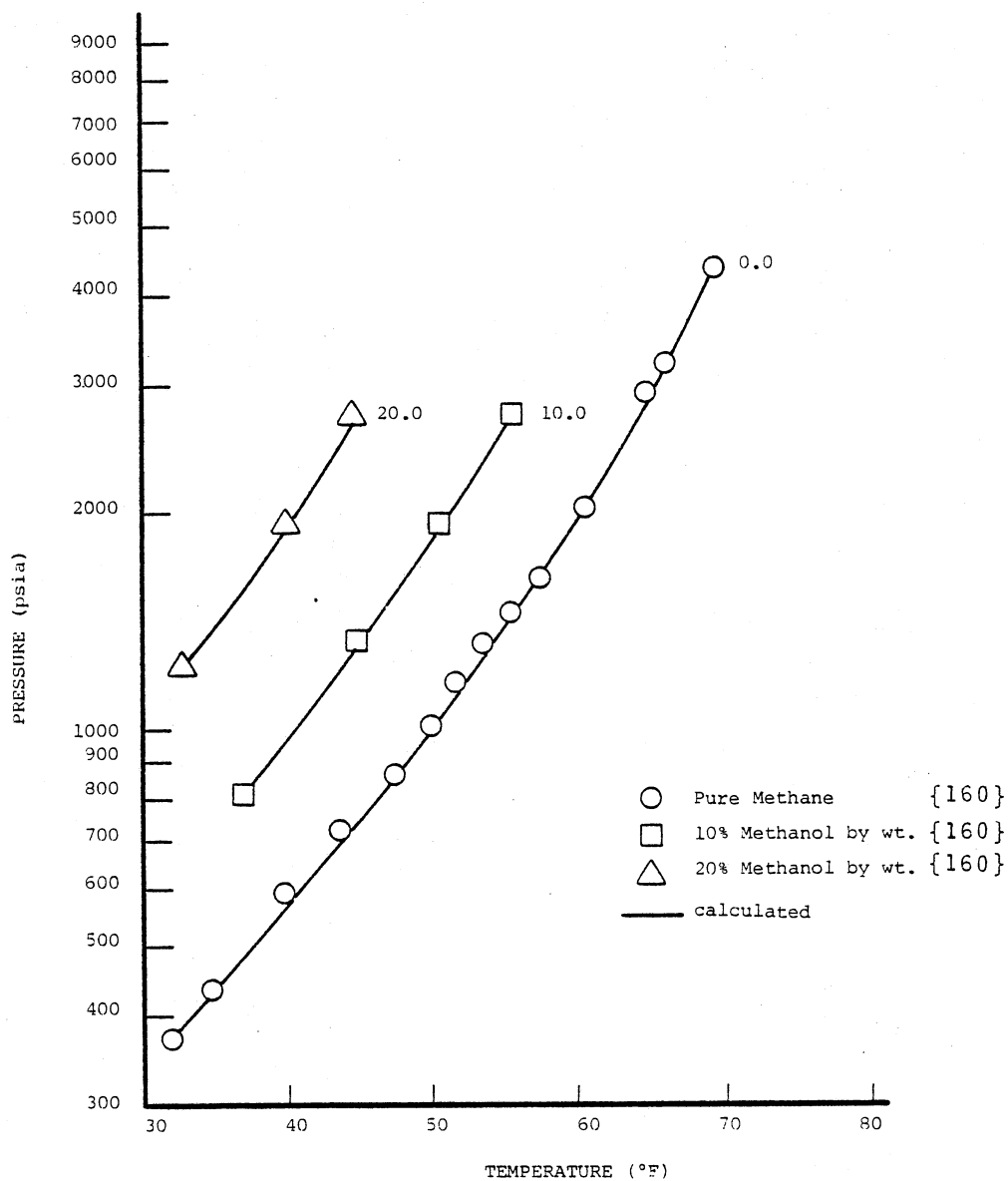


Figure 41. Effect of Methanol on Hydrate Forming Conditions for Methane

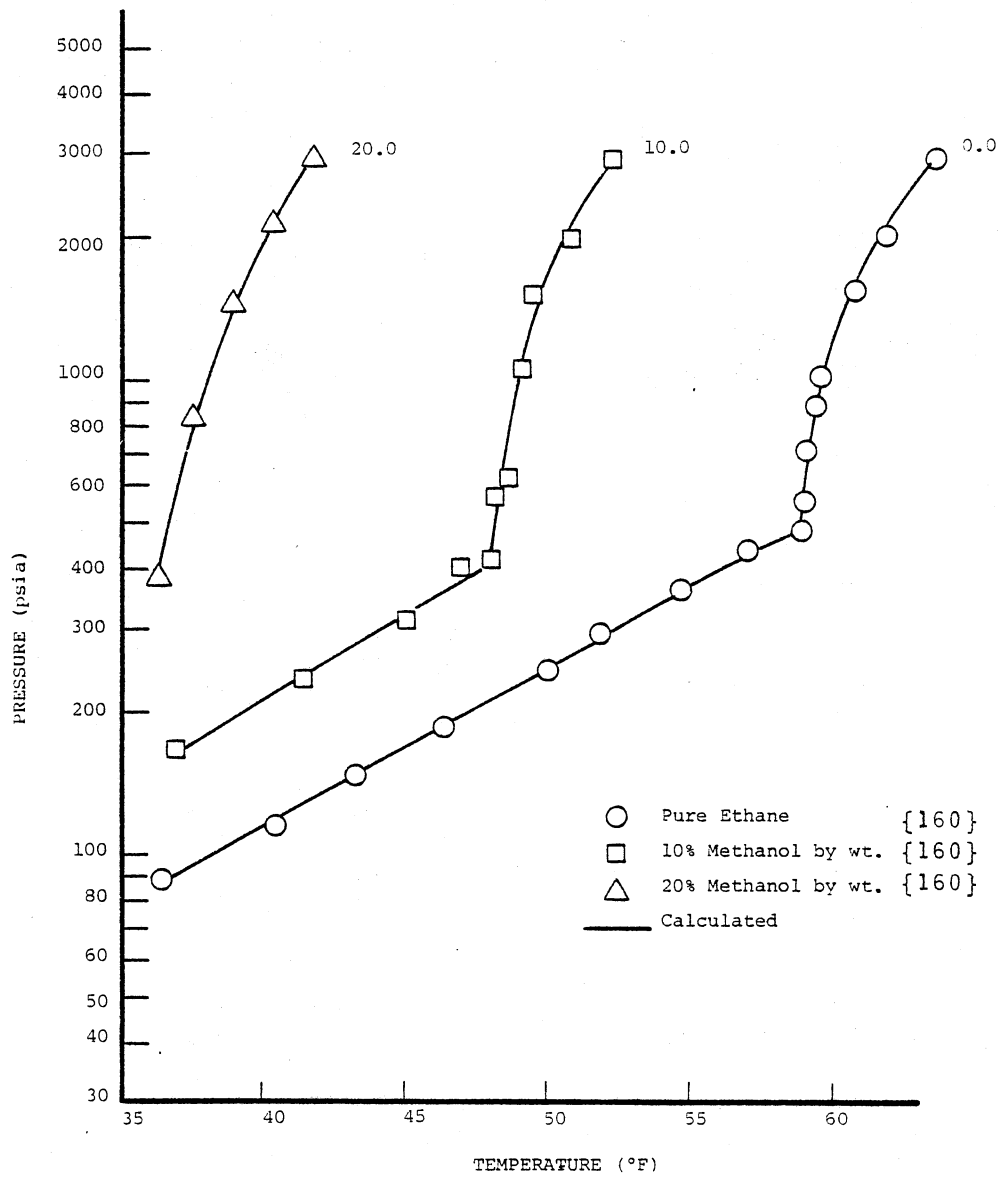


Figure 42. Effect of Methanol on Hydrate Forming Conditions for Ethane

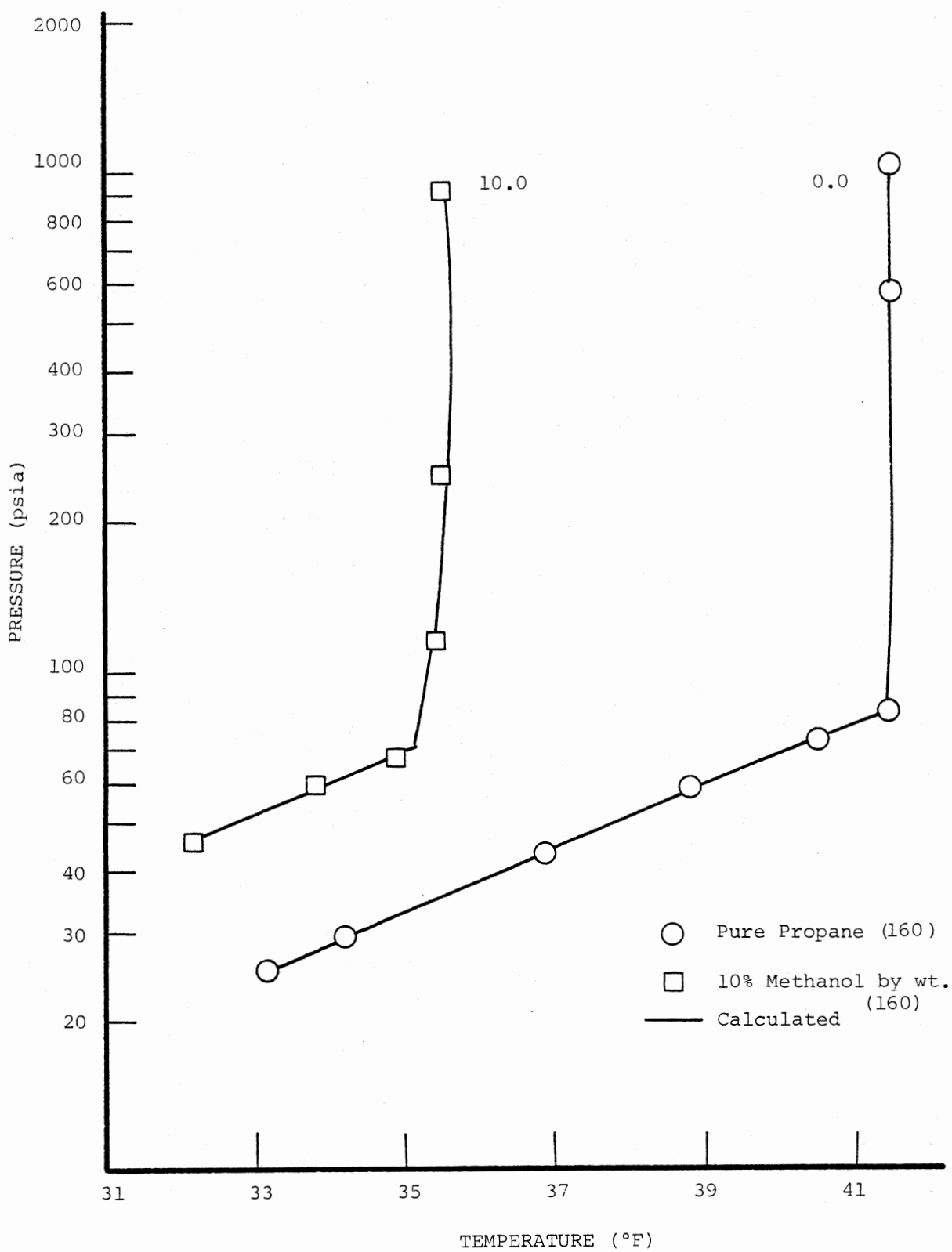


Figure 43. Effect of Methanol on Hydrate Forming Conditions for Propane

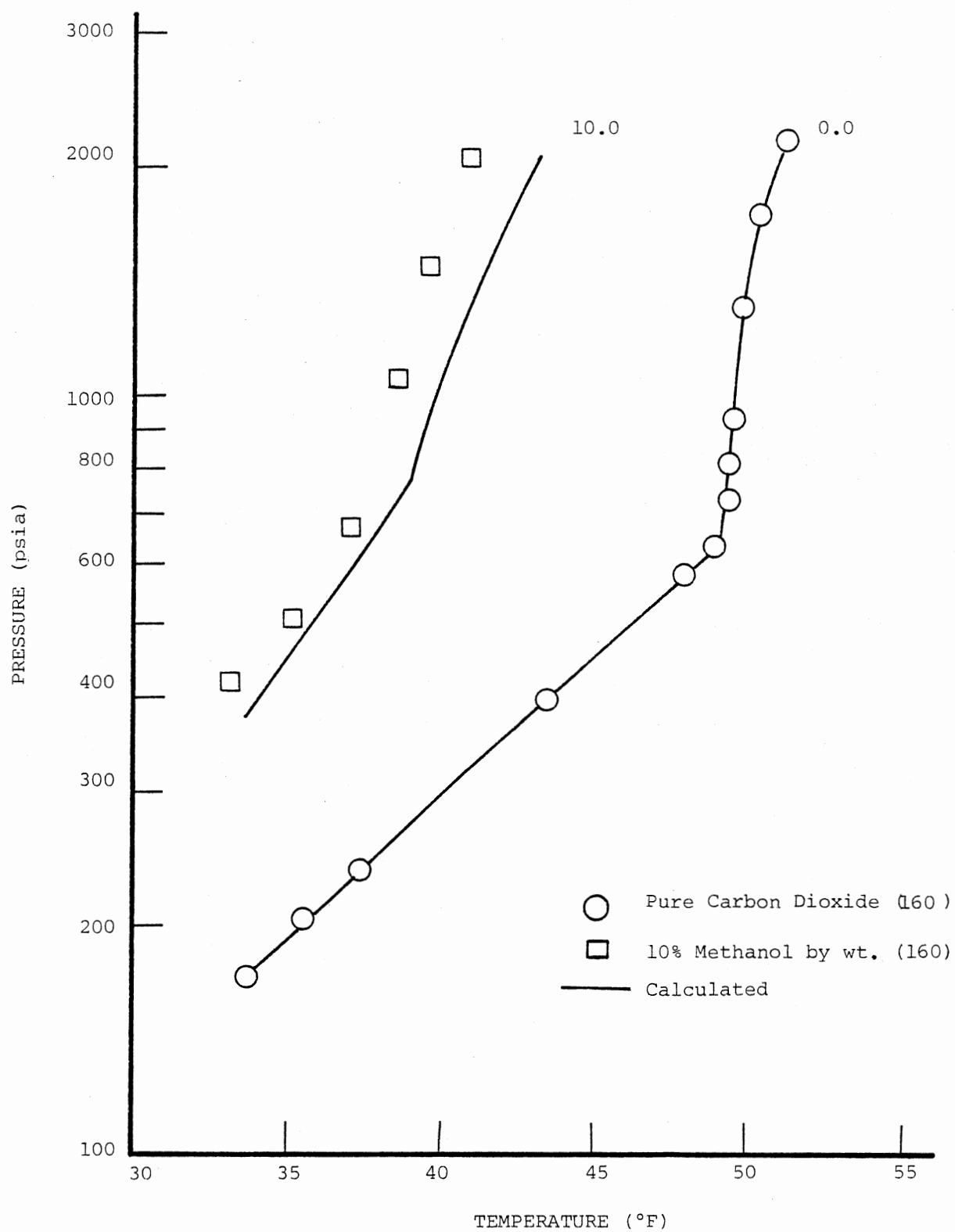


Figure 44. Effect of Methanol on Hydrate Forming Conditions for Carbon Dioxide

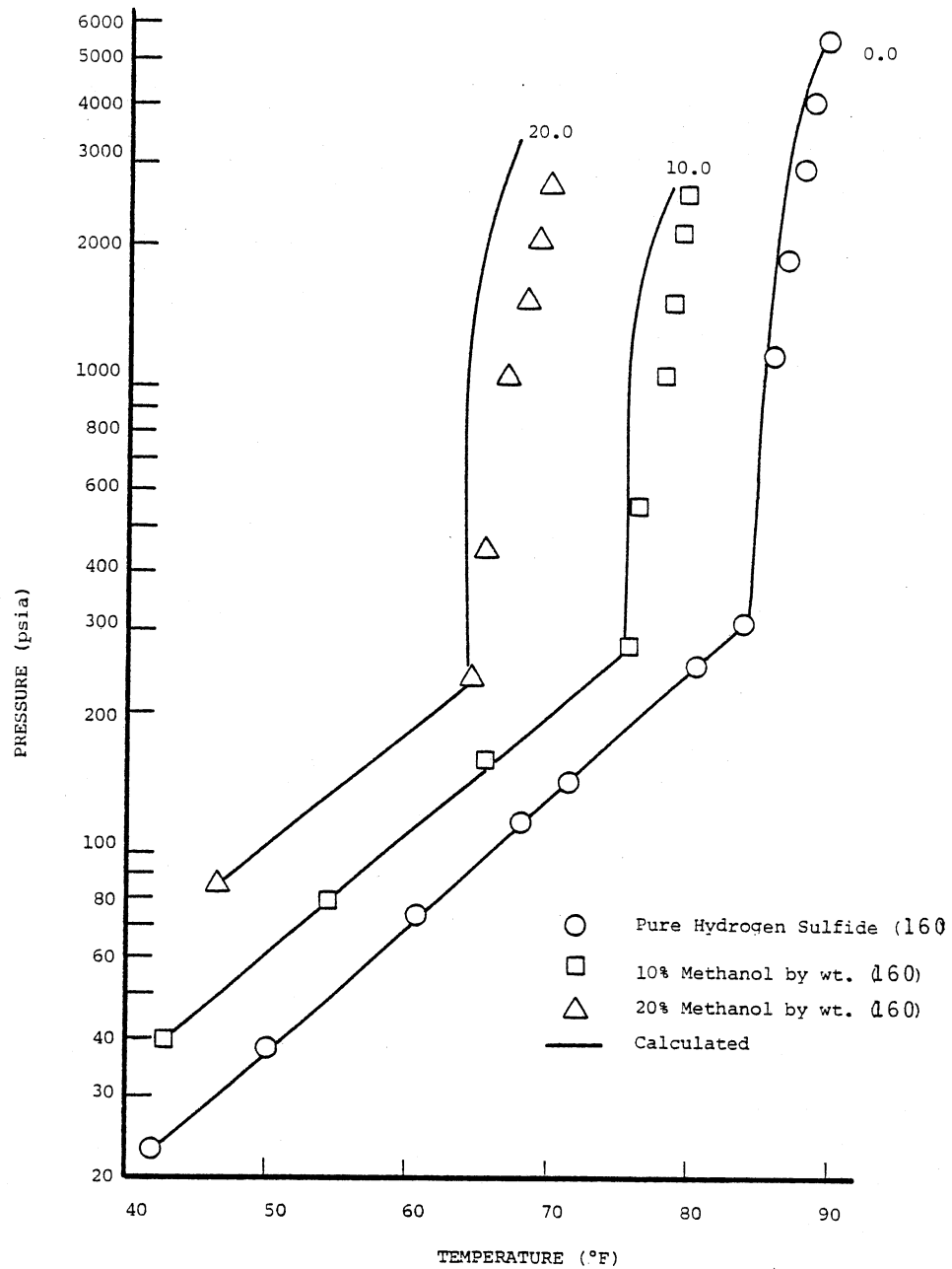


Figure 45. Effect of Methanol on Hydrate Forming Conditions for Hydrogen Sulfide

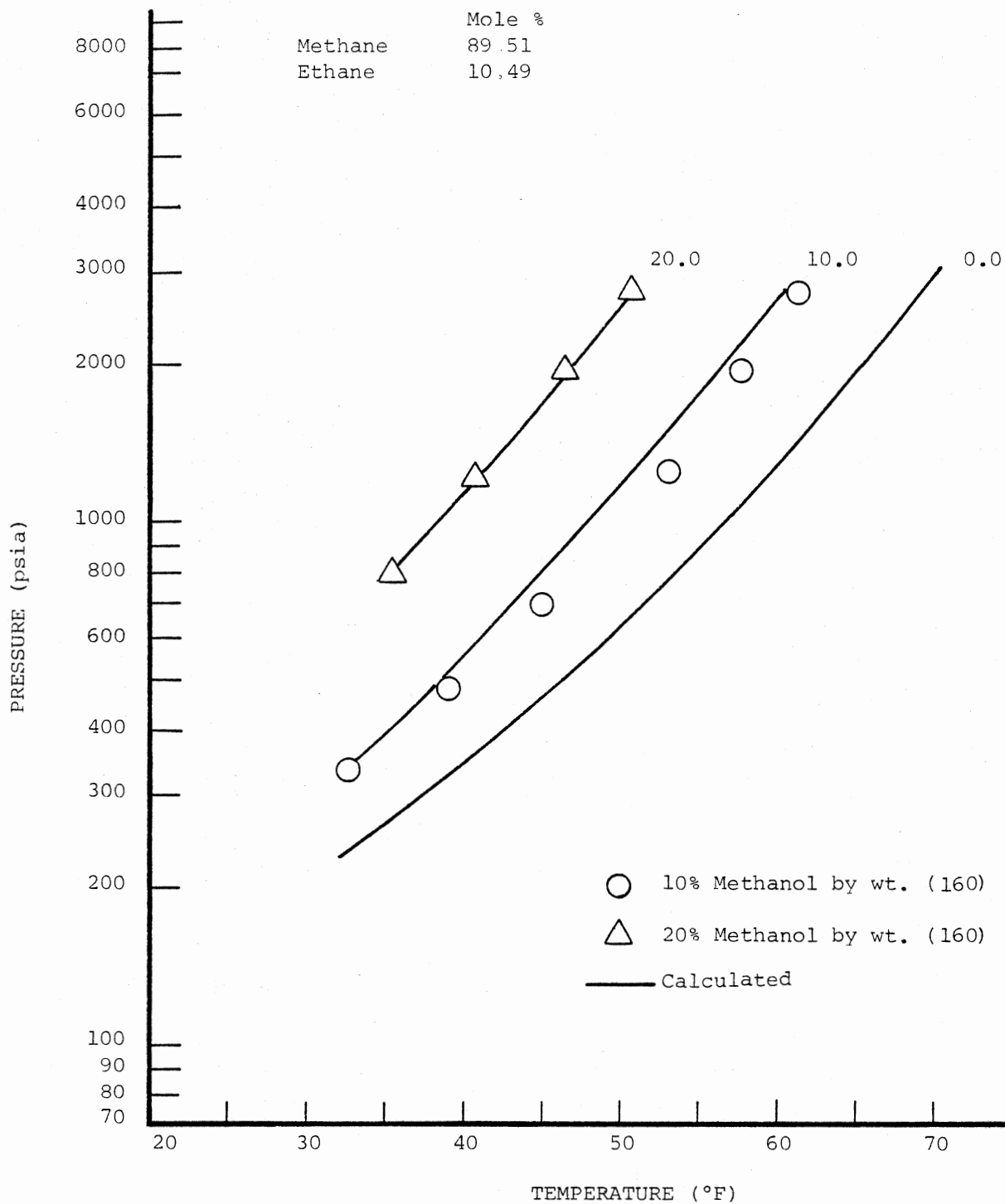


Figure 46. Effect of Methanol on Hydrate Forming Conditions for a Mixture Containing 89.51 Mole % Methane and 10.49% Ethane

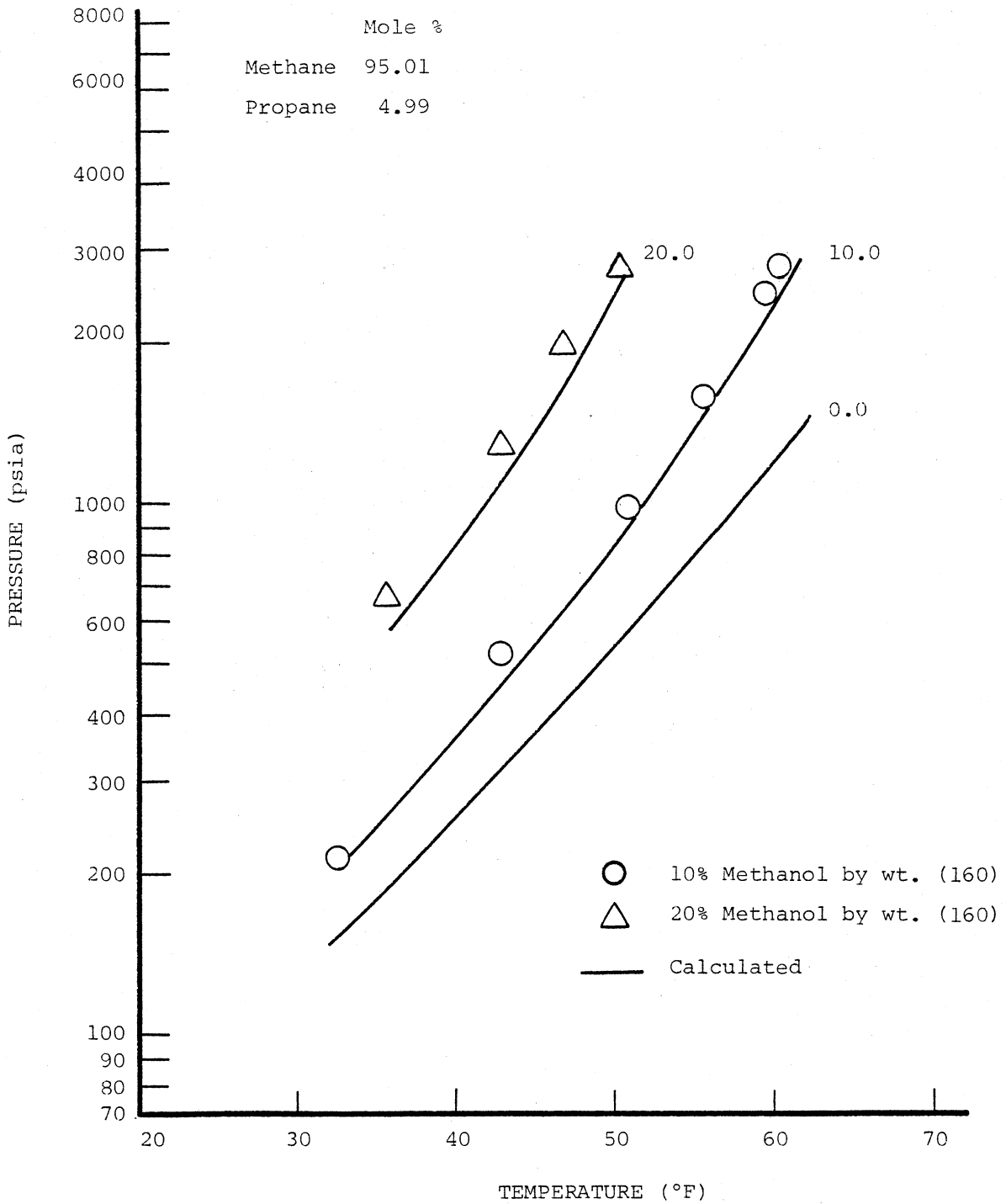


Figure 47. Effect of Methanol on Hydrate Forming Conditions in a Mixture Containing 95.01 Mole % Methane and 4.99 Mole % Propane

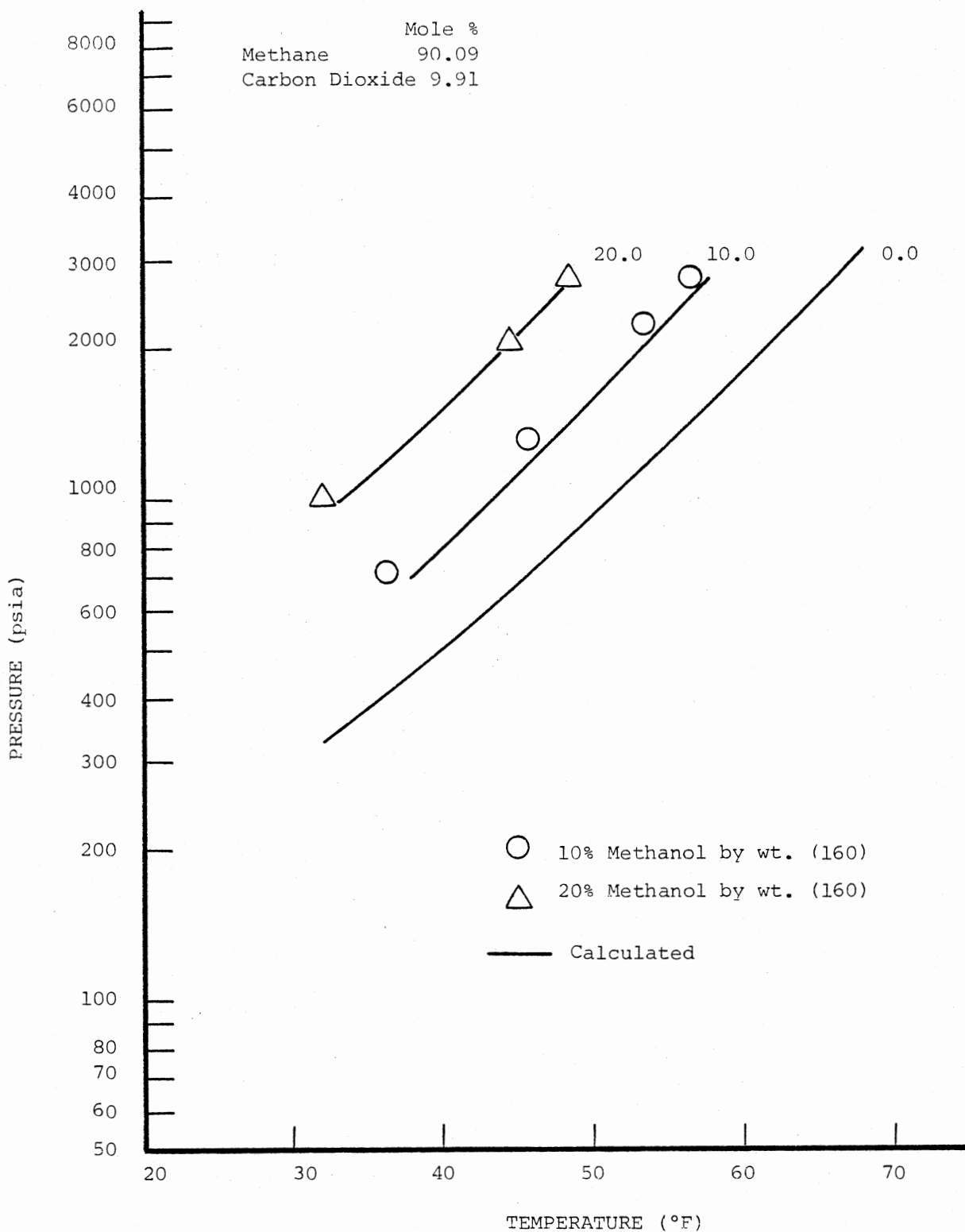


Figure 48. Effect of Methanol on Hydrate Forming Conditions for a Mixture Containing 90.09 Mole % Methane and 9.91 Mole % Carbon Dioxide

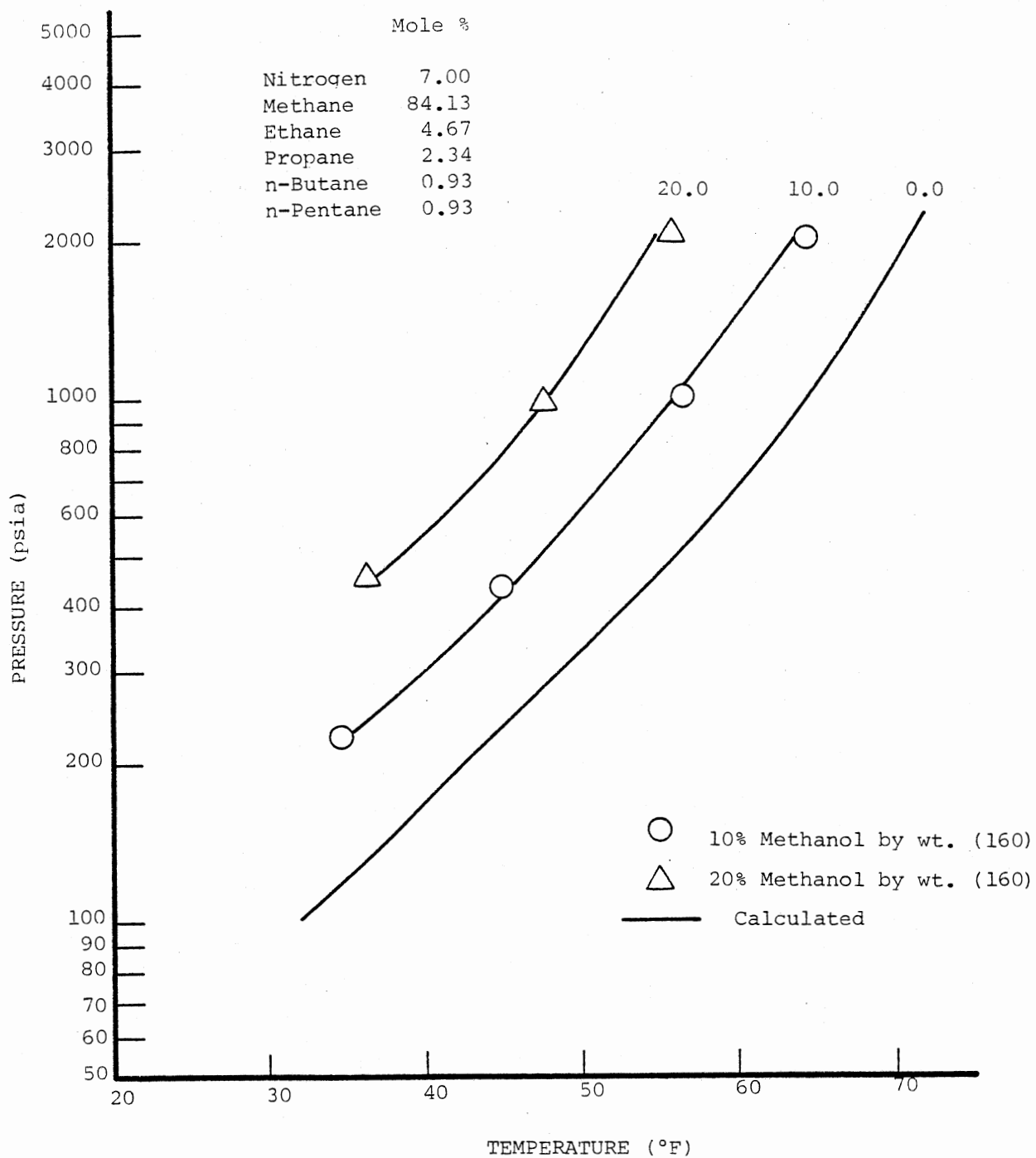


Figure 49. Effect of Methanol on Hydrate Forming Conditions in a Synthetic Natural Gas Mixture

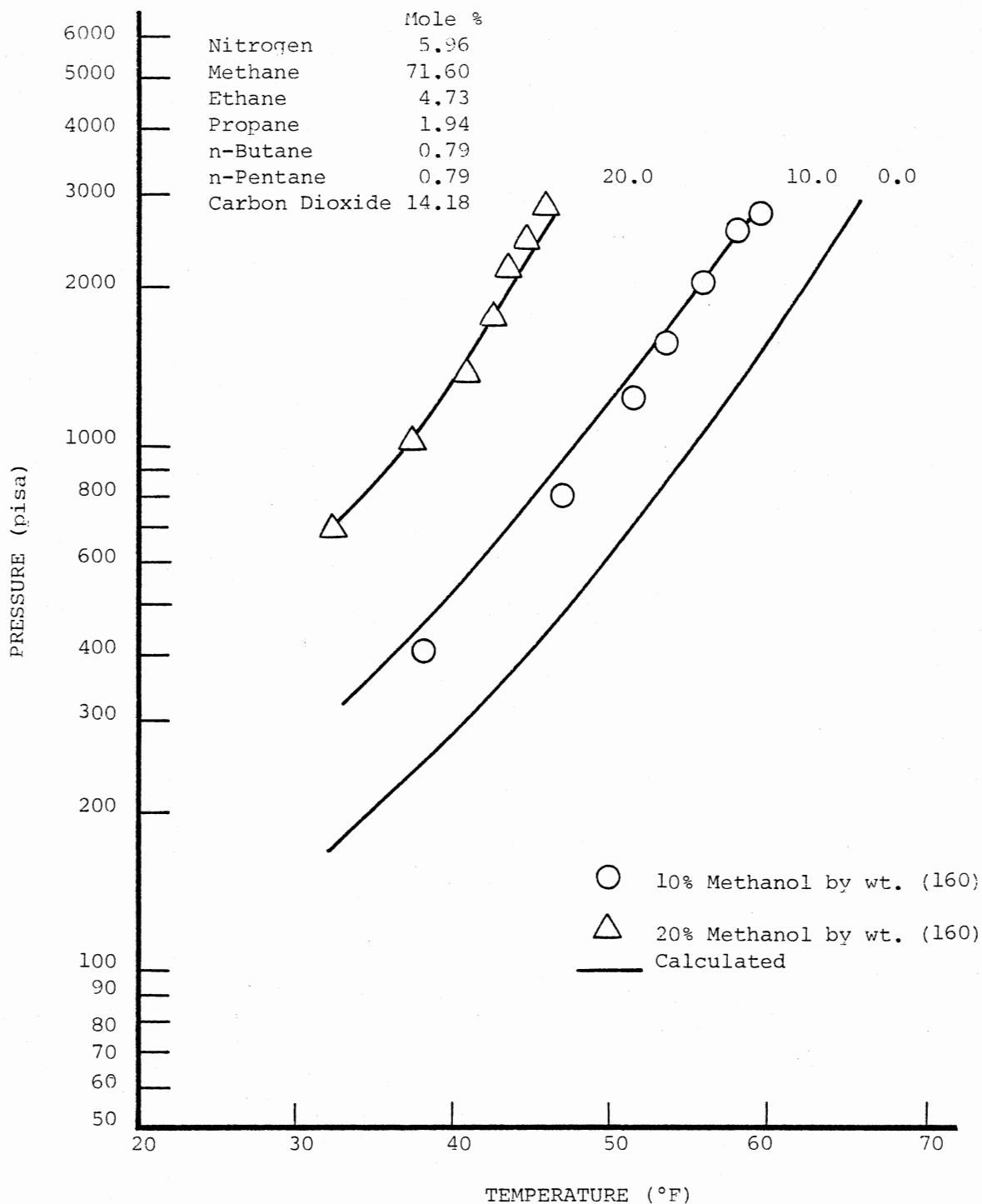


Figure 50. Effect of Methanol on Hydrate Forming Conditions for a Synthetic Gas Mixture Containing Carbon Dioxide

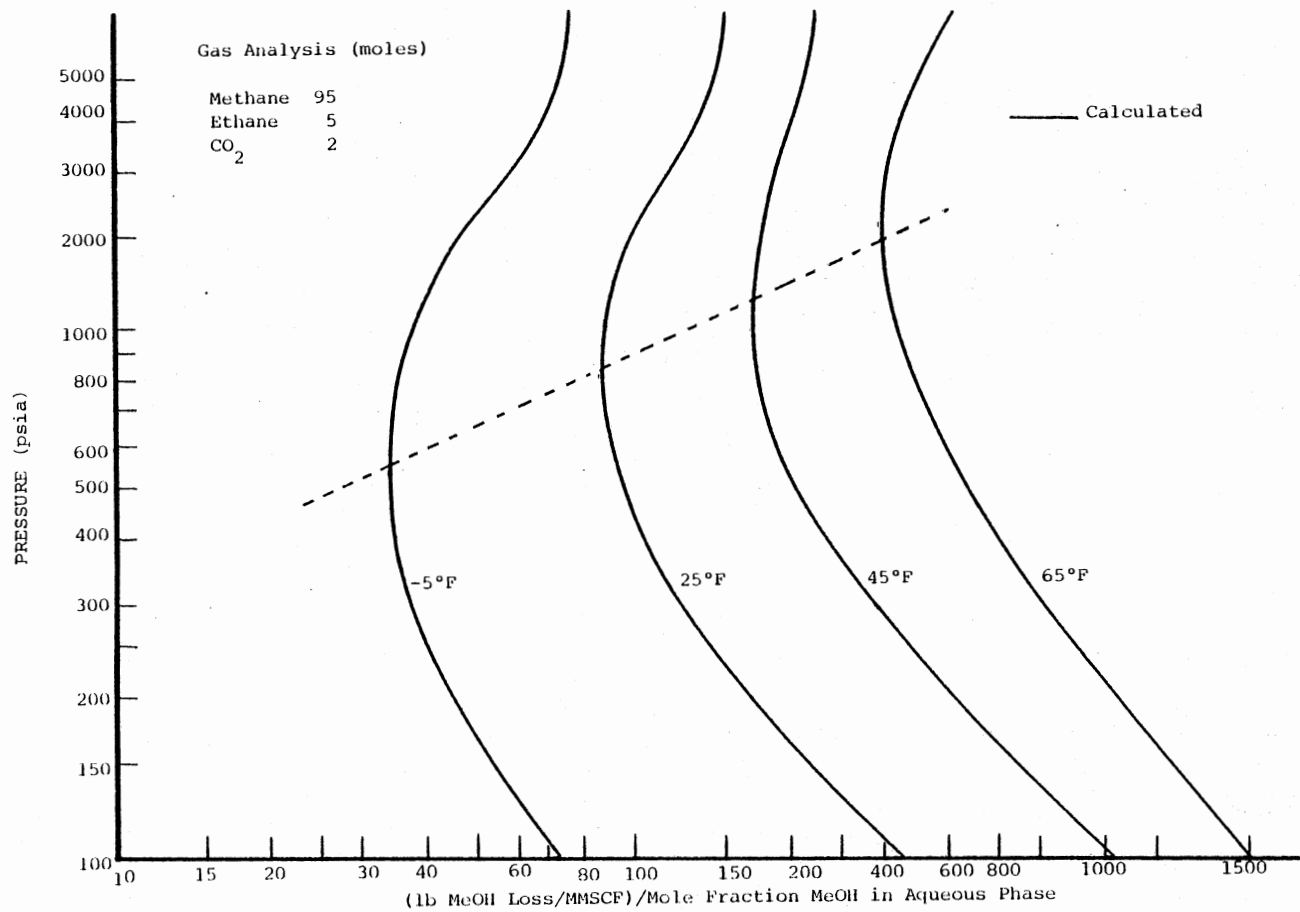


Figure 51. Ratio of Vapor to Liquid Composition for Methanol-Natural Gas Mixture

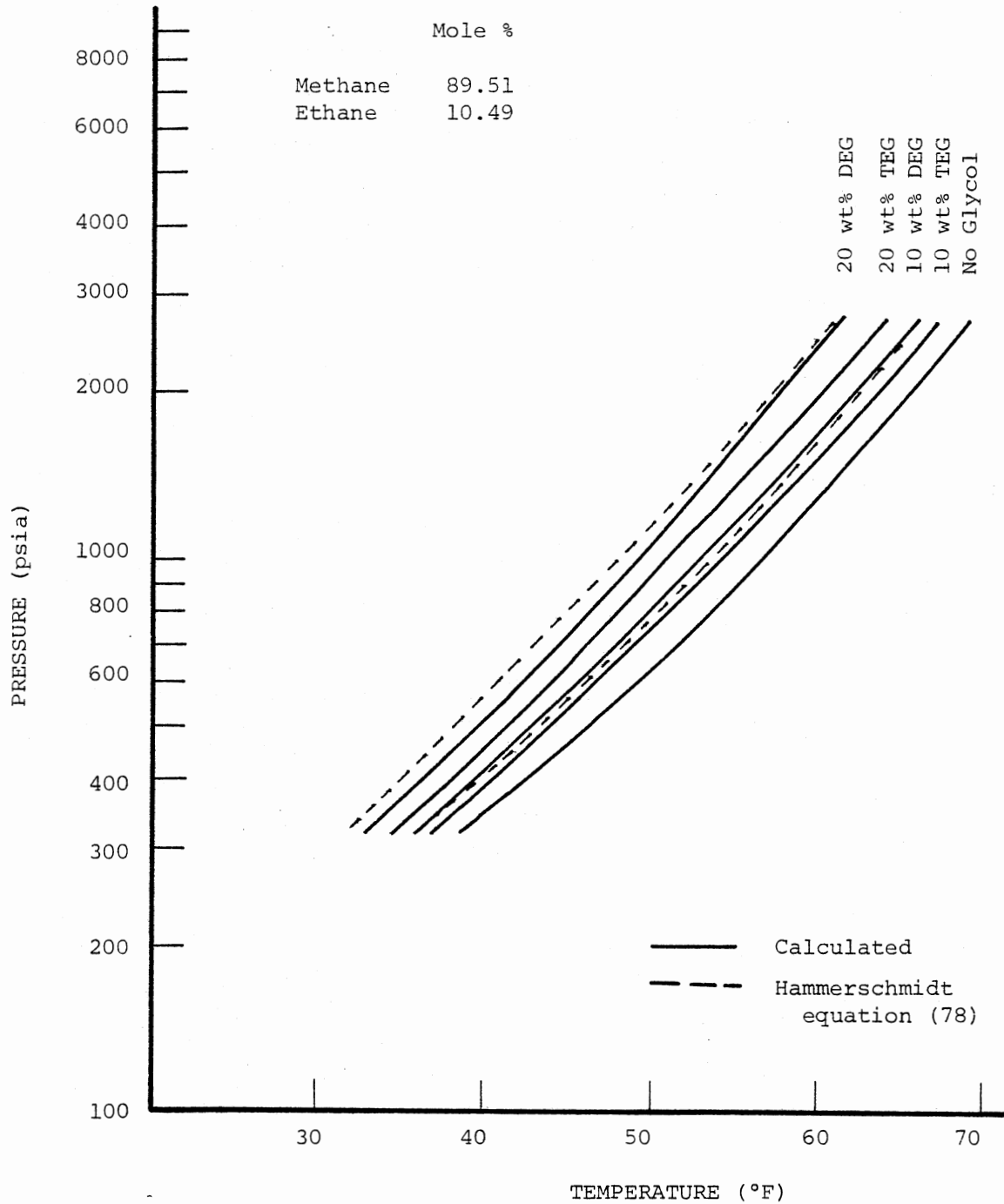


Figure 52. Effect of Glycols on Hydrate Forming Conditions for a Mixture Containing 89.51 Mole % Methane and 10.49 Mole % Ethane

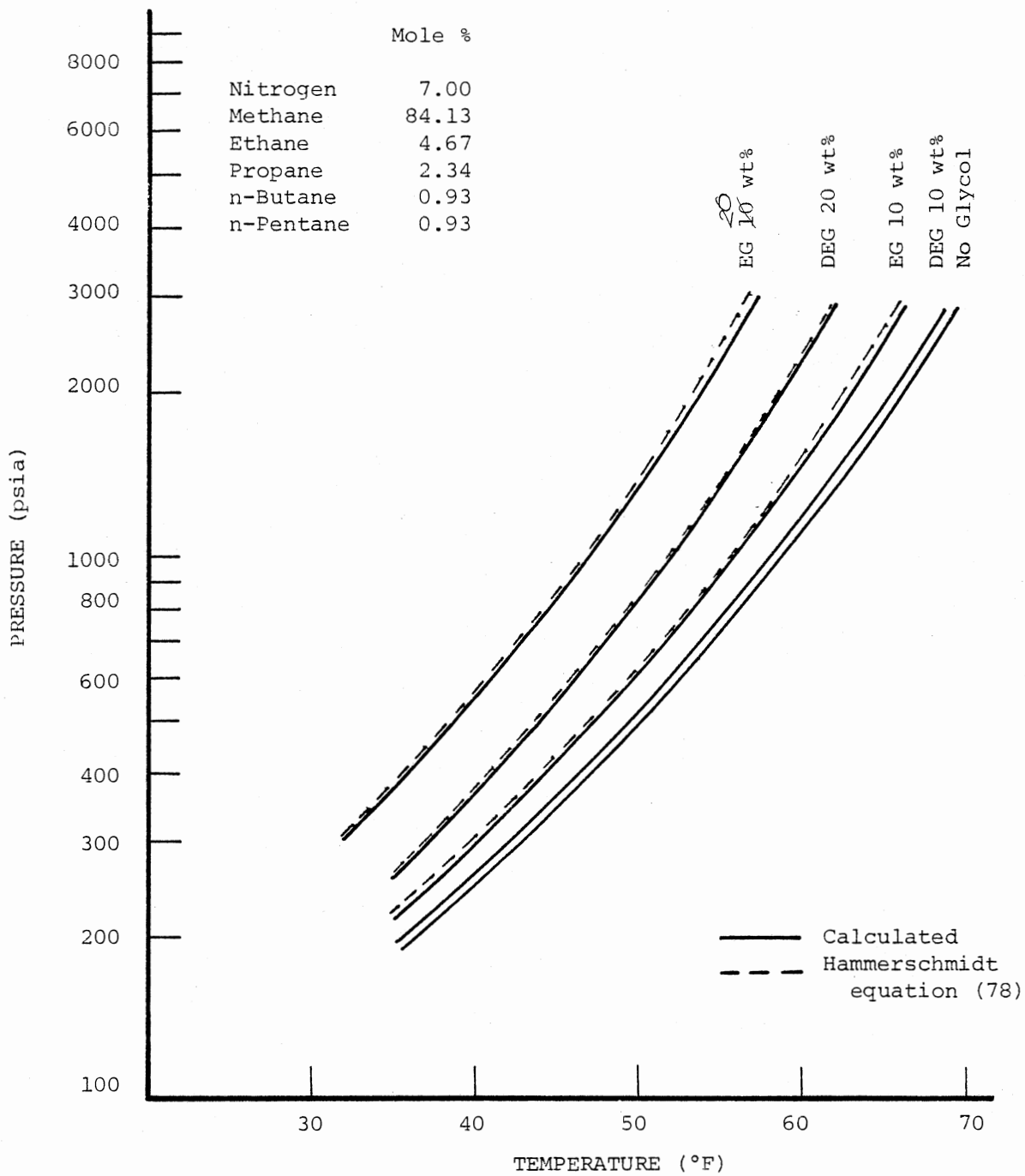


Figure 53. Effect of Glycols on Hydrate Forming Conditions in a Synthetic Natural Gas Mixture

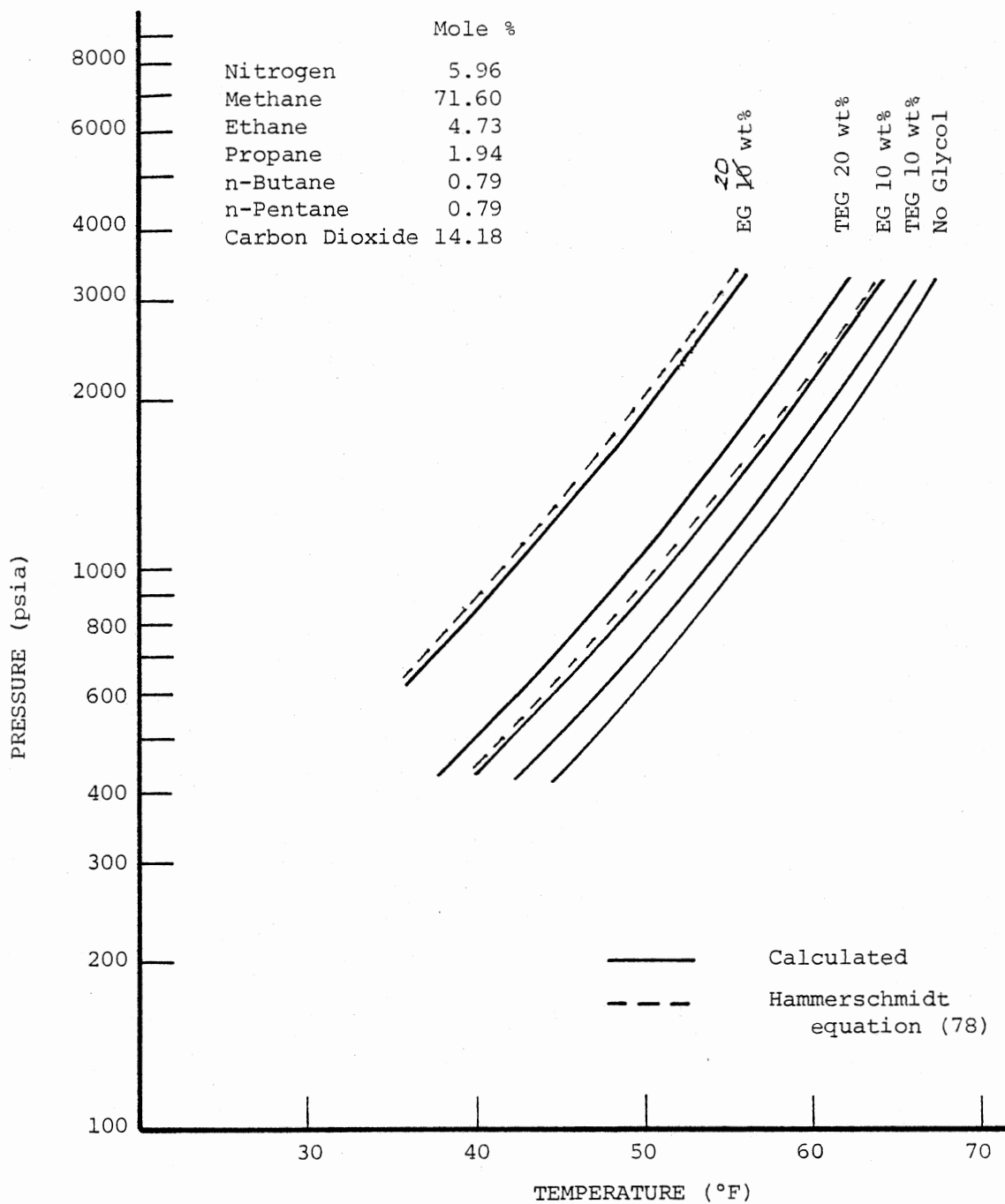


Figure 54. Effect of Glycols on Hydrate Forming Conditions for a Synthetic Gas Mixture Containing Carbon Dioxide

CHAPTER V

DISCUSSION OF RESULTS

For systems containing light hydrocarbons, nitrogen, carbon dioxide, hydrogen sulfide, methanol and glycols, the PFGC equation of state provides reliable gas phase fugacities, gas solubility in the aqueous phase, the activity coefficient of water, and the solubility of the components in the gas phase. These properties lead to accurate prediction of hydrate forming conditions using the technique developed by Parrish and Prausnitz (170). The use of the activity coefficient of water in the hydrate model as suggested by Menten, Parrish, and Sloan (148) is effective in calculating the inhibition of hydrate formation in the presence of methanol and glycols. The PFGC equation coupled to the new activity coefficient hydrate model provides a theoretically consistent alternative to the empirical Hammerschmidt equation (78).

Quality of Pure Component

Property Prediction

The root finding procedure based on the Richmond convergence scheme and the new fugacity expression proved to be very fast and reliable in solving the PFGC equation of state for pure component thermodynamic properties. Accurate prediction of a wide variety of component

properties is very important in the development of any equation of state. The PFGC equation reliably predicts the vapor pressure, volumetric properties and enthalpy departures for the liquid and vapor phases for paraffins, olefins, cycloparaffins, aromatics, some inorganics, methanol, and glycols. The quality of prediction of pure component thermodynamic properties varies with the number and type of different functional groups in each molecule. As a general rule, quality of property prediction deteriorates with increasing chain length and molecular complexity.

The quality of vapor pressure prediction for paraffin hydrocarbons is excellent considering the small number of parameters involved. Methane was considered an independent group. Ethane was used to derive parameters for the methyl group. Primary estimates of the methylene group were made from data on n-hexane. The final values for the methyl and methylene group interaction coefficients were derived from a simultaneous regression of data on butane, hexane, octane, and heptadecane. Some compromise in regressing the properties of the light and heavy ends was made to obtain acceptable vapor pressure predictions. The same strategy was followed for the other functional groups. Only sixteen groups are used to describe the vapor pressures of a large number of paraffins, olefins, cycloparaffins, and aromatics. In many cases, several components require group parameters and group interaction coefficients for the same group. If the same group was identified in more than one component, then the components containing that group were all regressed simultaneously. To be able to predict the vapor pressures of some components within five percent absolute average error, vapor pressures of other components containing the same type of groups had to

be compromised.

Parameters for most polar components and non-hydrocarbons were derived by considering the component as a single group. Vapor pressure predictions for carbon dioxide, hydrogen sulfide, water, nitrogen, carbon monoxide, and sulfur dioxide are well within the five percent target for absolute average error in the predicted value. The glycols were represented by two groups. The vapor pressure data for ethylene glycol, diethylene glycol, and triethylene glycol were used to simultaneously regress for the group parameters and binary group interaction coefficients. The decomposition of triethylene glycol at atmospheric pressure is the biggest deterrent to good data and consequently a major problem in obtaining a good vapor pressure fit. The absolute average error in predicted vapor pressure is still about 5 percent for all three glycols. The vapor pressure of methanol was well represented by considering methanol as a single group. The 5 to 6 percent deviation in vapor pressure of methanol may be due to the effect of dissociation in data acquisition. The ability of the PFGC equation of state to predict pure component properties for hydrocarbons, polar compounds, and glycols is very encouraging.

While the primary target for the error minimization was 1 to 5 percent absolute average error in vapor pressure results, volumetric properties and enthalpy departure predictions were not neglected. To prevent unreasonable volumetric and enthalpy predictions from the PFGC equation at any temperature and pressure, vapor pressure data from the critical point to the triple point were used whenever available. The calculated volumes and enthalpy departures at different temperatures and

pressures were checked for anomalous behavior. For components where such extensive data were unavailable, an attempt was made to extend existing data using extrapolation techniques. Vapor pressure data were extrapolated using the technique outlined by Korvezee and Gottschal (69). The Rackett equation (176) was used for liquid volumes. Vapor compressibility factors, and enthalpy departures, were obtained using the Pitzer (172) correlation. The liquid enthalpy departure was calculated using the heat of vaporization from the Watson (258) relationship and the vapor enthalpy departure.

Several difficulties were encountered in fitting the PFGC equation to pure component data. The major problems arose from lack of good experimental data. Very little high temperature vapor pressure data are available for paraffins heavier than octane, olefins, cycloparaffins and aromatics. The vapor pressure data on most non-hydrocarbons are unreliable. For glycols, the vapor pressure data are inconsistent, especially at atmospheric pressure. The lack of good experimental data leads to two very serious problems. First, some group parameters and interaction coefficients are derived from a limited range of vapor pressure data. Limited range of data affects the ability to describe volumetric and enthalpy departures over a wide range of conditions. Second, the unavailability of good volumetric or enthalpy departure data makes it difficult to evaluate these properties once they are predicted.

Another problem with enthalpy departure data lies with the ideal gas state enthalpy equation. For most components, ideal gas state enthalpy data are tabulated at intervals of about 100 degrees Kelvin. Most vapor pressure data fall between 100 to 300 degree Kelvin. It is impossible to take the three enthalpy departure data points, fit to

a polynomial and expect good ideal gas state enthalpy values for the entire saturation curve. This problem leads to the physically impossible results of positive vapor phase enthalpy departures at low temperatures for some components. Other problems originate from the group contribution method itself. The group contribution technique does not distinguish between molecule orientation. For this reason, cis-2-butene and trans-2-butene utilize the same group parameters, and the vapor pressure representation for cis-2-butene is not good. To avoid this problem in working with the xylenes, ortho, meta, and para xylene were represented by different functional groups for the three orientations. In spite of the difficulties mentioned above, the pure component thermodynamic properties are very well represented by the PFGC equation of state.

Quality of Vapor-Liquid Equilibrium

Predictions for Mixtures

Introduction of an interaction coefficient into the PFGC equation of state for every binary pair of groups is an effective way of predicting vapor-liquid equilibrium in multicomponent mixtures. The quality of equilibrium K-ratio predictions for a wide variety of binary and multicomponent systems is briefly discussed below.

Dry Light Hydrocarbon Systems

Several dry light hydrocarbon binary mixtures containing carbon dioxide, nitrogen, hydrogen sulfide, methane, ethane, ethylene, propane, benzene, toluene and a variety of cycloparaffins were regressed and evaluated using the PFGC equation of state.

The equilibrium K-ratio data for binary mixtures are scattered over a broad range of temperature and pressure. Consequently, it is incorrect to make generalizations on the behavior of the PFGC equation of state based solely on the percent absolute average deviations in calculated and experimental values. The percent absolute average error is only one of several criteria needed for evaluation of equilibrium K-ratio data. It is important to plot the calculated and experimental equilibrium K-ratios and do a qualitative evaluation based on the distribution of the errors, nature and shape of the plots, temperature and pressure conditions, molecular weights of individual components, and reliability of the data source. The equilibrium K-ratios vary over several orders of magnitude for a given mixture. No single statistical error analysis technique is flexible enough to allow a fair representation of the quality of predicted equilibrium K-ratios.

While the percent absolute average deviation in equilibrium K-ratios was considered an important criterion for the error minimization technique, selected results from the PFGC equation were plotted and qualitatively evaluated. The final values of the group parameters and binary interaction coefficients for use in the PFGC equation are listed in Table VII and VIII and are a result of these exhaustive evaluations. These parameters will provide reliable equilibrium K-ratios over a wide range of temperature and pressure conditions for the components evaluated.

Lack of good, reliable and consistent experimental data on equilibrium K-ratios was a major problem. Available data for binary systems from different sources were plotted and gross inconsistencies were discovered. In some cases the entire set of available data were plotted

and cross plotted to exclude inconsistent data points. Another major difficulty arose from the nature of the group contribution technique. Several binary group interaction parameters were fitted using vapor pressure data. Since the equation of state should have the ability to predict pure component properties, these binary group interaction parameters cannot be changed when regressing equilibrium K-ratios. The number of binary group interaction parameters that can be used to fit vapor liquid equilibrium data is, therefore, limited. Another problem that arises is the effect of the binary group interaction coefficient in a pure component versus a multicomponent mixture. If the binary group interaction coefficient was fitted to a binary mixture containing an equal number of both groups, it may not represent the behavior of a multicomponent mixture where, the number of groups of each type may not be the same. A good example of this problem is the paraffin-toluene system. The binary interaction coefficient between the $-\text{CH}_3$ and $=\text{CH}_2$ groups in toluene was optimized, using the vapor pressure data for toluene. For a certain percent absolute average error in vapor pressure prediction of toluene, the binary interaction coefficient between the two groups is a fixed number. Unfortunately, the same binary interaction coefficient is the key variable in obtaining good representation of toluene equilibrium K-ratios in paraffins. To be able to predict both the vapor pressure of toluene and its vapor-liquid equilibrium with paraffins, the binary interaction coefficient was fitted with great care. This problem is characteristic of a group contribution technique, where the number of groups is far less than the number of components. The group parameters and the binary interaction coefficients, represent a delicate balance between the ability to predict pure component

thermodynamic properties, and representation of vapor-liquid equilibrium data.

Aqueous Light Hydrocarbon Systems

Mixtures of water with paraffins, olefins, carbon dioxide, hydrogen sulfide, nitrogen and carbon monoxide were used to derive the vapor-liquid-liquid equilibrium of aqueous light hydrocarbon systems. Two interaction coefficients were defined for the various phases present; one binary interaction coefficient for both the hydrocarbon-rich liquid and vapor phase and another interaction coefficient per binary pair for the aqueous liquid phase. Some of the aqueous liquid phase binary interaction coefficients were found to be linearly dependent on absolute temperature. Also, the binary interaction coefficients for non-aqueous pairs in the aqueous liquid phase and vapor (and hydrocarbon-rich liquid) phase were assumed to be the same. The improvement in vapor-liquid-liquid equilibrium predictions by introducing an additional parameter is ineligious.

The lack of good vapor-liquid-liquid equilibrium data on light hydrocarbon systems was the major problem in deriving the binary interaction coefficients. Since the number of groups is much less than the number of components, the available data were adequate for developing the binary interaction coefficients. Additional vapor liquid liquid equilibrium data are needed on the higher molecular weight components to check the quality of predictions. The literature data on the binary systems of isobutane-and isopentane-water are very scarce. Another problem in predicting vapor-liquid-liquid behavior of aqueous systems lies in the temperature dependence of the binary interaction coefficient.

In most cases the relationship of the binary interaction coefficient with absolute temperature is linear. There are, however, instances where the optimal binary interaction coefficient has a slightly parabolic dependence on absolute temperature. In these cases, the binary interaction coefficient was fitted to the data with extreme caution to avoid serious errors at temperatures and pressures other outside the range of the experimental values.

The quality of the vapor-liquid-liquid equilibrium predictions from the PFGC equation show an improvement over the work of Moshfeghian, Shariat, and Erbar (153). For paraffins and olefins the PFGC equation gives excellent predictions of the concentrations of the vapor, hydrocarbon-rich liquid, and the water-rich liquid phases for pressure up to 9000 psia. Vapor-liquid-liquid predictions for binary systems containing carbon dioxide and hydrogen sulfide are very good up to 3000 psia. The reliability of most vapor liquid liquid equilibrium data above these pressures is very doubtful (57). The prediction of the solubilities of paraffins, olefins, carbon dioxide, hydrogen sulfide, nitrogen and oxygen in water is of importance in the hydrate prediction calculation. The ability of the PFGC to handle aqueous mixtures well is due to its strong theoretical dependence on a liquid activity coefficient model. The accuracy in predicting vapor liquid liquid equilibrium conditions for a variety of components is a demonstration of this ability of the PFGC equation.

Methanol and Glycol Systems

Vapor liquid equilibrium data for methanol and glycol binary systems with paraffins, olefins, aromatics, nitrogen, carbon dioxide, hydrogen sulfide and water are generally well represented by the PFGC equation of state. The vapor liquid equilibrium behavior of the methanol-water system is very difficult to predict using other equations of state. The PFGC equation provides reliable vapor-liquid equilibrium prediction of methanol with water. Binary systems of methanol with carbon dioxide, nitrogen, hydrogen sulfide, methane, ethane, and ethylene are also remarkably well represented. While data on the C₅ to C₈ range hydrocarbon-methanol systems are available in the literature, the data for lighter hydrocarbons in equilibrium with methanol are very sparse. For example, very little experimental data have been collected on the methanol-methane system. Most of what appears in the literature as vapor-liquid equilibrium data are extrapolations of the data taken by Hammerschmidt (78). At low temperatures, the vapor phase mole fraction of methanol in the methanol-methane binary system is very small. A small error in the vapor phase mole fraction of methanol can lead to large errors in vaporization loss estimation calculations. The experimental data are very unreliable when the mole fraction of methanol is less than 10⁻⁴. The results from the vapor-liquid equilibrium predictions of the methanol-methane system were plotted, and the methanol vaporization losses were compared with those given by Nielsen and Bucklin (161). The PFGC is a very promising tool in providing a reliable and consistent basis for methanol vaporization loss calculations.

In fitting the vapor-liquid equilibrium data for glycol systems to

the PFGC equation of state, the glycol-water system was the most difficult to regress. Ethylene glycol, diethylene glycol, and triethylene glycol are all represented by two functional groups. Fitting the vapor pressure data of diethylene and triethylene glycols fixed all the group parameters and the binary interaction parameters between these two groups. Only two adjustable parameters were used to describe the vapor-liquid equilibrium of all three glycols with water. The parabolic dependence of the binary interaction coefficients on absolute temperature, the decomposition of triethylene glycol near atmospheric pressure, and the absence of good, reliable experimental data added to the problem. Similar difficulties were encountered with other glycol systems. The final values for the two glycol functional group parameters and the binary interaction coefficients with other groups are optimal for the existing data on glycol systems.

Multicomponent Test Mixtures

Most real life applications of vapor-liquid equilibrium calculations involve the use of multicomponent mixtures. The group parameters and the binary group interaction coefficients for the PFGC equation of state were developed using binary mixtures. Selected multicomponent test mixtures were used to verify the applicability of the PFGC equation to mixtures of several components. The test mixtures were selected as being representative of a particular application. The comparison of predicted and experimental vapor phase water solubilities for a typical light hydrocarbon mixture containing carbon dioxide is done using Test Mixture I. The values predicted by the PFGC equation agree very well with experimental data. The PFGC equation shows promise for

application to mixtures of light hydrocarbons, water, carbon dioxide, hydrogen sulfide, and nitrogen. The ability of the PFGC equation to predict equilibrium K-ratios for components in a multicomponent mixture was tested using Test Mixture II which is a simulated natural gas mixture. The predicted equilibrium K-ratios compare well with the experimental values. In general, the PFGC equation tends to be more accurate in predicting equilibrium phase properties of multicomponent mixtures than binaries due to compensating errors.

The purpose of selecting Test Mixture III was the comparison of predicted and calculated equilibrium liquid and vapor phase densities for a typical sour gas system. Comparison of the predicted and experimental densities provides a very strict test for the reliability of the PFGC equation of state for volumetric prediction. The calculated and experimental equilibrium liquid and vapor phase densities agreed to within 7 percent. The PFGC equation is useful in providing accurate liquid and vapor densities for typical hydrocarbon mixtures. Applicability of the PFGC equation to a synthetic natural gas with a high nitrogen content was tested using Test Mixture IV. The calculated and experimental bubble point pressures agreed very well. The verification of the correct phase separation and density prediction was done using liquid volume fraction data. The experimental liquid volume fraction curves at different temperatures were matched very well by the PFGC equation. The results from the PFGC equation for high nitrogen content gases are very encouraging.

Test Mixture V was used as an extreme test of the PFGC equation in predicting phase behavior of synthetic oils with a high carbon dioxide content. The results from the PFGC equation were very

encouraging. Using the equation parameters and binary interaction coefficients derived from binary carbon dioxide mixtures, the equation predicted reasonably well the bubble point curves of Test Mixture V where the carbon dioxide content ranged from 20 to 97 percent. This is a demonstration of the application of the PFGC equation to a synthetic oil contained carbon dioxide. The absence of the critical temperature and pressure and the acentric factor as a correlating parameter was a great advantage in a synthetic oil application. The PFGC equation shows promise for prediction of the vapor-liquid equilibrium of heavy oils containing heavy carbon dioxide content. In addition to the test mixtures mentioned above, the PFGC equation was evaluated for multicomponent mixtures using data from several proprietary sources. The PFGC shows the potential of being a very useful tool for predicting the vapor-liquid equilibrium of multicomponent mixtures.

Quality of Predictions of Hydrate Forming

Conditions for Pure Components

The thermodynamic properties predicted by the PFGC equation were used to calculate hydrate forming conditions for methane, ethane, propane, butanes, ethylene, propylene, carbon dioxide, sulfur dioxide, nitrogen, and oxygen. The perturbation type model proposed by Holder, Papadopolous, and John (87) to add a correction factor to the Langmuir constant was evaluated. A correction factor to account for the non-idealities in the molecular interactions is needed, but the correction proposed by Holder, Papadopolous and John (87) does not adequately define the contributions in the various cavities. The choice of the correlating parameters in the proposed modification, i.e., the Kihara size parameter, the Kihara

energy parameter, and the acentric factor in the proposed modification may be a good one, but the functional form of the correction needs to be improved. Consequently, the new model did not improve the prediction of the dissociation pressures for the hydrate forming gases. The basic Van der Waals and Platteeuw (256) model as developed by Parrish and Prausnitz (170) was used with the activity coefficient correction suggested by Menten, Parrish, and Sloan (148).

The new Kihara parameters for use in the hydrate model were derived by minimizing the absolute difference in experimental and calculated hydrate forming temperatures. As noted by Holder, Papadopolous, and John (87) there are several sets of Kihara parameters that would predict the hydrate forming curves for pure components. There is only one set of parameters that is theoretically correct and would accurately describe the behavior of the gas in a multicomponent mixture. The final values of the Kihara parameters agree well with the values reported by Parrish and Prausnitz (170). The parameters reported by Parrish and Prausnitz (170) are very similar to the Kihara parameters derived from second virial coefficient or viscosity data, and were used to predict hydrate forming conditions in multicomponent mixtures. The prediction of the hydrate forming temperature for the majority of pure components fitted are accurate to within 4°F. The hydrate dissociation pressures for pure components are predicted within 10% of the experimental values. The results from the new hydrate model coupled to the PFGC equation are very encouraging.

Quality of Prediction of Multicomponent Hydrate Forming Conditions

The pure component Kihara parameters developed for the hydrate model were used to evaluate the quality of prediction of multicomponent hydrate forming conditions. The proportionality constant and binary interaction constant suggested by Ng and Robinson (159) were introduced into the hydrate model to provide one adjustable parameter per binary pair of components. Using this adjustable parameter, the hydrate model can be closely fitted to a given set of data on hydrate forming conditions. However, the biggest drawback in introducing a binary interaction constant between components in the hydrate model is the loss of predictive capability for a broader range of conditions. While considerable improvement for a specific mixture can be achieved by the introduction of a binary interaction constant the lack of a theoretical basis for this adjustment can lead to erroneous predictions for other mixtures. For this reason, no binary interaction constant were used in the hydrate model. To obtain a good fit of experimental data on hydrate forming conditions of mixtures, the Kihara parameters obtained from fitting pure component hydrate data were finely adjusted. It is possible to have more than one set of Kihara parameters for pure component hydrate prediction, but only one of them gives the correct result in predicting hydrate forming conditions for mixtures. Therefore, selection of the correct Kihara parameters to predict both pure component and mixture hydrate data involved a careful trial and error adjustment. The final values of the Kihara parameters will predict hydrate forming conditions for most light hydrocarbon mixtures containing hydrogen sulfide, carbon dioxide, nitrogen, and oxygen to within

4°F. Errors tend to be higher if the concentrations of hydrogen sulfide or carbon dioxide in the gas mixture are greater than about 10 percent.

Quality of Prediction of the Effect of Methanol

Glycols as Hydrate Inhibitors

The PFGC equation of state was coupled to the hydrate prediction model and the activity coefficient modification suggested by Menten, Parrish, and Sloan (148) was used to calculate the inhibition of hydrate formation in the presence of methanol and glycols.

The ability to predict the inhibition of hydrate formation in the presence of methanol and glycols was the most important test for the usefulness of the new model. The agreement with the experimental data on the effect of methanol on hydrate forming conditions for methane, ethane, propane, carbon dioxide, hydrogen sulfide, and several light hydrocarbon mixtures was excellent. The PFGC equation of state and the new hydrate model performed remarkably well over the entire range of available data. For pure components the hydrate forming temperature predictions were accurate to within 3°F. The hydrate forming temperature predictions were well within 4°F for most mixtures. The errors for mixtures containing carbon dioxide in amounts greater than about 10 mole percent tend to be higher than 4°F. Methanol vaporization losses are predicted by vapor-liquid-liquid equilibrium calculations. The methanol vaporization losses are generally well represented except at temperatures below 0°F where the mole fraction of methanol in the vapor phase becomes less than 10^{-4} and is too small to be significant.

No experimental data are available on the effect of ethylene glycol, diethylene glycol, and triethylene glycol on hydrate-forming conditions.

The results from the PFGC equation and the new hydrate model were qualitatively evaluated. If an equal number of moles of ethylene glycol, diethylene glycol, and triethylene glycol are added to a mixture, the effect of triethylene glycol on hydrate forming conditions is the strongest of the three glycols. The inhibition of the hydrate-forming conditions in the presence of glycols compared favorably with the Hammerschmidt equation at low glycol concentrations in the aqueous liquid phase. As new hydrate formation data in the presence of glycols are published, the new hydrate model can be evaluated and the prediction of hydrate inhibition can be improved.

CHAPTER VI

CONCLUSIONS AND RECOMMENDATIONS

Conclusions

1. The PFGC equation has demonstrated the capability to reliably predict the pure component vapor pressures, volumetric properties and enthalpy departures for paraffins, olefins, cycloparaffins, aromatics, nitrogen, carbon dioxide, hydrogen sulfide, methanol, glycols, and water.

2. Vapor-liquid equilibrium prediction using the PFGC equation for binary mixtures of light hydrocarbons with carbon dioxide, nitrogen, hydrogen sulfide, methane, ethane, ethylene, propane, benzene, toluene, and a variety of cycloparaffins are in good agreement with available experimental data.

3. The predictions from the PFGC equation for the concentrations of the vapor, hydrocarbon-rich liquid and the water-rich liquid phases for aqueous mixtures with paraffins, olefins, carbon dioxide, hydrogen sulfide, nitrogen, and carbon monoxide are accurate and reliable.

4. Methanol, ethylene glycol, diethylene glycol and triethylene glycol systems with paraffins, olefins, aromatics, nitrogen, carbon dioxide, hydrogen sulfide, and water are generally well represented by the PFGC equation. Therefore the activity coefficient of water in the presence of the methanol or glycols can be used in the hydrate model.

5. The PFGC equation is a promising tool in predicting the vapor

liquid equilibrium for a broad variety of multicomponent mixtures. The thermodynamic properties for typical hydrocarbon mixtures containing natural gas, sour gas, high nitrogen content and heavy oils with large amounts of carbon dioxide show encouraging results from the PFGC equation of state.

6. The thermodynamic properties predicted by the PFGC equation are coupled to the hydrate model used by Parrish and Prausnitz (170). The activity coefficient correction suggested by Menton, Parrish and Sloan (148) is used in the hydrate model. Hydrate forming temperatures for methane, ethane, propane, butanes, ethylene, propylene, carbon dioxide, sulfur dioxide, nitrogen, and oxygen are predicted within 4°F.

7. Hydrate-forming conditions for multicomponent mixtures containing light hydrocarbons with hydrogen sulfide, carbon dioxide, and nitrogen are predicted within 4°F using the Kihara parameters developed from the pure component hydrate-forming data.

8. The addition of methanol, ethylene glycol, diethylene glycol and triethylene glycol to inhibit hydrate formation is accurately represented by the PFGC equation and the hydrate model. The activity coefficient of water in the presence of methanol or glycols, calculated using the PFGC equation, accounts for the presence of the inhibitor in the aqueous liquid phase. Vaporization losses for methanol are given by the solubility of the methanol in the hydrocarbon-rich liquid phase. The PFGC equation and the hydrate model show encouraging results and provide a theoretically consistent alternative to the Hammerschmidt equation.

Recommendations

1. As new data on thermodynamic properties of pure components and

mixtures become available, the group parameters and binary group interaction coefficients in the PFGC equation should be evaluated and improved. The vapor and liquid equilibrium phase enthalpy departures and densities from the PFGC equation for hydrocarbon mixtures should be evaluated in greater detail.

2. The pure component and mixture hydrate formation data available in the future should be used to improve the predictions from the hydrate model. The predictions from the PFGC equation and the hydrate model should be checked against new data taken on the effect of methanol and glycols on hydrate-forming conditions of light hydrocarbon mixtures. The ability to predict the depression of the freezing point of water in the presence of methanol and glycols and the availability of liquid water to form hydrates below the ice point should be incorporated into the hydrate model.

3. The PFGC equation should be extended to systems containing hydrogen, physical absorbents for acid gas removal from synthetic and natural gases, aromatic molecules used in coal liquefaction, sulfur containing compounds in coal gasification, halogenated refrigerants, and other organic chemicals. The PFGC equation should be used with another ionic activity coefficient model to predict the behavior of ionic solutions. If a breakdown of different types of groups in a compound is available from a C^{13} Nuclear Magnetic Resonance, the PFGC equation can be used for the characterization of heavy components. This will improve predictions of the properties for reservoir fluids and natural gas systems.

4. Improved calculation techniques to handle multiple liquid phases should be developed. The PFGC equation can be incorporated

into the new techniques to provide a better understanding of complex phenomena like multiphase distillation and high carbon dioxide content reservoir simulation.

5. Different group prediction models should be studied and evaluated for the prediction of other physical properties. Other equations of state should be tested and incorporated into the hydrate model. Theoretically sound correction factors and mixing rules should be developed and introduced into the existing hydrate model to improve the predictions for hydrate formation in mixtures. Better models for predicting hydrate forming conditions should be developed.

6. Techniques to provide theoretically sound initial estimates for group parameters and binary group interaction parameters in the PFGC equation should be developed. The same techniques should be extended for use in developing initial estimates for Kihara parameters in the hydrate model.

7. The thermodynamic properties used in the development of the PFGC equation should be used to evaluate and develop other equations of state. Efforts should be made to keep these data current by adding new data as they are published.

8. The PFGC equation show promise as a source of reliable thermodynamic properties for application in process design and evaluation, process simulation, design and operation of distillation equipment, reservoir simulation, cryogenic processes and a variety of other applications.

BIBLIOGRAPHY

1. Akers, W. W., Burns, J. F., and Fairchild, W. R.,
Ind. Eng. Chem., 46(12), pp. 2531-2534, (1954).
2. Akers, W. W., Kehn, D. M., and Kilgore, C. H.,
Ind. Eng. Chem., 46(12), pp. 2536-2539, (1954).
3. Akers, W. W., Kelley, R. E., and Lipscomb, T. G.,
Ind. Eng. Chem., 46(12), pp. 2535-2536, (1954)
4. Ambrose, D., and Hall, D. J., J. Chem. Thermo.,
13, pp. 61-66, (1981).
5. Amick, E. H., Winford, B. J., and Barrett, D.,
Chem. Eng. Prog. Symp. Ser. No 3,
48, pp. 65-72 (1952).
6. Anthony, R. G., and McKetta, J. J., J. Chem. Eng. Data,
12(1), pp. 17-20, (1957).
7. Arnold, E. W., Liou, D. W., and Eldridge, J. W.,
J. Chem. Eng. Data, 10(2), pp. 88-92, (1965).
8. ASHRAE Handbook, Fundamentals 1981, American Society of
Heating, Refrigerating and Air Conditioning
Engineers, Third Printing, pp. 17.49, (1982).
9. Azarnoosh, A., and McKetta, J. J., J. Chem. Eng. Data,
4(3), pp. 211-212, (1959).
10. Azarnoosh, A., and McKetta, J. J., Petroleum Refiner,
37(11), pp. 275-278, (1958).
11. Benedict, M., Johnson, C. A., Solomon, E., and Rubin, L. C.,
Paper Presented at the Philadelphia-Wilmington
Section, AIChE Meeting, April 10, (1945).
12. Besserer, G. J. and Robinson, D. B., J. Chem. Eng. Data,
18(3), pp. 298-301, (1973).
13. Besserer, G. J. and Robinson, D. B., J. Chem. Eng. Data,
18(3), pp. 301-304, (1973).
14. Besserer, G. J. and Robinson, D. B., J. Chem. Eng. Data,
18(4), pp. 416-419, (1973).

15. Besserer, G. J. and Robinson, D. B., J. Chem. Eng. Data, 20(1), pp. 93-96, (1975).
16. Bierlein, J. A., and Webster, B. K., Ind. Eng. Chem., 45(3), pp. 618-624, (1953).
17. Blake, R. J., Oil and Gas Journal, 65(2), pp. 105-107, (1967).
18. Bradbury, E. J., McNulty, D., Savage, R. L., and McSweeney, E. E., Ind. Eng. Chem., 44(1), pp. 211-212, (1952).
19. Brewer, J., Rodewa, H. N., and Kurata, F., AIChE J., 7(1), pp. 13-19, (1961).
20. Brown, I., and Ewald, A. H., Australian J. Sci. Res., 4A, pp. 198-212, (1951).
21. Brunner, G., Peter, S., and Wenzel, H., Chem. Eng. J., 7, pp. 99-104, (1974).
22. Burgess, M. P., and Germann, R. P., AIChE J., 15(2), pp. 272-275, (1967).
23. Byk, S. S., and Formina, V. I., Russ. Chem. Rev., 37(6), pp. 469, (1968).
24. Campbell, J. M., " Gas Conditioning and Processing ", Vol II, Campbell Petroleum Series, (1981).
25. Canjar, L., and Manning, F., "Thermodynamic Properties and Reduced Correlations for Gases", Gulf Publishing Corporation, Houston, Texas, (1966).
26. Chandler, J. P. and Leon, L. W., "Modification of Marquardt's Non-Linear Fit Program, Dept. of Computing and Information Sciences, Oklahoma State University, Stillwater, Oklahoma, (1978).
27. Chang, H. L., Hurt, L. J., and Kobayashi, R., AIChE J., 12(6), pp. 1212-1216, (1966).
28. Chang, H. L., and Kobayashi, R., J. Chem. Eng. Data, 12(4), pp. 517-523, (1967).
29. Chang, S. D., Lu, B. C. Y., Chem. Eng. Prog. Symp. Ser., 63(81), pp. 18-27, (1967).
30. Chu, T. C., Chen, R. J. J., Chappellear, P. S., and Kobayashi, R., J. Chem. Eng. Data, 21(1), pp. 41-43, (1976).

31. Cines, M. R., Roach, J. J., Hogan, R. J., and Roland, C. H., Chem. Eng. Symp. Ser. No. 6, 49, pp. 1-10, (1956).
32. Clarke, E. C., Ford, R. W., and Glen, D. N., Can. J. Chem., 42, (1964).
33. Claussen, W. F., J. Chem. Phys., 19, pp. 1425, (1951).
34. Cleef, Van A, and Diepen, G. A. M., Rec. Trav. Chim, 69, pp. 593-603, (1960).
35. Cleef, Van A, and Diepen, G. A. M., Rec. Trav. Chim, 79, pp. 583-587, (1960).
36. Cleef, Van A, and Diepen, G. A. M., Rec. Trav. Chim, 81, pp. 425-429, (1962).
37. Cleef, Van A, and Diepen, G. A. M., Rec. Trav. Chim, 84, pp. 1085-1093, (1965).
38. Coan, C. R., and King, A. D., J. Am. Chem. Soc., 93(8), pp. 1857-1862, (1971).
39. Cunningham, J. R., "Calculation of Parameters From Group Contributions for the PFGC Equation of State", M. S. Thesis, Brigham Young University, Provo, Utah, (1974).
40. Cunningham, J. R., and Wilson, G. M., Paper Presented at the Gas Processors Association Meeting, Technical Section F, March 25, Denver, Colorado, (1974).
41. Dalager, P., J. Chem. Eng. Data., 14(3), pp. 298-301, (1969).
42. Danniel, A., Todheide, K., and Franck, E. U., Chem. Ing. Techn., 39(13), pp. 816-821, (1967).
43. Davalos, J., Anderson, W., Phelps, R., and Kidnay, A. J., J. Chem. Eng. Data, 21(1), pp. 81-84, (1976).
44. Davis, J. E., and McKetta, J. J., J. Chem. Eng. Data, 5(3), pp. 374-375, (1960).
45. Deaton, W. M., and Frost, E. M., United States Bur. Mines Monograph 8, (1946).
46. Djordjevich, L., and Budenholzer, R. A., J. Chem. Eng. Data, 15(1), pp. 10-12, (1970).
47. Donnelly, H. G., and Katz, D. L., Ind. Eng. Chem., 46(3), pp. 511-517, (1954).

48. Douglas, G. E., Chen, R. J. J., Chappellear, P. S., and Kobayashi, R., J. Chem. Eng. Data, 19(1), pp. 71-77, (1974).
49. Dow Chemical Handbook, "Properties of Glycols," pp. 1-20, Dow Chemical Company.
50. Edmister, W. C., Hydrocarbon Processing, 51(12), pp. 93-101, (1972).
51. Elbishlawi, M., and Spencer, J. R., Ind. Eng. Chem., 43(8), pp. 1811-1815, (1951).
52. Engineering Sciences Data Unit, Chemical Engineering Series, Physical Data, Volume 5, 251-259 Regent Street, London W1R 7AD, August, (1975).
53. Erbar, J. H., "Documentation on the GPA*SIM Program", August, (1980).
54. Erbar, J. H., "Comments on the Multiproperty and Multicomponent Fit Program MPMCGC for the PFGC Equation of State, LINDE AG, Munich, W. Germany, (1980).
55. Erbar, J. H., Personal Communication. Oklahoma State University, Stillwater, Oklahoma, 1981.
56. Erbar, J. H., Personal Communication. Oklahoma State University, Stillwater, Oklahoma, 1982.
57. Erbar, J. H., Jagota, A. K., Muthswamy, S., and Moshfeghian, M., Gas Processors Association, Research Report, RR-42, August, (1980).
58. Erichson, L., Leu, A. D., Ng, H. J., and Robinson, D. B., "Hydrate Formation Conditions in the Presence of Methanol", Report Presented to Canadian Gas Processors Association, Edmonton, Alberta, June 11, (1981).
59. Faraday, M., Trans. Roy. Soc. (London), A22, 160, pp. 1823, (1823).
60. Ferrell, J. K., Rousseau, R. W., and Bass, D. G., "The Solubility of Acid Gases in Methanol", EPA Report No. EPA-600/7-97-097, April, (1979).
61. Fredenslund, A., Mollerup, J., and Hall, K. R., Off-Print from J. of Chem. Soc., Faraday Transactions I, (1974).
62. Fredenslund, A., Mollerup, J., J. Chem. Soc., Faraday Transactions I, 70, pp. 1653-1659, (1974).
63. Gilliland, E. R., and Scheeline, H. W., Ind. Eng. Chem., 32(1), pp. 48-54, (1940).

64. Glanville, J. W., Sage, B. H., and Lacey, W. N.,
Ind. Eng. Chem., 42(3), pp. 508-513, (1950).
65. Gmehling, J., and Onken, U., "Vapor Liquid Equilibrium
Data Collection," 1(1), pp. 201-204, DECHEMA, Frankfurt,
W. Germany, 1977.
66. Gmehling, J., and Onken, U., "Vapor Liquid Equilibrium
Data Collection," Supplement, pp. 352-353, DECHEMA,
Frankfurt, W. Germany, 1978.
67. Goodwin, R. D., "The Thermophysical Properties of Methane
from 90 to 500 K at Pressures to 700 Bar",
Nat. Bur. Stand. (U.S.), Tech Note 653, (1974).
68. Goodwin, R. D., "The Thermophysical Properties of Ethane
from 90 to 600 K at Pressures to 700 Bar",
Nat. Bur. Stand. (U.S.), Tech Note 684, (1976).
69. Gottschal, A. J., and Korvezee, A. E., Rec. Trav. Chim.,
72, pp. 465-481, (1953).
70. GPA*SIM Program, Gas Processors Association, Tulsa,
Oklahoma, (1980).
71. Green, S. J., and Vener, R. E., Ind. Eng. Chem., 47(1),
pp. 103-109, (1955).
72. Grenier-Loustalot, M., Potin-Gautier, M., and Grenier, P.,
Analytical Letters, 14(A16), pp. 1335-1349, (1981).
73. Griswold, J., and Wong, S. Y.,
Chem. Eng. Sci. Symp. Ser. No. 3, 48(2),
pp. 18-34, (1952).
74. Hakuta, T., Nagahama, K., Suda, S.,
Kogaku Kagaku, 33(9), pp. 904-907, (1969).
75. Hamam, S. E. M., and Benjamin, C.,
Can. J. Chem. Eng., 52, pp. 282-286, (1974).
76. Hamam, S. E. M., Lu, Y., and Benjamin, C.,
J. Chem. Eng. Data, 21(2), pp. 200-204, (1976).
77. Hammerschmidt, E. G., Ind. and Eng. Chem.,
26(8), pp. 851-855, (1934).
78. Hammerschmidt, E. G., Oil and Gas J., 37,
pp. 66-72, (1939).
79. Hanson, G. A., Hogan, R. J., Nelson, W. T., and Cines M. R.,
Ind. Eng. Chem., 44(3), pp. 604-609, (1952).

80. Hanson, G. H., Hogan, R. J., Ruchlen, F. N., and Cines, M. R., Chem. Eng. Symp. Ser. No. 6, 49(6), pp. 37-44, (1953).
81. Hirata, M., Nagahama, K., and Bae, H., J. Chem. Eng. Data, 27(1), pp.25-27, (1982).
82. Hirata, M. and Suda, S., Kagaku Kogaku, 31(8), pp. 759-766, (1967).
83. Hiza, M. J., Kidnay, A. J., and Miller, R. C., J. Chem. Thermodynamics, 9, pp. 167-178, (1977).
84. Holder, G. D., " Multiphase Equilibria in Methane-Ethane-Propane-Water Hydrate Forming Systems", Ph. D. Thesis, Univ. of Michigan, (1976).
85. Holder, G. D., Corbin, G., and Papadopoulos, K. D., Ind. and Chem. Fundam., 19, pp. 282-286, (1980).
86. Holder, G. D., and Hand, J. H., AIChE J., 28(3), pp. 440-447, (1982).
87. Holder, G. D., Papadopoulos, K. D., and John, V. T., Manuscript submitted to AIChE Journal, (1983).
88. Hudson, J. W., and Winkle, M. Van, J. Chem. Eng. Data, 14(3), pp. 310-318, (1969).
89. Hughes, H. E., and Maloney, J. O., Chem. Eng. Progr., 48(4), pp. 192-200, (1952).
90. IUPAC "International Thermodynamic Tables of the Fluid State", Chem. Data Series No. 25, Propylene, Pergamon Press, London, (1980).
91. IUPAC "International Thermodynamic Tables of the Fluid State", Chem. Data Series No. 7, Carbon Dioxide, Pergamon Press, London, (1980).
92. Jacoby, R. H., "Vapor Liquid Equilibrium Data for the Use of Methanol in Preventing Gas Hydrates, Gas Hydrate Control Conference, May 5-6, Extension Division, University of Oklahoma, Norman, (1953).
93. John, V. T., and Holder, G. D., J. Phys. Chem., 85(13), pp. 1811-1814, (1981).
94. John, V. T., and Holder, G. D., J. Phys. Chem., 86(4), pp. 455-459, (1982).
95. Kahre, L. C., J. Chem. Eng. Data, 19(1), pp. 67-71, (1974).

96. Kahre, L. C., J. Chem. Eng. Data, 20(4), pp. 363-367, (1975).
96. Kaminishi, G., Arai, Y., Saito, S., and Maeda, S., J. Chem. Eng. of Japan, 1(2), pp. 109-116, (1968).
97. Katayama, T., Ohgaki, K., Maekawa, G., Goto, M., and Nagano, T., J. Chem. Eng. of Japan, 8(2), pp. 89-92, (1975).
98. Katayama, T. and Ohgaki, K., J. Chem. Eng. Data, 21(1), pp. 53-54, (1976).
99. Kato, M., Konishi, H., and Hirata, M., J. Chem. Eng. Data, 15(4), pp. 501-505, (1970).
100. Katz, D. L., Handbook of Natural Gas Engineering, 2nd Ed., McGraw Hill Book Co., New York, (1959).
101. Katz, D. L., "Prediction of Conditions for Hydrate Formation in Natural Gases", Amer. Inst. Mining and Metall. Eng., Technical Publication No. 1748.
102. Katz, D. L. and Carson, D. B., Trans. AIME, 146, pp. 150, (1942).
102. Kay, W. B., and Brice, D. B., Ind. Eng. Chem., 45(3), pp. 615-624, (1953).
103. Kazunari, O., and Katayama, T., Fluid Phase Equilibria, 1, pp. 27-32, (1977).
104. Kidnay, A. J., and Somait, F. A., J. Chem. Eng. Data, 23(4), pp. 301-305, (1978).
105. Kidnay, A. J., Hegarty, M. J., Gardner, G. C., and Gupta, M. K., J. Chem. Eng. Data, 25(4), pp. 313-318, (1980).
106. Kidnay, A. J., Hiza, M. J., and Miller, R. C., J. Phys. Chem. Ref. Data, 8(3), pp. 799-816, (1979).
107. Kidnay, A. J., Miller, R. C., Parrish, W. R., and Hiza, M. J., Cryogenics, 15(6), pp. 531-541, (1975).
108. Kobayashi, R., and Katz, D. L., Ind. Eng. Chem., 45(2), pp. 440-451, (1953).
109. Kobayashi, R., and Price, A. R., J. Chem. Eng. Data, 4(1), pp. 40-52, (1959).
110. Kobayashi, R., Chappellear, P. S., and Leland, T. W., Gas Processors Association, Technical Publication, TP-4, April 1974.

111. Kobayashi, R., Chappellear, P. S., and Stryjek R.,
J. Chem. Eng. Data, 19(4), pp. 334-339, (1974).
112. Kobayashi, R., Chappellear, P. S., and Stryjek R.,
J. Chem. Eng. Data, 19(4), pp. 340-343, (1974).
113. Kobayashi, R., Withrow, H. J., Williams, G. B., and Katz, D. L.,
Proc. Nat. Gas. Assn. Am. 30th Ann. Conf.,
pp. 27, (1951).
114. Kohn, J. P. and Beaudoin J. M.,
J. Chem. Eng. Data, 12(2), pp. 189-191, (1967).
115. Kohn, J. P. and Bradish, W. F.,
J. Chem. Eng. Data, 9(1), pp. 5-8, (1964).
116. Kohn, J. P. and Kurata, F., AIChE. J.,
4(2), pp. 211-217, (1958).
117. Kohn, J. P. and Ma Y. H., J. Chem. Eng. Data,
9(1), pp. 3-5, (1954).
118. Kohn, J. P. and Shipman L. M.,
J. Chem. Eng. Data, 11(2), pp. 176-180, (1966).
118. Kohn, J. P., Merrill, R. C., and Luks, K. D.,
Gas Processors Association, Research Report,
RR-40A, February, (1982).
119. Kojima, T., and Tochigi, K., Kagaku Kogaku, 32(2),
pp. 149-153, (1968).
120. Korvezee, A. E., and Scheffer, F. E. C.,
Rec. Trav. Chim., 50, pp. 256, (1931).
121. Kurata, F. and Swift, G. W.,
Gas Processors Association, Research Report,
RR-5, December 1971.
122. Lacey, W. N., Sage, B. H., and Lavender, H. M.,
Oil and Gas J., July 11, pp. 47-49, (1940).
123. Lapidus, L., "Digital Computation for Chemical Engineers",
McGraw Hill Book Co., New York, (1962).
124. Laugier, S., Legret, D., Desteve, J., Richon, D., and Renon H.,
Gas Processors Association, Research Report,
RR-59, June 1982.
125. Laurance, D. R., and Swift, G. W., J. Chem. Eng. Data,
17(3), pp. 333-337, (1972).
126. Le Breton, J. G., and McKetta, J. J., Hydrocarbon Processing,
43(6), pp. 136-138, (1964).

127. Li, Y. H., Dillard, K. H., and Robinson, R. L.,
J. Chem. Eng. Data, 26(1), pp. 53-55, (1981).
128. Lin, Y. N., Chen, R. R. J., Chappellear, P. S., and Kobayashi, R.,
J. Chem. Eng. Data, 22(4), pp. 402-408, (1977).
129. Lin, Y. N., Hwang, S. C., and Kobayashi, R.,
J. Chem. Eng. Data, 23(3), pp. 231-237, (1978).
130. Lin, H., Sebastian, H. M., Simnick, J. J., and Chao, K. C.,
J. Chem. Eng. Data, 24(2), pp. 146-149, (1979).
131. Liu, E. K., and Davison, R. R., J. Chem. Eng. Data, 26(1),
pp. 85-88, (1981).
132. Lu, C. Y., and Poon, D. P. L., Advan. Cryog. Eng.,
19, pp. 292-299, (1969).
133. Makranczy, J., Bela, M., Sandor, P., and Laszlo, R.,
Veszpremi Vegyipari Egyetem Kozlemennei, 8,
pp. 213-224, (1964).
134. Manley, D. B., and Swift, G. W., J. Chem. Eng. Data,
16(3), pp. 301-307, (1971).
135. Mantor, P. D., "The Solubility of Methane, Carbon Dioxide, and
Hydrogen Sulfide in Oxygenated Compounds at Elevated
Pressures." (Unpub. M.S. thesis, The Rice Institute,
Houston, Texas, 1960.)
136. Maripuri, V. O., and Ratcliff, G. A., J. Chem. Eng. Data,
17(3), pp. 366-369, (1972).
137. Marshall, D. R., Saito, S., and Kobayashi, R.,
AIChE J., 10(5), pp. 734-740, (1964).
138. Marshall, D. R., " Gas Hydrates at High Pressure ",
Ph. D. Thesis, Rice University, Houston, (1962).
139. Matschke, D. E., and Thodos, G., J. Chem. Eng. Data, 7(2),
pp. 232-234, (1962).
140. McCurdy, J. L., and Katz, D., Ind. Eng. Chem., 36(2),
pp. 674-680, (1944).
141. McKay, R. A., Reamer, H. H., Sage, B. H., and Lacey, W. N.,
Ind. Eng. Chem., 43(9), pp. 2112-2117, (1951).
142. McKetta, J. J., and Azarnoosh, A., J. Chem. Eng. Data,
8(4), pp. 494-496, (1963).
143. McKetta, J. J., and Lehigh, W. R., J. Chem. Eng. Data,
11(2), pp. 180-182, (1966).

144. McKetta, J. J., and Li, C. C., J. Chem. Eng. Data, 8(2), pp. 271-275, (1963).
145. McKoy, V., and Sinanoglu O., J. Chem. Phys., 38, pp. 2946, (1963).
146. McLeod, H. O., and Campbell, J. M., Trans. AIME, 222 pp. 590, (1961).
147. Mehra, V. S., and Thodos, G., J. Chem. Eng. Data, 10(3), pp. 211-214, (1965).
148. Menton, P. D., Parrish, W. R., and Sloan, E. D., Ind. Eng. Chem. Proc. Des. Dev., 20(2), pp. 399-401, (1981).
149. Miller, P., and Barnett D., Ind. Eng. Chem., 32(3), pp. 434-438, (1940).
150. Miller, R. C., Kidnay, A. J., and Hiza, M. J., J. Phys. Chem. Ref. Data, 9, pp. 721-734, (1980).
151. Mollerup, J., Fredenslund, A., and Grauso, L., Institute for Kemiteknik, Tech. Univ. of Denmark, Paper Presented at the Centinneial ACS Meeting in New York (1976).
152. Mollerup, J., J. Chem. Soc., Faraday Transactions I, 71(12), pp. 2351-2360, (1975).
153. Moshfeghian, M., Shariat, A. and Erbar, J. H., Paper Presented at NBS/NSF Symposium on Thermodynamics of Aqueous Systems with Industrial Application, Airlie House, Virginia, October 22-25, (1979).
154. Mraw, S. C., Hwang, S. C., and Kobayashi, R., J. Chem. Eng. Data, 23(2), pp. 135-139, (1978).
155. Myers, H. S., Petroleum Refiner, 36(3), pp. 175-178, (1957).
156. Nagahama, K., Konishi, H., Hoshino, D., and Hirata, M., J. Chem. Eng. Japan, 7(5), pp. 323-328, (1974).
157. Nagata, I. and Kobayashi, R., Ind. and Eng. Chem. Fundam., 5(3), pp. 344-348, (1966).
158. Nagata, I. and Kobayashi, R., Ind. and Eng. Chem. Fundam., 5(4), pp. 466-469, (1966).
159. Ng, H. J., and Robinson, D. B., Ind. and Eng. Chem. Fundam., 15(4), pp. 293-298, (1976).
160. Ng, H. J., and Robinson, D. B., Gas Processors Association, Research Report 66, April, 1983.

161. Nielsen, R. B., and Bucklin, R. W., Proc. 31st Ann. Gas Cond. Conf., March 2-4, Norman, Oklahoma, (1981).
162. Nielsen, R. L., and Weber, J. H., J. Chem. Eng. Data, 4(2), pp. 145-151, (1959).
163. Noaker, L. J., and Katz, D. L., Trans. AIME, 201, pp. 237, (1954).
164. Ogorodnikov, S. K., Kogan, V. B., and Nemtsov, M. S., Zh. Prik. Khimii, 33(12), pp. 2685-2693, (1960).
165. Olds, R. H., Sage, B. H., and Lacey, W. N., Ind. Eng. Chem., 34(80), pp. 1008-1013, (1942).
166. Olds, R. H., Sage, B. H., and Lacey, W. N., Ind. Eng. Chem., 34(10), pp. 1223-1227, (1942).
167. Olds, R. H., Sage, B. H., and Lacey, W. N., Ind. Eng. Chem., 41(3), pp. 475-482, (1949).
168. Othmer, D., and Benenati, R. F., Ind. Eng. Chem., 37(3), pp. 299-303, (1945).
169. Parrish, W. R., and Hiza, M. J., Advan. Cryog. Eng., 19, pp. 300-309, (1973).
170. Parrish, W. R., and Prausnitz, J. M., Ind. Eng. Chem. Proc. Des. Dev., 11(1), pp. 26-35, (1972).
171. Pauling, L., and Marsh, R. E., Proc. Nat. Acad. Sci., 38(1), pp. 112, (1952).
172. Pitzer, K. S., and Curl, R. F., "The Thermodynamic Properties of Fluids", Institution of Mechanical Engineers, London, (1957).
173. Powell, H. M., J. Chem. Soc., pp. 61, (1948).
174. Price, R. A., and Kobayashi, R., J. Chem. Eng. Data, 4(1), pp. 40-52, (1959).
175. Prodany, N. W., and Williams, B., J. Chem. Eng. Data, 16(1), pp. 1-6, (1971).
176. Rackett, H. G., J. Chem. Eng. Data, 15, pp. 514, (1970).
177. Reamer, H. H., Carmichael, L. T., and Sage, B. H., Ind. and Eng. Chem., 44(9), pp. 2219-2226, (1952).
178. Reamer, H. H., Sage, B. H., and Lacey, W. N., Ind. Eng. Chem., 5(1), pp. 44-50, (1940).

179. Reamer, H. H., Olds, R. H., Sage, B. H., and Lacey, W. N.,
Ind. Eng. Chem., 34(12), pp. 1526-1531, (1942).
180. Reamer, H. H., Olds, R. H., and Lacey, W. N.,
Ind. Eng. Chem., 35(7), pp. 790-793, (1943).
181. Reamer, H. H., Sage, B. H., and Lacey, W. N.,
Ind. Eng. Chem., 42(3), pp. 534-539, (1950).
182. Reamer, H. H., Sage, B. H., and Lacey, W. N.,
Ind. Eng. Chem., 43(4), pp. 976-981, (1951).
183. Reamer, H. H., and Sage, B. H., Ind. Eng. Chem., 43(7),
pp. 1628-1634, (1951).
184. Reamer, H. H., and Sage, B. H., Ind. Eng. Chem., 43(11),
pp. 2515-2520, (1951).
185. Reamer, H. H., Sage, B. H., and Lacey, W. N.,
J. Chem. Eng. Data, 1(1), pp. 29-41, (1956).
186. Reamer, H. H., and Sage, B. H., J. Chem. Eng. Data,
7(2), pp. 161-168, (1962).
187. Reamer, H. H., Sage, B. H., and Lacey, W. N.,
Ind. Eng. Chem., 44(2), pp. 609-615, (1962).
188. Reamer, H. H., Sage, B. H., and Lacey, W. N.,
Ind. Eng. Chem., 45(8), pp. 1805-1809, (1953).
189. Reamer, H. H., and Sage, B. H., J. Chem. Eng. Data,
9(1), pp. 24-28, (1964).
190. Reamer, H. H., and Sage, B. H., J. Chem. Eng. Data,
11(1), pp. 17-24, (1966).
191. Reamer, H. H., Selleck F. T., and Sage, B. H.,
Petroleum Trans, AIME, 195, pp.197-202, (1952).
192. Reamer, H. H., Selleck, F. T., Sage, B. H., and Lacey, W. N.,
Ind. Eng. Chem., 45(8), pp. 1810-1812, (1953).
193. Richards, A. R., Hargreaves, E., Ind. Eng. Chem., 36(9),
pp. 805-808, (1944).
194. Rigby, M., and Prausnitz, J. M., J. Phys. Chem., 72(1),
pp. 330-334, (1968).
195. Roberts, D. L., Brownscombe, E. R., Home, L. S.,
and Ramser, H., The Petroleum Engineer,
March (1941).
196. Roberts, L. R., and McKetta, J. J., AIChE. J.,
7(1), pp. 173-174, (1961).

197. Robinson, D. B., Proceedings 53th GPA Annual Convention, pp. 14-15, (1971).
198. Robinson, D. B., and Bailey, J. A., Can. J. Chem. Eng., 35(4), pp. 151-158, (1957).
199. Robinson, D. B., Lorenzo, A. P., and Macrygeorgos, C. A., Can. J. Chem. Eng., 37(6), pp. 212-217, (1959).
200. Robinson, D. B., and Besserer, G. J., Can. J. Chem. Eng., 49, pp. 651-656, (1971).
201. Robinson, D. B., and Besserer, G. J., Gas Processors Association, Research Report, RR-7, June 1972.
202. Robinson, D. B., and Besserer, G. J., J. Chem. Eng. Data, 20(2), pp. 157-161, (1975).
203. Robinson, D. B., Chen, C. J., and Ng, H. J., Gas Processors Association, Research Report, RR-58, March 1981.
204. Robinson, D. B., Huang, S. S., and Leu, A. D., Gas Processors Association, Research Report, RR-51, March 1981.
205. Robinson, D. B., Hughes, R. E., and Sandercock, J. A. W., Can. J. Chem. Eng., 42(7), pp. 143-151, (1964).
206. Robinson, D. B., and Hutton, J. M., J. Can. Pet. Tech., March, pp. 6-9, (1967).
207. Robinson, D. B., and Jhaveri, J., Can. J. of Chem. Eng., April, pp. 75-78, (1965).
208. Robinson, D. B., and Kalra, H., Cryogenics, 15(7), pp. 409-412, (1975).
209. Robinson, D. B., and Kalra, H., Gas Processors Association, Technical Publication, TP-45, March 1975.
210. Robinson, D. B., Kalra, H., Ng, H. J., and Kubota, H., J. Chem. Eng. Data, 25(1), pp. 51-55, (1980).
211. Robinson, D. B., Kalra, H., Ng, H. J., and Kubota, H., J. Chem. Eng. Data, 23(4), pp. 317-321, (1978).
212. Robinson, D. B., Kalra, H., Ng, H. J., and Miranda, R. D., J. Chem. Eng. Data, 23(4), pp. 321-324, (1978).
213. Robinson, D. B., Krishnan, T., and Kalra, H., Ind. Eng. Chem., 21(2), pp. 222-225, (1976).
214. Robinson, D. B., and Ng, H. J., J. Chem. Eng. Data, 23(4), pp. 325-327, (1976).

215. Robinson, D. B., and Ng, H. J.,
AIChE J., 22(4), pp. 656-661, (1976).
216. Robinson, D. B., and Ng, H. J., Gas Processors Association,
Research Report, RR-29, March 1978.
217. Robinson, D. B., Ng, H. J. and Wu B. J.,
J. Chem. Thermodynamics, 8, pp. 461-469, (1976).
218. Robinson, R. L., Li, Y. H., Hulsey, B. J., and Gupta, M. K.,
J. Chem. Eng. Data, 27(1), pp. 55-57, (1982).
218. Robinson, D. B., Kalra, H., and Rempis, H.,
Gas Processors Association, Research Report,
RR-31, May, (1978).
219. Rouher, O. S. and Barduhn, A. J., Desalination,
6, pp. 57-73, (1969).
220. Sage, B. H., Hicks, B. L., and Lacey, W. N.,
Ind. Eng. Chem., 32(8), pp. 1085-1092, (1940).
221. Sage, B. H., Jacobs, J., and Wiese, H. C.,
J. Chem. Eng. Data, 15(1), pp. 82-91, (1970).
222. Sage, B. H., and Lacey, W. N., Ind. Eng. Chem., 32(7),
pp. 992-996, (1940).
223. Sage, B. H., Reamer, H. H., Olds, R. H., and Lacey, W. N.,
Ind. Eng. Chem., 34(9), pp. 1108-1116, (1942).
224. Sage, B. H., and Reamer, H. H.,
J. Chem. Eng. Data, 8(4), pp. 508-513, (1963).
225. Saito, S., and Kobayashi, R. AIChE J.,
11(1), pp. 96-99, (1965).
226. Sanchez, M., and Lentz, H., High Temp. High Pres., 5,
pp. 689-699, (1973).
227. Scauzillo, F. R., J. of Pet. Tech.,
pp. 698-701, July, (1961).
228. Schlinder, D. L., Swift, G. W., and Kurata, F.,
Hydrocarbon Processing, 45(11), pp. 205-210, (1966).
229. Schroeder, W., "Sammlung Chemischer und Chemischtechnischer
Vortrage," pp. 21-71, (1926).
230. Selected Values of Properties of Hydrocarbons and Related
Compounds, API Research Project 44, Texas A & M
University, Updated (1979).

231. Sebastian, H. M., Simnick, J. J., Lin, H. M., and Chao, K. C.,
J. Chem. Eng. Data, 25(3), pp. 138-140, (1980).
232. Sebastian, H. M., Simnick, J. J., Lin, H. M., and Chao, K. C.,
J. Chem. Eng. Data, 25(3), pp. 246-248, (1980).
233. Selleck, F. T., Carmichael, L.T., and Sage, B. H.,
Ind. Eng. Chem., 44(9), pp. 2219-2226, (1952).
234. Shenderei, E. R., Zelvenskii, Y. D., and Ivanovskii, F. P.,
Zh. Prikl. Khim., 35(3), pp. 690-693, March, (1962).
235. Shim, J., and Kohn, J. P.,
J. Chem. Eng. Data, 7(1), pp. 3-8, (1962).
236. Sieg, L., Chem. Ing. Tech, 22(15), pp. 322-326, (1950).
237. Skripka, V. G., Khimiya. Tekn. Topliv i. Masel, 2,
pp. 13-14 (1975).
238. Smith, J. M., Chem. Engr. Prog., 44(7),
pp. 521-528, (1948).
239. Sobocinski, D. P., and Kurata, F., AIChE. J.,
5(4), pp. 545-551, (1959).
240. Stackelberg, Von M., and Muller, H. R., Z. Electrochem.,
58, pp. 25, (1954).
241. Steam Tables, Properties of Saturated and Superheated Steam
from 0.08865 to 15,500 psia, Values Reprinted from
1967 ASME Steam Tables by the American Society
of Mechanical Engineers, 4th Printing, (1976).
241. Strobridge, T. R., "The Thermodynamic Properties of Nitrogen
from 64 to 300 K between 0.1 and 200 Atmospheres",
Nat. Bur. Stand., Tech Note 129, (1962).
242. Stroud, L., and Brandt, L. W., Ind. Eng. Chem.,
50(5), pp. 849-852, (1958).
243. Sultanov, R. G., Skripka, V. G., and Namiot, Y.,
Gazonov Prom., 4, pp. 6-8, (1971).
244. Takenouchi, S., and Kennedy, G. C., Amer. J. of Science,
262, pp. 1055-1074, (1964).
245. Thodos, G., and Mehra, V. S., J. Chem. Eng. Data, 10(4),
pp. 307-309, (1965).
246. Todheide, K., and Franck, E. U., Zeitschrift fur Physikalische
Chemie Neue Folge, 37, pp. 387-401, (1963).

247. Tongberg, C. O., and Johnston, F., Ind. Eng. Chem., 25(7), pp. 733-735, (1933).
248. Toshikatsu, H., Nagahama, K., and Suda, S., Kagaku Kogaku, 33(9), pp. 904-907, (1969).
249. Trimble, H. M., and Potts, W., Ind. Eng. Chem., 27(1), pp. 66-68, (1935).
249. Turek, E. A., Metcalfe, R. S., Yarborough, L., Robinson, R. L., Paper Presented at 55th Annual Fall Conference of the Society of Petroleum Engineers, September 21-24, (1980).
250. Unruh, C. H., and Katz, D. L., Trans. AIME, 186, pp. 83, (1949).
251. Vaughan, W. E., and Collins, F. C., Ind. Eng. Chem., 34(7), pp. 885-890, (1942).
252. Verhoeve, L., and Schepper H., J. Appl. Biotechnol., 23, pp. 607-619, (1973).
253. Verma, V. K., " Gas Hydrates from Liquid Hydrocarbon-Water Systems ", Ph. D Thesis, Univ. of Michigan, (1974).
254. Villard, P., Compt. Rend., 106, pp. 1602-1603, (1888).
255. Villard, P., Compt. Rend., 107, pp. 395-397, (1888).
256. Waals, Van der, and Platteeuw, J. C., Advan. Chem. Phys., 2(1), pp. 91-96, (1959).
257. Walch, N., Nat. Chemie Ing. Techn., 40(5), pp. 241-244, (1968).
258. Watson, K. M., Ind. Eng. Chem., 35, pp. 398, (1943).
259. Webster, B. K., and Robert, E. A., Ind. Eng. Chem., 48(3), pp. 422-426, (1956).
260. Wehe, A. H., and McKetta, J. J., J. Chem. Eng. Data., 6(2), pp. 167-172, (1961).
261. West, J. R., Chem. Engr. Prog., 44(4), pp. 287-292, (1948).
262. Wichterle, I., Kobayashi, R., J. Chem. Eng. Data, 17(1), pp. 4-8, (1972).
263. Wichterle, I., Kobayashi, R., J. Chem. Eng. Data, 17(1), pp. 9-12, (1972).

264. Wiese, H. C., Reamer, H. H., and Sage, B. H.,
J. Chem. Eng. Data, 15(17), pp. 75-82, (1970).
265. Wiese, H. C., Jacobs, J., and Sage, B. H.,
J. Chem. Eng. Data, 15(17), pp. 82-91, (1970).
266. Wilcox, W. J., Carson, D. B., and Katz, D. L.,
Ind. Eng. Chem., 33(5), pp. 662-665, (1941).
267. Wilson, G. M., "Equation of State Analogies to Excess Free Energy of Mixing Equations", Contribution No. 29 from the Center of Thermochemical Studies, Brigham Young University, Provo, Utah, March (1972).
268. Wilson, G. M., Personal Communication. Brigham Young University, Provo, Utah, April 1980.
269. Wilson, G. M., and Gillespie, P. C., Gas Processors Association, Research Report, RR-48, 1982.
270. Yang, C. P., and Van Winkle, M., Ind. Eng. Chem., 47(2), pp. 293-296, (1955).
271. Yorizane, M., Sadamota, S., and Yoshimura, S.,
Kagaku Kogaku, 32(3), pp. 257-264, (1968).
272. Yorizane, M., Yoshimura, S., and Masuoka, H.,
Kagaku Kogaku, 34(9), pp. 953-957, (1970).
273. Yorizane, M., Yoshimura, S., and Masuoka, H.,
Kagaku Kogaku, 30(12), pp. 1093-1097, (1966).
274. Zais, E. J., and Silberberg, I. H., J. Chem. Eng. Data, 15(2), pp. 253-256, (1970).
275. Zandijcke, F., and Verhoeve, L., J. Appl. Biotechnol, 24, pp. 709-724, (1974).
276. Zenner, G. H., and Dana, L. I.,
Chem. Engr. Progr. Symp. Ser. No 44, 59, pp. 36-41, (1963).

2
VITA

Ali Iftikhar Majeed

Candidate for the Degree of

Doctor of Philosophy

Thesis: PREDICTION OF INHIBITION OF HYDRATE FORMATION USING THE
PFGC EQUATION OF STATE

Major Field: Chemical Engineering

Biographical:

Personal Data: Born in Rawalpindi, Pakistan on September 11, 1956,
to Haji Abdul and Tanvir Arshad Majeed.

Education: Started elementary education at Trinity Private School,
Karachi in August 1961. Also attended Presentation Convent
School, Rawalpindi and Saint Anthony School, Lahore. Middle
school education began at LaSalle School, Multan and finished
at Grammar School, Karachi. High School education started at
Cadet College, Hasanabdal in May 1969. Received the Matricu-
lation Certificate with distinction in 1972. Left Cadet
College, Hasanabdal as the top high school graduate in the
nation in August 1974 to attend Middle East Technical University,
Ankara, Turkey on a CENTO Technical Merit Scholarship.
Transferred to Boğaziçi University, Istanbul, Turkey in
February 1976. Received Bachelor of Science in Chemical
Engineering in July 1979 from Boğaziçi University. Admitted
to the graduate college at Oklahoma State University,
Stillwater in August 1980. Awarded the Master of Science
degree in Chemical Engineering in December 1981. Completed
requirements for the degree of Doctor of Philosophy in
Chemical Engineering at Oklahoma State University in December
1983.

Membership in Scholarly or Professional Societies: Member Omega
Chi Epsilon, Honorary Chemical Engineering Fraternity. Student
member of the American Institute of Chemical Engineers. Student
member of the National Society of Professional Engineers.
Recipient of the National Talent Gold Medal 1974. Recipient
of the CENTO Merit Scholarship 1974-1979.

Professional Experience: Independent Consultant to Chemical Process Consultants, Stillwater, Oklahoma, June 1981 to July 1983; Research Assistant, National Center for Groundwater Research, Stillwater, Oklahoma, June 1981 to July 1983; Research Assistant, OSU Foundation Thermodynamics Study, June 1982 to July 1983; Teaching Assistant, Oklahoma State University, September 1981 to May 1982; Research Assistant, Effect of Wheat Processing on Bran, January 1981 to May 1981; Training Engineer, Packages Limited, Lahore Pakistan, February 1980 to April 1980; Chemical Engineer, Industrial Development Bank, Istanbul, Turkey, July 1979 to September 1979. Training Engineer, Dawood Hercules Urea Complex, Lahore, Pakistan, July 1978 to September 1978; Training Engineer, Pakistan Refinery Limited, Karachi Pakistan, July 1977 to September 1977.